Investigation into Tipifarnib as an anti-mitotic agent and Spindly as the mitotic target

by

Joanne Dawn Smith

A thesis submitted in partial fulfillment of the requirements for the degree of

Master of Science

In

Cancer Sciences

Department of Oncology

University of Alberta

ABSTRACT

The mitotic checkpoint is a failsafe mechanism for the cell to ensure correct chromosome segregation. The evolutionarily conserved kinetochore RZZ complex is an essential component of the mitotic checkpoint. Spindly interacts with the RZZ complex in a farnesylation dependent manner and acts as a dynein adaptor at kinetochores. Spindly knockdown results in prometaphase delay, alignment defects, and loss of dynein kinetochore localization. The knockdown of Spindly phenocopies farnesyl transferase inhibitor (FTI) treatment of cells suggesting that Spindly is the mitotic target of FTIs. FTIs were originally developed to target the *RAS* oncogene, but have been abandoned as inhibitors of the Ras pathway. Our findings indicate a possibility in repurposing FTIs for cancer treatment, especially in combination treatment strategies.

We found that upon treatment of HeLa cells with Tipifarnib (an FTI) there was loss of Spindly KT localization. This lack of Spindly KT localization also caused a prometaphase arrest and prolonged mitotic duration that increased in a dose dependent manner. This is consistent with other FTIs that have been tested. However, neither Spindly nor Farnesyltransferase beta subunit protein levels corresponded to sensitivity or resistance, and more investigation is required to determine what acts as a marker for sensitivity or resistance to Tipifarnib.

Adavosertib, a Wee1 kinase inhibitor results in mitotic catastrophe and our lab found that it enhanced the activity of other anti-mitotic agents including an FTI. Based on this we wished to test the combination of Tipifarnib and Adavosertib in a range of cell lines and determine if the combination is synergistic. Our data indicate that the synthetic lethal relationship between

Tipifarnib and Adavosertib, both of which are being used in clinical trials for breast cancer individually, is conserved in a subset of breast cancer cells. The combination treatment was synergistic to varying extents depending on the cell line tested and this was not molecular subtype specific. The combination treatment of Tipifarnib and Adavosertib represents a potential new treatment for breast cancers.

Since neither Spindly nor FNTB protein levels served as a marker for Tipifarnib resistance, we wished to examine the mechanism of resistance, by generating Tipifarnib resistant cells. I found that while the resistant cells had increased Spindly and FNTB levels, this did not correspond to Spindly KT localization in the presence of Tipifarnib. These resistant cells will be invaluable reagents for future examination of Tipifarnib resistance mechanism, and potentially aid in determining how the resistance occurs.

PREFACE

This thesis is the original work by Joanne Dawn Smith and no part of this thesis has been previously published.

ACKNOWLEDGEMENTS

I would like to thank my supervisor Dr. Gordon Chan for taking me into his lab and for his patience, and support during my Masters. His mentorship and guidance were invaluable developing my skills as a researcher and for the work presented in this thesis. I would also like to thank all the members of the Chan laboratory, Dr. Cody Lewis for all of his assistance with learning new techniques and having always being willing to help bounce ideas. Kaushiki Roy, for her invaluable help writing the kinetochore localization quantification code. Our project and summer students for teaching me how to be a successful mentor. Specifically, I would like to thank Sargun Sokhi and Edric Xiao, for their assistance with experiments.

I would also like to thank my supervisory committee Dr. Michael Hendzel and Dr. Roseline Godbout for all their advice and feedback during the course of my Masters. I would also like to thank members of the Weinfeld, Godbout and Gamper laboratories for sharing equipment and reagents. I would like to thank Courtney Mowat for her friendship, helping me throughout my course by being a second pair eyes, dealing with my panic before exams and always being willing to sit in on my mock talks.

I would also like to thank Dr. Xuejun Sun, Dr. Guobin Sun and Gerry Barron in the Cell Imaging Facility for all of their assistance with my numerous imaging experiments. Thank you to Dr. Anne Galloway for her assistance sorting cells. In the Oncology department we have several fantastic laboratory assistants, thank you April Scott for all your help preparing solutions and helping with other tasks that made experiment run that much smoother. Special thank you for filling thousands of 10µL of pipette tips some months.

I would like to thank my funding sources for the duration of my Masters. The University of Alberta for awarding me the Queen Elizabeth II graduate scholarship and Alberta Graduate excellence scholarship, CRINA for awarding me the La Vie en Rose Scholarship for Breast Cancer Research.

Finally, I would like to thank my fiancé Jake Hadfield for always supporting and encouraging me during stressful times. And always telling me it will be alright when I am panicking.

TABLE OF CONTENTS

LIST OF TABLES

LIST OF FIGURES

LIST OF RECURRING ABBREVIATIONS

1μM Tipi^R	1μM Tipifarnib resistant cell line
2μM Tipi^R	2μM Tipifarnib resistant cell line
ACA	Anti-centromere antigen
APC/C	Anaphase promoting complex/cyclosome
ATM	Ataxia telangiectasia mutated
ATR	Ataxia telangiectasia and Rad3 related kinase
BSA	Bovine serum albumin
Bub1	Budding uninhibited by benzimidazole 1
BubR1	Bub1 related kinase 1
Bub3	Budding uninhibited by benzimidazole 3
C-terminus	Carboxyl terminus
CAK	CDK activating kinase
CCAN	Constitutive centromere associated network
Cdc25C	Cell division cycle 25C phosphate
Cdk1	Cyclin-dependent kinase 1 (also known as Cdc2)
CENP-A	Centromere protein A
CENP-F	Centromere protein F
Chk1	Checkpoint kinase 1
Cip	CDK interacting protein
CPC	Chromosomal passenger complex
DAPI	4',6-diamino-2-phenylindole
DNA	Deoxyribonucleic acid
DMEM	Dulbecco's Modified Eagle's Medium
EGFR	Epidermal growth factor receptor
FTI	Farnesyl transferase inhibitor
G1	Gap phase 1
G2	Gap phase 2
GFP	Green fluorescent protein
hrs	Hours
H3	Histone H3
KDa	Kilo dalton
Kip	Kinase inhibitory protein
KNM	Knl1, Ndc80, and Mis12
M	Mitosis phase
Mad1	Mitotic arrest deficient 1
Mad2	Mitotic arrest deficient 2
C-Mad2	Closed mitotic arrest deficient 2
O-Mad2	Open mitotic arrest deficient 2
MCAK	Mitotic centromere-associated kinesin
MCC	Mitotic checkpoint complex
mCherry	Monomeric Cherry fluorescent protein
min	Minutes
Mps1	Monopolar spindle 1

Myt1 (PKMYT1)	Protein kinase, membrane associated tyrosine/threonine 1
n	Number of samples
N-terminus	Amino terminus
NEBD	Nuclear envelope breakdown
ng	Nanogram
nm	Nanometer
nM	Nanomolar
ns	Not significant
OD_{600}	Optical density at 600 nm
PBS	Phosphate buffered saline
Plk1	Polo-like kinase 1
PP1	Protein phosphatase 1
PP2A	Protein phosphatase 2A
Rod	Roughdeal
RZZ	Roughdeal, Zwilch and Zeste-white 10
S	Synthesis (DNA replication) phase
SAC	Spindle assembly checkpoint
SD	Standard deviation
SDS	Sodium dodecyl sulfate
SEM	Standard error of mean
Ska	spindle and kinetochore associated complex
Spy	Spindly
TBS	Tris buffered saline
TBS-T	Tris buffered saline with tween
TipiR	Tipifarnib resistant cell line
µg	Microgram
µM	Micromolar
µm	Micrometer
ZW-10	Zeste-white 10

CHAPTER 1: INTRODUCTION

1.1 The cell cycle

1.1.1 Cell cycle phases

Cell division is required for all cellular organisms. The cell cycle is the process in which a cell divides to produce 2 daughter cells. When cell division fails, it can lead to chromosome loss, cell death, and inaccurate chromosome segregation that results in aneuploidy which can lead to cancer development.[1]

The cell cycle has 2 major parts: interphase and M-phase which are characterized by DNA replication and the segregation of the replicated chromosomes into 2 daughter cells respectively.[2] Interphase is made up of 3 individual phases, 2 Gap phases (G1 and G2) which are separated by synthesis (S). During G1 the cells increase in size and accumulate the necessary components for DNA replication and cell division. In S phase, the cell duplicates its DNA and in G2 the cell prepares for mitosis.[2] M Phase is divided into 2 components, mitosis or the division of chromosomes and cytokinesis, or the division of cytoplasm (Figure 1.1).

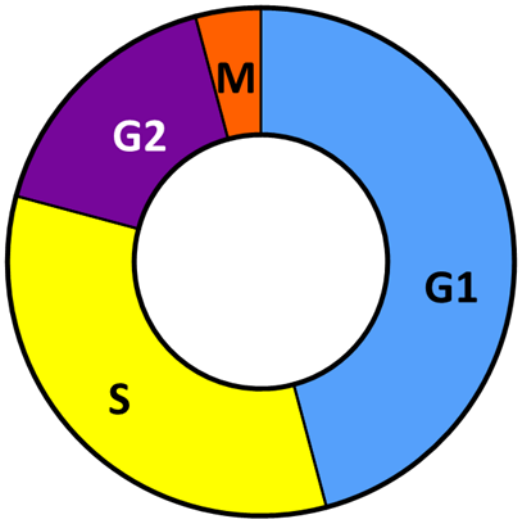

Figure 1.1 Phases of the cell cycle. The phases of the cell cycle are shown, interphase (G1, S and G2) and mitosis (M).

1.1.1.1 Cdks drive the cell cycle.

The cell cycle is controlled by cyclin dependent kinases or Cdks, a family of Ser/Thr kinases. Cdks are inactive as a monomer and require binding of cyclins, forming the active heterodimer[3]. Cdk levels remain consistent throughout the cell cycle however cyclin levels oscillate with the cell cycle, increasing in the phase in which they are active and then are degraded upon entry to the next phase of the cell cycle.[4] The Cdk-Cyclin complex can be activated or inhibited by different mechanisms. Cyclin activating kinases (CAKs) phosphorylate the complex, increasing its activity, while cyclin dependent kinase inhibitors (CKI) bind and inhibit Cdk (Figure 1.2A).[3] For full Cdk-Cyclin activation, Cdk requires phosphorylation by CAK that induces conformational changes enhancing the binding of cyclins. In the case of the Cdk1-CyclinB complex it is inhibited by phosphorylation, where Wee1 or Myt1 kinase phosphorylate Cdk on Thr14 or Tyr15 , which must be de-phosphorylated before the Cdk1-Cyclin B can be activated and the cell proceed into mitosis (Figure 1.2B).[2]

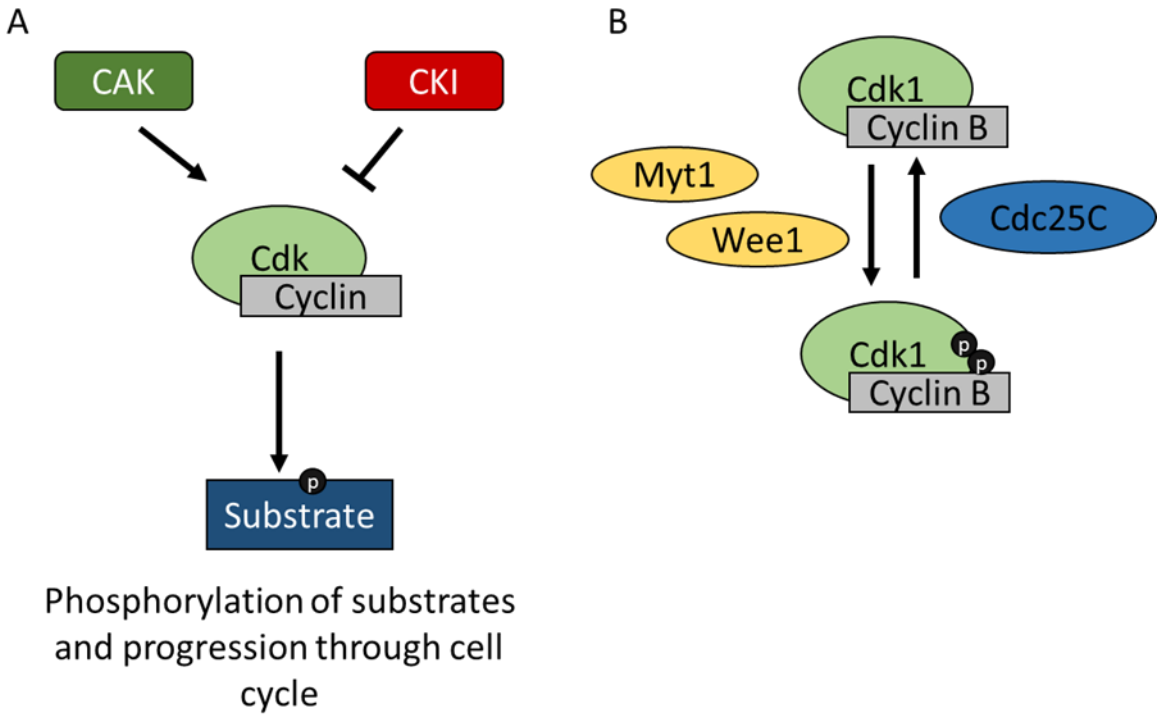

Figure 1.2 Cdk activity requires cyclin partner binding. A) Cdk-Cyclin complexes are activated by CAKs and inhibited by CKIs. When the Cdk-Cyclin complex is active it phosphorylates its substrates for progression through the cell cycle. B) Cdk1-CyclinB complex is inhibited by Wee1 and Myt1 mediated phosphorylation and activated be Cdc25C mediated de-phosphorylation.

1.1.1.2 Cell cycle checkpoints

Progression through the cell cycle is regulated by cell cycle checkpoints. These are checkpoints which if activated result in cell cycle arrest until conditions are correct. The G1/S checkpoint, or the restriction point, is the point in late G1 where past this point the cell has committed to cell division (Figure 1.3). This checkpoint ensures that the cell is large enough, and that there is a favorable environment for cell division. If cells have been starved of nutrients or growth factors, the cell will arrest in G1.[5]

Following entry to S phase, the next checkpoint is the Intra-S checkpoint, which is activated upon DNA damage, resulting in the inhibition of origins of replication firing until the damage has been repaired. This checkpoint is controlled by 2 different kinases, ataxia-telangiectasia-mutated (ATM) and ataxia telangiectasia and Rad3-related (ATR), which respond to double strand breaks or single strand breaks, respectively. Upon activation, they phosphorylate downstream effectors, resulting in inhibition of DNA replication. Upon DNA damage repair, the cell cycle continues.[6]

The G2/M checkpoint prevents cells from entering mitosis if they have DNA damage from either G2 or unrepaired damage from the earlier phases of the cell cycle. The main target of this checkpoint is the Cdk1-Cyclin B complex, whose inhibition prevents entry into mitosis.[6] This inhibition is carried out by Wee1 and Myt1 kinases, which place inhibitory phosphorylation on Cdk1 at Thr14 and Tyr15. [7]

The mitotic checkpoint, or the spindle assembly checkpoint, ensures that all the chromosomes are properly aligned at the metaphase plate before the cell proceeds into anaphase and the completion of mitosis. This checkpoint will be discussed in more detail in section 1.3.

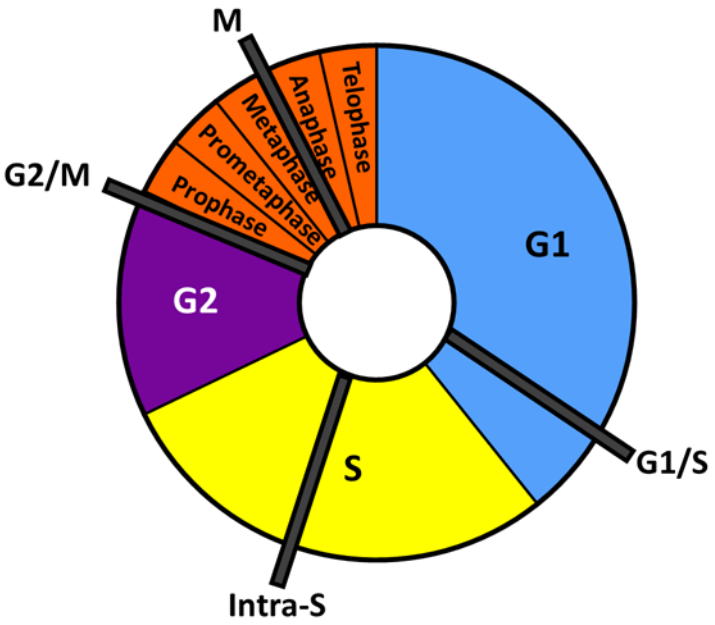

Figure 1.3 Cell cycle checkpoints. The cell cycle has 4 checkpoints, G1/S (or Restriction point), Intra-S, G2/M and Mitotic checkpoint.

1.1.1.2 Stages of Mitosis

Mitosis was first noted by Walther Flemming in 1882[8], and correct chromosome segregation during mitosis is critical to maintain genomic stability. Proper mitosis requires the activity of many different proteins for completion. Mitosis consists of 5 phases: prophase, prometaphase, metaphase, anaphase, and telophase (Figure 1.4A). These phases have distinct events occurring, and once these events have concluded the cell will progress to the next. Following cytokinesis and the generation of 2 daughter cells, the cell can re-enter G1, or enter G0, the quiescent state.

In prophase, the chromosomes condense, the nuclear envelope breaks down, and this breakdown marks the transition from prophase to prometaphase (Figure 1.4B). In prometaphase the attachment of microtubules to the sister chromatids occurs. The attached chromosomes

begin moving, resulting in chromosome congression at the spindle equator, beginning metaphase. In metaphase, all the chromosomes are aligned at the spindle equator and at the end of metaphase, the cohesion between the sister chromatids is broken, resulting in the separation and the beginning of anaphase. Anaphase is composed of anaphase A and B, in anaphase A, the daughter chromosomes move poleward and in anaphase B the poles separate from one another. In telophase, the chromosomes decondense and the nuclear envelop reforms, finally cytokinesis occurs, dividing the cytoplasm, resulting in 2 daughter cells.[9]

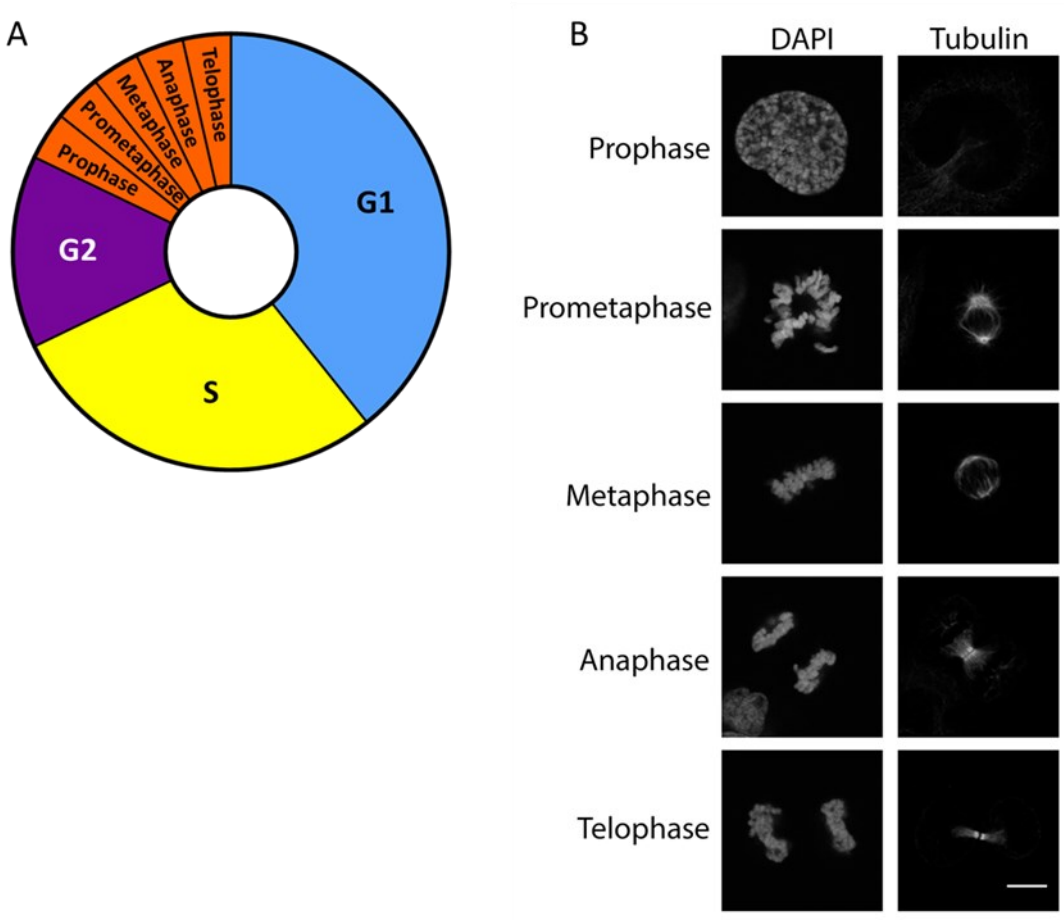

Figure 1.4 Stages of Mitosis. A) Mitosis is made up of 5 different phases: prophase, prometaphase, metaphase, anaphase, and telophase. B) Chromosome morphology for each

stage of mitosis is shown. HeLa cells were imaged for the chromosomes (DAPI) and mitotic spindle (tubulin). Cells in each stage of mitosis were imaged. Single z-stack image is shown, scale bar = 10µm.

1.2 The Kinetochore

The kinetochore (KT) is a trilaminar structure with the most prominent being an electron opaque outer plate, separate by light staining electron translucent middle plate from the inner plate that is associated with the surface of the pericentric heterochromatin.[10] The kinetochore requires the coordination of >100 different proteins to assemble this multilayered structure.[10] Following kinetochore assembly it must interact with additional proteins to provide the force to move chromosomes. The motor proteins move in either minus end directed, such as dynein/dynactin, or plus end directed such as Kinesin-7. These proteins are responsible for chromosome congression as well as poleward chromosome movement for mitotic progression (Figure 1.5). [10]

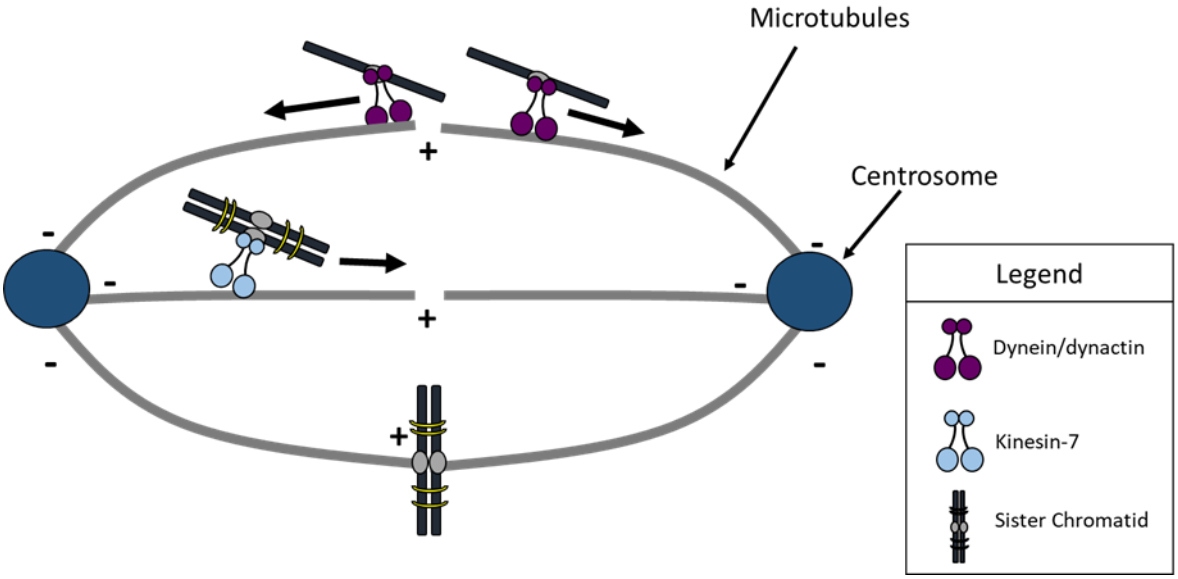

Figure 1.5 Mitotic motor proteins. Examples of some of the mitotic motor proteins involved in chromosome congression and separation. Kinesin-7, a plus end directed motor

protein is involved in chromosome congression and movement of sister chromatids to the metaphase plate. Dynein/dynactin are minus end directed, involved in poleward chromosome migration.

The inner plate of the KT interfaces with the centromeric heterochromatin which promotes the assembly of the KT due to the presence of histone H3 variant CENP-A which specifies centromeric chromatin.[10,11] The inner plate is made up of the constitutive centromere associated network (CCAN), a group of 16 proteins that are constitutively associated with the centromere throughout the cell cycle, and serves as the building platform for the KT (Figure 1.6).[11]

In late G2, KT assembly begins, and is fully matured after NEBD, following the exit from mitosis they rapidly disassemble.[10] During mitosis the kinetochore must form direct physical connection with microtubules (MT) from the mitotic spindle.[10] The outer KT serves as the MT binding surface, the core of which is the KMN network, a 10 subunit super complex made up of Knl1, Mis12 and the Ndc80 complexes (Figure 1.6).[11] The KMN network serves as main MT receptor at the KT and also as recruitment platform for other proteins including mitotic checkpoint proteins and additional regulators of KT-MT attachment, such as the Ska1 complex, MCAK, CENP-E and dynein.[11]

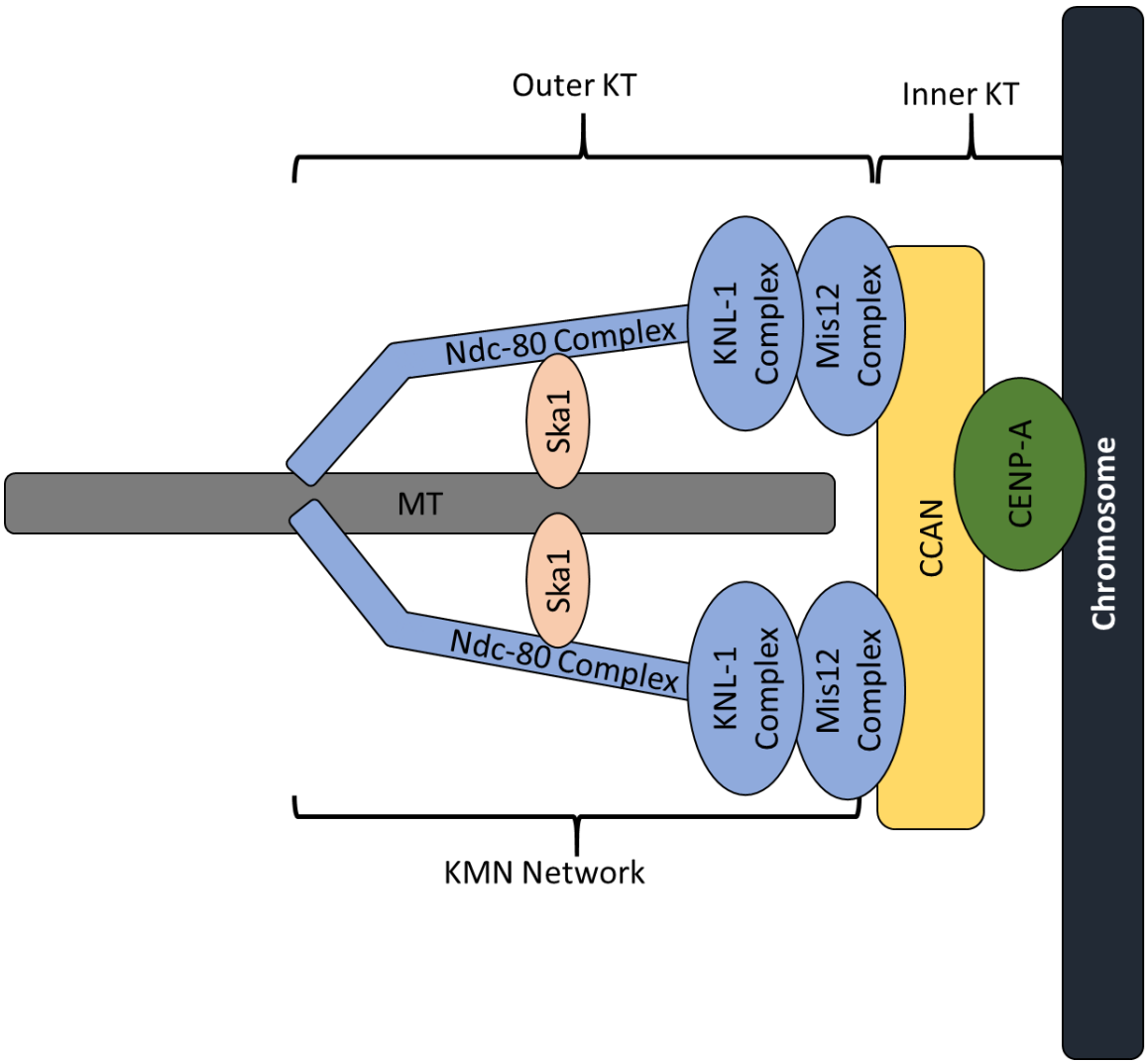

Figure 1.6 The kinetochore. The inner kinetochore, where the H3 variant CENP-A, and the constitutive centromere associated network (CCAN) connect the chromosome to the outer kinetochore proteins. The KMN network (Ndc-80, KNL-1 and Mis12 complexes) and Ska1 bind the microtubules.

1.2.1 KT-MT attachments

There are 2 different ways in which the KT can attach to a MT. Lateral interactions, where the KT interacts with the side of the MT, this allows the KT to initially capture the MT and be

moved along.[10] Stable KT-MT interactions require end on attachments, where the MT plus end is embedded in the KT.[10]

The KT-MT attachments that are formed must also be in the proper amphitelic attachments where sister KT are attached to spindle MTs from opposite poles (Figure 1.7 right panel). If improper KT-MT attachments occur, they must be corrected. Examples of these are shown in Figure 1.7, monotelic, where only one sister KT is attached to MT from a spindle pole and the other sister KT is unattached; syntelic, where both sister KTs are attached to MT from the same spindle pole; merotelic, where a single KT is attached to MT from opposite spindle poles. These improper attachments must be resolved, and this is done through an error correction mechanism mediated through Aurora B kinase signaling.[12]

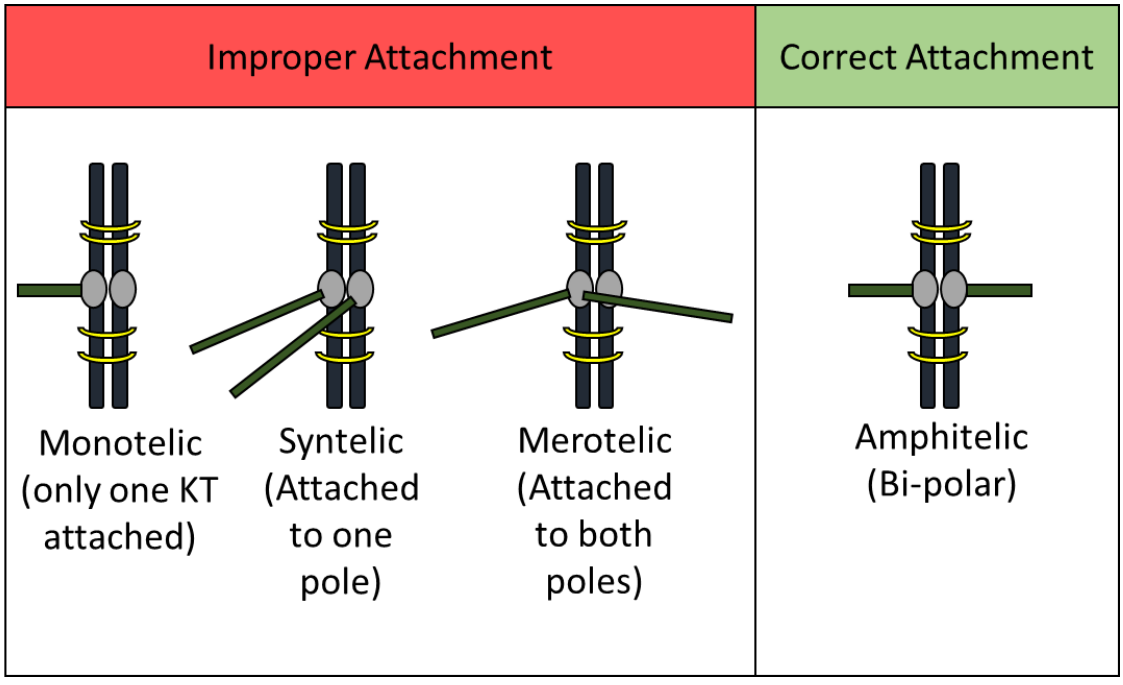

Figure 1.7 Kinetochore Microtubule attachments. There are proper and improper KT-MT attachments. Monotelic, syntelic and merotelic are improper KT-MT attachment that must be corrected until proper amphitelic attachments are made.

1.2.2 Dynein and Dynactin.

In eukaryotic cells, cytoplasmic dynein-1 (dynein) and various kinesins are responsible for the movement of vesicles, organelles, proteins, and mRNA. Dynein is a member of the AAA+ ATPase superfamily, and is the major minus end directed MT motor in most eukaryotic cells.[13] Dynactin is a dynein regulator that has been implicated in almost all functions of dynein, including its recruitment to the kinetochore, as dynein is in an inactive conformation when unbound.[13] While dynactin is able to increase dynein processivity on its own, the addition of a cargo adaptor, converts dynein into a highly processive motor.[14,15]

Each dynein/dynactin complex contains a single cargo adaptor molecule, which functions as the link between dynein/dynactin and the cargo; forming a stable complex that is capable of MT minus end directed movement. The N-terminal region of the adaptor protein binds to dynein/dynactin, while the C-terminal region binds the specific cargos[15] (Figure 1.8). In the absence of this adaptor, dynein and dynactin have low affinity for each other and processive motion will not occur. Currently there are 4 members of the BICD family of dynein/dynactin adaptors that have been studied, BICD2, Rab11-FIP3, Hook3 and Spindly. These 4 adaptor proteins link dynein/dynactin to their cargos and are required for the highly processive dynein/dynactin complexes[14].

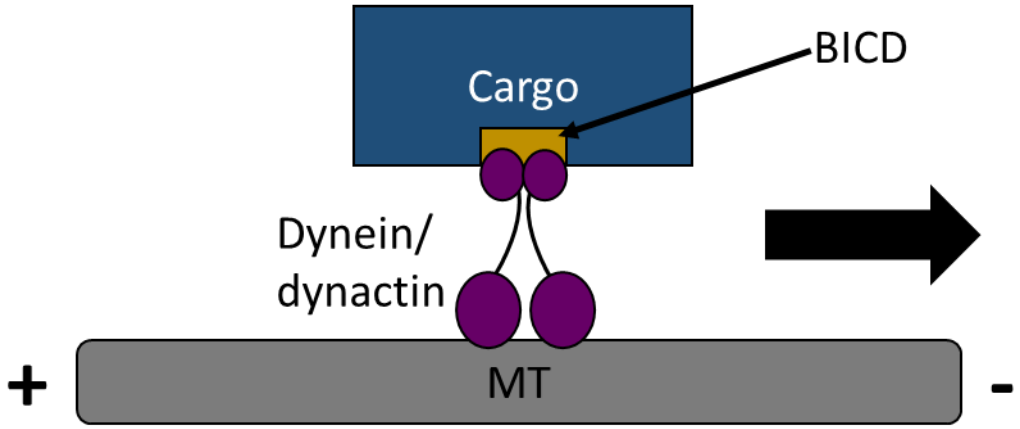

Figure 1.8 Dynein/dynactin is the major minus end directed motor protein.
Dynein/dynactin require the presence of an adaptor protein (BICD) bind to the cargo. This complex then moves poleward on the microtubule.

Dynein/dynactin plays 2 major roles in mitosis, chromosome congression and silencing of the mitotic checkpoint. KT bound dynein captures MT that are passing the KT, which allows for the rapid movement of chromosomes along MT toward the spindle poles before alignment at the metaphase plate. Following sister chromatid bi-orientation, dynein/dynactin mediates the transport of mitotic checkpoint proteins such as Mad1, Mad2, BubR1, the RZZ complex and Spindly away from the KT to the spindle poles, silencing the mitotic checkpoint.[16]

1.2.3 CENP-F

Centromere protein F (CENP-F), is a human KT protein that is important for chromosome alignment and is essential for cells to sustain prolonged mitotic arrest in response to unattached KT. Mammalian CENP-F interacts with a variety of partners involved in various cellular processes including cell division.[17] CENP-F depletion results in cells with reduced KT localization of mitotic checkpoint proteins Mad1, Mad2, hBubR1, hBub1 and hMps1.[18]

CENP-F is farnesylated at its C-terminus and this farnesylation is required for nuclear envelope localization, KT localization and degradation post mitosis. [19,20] Unlike Spindly, CENP-F KT localization does not depend on the RZZ complex, rather Bub1 is required for CENP-F KT localization.[21]

1.2.4 Bubs and Mads

Mitotic checkpoint proteins were first identified in yeast mutants that failed to arrest in mitosis in the presence of MT poisons. The first group was the Mitotic Arrest Deficient (Mad) 1, Mad2, and Mad3;[22] the second group was the Budding Uninhibited by Benzimidazole (Bub) 1, Bub2, and Bub3.[23] Monopolar spindle (Mps1) kinase, was identified in a yeast mutant that failed to arrest in mitosis when spindle formation was impaired.[24] These proteins, excluding Bub2 are all evolutionarily conserved in all eukaryotic organisms forming the core mitotic checkpoint proteins.[25] Since the discovery of these proteins, more mitotic checkpoint proteins have been identified that play roles in arresting cells in mitosis upon different conditions. Mammalian Mad1, Mad2, Mad3 (BubR1), Bub1, Bub3 and Mps1 all preferentially localize to unattached KT.

1.3 The Mitotic checkpoint

The mitotic checkpoint is the failsafe mechanism that monitors chromosome bi-orientation on the mitotic spindle, and as long as any unattached chromosomes remain, it prevents the progression from metaphase to anaphase allowing more time to achieve proper bipolar chromosome alignment.[12] Sister chromatids are held together by the cohesin complex, and prior to anaphase, securin inhibits separase preventing cohesin cleavage (Figure 1.9, top panel). At anaphase onset, the E3 ubiquitin ligase Anaphase Promoting Complex/Cyclosome

(APC/C), targets securin for degradation. This results in free separase which then cleaves cohesin resulting in sister chromatid separation (Figure 1.9, bottom panel). Premature chromosome separation must be prevented to ensure proper chromosome segregation, and this is done by the mitotic checkpoint.[10,24] The presence of incorrect or missing MT attachment at the KT results in checkpoint signal that can diffuse through the rest of the cell and results in inhibition of the cell cycle.[10,12]

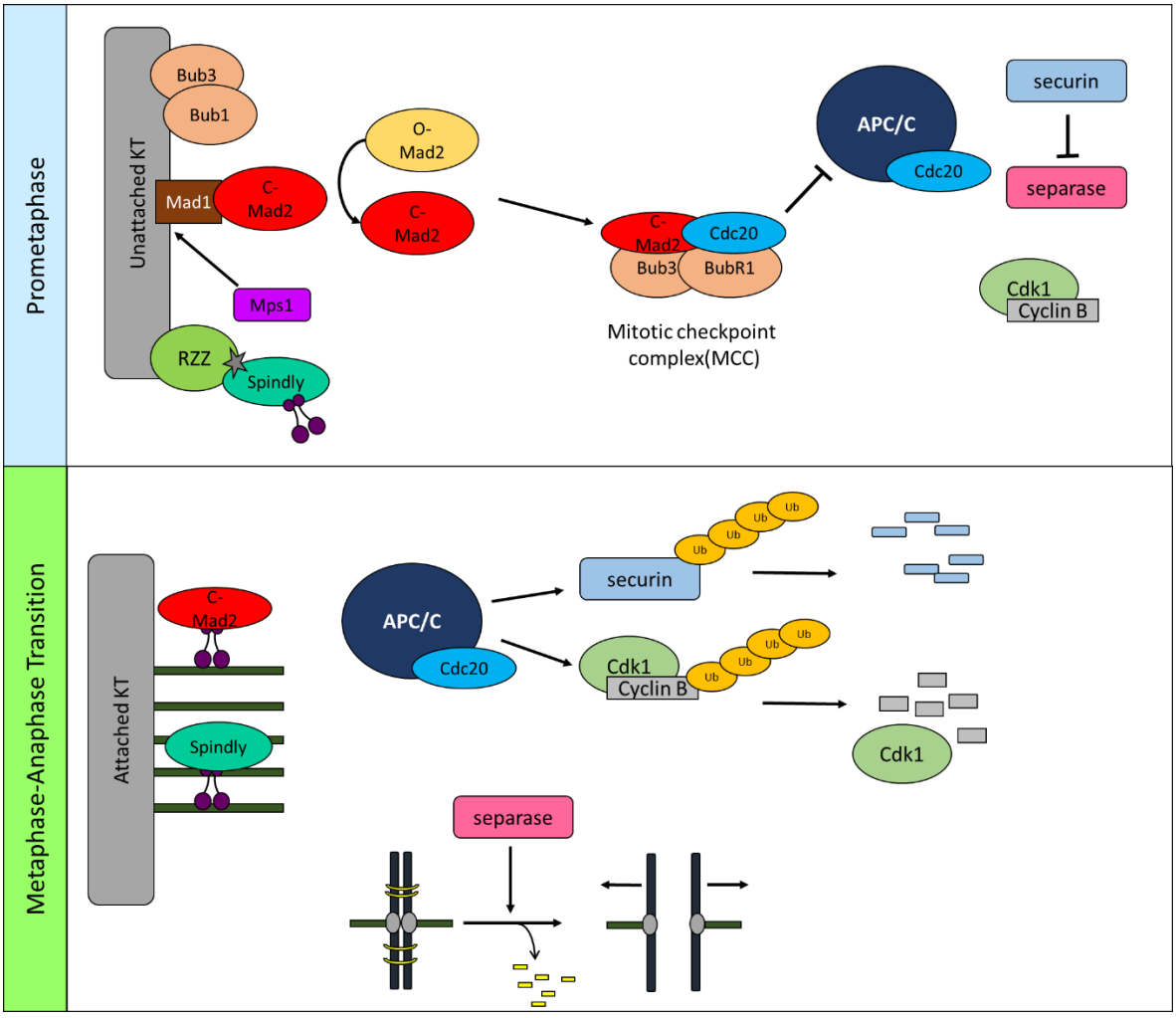

Figure 1.9 The mitotic checkpoint. In Prometaphase, the Mitotic checkpoint complex (MCC) inhibits APC/C preventing degradation of securin and Cyclin B. O-Mad2, inactive conformation of Mad2; C-Mad2- active conformation of Mad2. C-Mad2 interacts with Mad1 at

KT, serves as a template to convert more O-Mad2 to C-Mad2. C-Mad2 forms the MCC with BubR1, Bub3, Cdc20 and binds to APC/C as a pseudo-substrate, inhibiting its activity. During the metaphase to anaphase transition, MCC is disassembled, APC/C is now active, securin and Cyclin B are degraded. Separase cleaves cohesin, resulting in separation of the sister chromatids.

1.3.1 APC/C

Progression through mitosis into anaphase requires the activity of APC/C, an E3 ubiquitin ligase that controls the polyubiquitylation of cell cycle regulators.[26] Polyubiquitylated proteins are recognized and degraded by the 26S proteasome.[26] APC/C is a multi-subunit complex, with a Cullin-RING ubiquitin ligase-like catalytic core, structural linkers and various subunits, such as Cdc20. Cdc20 is an activator of APC/C and acts as a substrate specific receptor for KEN and D box degrons.[26] Following mitotic checkpoint silencing, APC/C-Cdc20 activity results in the polyubiquitylation of Cyclin B and securin which allows for anaphase onset, the separation of sister chromatids, and mitotic exit (Figure 1.10).[27]

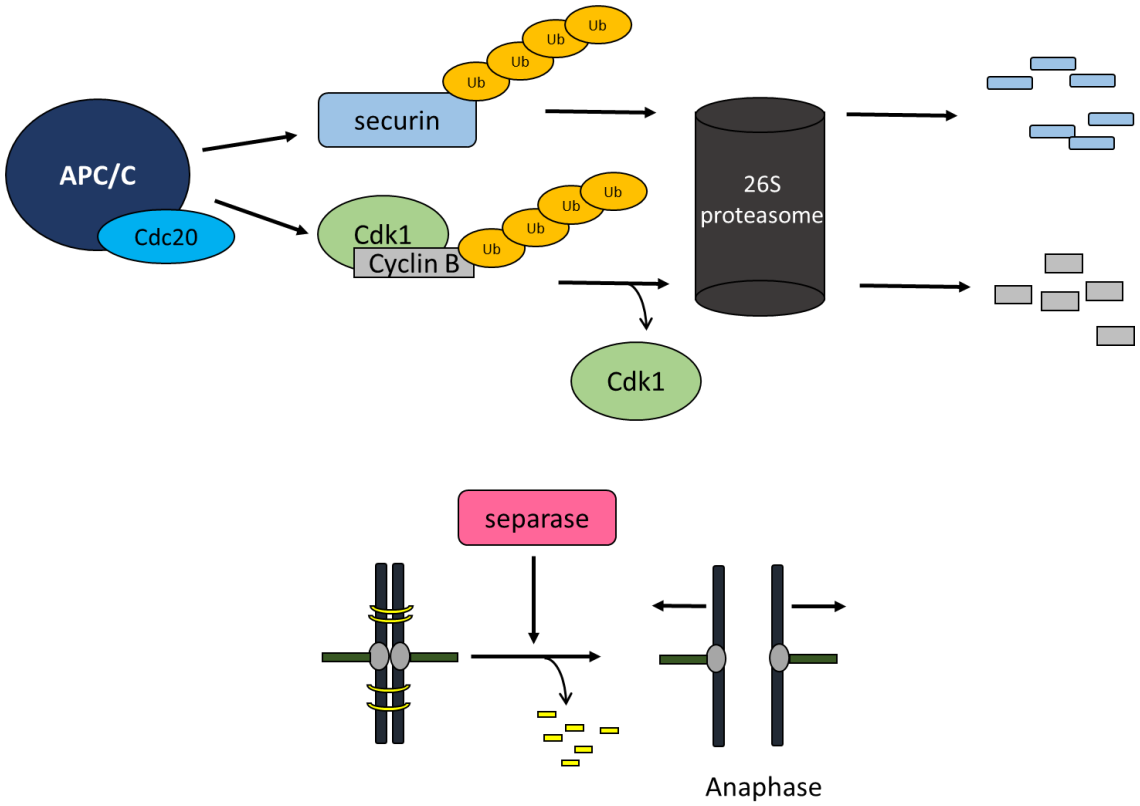

Figure 1.10 Active APC/C results in mitotic progression. The APC/C is phosphorylated by Cdk1 and once bound to Cdc20 is now active. It targets substrates containing D or Ken box degrons for degradation via the ubiquitin-proteasome-system. This allows the metaphase to anaphase transition to occur, degradation of cohesin by separase and the separation of sister chromatids.

1.3.2 MCC Complex

The Mitotic Checkpoint Complex (MCC), functions as the inhibitor of APC/C preventing premature entry into mitosis. The MCC is comprised of Mad2, BubR1, Bub3 and Cdc20. BubR1 contains 2 KEN domains, which are involved in the binding of Cdc20 to the MCC.[12] Mad2 is recruited to the kinetochore through interaction with Mad1, where it then can bind and sequester Cdc20 in the MCC. Mad2 has 2 different conformations, open-Mad2 (O-Mad2) the inactive, unbound pool of Mad2; and closed-Mad2 (C-Mad2) the active conformation, which

interacts with Mad1 and Cdc20.[28] Mad1-C-Mad2 at the kinetochore serves as a template for the conversion of O-Mad2 to C-Mad2 that is then able to bind Cdc20 and be incorporated into the MCC (Figure 1.9, top panel).[28] The removal of Mad1-C-Mad2 from the kinetochore upon proper microtubule attachment is performed by the RZZ complex and Spindly, which are required for proper mitotic checkpoint silencing (Figure 1.9, bottom panel).[12]

Mad2 is required for BubR1 binding of Cdc20, resulting in inhibition of Cdc20 mediated activation of APC/C.[12] The MCC functions as a pseudo-substrate for APC/C inhibiting its activity (Figure 1.11, left panel).[12] Loss of Mad2 results in premature degradation of cyclin B during prometaphase, causing premature chromosome separation, due to the lack of APC/C inhibition. Upon mitotic checkpoint silencing, the MCC disassembles, and APC/C-Cdc20 is free, resulting in polyubiquitylation of target substrates such as cyclin B and securin (Figure 1.11, right panel). [29]

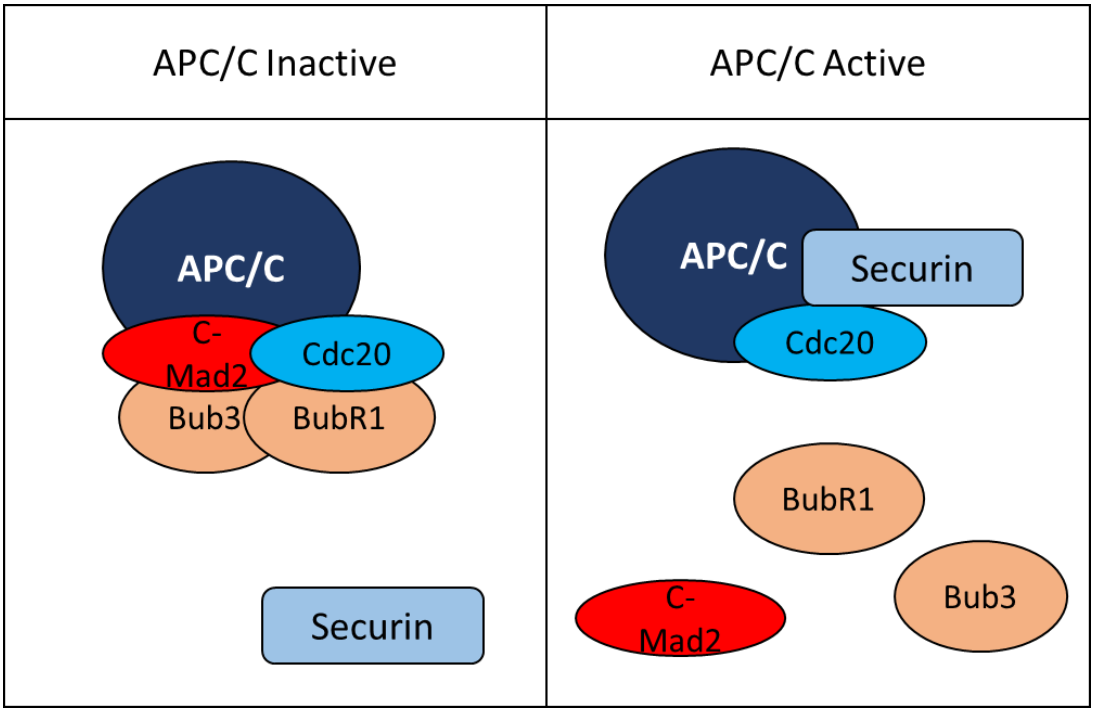

Figure 1.11 MCC acts as a pseudo-substrate for APC/C. When MCC is bound to APC/C as a pseudo-substrate, it prevents APC/C-Cdc20 from binding substrates. Upon mitotic checkpoint silencing, APC/C-Cdc20 is able to bind substrates such as securin, resulting in degradation.

1.3.3 The RZZ Complex

The RZZ complex is an essential mitotic checkpoint component at the KT, composed of Roughdeal (Rod), ZesteWhite10 (Zw10) and Zwilch. In cells lacking RZZ components, cells no longer arrest in mitosis following spindle damage, but will instead proceed to exit from mitosis.[30] The RZZ complex is recruited to the KT via the Bub1/Bub3 complex, where it then recruits other mitotic checkpoint proteins.[31] The RZZ complex is required for the recruitment of Mad1, Mad2 and Spindly to KTs (Figure 1.12).[28,32,31,33] The RZZ complex contributes to checkpoint activation by promoting Mad2 recruitment, allowing for formation of the MCC. When metaphase chromosome alignment is achieved, mitotic checkpoint silencing begins with shedding of Mad2 along MT fibers along with RZZ and Spindly.[33]

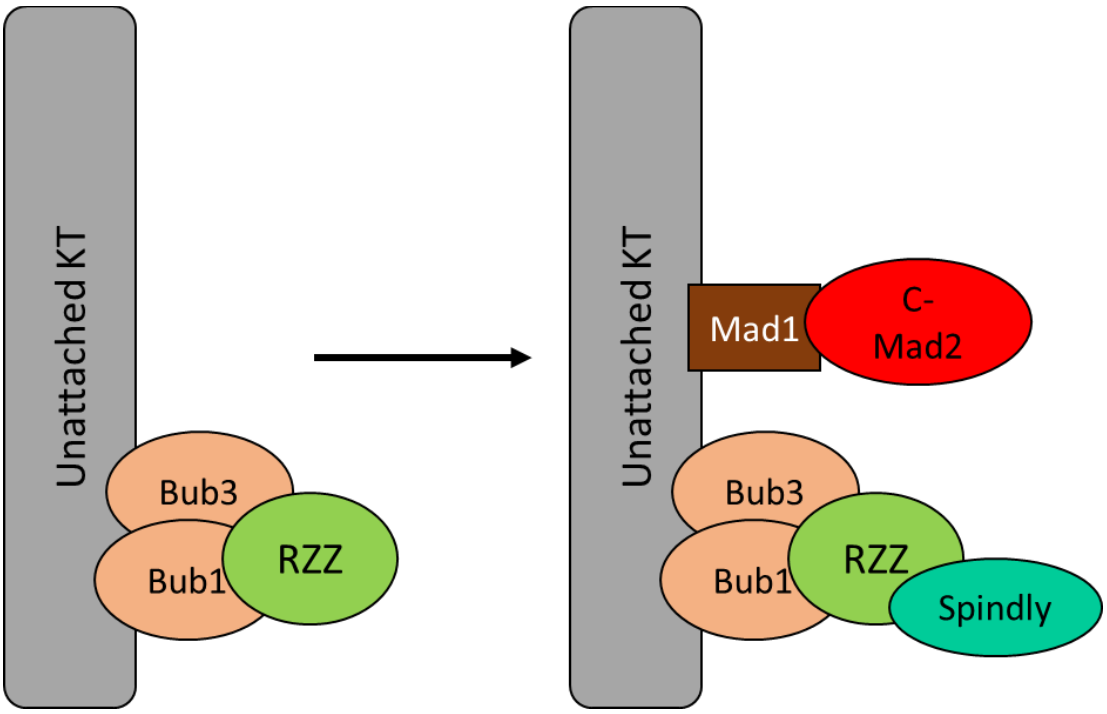

Figure 1.12 RZZ KT recruitment. The RZZ complex is recruited via Bub1, where it then can recruit Spindly an Mad1-Mad2 to the kinetochore.

1.3.4 Aurora B Kinase and Mps1

Improper KT-MT attachment needs to be remedied, this is controlled by a variety of mitotic kinases including Aurora B, Mps1, Plk1, Bub1 and Cdk1. In some cases these kinases will act globally, for example Cdk1 dependent phosphorylation ensures KT function and assembly state change are simultaneously controlled at each KT to alter its function at cell cycle transitions.[10]

Aurora B is a Ser/Thr protein kinase that is part of the chromosome passenger complex (CPC) located in the inner KT. Aurora B phosphorylates outer KT substrates to promote proper KT-MT attachments, in response to lack of tension. [10,12] Lack of tension allows Aurora B to directly inhibit components of the KT-MT interface, including the Ndc80 and Ska1 complexes, which eliminates incorrect KT-MT attachments, resetting KT to unattached state from which proper KT-MT attachments can be re-established (Figure 1.13, left panel).[10] Upon proper KT-MT attachments, the KT is under tension, which results in the spatial separation of Aurora B from its substrates, preventing its activity. (Figure 1.13, right panel).[9,10,12] In addition to Aurora B, there are phosphatases that are localized to the KT, that following activation, ensure that KT substrates are dephosphorylated.[10]

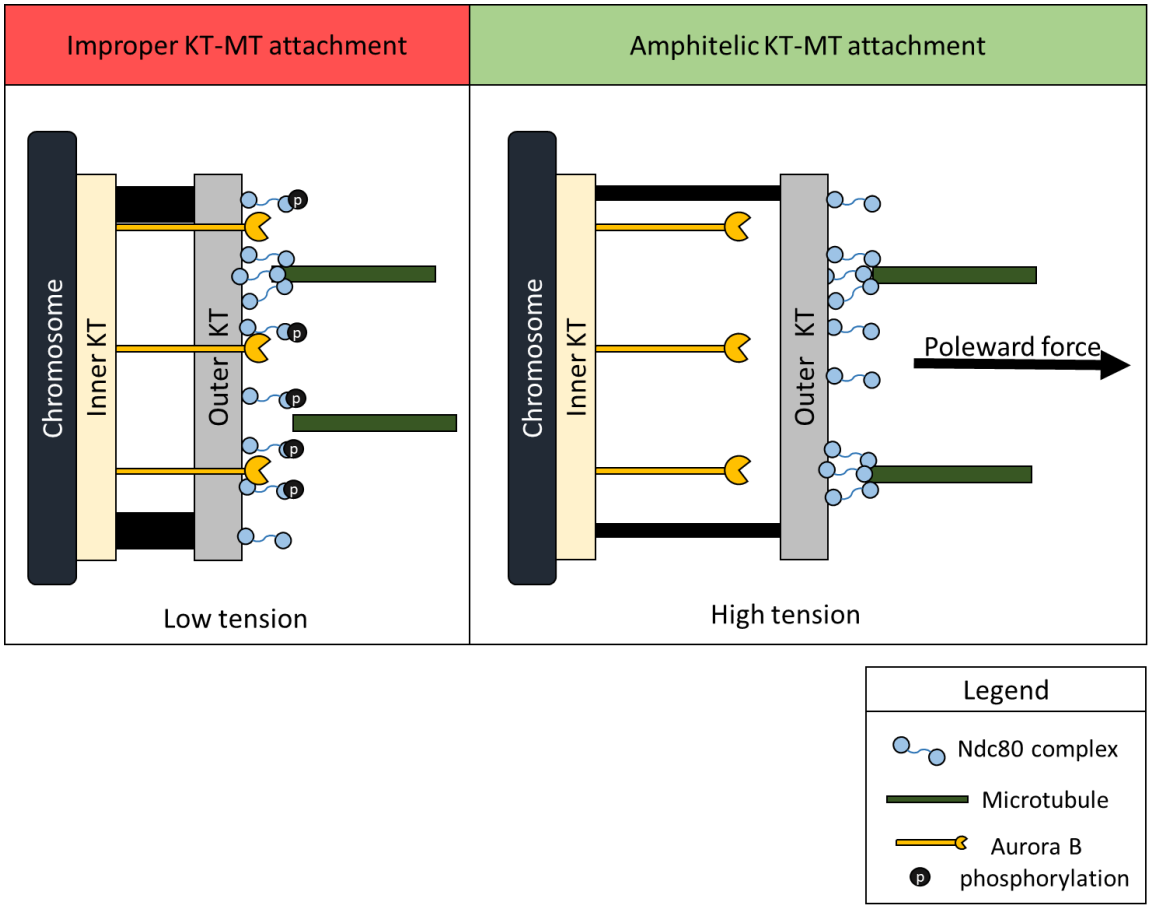

Figure 1.13 Aurora B kinase corrects improper KT-MT attachments. Improper KT-MT attachments result in lack of tension between the sister KT. This allows Aurora B to be in proximity to Ndc80 to phosphorylate it and reset the KT to an unattached state. Upon proper amphitelic attachments, tension across the KT results in spatial separation of Aurora B kinase from its substrates.

Mps1 kinase is involved in the proper biorientation of sister chromatids on the mitotic spindle. Mps1 is recruited to the kinetochore in response to Aurora B mediated phosphorylation of Ndc80. Mps1 mediated phosphorylation, recruits mitotic checkpoint proteins such as Bub1, Bub3, Mad1 to the KT resulting in the activation of the mitotic checkpoint (figure 1.14).[12]

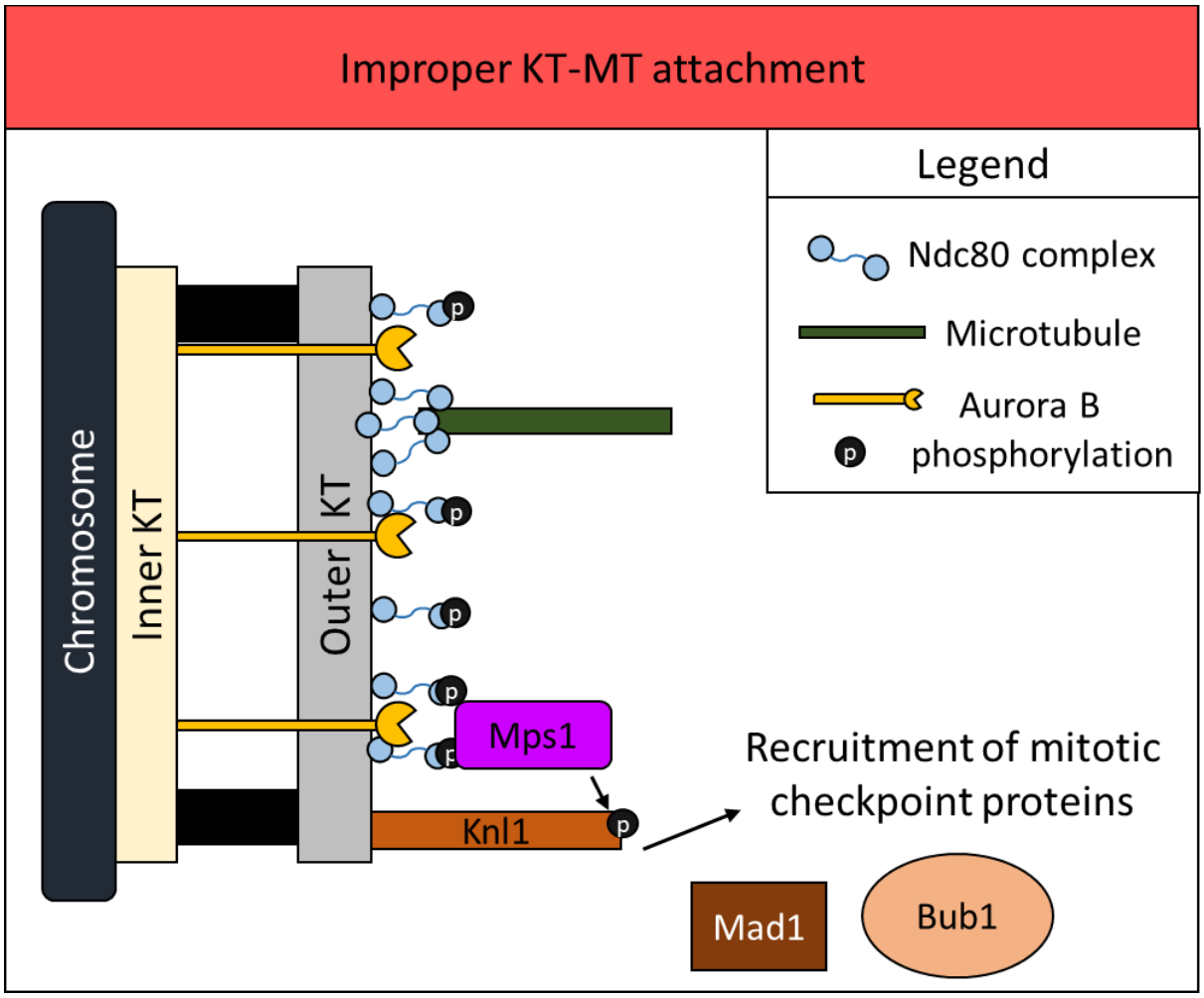

Figure 1.14 Mps1 mechanism of action. Phosphorylated Ndc80 recruits Mps1 to the KT. Mps1 then phosphorylates Knl1, resulting in the recruitment of mitotic checkpoint proteins.

1.4 Spindly

1.4.1 Discovery of Spindly

Spindly was identified through an RNAi screen in *Drosophila* S2 cells looking for novel components of the mitotic checkpoint.[34] In *C. elegans*, Spindly (SPDL-1) was identified though an RNAi based genome-wide screen for interactors with known SAC components.[35] Through a BLAST

search using a 32 amino acids region conserved between *D. melanogaster*, *A. gambiae* and *A. aegypti*, human Spindly (hSpindly, CCDC99) was discovered.

1.4.2 Spindly Localization

In interphase hSpindly is mainly nuclear. Following entry to mitosis, hSpindly KT localization is first detectable after nuclear envelope breakdown. hSpindly KT levels are the highest during prometaphase, after which they decrease and the majority of hSpindly is degraded upon mitotic exit, with a small pool of hSpindly remaining (Figure 1.15).[36,37,38] When KT are unattached, hSpindly expands into a crescent like morphology,[38] consistent with its localization to the fibrous corona. The levels of hSpindly are highest at unattached KT and decrease upon proper MT attachment. In addition to its role during mitosis, hSpindly also localizes to the leading edge of migrating cells and is required for mediating dynein/dynactin function in cell migration and timely migration of cells.[39]

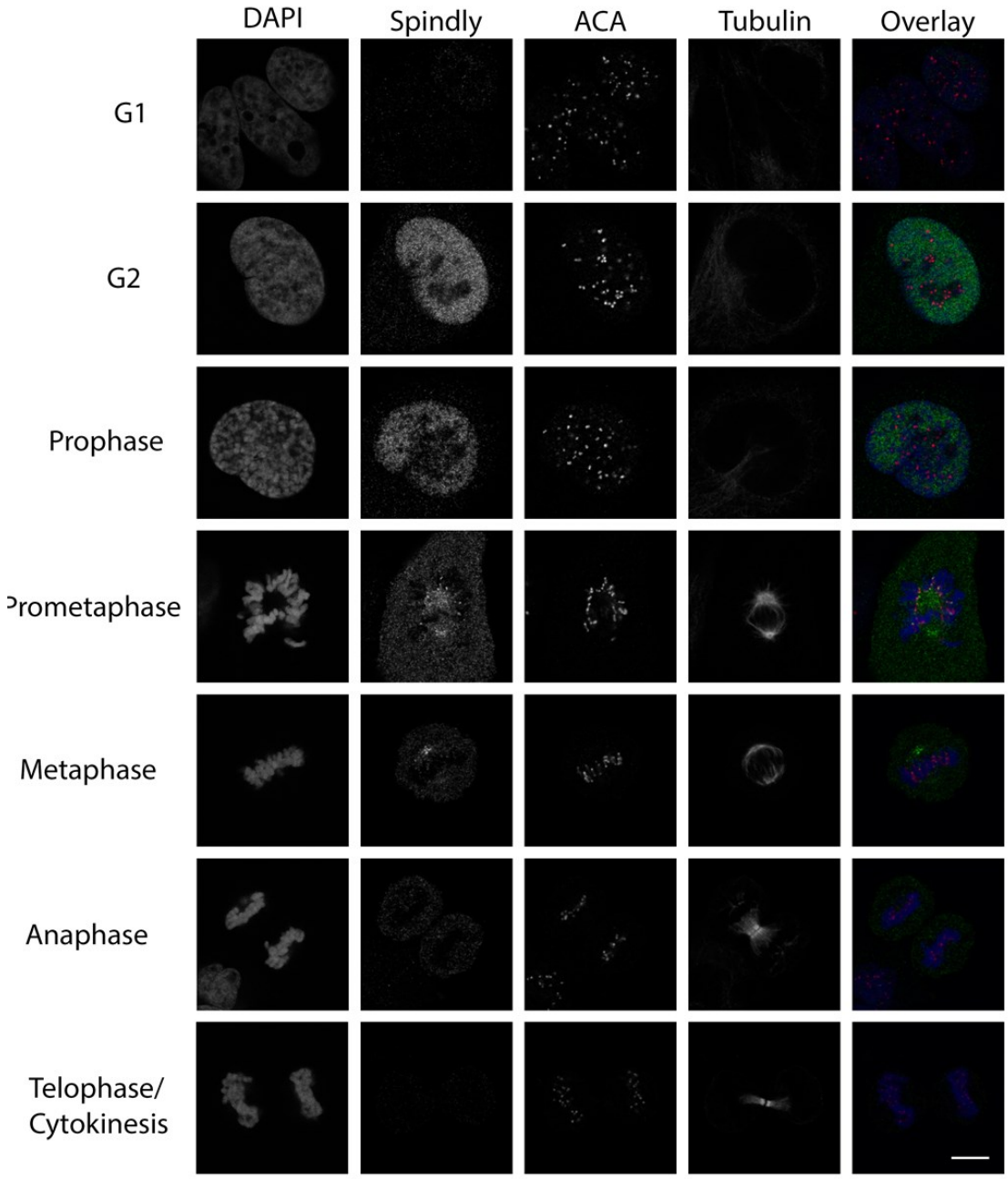

Figure 1.15 Spindly cell cycle localization. Spindly cell cycle localization in HeLa cells is shown. HeLa cells were imaged at each phase of mitosis, and Spindly, the kinetochore (ACA), mitotic spindle (Tubulin) and DNA (DAPI) were imaged. Overlay of Spindly (green), ACA (red) and DAPI (blue) is shown. Single slice, scale bar = 10µm.

1.4.3. Spindly domains

1.4.3.1 Evolutionary conservation of Spindly.

hSpindly is a 605 amino acid protein comprised predominately of coiled coil structure, that shows only 14% identity between human and *Drosophila.*[34] Aside from the Spindly Box (the 32 conserved amino acids) there is almost complete divergence from the rest of the protein sequence. There are 2 highly conserved residues S256 and F258 (human), F199 and S234 (*C. elegans* and Drosophila*)*. These residues are essential for the interaction of Spindly with dynein (and dynactin in the case of *C. elegans* and human cells).[40] This shows that even though Spindly's function is conserved as a dynein adaptor across these different species, sequence conservation is limited.

1.4.3.2 Spindly Box

hSpindly has 2 putative coiled coil domains, which are separated by a conserved Spindly box (SB).[37] The Spindly Box is a short evolutionarily conserved motif (Figure 1.16) that is used to define this protein family. When 2 conserved residues in the SB are mutated, this mutant localizes to the kinetochore, but fails to recruit dynein/dynactin. This then results in retention of Spindly, Mad1, Mad2, and CENP-E at the KT of aligned chromosomes.[38] This persistent KT localization demonstrates the requirement of hSpindly SB in the recruitment of dynein/dynactin for proper mitotic checkpoint silencing.

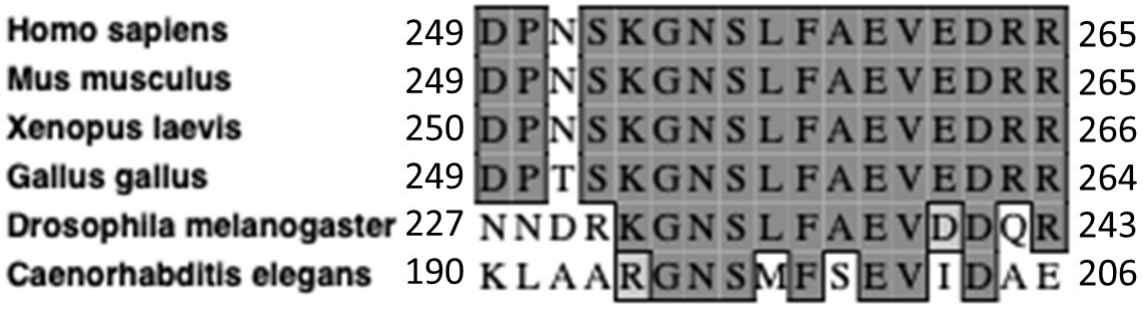

Figure 1.16 The Spindly Box is evolutionarily conserved. Spindly Box sequence alignment of human (Homo sapiens), mouse (Mus musculus), Xenopus (Xenopus laevis), Chicken (Gallus gallus), Drosophila (Drosophila melanogaster), and C. elegans (Caenorhabditis elegans) is shown. Conserved amino acids are highlighted with the grey box.

1.4.2.3. CC1 and CC2 motif

hSpindly has both CC1 and CC2 box domains, a characteristic of BICD family member proteins (Figure 1.17), through which Spindly interacts with dynein/dynactin. BICD family members serve as adaptor proteins for dynein, the C-terminal portion binds the cargo to be transported and the N-terminal portion is then available to bind dynein and induce minus end directed transport.[41] Mutations in either CC1 or CC2 results in impaired recruitment of Dynein/Dynactin.[42] It is through the CC1, CC2 and Spindly box that hSpindly can interact with dynein and dynactin.

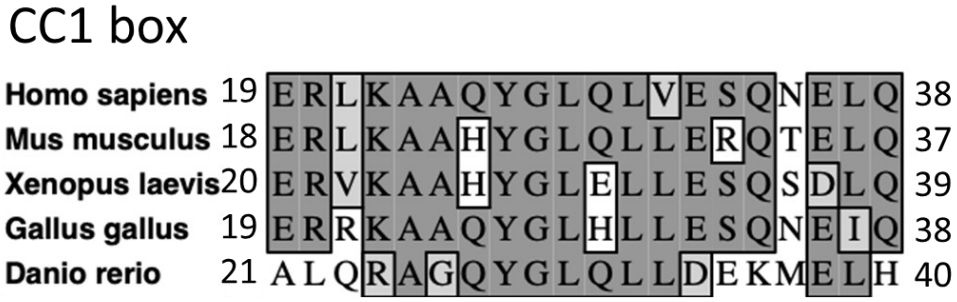

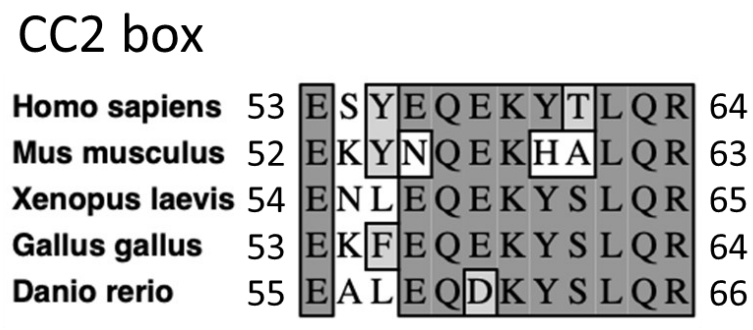

Figure 1.17 CC1 and CC2 boxes are evolutionarily conserved. CC1 and CC2 box sequence alignment of human (Homo sapiens), mouse (Mus musculus), Xenopus (Xenopus laevis), Chicken (Gallus gallus), and Zebrafish (Danio rerio) is shown. Conserved amino acids are highlighted with the grey box.

1.4.2.4 CAAX farnesylation motif

Through screening of deletion and random insertion mutants the extreme C-terminus was found to be essential for hSpindly KT localization.[37,43] The C-terminal amino acids make up the CAAX farnesylation motif (Figure 1.18), that when altered prevents hSpindly kinetochore localization[44] due to lack of farnesylation.

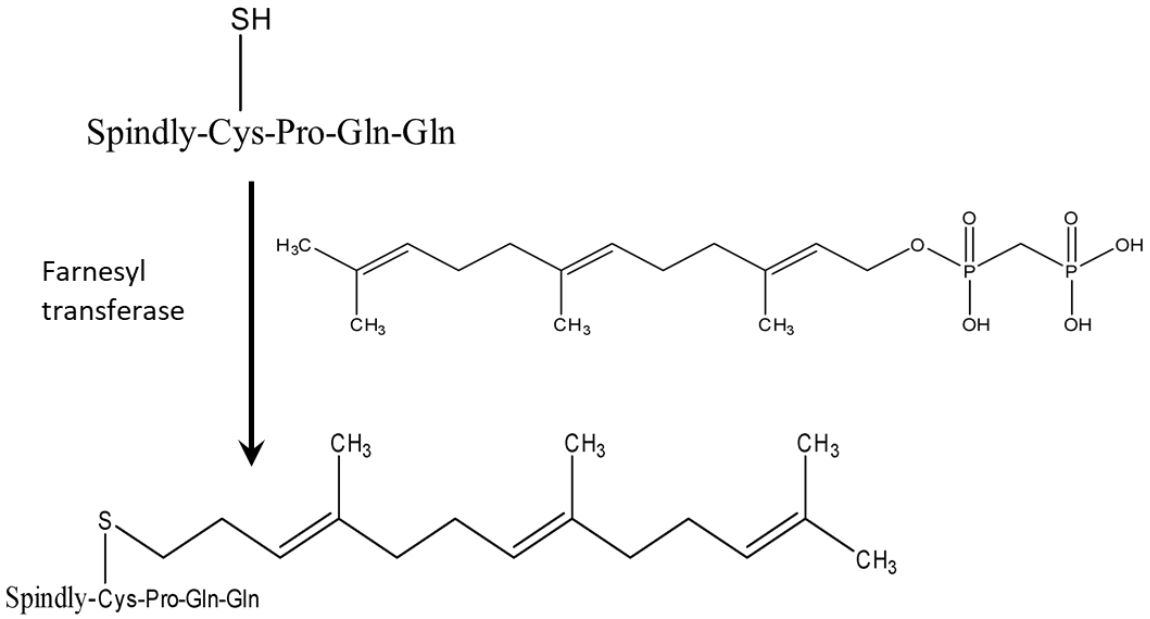

Figure 1.18 Spindly is farnesylated. The C-terminus CAAX of Spindly is farnesylated by farnesyltransferase.

1.4.4 Spindly Kinetochore localization

Spindly is recruited to the kinetochore through interaction with the RZZ complex (Figure 1.19 top panel), and loss of the RZZ complex subunits results in the abolishment of Spindly kinetochore localization.[37,36] Spindly interaction with the RZZ complex requires farnesylation. When farnesylation is inhibited by FTI treatment, Spindly no longer interacts with the RZZ complex (figure 1.19, bottom panel).[43,44] This loss of interaction is because farnesylated Spindly interacts with Leu120 of Rod's β-propeller,[45] and loss of farnesylation results in loss of this interaction.[46]

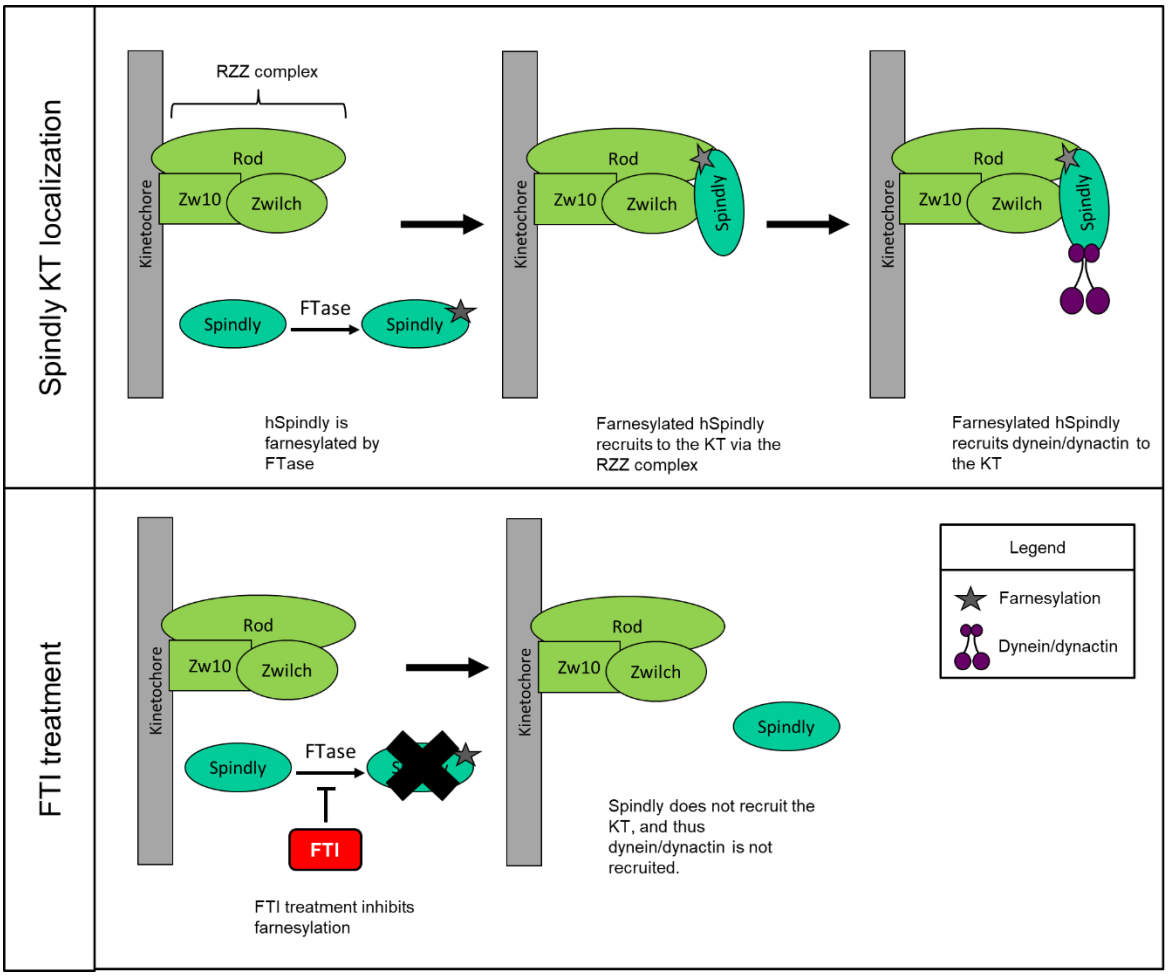

Figure 1.19 Spindly KT localization. Spindly is recruited to the KT through farnesyl dependent interaction with RZZ complex. Top panel) Spindly is farnesylated by FTase, is recruited to the KT through interactions with Leu120 of Rod. Dynein/dynactin is then recruited to the KT. Bottom panel) inhibition of Spindly farnesylation inhibits Spindly KT localization and dynein/dynactin KT localization.

Spindly kinetochore localization is dependent on its farnesylation; however, the specific farnesylation motif does not matter as long as it meets the criteria to be a farnesylation motif. When hSpindly farnesylation motif was substituted for CENP-E or CENP-F farnesylation motifs, hSpindly still localizes to the kinetochore during prometaphase.[44] However if the farnesylation motif is substituted for one that will be geranylgeranylated, hSpindly is not recruited to the

kinetochore during prometaphase.[44] This further highlights farnesylation and not alternative prenylation is required for hSpindly kinetochore recruitment during prometaphase.

1.4.5 Functions of Spindly

hSpindly is required for proper chromosome alignment and mitotic spindle formation[34] hSpindly functions as the kinetochore adaptor for dynein/dynactin[41] and depletion of hSpindly results in loss of dynein/dynactin from the kinetochore,[36] which is the mechanism that results in the observed prometaphase arrest.

1.4.5.1 Spindly and dynein/dynactin

hSpindly forms a complex with dynein and dynactin *in vitro*, interacting with both dynein light intermediate chain and dynactin's pointed end complex. [46] Spindly interacts with dynein via its N-terminus[46] showing that while the C-terminus of hSpindly is required for its interaction with the RZZ complex and recruitment to kinetochores, the N-terminus is what is necessary for dynein recruitment consistent with other dynein/dynactin cargo adaptors. While hSpindly depletion prevents recruitment of dynein/dynactin to KT, resulting in KT that resemble those found in cells lacking dynein;[34] it does not affect dynein/dynactin localization to the spindle, spindle poles, cell cortex or microtubule plus ends in interphase cells.[38] Thus, hSpindly depletion specifically affects the recruitment of dynein/dynactin to kinetochores, without affecting the other roles of dynein/dynactin outside of mitosis.

1.4.5.2 Spindly and chromosome congression

hSpindly is required for chromosome congression by acting as the adaptor protein in the recruitment of dynein/dynactin to kinetochores. When hSpindly is mutated or depleted,

chromosome congression is impaired, with the majority of peripheral chromosomes failing to reach the metaphase plate while chromosomes more centrally located are able to align properly.[37] hSpindly SB mutants lacking the ability to recruit dynein/dynactin, but still capable of KT localization, partially rescued the chromosome alignment defect seen when hSpindly was depleted.[38] These hSpindly mutants resulted in aligned sister KT under tension comparable to KT with wild-type hSpindly bound.[38] This indicates a yet undefined dynein/dynactin independent role for hSpindly in chromosome congression.

1.4.5.3 Spindly and the mitotic spindle

hSpindly is required for maintenance of spindle morphology. Depletion of hSpindly results in multi-polar spindles and spindles that were either very long, bent or twisted with their spindle poles often displaced off the spindle axis.[37] This is believed to be due to the lack of hSpindly mediated dynein/dynactin poleward movement that counters the ejection forces of chromokinesin hKid.[37]

1.4.5.4 Spindly regulation of the Mitotic Checkpoint

The mitotic checkpoint is silenced when the MCC is disassembled and mitotic checkpoint proteins have been shed from the KT. This shedding is dependent on dynein/dynactin, and therefore on hSpindly KT localization.[34] Aurora B kinase regulates the mitotic checkpoint through the recruitment of some checkpoint proteins[47] and inhibition of premature removal of checkpoint proteins.[48] When Aurora B kinase is inhibited, hSpindly KT localization is lost, due to premature shedding of the mitotic checkpoint proteins.[36]

When Spindly is mutated and not able to bind dynein/dynactin, mitotic checkpoint components are still localized to bi-oriented chromosomes, resulting in prolonged checkpoint activity.[38] The mitotic arrest that occurs upon hSpindly depletion occurs in a Mad2 dependent mechanism; as when both Mad2 and hSpindly are depleted the cells exit mitosis.[37] This highlights the importance of Spindly in silencing of the mitotic checkpoint through the recruitment of dynein/dynactin and the following poleward movement of the mitotic checkpoint components.

1.4.5.5 Spindly and cell migration

hSpindly localization to focal adhesions is required for cell migration, through the recruitment of dynein/dynactin. hSpindly colocalizes with the p50 dynamitin subunit of dynactin on what is thought to be an actin-based structure. Depletion of hSpindly results in decreased migration comparable to that of dynactin depletion.[39] This shows that hSpindly acts as a dynein/dynactin cargo adaptor in both interphase and mitosis.; and in interphase is required for cell migration.

The involvement of Spindly in migration has also been investigated in *Drosophila* ovarian border cells. When Spindly is depleted, the border cell cluster will migrate faster along the anterior posterior axis towards the oocyte, and when Spindly is overexpressed it causes incomplete border cell migration.[40] Spindly in both human and *Drosophila* is involved in proper cell migration, but in different ways. In the case of *Drosophila* ovarian border cells, depletion of Spindly results in faster migration, while hSpindly depletion results in decreased migration. This shows the need to continue to study the roles of Spindly in the different organisms to see what roles it plays, as this role does not appear to be consistent across different species.

Recently, hSpindly has also been shown to interact with the de-ubiquitylating enzyme (DUB) USP45. hSpindly is mono-ubiquitylated and USP45 removes this ubiquitylation. Depletion of USP45 resulted in impaired wound healing similar to that seen with hSpindly depletion. However, USP45 depletion had no effect on mitotic progression, so it does not affect hSpindly's role in mitosis.[49] While the role of hSpindly is more clearly understood in mitosis, there are other roles for hSpindly in interphase that are currently not fully understood.

1.4.6 Spindly and Anti-mitotic agents

hSpindly depletion results in a prometaphase arrest due to the lack of dynein/dynactin recruitment to KT. hSpindly expression in lung cancer cell lines was compared to non-tumorigenic control and showed increased mRNA and proteins levels.[50] When hSpindly depletion was combined with a low dose of paclitaxel (an anti-mitotic agent that targets tubulin), it resulted in prolonged mitotic arrest, decreased cell viability and decreased colony forming capacity.[50] This combination treatment altered the way in which the cells were dying. hSpindly depletion results in cells dying in mitosis, but when hSpindly depletion was combined with paclitaxel the majority of the cells died in the interphase following mitosis or were arrested in interphase. This combination also resulted in more cells dying from apoptosis compared to hSpindly depletion alone.[50] Both hSpindly depletion and paclitaxel treatment resulted in a similar number of multipolar spindles, when the two were combined almost all spindles observed were multipolar and lead to increased multinucleated cells.[50] Treatment with farnesyltransferase inhibitors (FTI) phenocopies hSpindly depletion, as it results in loss of hSpindly KT localization. Loss of hSpindly KT localization, either through FTI treatment or depletion; combined with other anti-mitotic agents shows a possible therapeutic treatment option.

1.5 Farnesylation and Farnesyltransferase inhibitors

1.5.1 Protein Prenylation

Protein prenylation is a post-translational modification that results in the addition of an isoprenoid lipid group onto a protein, promoting membrane interaction and biological activities (Figure 1.20).[51] Farnesylation was first observed in the mating factor of *R. toruloides*, that was found to contain a farnesylated cysteine in its C-terminus.[52] Previous studies had shown that there were cellular requirements for mevalonic acid that was unrelated to cholesterol. Radiolabelled protein was detected in cells subjected to metabolic labeling with radioactive mevalonic acid demonstrating that mevalonate was converted to an isoprenoid compound and covalently incorporated into proteins.[53] Mevalonic acid is the precursor to both geranyl pyrophosphate (GPP) and farnesyl pyrophosphate (FPP) as well as other isoprenoid intermediate in the cholesterol biosynthesis pathway (Figure 1.21).[54] It was found that both Ras and the α-mating pheromone in *S. cerevisiae* were farnesylated at their C-terminus. When the amino acid sequences were examined the only region that showed similarity was the C-terminus where both contained a CAAX motif. This conserved farnesylation motif has a cysteine residue followed by 2 aliphatic amino acids and a C-terminal residue.[55]

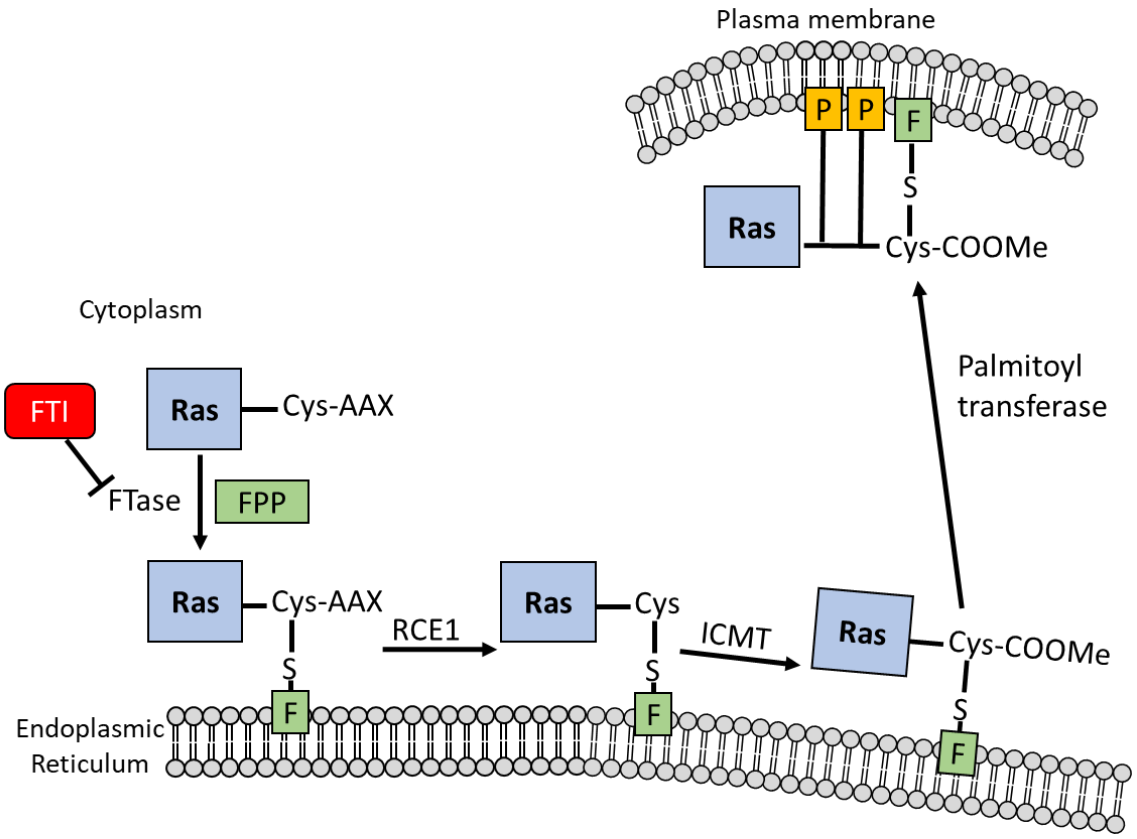

Figure 1.20 Ras farnesylation. Proteins with a CAAX motif are farnesylated by FTase in the cytoplasm. Farnesylated Ras then moves to the endoplasmic reticulum where the C-terminal AAX residues are cleaved and then methylated. Finally, at the cell membrane, the protein is then also palmitoylated. FPP, Farnesyl pyrophosphate; FTase, Farnesyl transferase; F, Farnesyl isoprenoid lipid; FTI, farnesyltransferase inhibitor; RCE1, Ras converting enzyme; ICMT, isoprenylcysteine methyltransferase; P, fatty acid covalently bound to Cys residue i.e. palmitic acid.

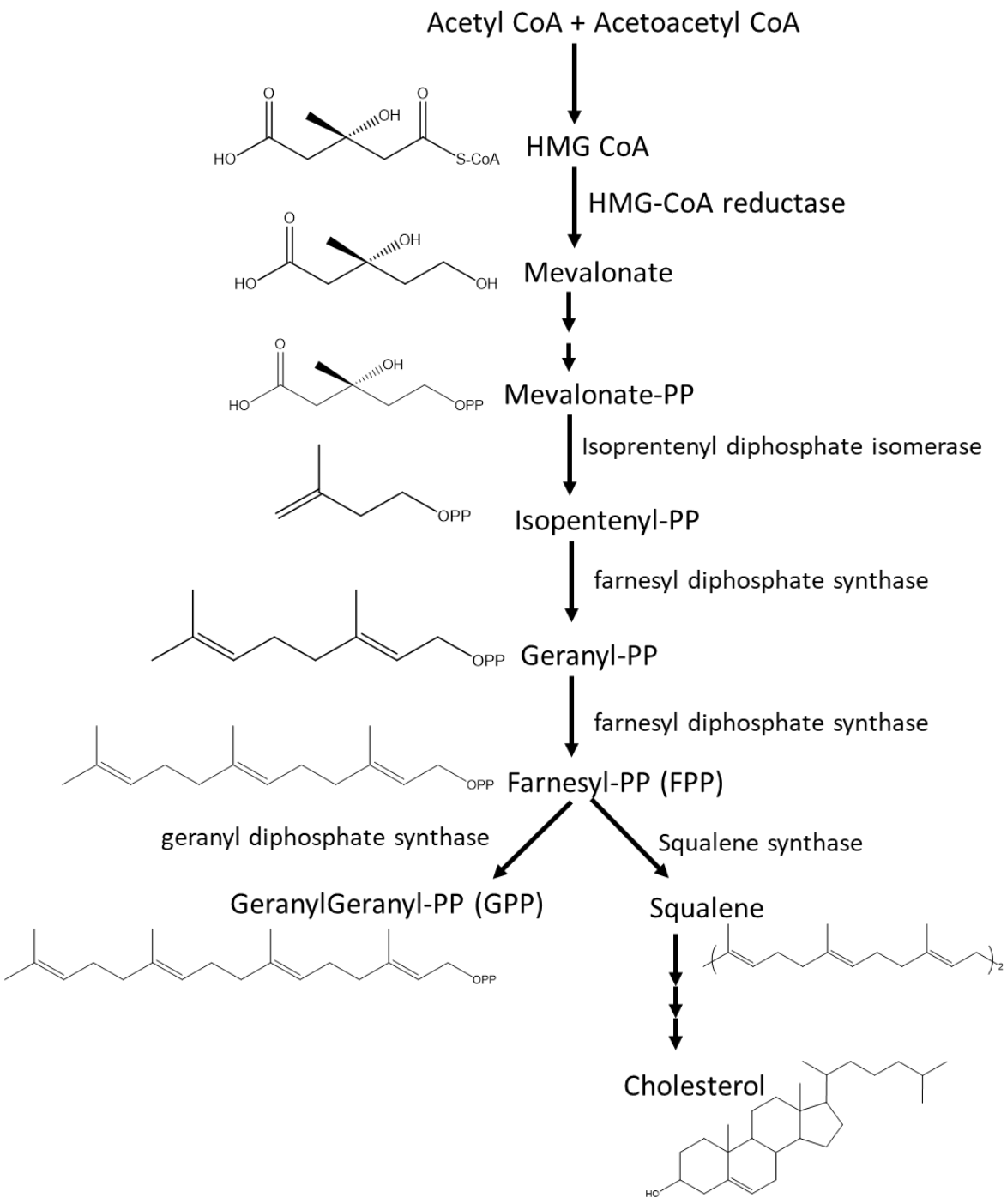

Figure 1.21: Mevalonate pathway in animal cells. Mevalonate metabolism pathway resulting in the production of farnesyl pyrophosphate (FPP) and geranylgeranyl pyrophosphate (GGPP) in the cholesterol biosynthesis pathway.

1.5.2 Farnesylation and Geranylgeranylation

1.5.2.1 Farnesyltransferase

The farnesyltransferase (FTase) enzyme was first purified from rat brain cytosol as an enzyme that transfers the farnesyl moiety (15 carbon) from FPP to the Cys of $p21^{Ras}$. This enzyme is competitively inhibited by peptides containing the CAAX motif, even ones as short as 4 residues.[56] Since then FTase has been found in many other mammalian cells and tissues.[57] The purified FTase was found to be a heterodimer containing an α and β subunit. The α subunit is 377 amino acids and ~49kDa,[58] while the β subunit is 438 amino acids and is ~46 kDa. Additionally, the β subunit contains the recognition site for the peptide substrate[59] and FPP.[60] Neither the FTase α or β subunit have FTase activity without the other being present.[58,59]

FTase is a metalloenzyme, requiring Zinc to bind the protein substrate while FPP binding to FTase is independent of the presence of either zinc or magnesium.[61] The zinc molecule coordinates the thiol group(s) in the peptide substrate in a ternary complex of the enzyme-isoprenoid-peptide substrate.[60] The transfer of the farnesyl moiety from FPP to the substrate protein requires the presence of magnesium.[61]

The FTase holoenzyme forms a stable complex with FPP, where it is not covalently bound but when the complex is incubated with an acceptor protein, the farnesyl group is transferred.[62] Mammalian FTase can bind either FPP or the protein substrate independently, but in order for the substrate to be farnesylated FTase must bind FPP first.[60] The release of the farnesylated product is the rate-limiting step in this reaction. FTase enzyme must encounter more FPP to release the farnesylated product (Figure 1.22).[60]

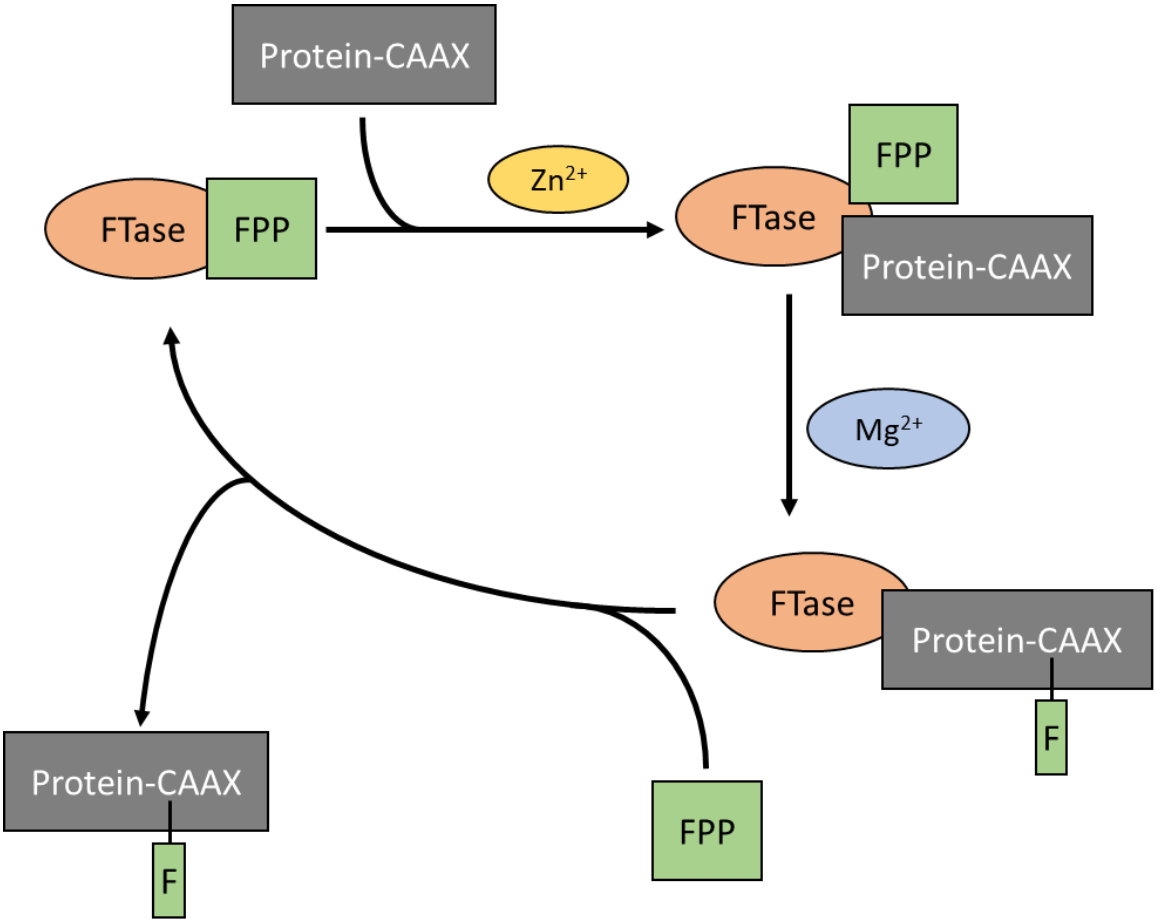

Figure 1.22: Farnesylated protein release from FTase. FTase binds FPP, and the protein substrate, this interaction requires the presence of a zinc (Zn). FTase then transfers the Farnesyl isoprenoid to the protein substrate, in the presence of magnesium (Mg). In order to release the farnesylated substrate protein FTase needs to bind new FPP.

FTase is essential for embryonic development, when FTase is ablated in mice, embryos did not proceed past embryonic stage 11.5, as well as having loss of embryonic layers, decreased cell proliferation and increased apoptosis.[63] Murine embryonic fibroblasts (MEFs) that were deficient in FTase did not grow to high density as well as maintained a discernable intracellular space. In addition, these MEFs had a flat morphology, reduced motility and slower proliferation rate than control MEFs.[63] Due to the early embryonic lethality of FTase knockout, mice were

induced for FTase knockout at 10 days old, and showed no FTase allele or FTase activity. These mice developed into adults and did not show any anatomical pathology or behavioral defects. Mice at 6 months old were tested for stress responses, including wound healing, and while they showed delayed wound healing by ~30%, the wounds did heal[63]. When FTase was depleted in 2 Ras oncogene driven tumor models (K-Ras and H-Ras) there was no effect on the number or size of tumors induced.[63] While it is known that FTase is dispensable for tumor development and embryonic lethal, it is not yet known what substrates are essential for the initiation, proliferation or survival of different cancers. Further understanding of the role of FTase and farnesylated protein in cancer development and progression will aid in understanding what patients would benefit from prenylation inhibitor treatment.

1.5.2.2 Geranylgeranyltransferase

In addition to farnesylation there is geranylgeranylation, which is the addition of a 20-carbon isoprenoid lipid onto proteins. It was first observed in HeLa cells and was determined to be a major isoprenoid modification.[64] FTase α subunit is the common regulatory subunit between FTase and Geranylgeranyl transferase (GGTase), while both have a unique catalytic β subunit (Figure 1.23).[63] Normal Ras function requires farnesylation not geranylgeranylation, however oncogenic Ras activity can be maintained by geranylgeranylation when farnesylation is inhibited.[65]

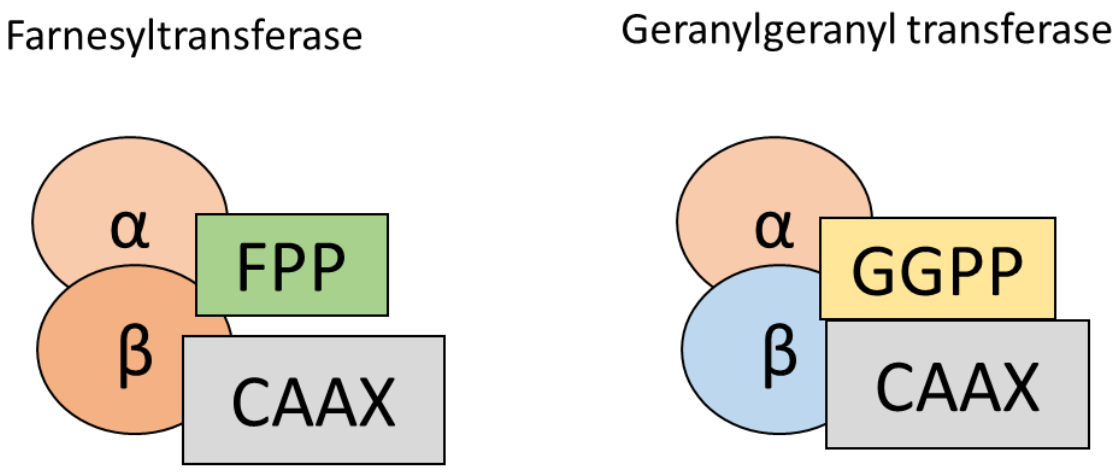

Figure 1.23 Farnesyltransferase and Geranylgeranyl transferase. Both Farnesyltransferase (FTase) and Geranylgeranyltransferase-1 (GGTase-1) share a common α-subunit and different β-subunits.

1.5.2.3 CAAX motif requirements

FTase and GGTase are 2 different and distinct enzymes.[66] When the cytosolic fraction of bovine brain was incubated with both FTase and GGTase substrates with radiolabelled FPP and GGPP, both substrates were labelled with radioactive isoprenoid moieties. Using peptide affinity column chromatography, Moores et al. purified 3 different enzymes: FTase, GGTase-1 and GGTase-2.[67] Both FTase and GGTase-1 rely on the CAAX motif to determine substrate specificity, while GGTase-2 catalyses the addition of 2 geranylgeranyl groups onto 2 cysteine residues in sequences that contain CXC or CCXX in the C-terminus of Rab proteins.[51] When X is Alanine, Serine, Methionine or Glutamine the protein is farnesylated.[68] When X= Leucine, Isoleucine or Phenylalanine the protein is geranylgeranylated.[66] However there is some overlap, such as in the case of Ras, where if farnesylation is inhibited it can instead be geranylgeranylated to maintain its activity.[69] What amino acids can be in A_1 is more relaxed than either A_2 or X. Basic and

aromatic side chains were tolerated in A_1 not A_2 position, and they appear to influence the efficiency of the isoprenylation but did not change the specificity of the reaction.[67] Proteins that are good substrates for FTase are poor substrates for GGTase-1 and vice versa.[67]

1.5.3 Farnesyltransferase inhibitors:

Farnesyltransferase inhibitors (FTI) were initially developed to inhibit Ras farnesylation, as oncogenic Ras requires farnesylation dependent membrane localization in order to cause malignant transformation. While Ras is both farnesylated and palmitoylated, Val^{12}K-Ras 4B is not palmitoylated but is farnesylated, membrane associated and fully transforming. When farnesylation was inhibited, Val^{12}K-Ras 4B failed to become membrane associated and did not transform 3T3 cells.[69] Based on the promising preclinical data, clinical trials with FTIs were carried out however they did not provide any survival advantage in patients with solid tumors.[70] It is believed that this failure was due to inappropriate stratification of patients,[71] and that many of the patients enrolled had advanced or metastatic disease. Additionally while it was known preclinically that K-Ras tumors were resistant to FTIs, Phase 3 trials were carried out in patients whose tumors contained K-Ras mutations.[72] This indicates that novel biomarkers are needed for patient stratification in future clinical trials for FTIs to ensure effective clinical outcomes.

Treatment of cancer cells with FTIs results in a range of cellular effects, including induction of apoptosis,[73,74] cell cycle arrest,[75,76,44] inhibition of cell proliferation, migration,[72,77,78,79,80] and angiogenesis.[81] FTI treatment results in the inhibition of both anchorage dependent and independent proliferation. FTIs can inhibit cell growth in cells with various mutations including K-Ras, p53 deletions, and cyclin dependent kinase inhibitor 2A silenced cells.[77,78] In the case of Ras

mutations, FTIs are able to inhibit growth in tumors with K-Ras and N-Ras mutations (but not regress it); while in tumors with H-Ras mutations, FTI treatment results in tumor regression.[72,79,80] In tissue culture cells, FTI treatment results in prometaphase arrest by preventing bipolar spindle formation and chromosome alignment, due to inhibition of hSpindly KT localization.[75,76,44] FTIs can induce apoptosis through various mechanisms including enhancing death receptor signals, inhibiting pro-survival signaling such as NF-κB, Inhibitor of Apoptosis (IAP) and Bcl-2.[72,73,74,] FTIs have been shown to inhibit angiogenesis, possibly through the inhibition of HIF-1α expression and hypoxia (Figure 1.24).[81]

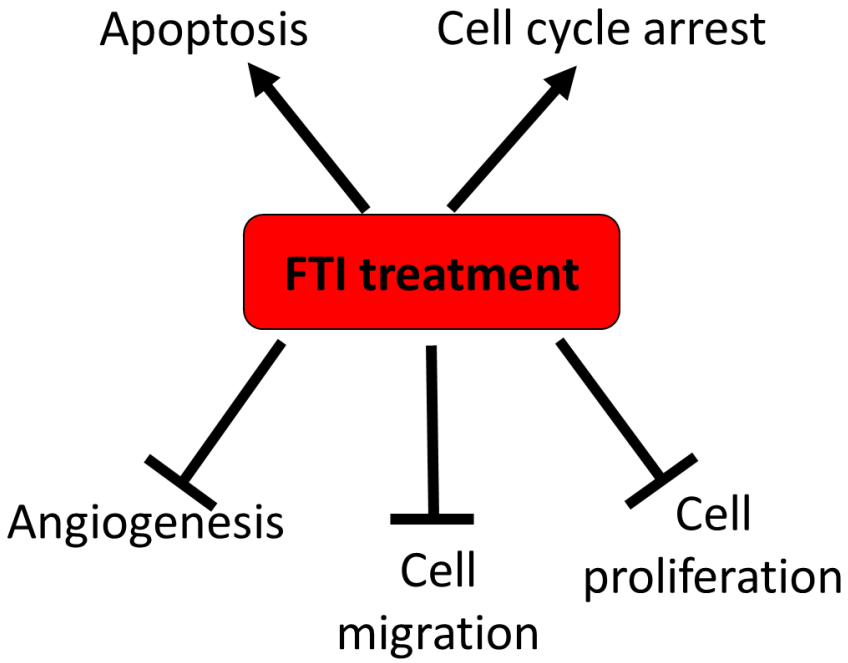

Figure 1.24 Farnesyltransferase inhibitor treatment cellular effects. Treatment with farnesyltransferase (FTI) results in inhibition of cell proliferation, cell migration, angiogenesis and promotes cell cycle arrest and apoptosis.

FTIs have been shown to be potent inhibitors of tumor cell growth in cell culture and in mouse models. While combination treatments of FTI and cytotoxic anti-neoplastic drugs (such as cisplatin, doxorubicin and fluorouracil) resulted in additive effects, when FTIs are combined with microtubule stabilization agents (i.e. Taxol and epothilones) the effect observed was synergistic, resulting in abnormal chromosome alignment and disordered spindle apparatus which is consistent with metaphase arrest.[82]

FTIs have also been used in the treatment of other diseases, such as Hutchinson-Gilford progeria syndrome (HGPS), a disease in which there is a mutation in the Lamin A gene, such that prelamin A (an FTase substrate) is not cleaved to mature Lamin A. This persistently farnesylated and non-functional Lamin A is termed progerin.[83,84] FTIs prevented the aberrant nuclear morphology in a HeLa cell HGPS model.[85] In HGPS mouse models, FTI treatment resulted in improved life span, body weight and bone integrity.[86] In Phase 2 clinical trials involving the treatment of HGPS patients with FTI, there was improved life span and bone integrity observed.[87,88,89] HGPS treatment remains a current area of study, with clinical trials continuing. In addition to HGPS, FTIs have also been used to treat various parasitic disease including: Malaria, Chagas disease, and African sleeping sickness.[90,91] Second generation FTIs have been designed to specifically inhibit parasite FTase.[92,93] These second generation FTIs result in toxicity to the parasite and parasite eradication in a malaria mouse model[94] without inhibition of mammalian FTase.[94]

1.5.4 Tipifarnib

Tipifarnib is a non-peptidomimetic FTI that competitively inhibits Ftase through interaction with the substrate protein binding site. Cells that have H-Ras or N-Ras mutations were found to be the most sensitive to Tipifarnib with IC_{50}<10nM. Tipifarnib is orally available and showed antiproliferative activity, increased apoptosis and anti-angiogenic effects in mouse tumor models.[95] Tipifarnib is one of 2 FTIs that have advanced to Phase 3 clinical trials and has been tested in variety of tumor models and clinical trial stages. As a monotherapy Tipifarnib has been tested in advanced bladder, colon cancer, NSCLC, and solid tumors with little response.[72] When tested in advanced breast cancer, there was a partial (11.8%) response, and all who responded had wild type Ras genes.[72] While Tipifarnib showed little effect as a monotreatment, when used in combination with other therapeutics it showed an improved response. Tipifarnib has been used in combination in various trials. In a Phase 1 trial in combination with gemcitabine and cisplatin it showed a 33.3% complete response and 26% partial response in patients with advanced solid tumors.[72] In Phase 2 clinical trials of both advanced and locally advanced breast cancer, Tipifarnib in combination with doxorubicin (Topoisomerase II inhibitor) and cyclophosphamide (DNA alkylating agent) improved response rate from 10% to 21.9% and 25% respectively.[72] Additionally, when FTase activity was examined in these trials, it was shown that FTase activity decreased by 55-100% for the advanced breast cancer trial and median FTase activity decreased by 91% in the locally advanced breast cancer trial. While in a clinical trial looking at Tipifarnib and tamoxifen in advanced breast cancer, the response rate was only 16.7%, and FTase activity had only decreased by 42-54%. This information indicates the need to determine what patients could benefit from Tipifarnib treatment, and what other therapies it would work best with in combination.[72] In a recent Phase 2 clinical trial, Tipifarnib and Fulvestrant

(a selective estrogen receptor degrader) was tested in post-menopausal metastatic breast cancer where some of the patients had aromatase inhibitor resistant disease and some did not. The combination treatment showed an improved clinical benefit rate of 47.6% compared to 32% for Fulvestrant alone for aromatase inhibitor resistant disease.[96] The combination treatment did not increase the response rate in hormone receptor positive metastatic breast cancer. This further highlights the need to ensure testing is occurring in the proper models. The increased response rate for the combination in the aromatase inhibitor resistant patients shows a need for further testing.

1.6 Wee1 and Adavosertib

1.6.1 Wee1 family of kinases

The Wee1 family of kinases is made up of Wee1 and Myt1 and was originally discovered in budding yeast, where Wee1 mutants resulted in smaller or "wee" progeny.[98] Wee1 and Myt1 are responsible for Cyclin B-Cdk1 inhibition, preventing premature entry into mitosis.[99]

1.6.2 Wee1 role in the cell cycle

Wee1 activity is regulated during the cell cycle. In interphase, Wee1 is phosphorylated and bound to 14-3-3, sequestering it in the cytoplasm (Figure 1.25).[99] Following DNA damage, Wee1 is activated resulting in inhibition of Cdk1 until the G2/M checkpoint is silenced when all DNA damage has been repaired. Cdc25C phosphatase removes the inhibitory phosphates on Cdk1, resulting in active Cdk1-Cyclin B and entry into mitosis (Figure 1.25).[7]

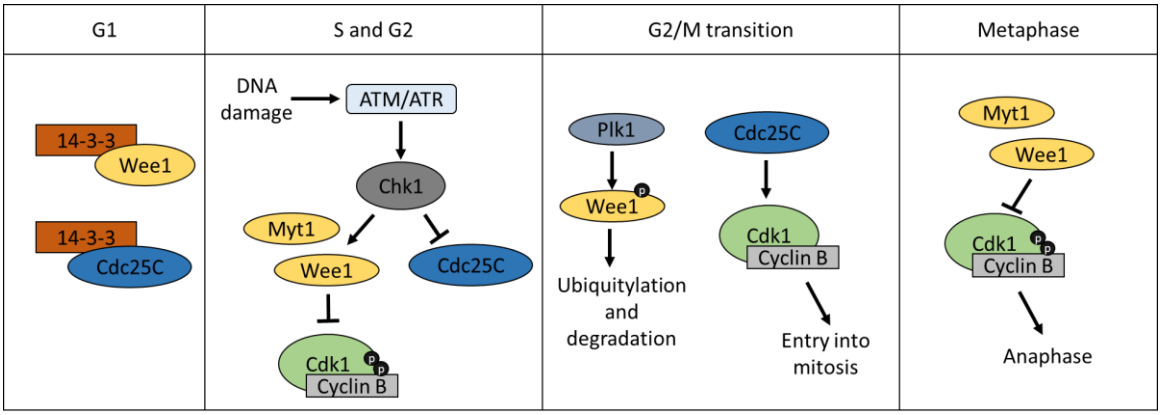

Figure 1.25 Wee1 activity in the cell cycle. In G1, Wee1 is sequestered by 14-3-3. During S and G2 upon checkpoint activation, Wee1 is activated and prevents entry into mitosis. Upon DNA damage repair at the G2/M transition Wee1 is ubiquitylated and subsequently degraded, and active Cdk1-Cyclin B drives entry into mitosis. During metaphase Wee1 phosphorylates and inhibits Cdk1-Cyclin B allowing progression into anaphase.

1.6.2.1 G2/M Checkpoint

The G2/M checkpoint prevents cells from entering mitosis if there is unrepaired DNA damage from earlier phases in the cell cycle.[6] Ataxia-Telangiectasia Mutated (ATM) and Ataxia Telangiectasia and Rad3-related (ATR) are the 2 kinases that are responsible for the response to DNA damage, with ATM responding to double stand breaks and ATR to replication stress. These 2 kinases phosphorylate a number of other proteins and kinases resulting in a signaling cascade which will pause the cell cycle until the DNA damage is either repaired or the cell will undergo cell death or senescence.[100] When the G2/M checkpoint is activated in response to DNA damage by ATM/ATR, Chk1 is phosphorylated, resulting in inhibition of Cdc25C and activation of Wee1, resulting in Cdk1-Cyclin B inhibition (Figure 1.25, middle panel).[101] Once the DNA damage has been repaired and the checkpoint silenced, Wee1 is phosphorylated by Polo like kinase (Plk1) and subsequently degraded via the proteasome. [102] Additionally, Cdc25C inhibition is weakened,

leading to activation of Cdc25C and subsequent activation of Cdk1-CyclinB through de-phosphorylation (Figure 1.25).[103]

1.6.2.2 Mitotic exit

During mitosis, for the progression from metaphase to anaphase, Wee1 activity is required to phosphorylate Cdk1, resulting in inhibition of Cdk1-Cyclin B activity. This allows the cell to proceed to anaphase and exit mitosis.[104] Lack of this Wee1 activity results in a prolonged mitotic arrest (Figure 1.25).[105]

1.6.3 Wee1 in cancer

Cancer cells frequently have altered G1 checkpoints, so the inhibition of Wee1 and the G2/M checkpoint allows for continued cell proliferation with unrepaired DNA damage.[106] Wee1 is highly expressed in several cancer types, including breast cancer. High expression of Wee1 has been reported in response to elevated replication stress and is associated with tumor progression and poor rates of disease free survival.[102] Other studies have reported the absence of Wee1 in colon cancer and this is correlated with poor prognosis.[102] These studies suggest that the mechanism through which these cancers survive varies. When cells have high Wee1 expression they most likely rely on the G2/M checkpoint for survival and mitosis, while those with absence of Wee1, most likely rely on not having the G2/M checkpoint present in order to survive.[102] Myt1 has been shown to be required in certain cancers. In glioblastoma, Myt1 was shown to be essential, and the redundancy between Myt1 and Wee1 had been lost.[107]

1.6.4 Adavosertib is a selective small molecule inhibitor of Wee1 activity.

Loss of Wee1 activity during interphase promotes premature mitotic entry, [108] resulting in abnormal mitotic cells that display mitotic slippage, apoptosis and micronuclei formation.[109] Whereas loss of Wee1 during metaphase prevents the initiation of anaphase resulting in mitotic arrest. Both premature entry into mitosis and mitotic arrest are a result of high ectopic Cdk1-CyclinB activity.[105]

Adavosertib (MK-1775 or AZD-1775) is a small-molecule inhibitor that inhibits Wee1 activity resulting in premature mitotic entry, and delayed mitotic exit, with a mitotic arrest at the metaphase to anaphase transition. These mitotic cells have centromere fragmentation, where the centromeres and kinetochores cluster away from the chromosomes.[105] When cells are deficient in p53, they are dependent on the G2/M checkpoint, as the lack of p53 results in inactivation of the G1 checkpoint. Adavosertib was first tested in p53 deficient cells and was shown to selectively lead to cell death when combined with DNA damaging agents such as gemcitabine and cisplatin in p53 deficient cells.[110] Adavosertib has been shown to result in enhanced killing when combined with other anti-mitotic compounds or DNA damaging agents.[105,109,111,110] In addition Adavosertib has been shown to regress tumor xenograft growth,[112] and has been tested in combination trials with other agents. One such combination is Adavosertib combined with the ATR inhibitor AZD6738, which resulted in tumor remission and inhibited metastasis with minimal side effects. This combination was synergistic, and resulted in cells with unrepaired or under replicated DNA entering mitosis resulting in mitotic catastrophe.[113]

1.7 Synergy

1.7.1 Synthetic Lethality

Synthetic lethality is when 2 genes, that when either alone is inhibited the cells will survive, however when both are simultaneously inhibited it leads to cell death. To exploit this, the identification and characterization of the mechanisms that cancer cells are dependent on allows targeting through treatment.[114]

An example of synthetic lethality that has been used previously is the use of PARP inhibitors in BRCA deficient breast cancers, where treatment with a PARP inhibition alone results in tumor specific cell death.[115] This death is due to persistent DNA damage that would normally be repaired by BRCA mediated DNA repair in cells with functional BRCA.[116]

Synthetic lethality can target specific cancer cell genetic mutations, hopefully aiding in determination of what patients will respond. In addition, synthetic lethality creates a large therapeutic window, or range of doses that can be used to treat a patient. This large therapeutic window allows lower efficacious doses of chemotherapy to be used to help limit adverse effects.[114]

1.7.2 Bliss Independence method

Synergy is the greater effects of drugs in combination than the simple additive effect expected from the combination of the 2 individual drugs.[117] Synergy, similar to synthetic lethality allows lower concentrations of treatment modalities used in combination than on their own. This created the potential for less side effects to occur.

The Bliss Independence method is an effect-based strategy that compares the effect of the combination of 2 drugs directly to the effects of the drugs as monotreatment.[118] We calculate the Bliss CI value from the equation shown in Figure 1.26b. The effect of each drug as a

monotreatment is shown in Figure 1.27a, and these correspond to the E_A and E_B values in the equation. The effect of the 2 drugs used in combination, or E_{AB} is shown in Figure 1.27a and this corresponds to the denominator of the equation. While E_AE_B expected effect of the combination treatment and if the observed combination treatment effect is greater than this, then the Bliss CI value is <1.0 making it synergistic. If the expected effect is greater, then the Bliss CI will be >1.0 making it an antagonistic combination.

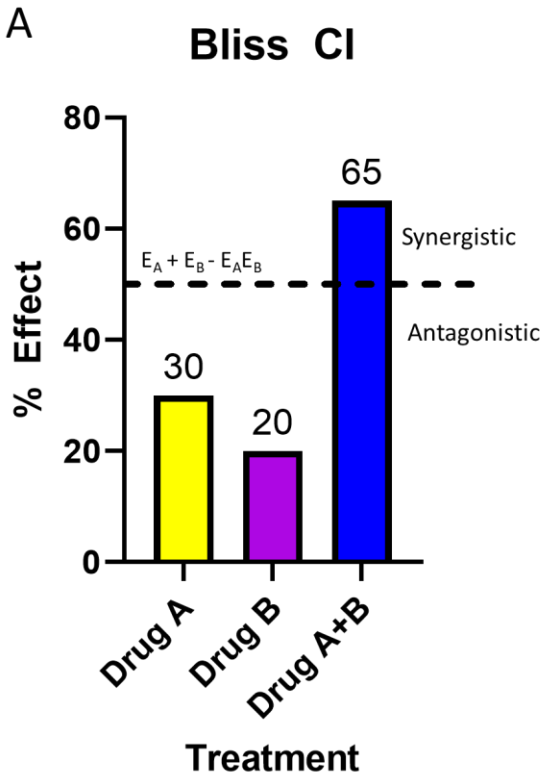

B

$$CI = \frac{E_A + E_B - E_AE_B}{E_{AB}}$$

C

CI Range	Classification
>1	Antagonistic
1.0	Additive
<1.0	Synergy
<0.7	Strong synergism

Figure 1.26 Bliss CI. A) Graphical representation of the data collected for the effect of 2 individual drugs and the combination treatment. B) Bliss CI equation, Effect of A (E_A), Effect of B (E_B), Effect of A and B combo treatment (E_{AB}). C) What each CI range signifies, >1 is antagonistic, 1.0 is additive, <1.0 is synergistic and <0.7 is strongly synergistic.

1.8 Breast Cancer

1.8.1 Breast Cancer molecular classifications

Breast cancer is the most diagnosed cancer among women, and most common cause of cancer related death.[119] Breast cancer is classified into different subtypes based on the expression of 3 receptors, estrogen (ER), progesterone (PR) and human epidermal growth factor receptor 2 (Her2). Breast cancer was originally classified based on IHC into Luminal, Her2 overexpression and basal-like (triple negative). However, modern breast cancer classification is based off the expression of the 3 different receptors. Luminal breast cancer is sub-classified as Luminal A, or Luminal B based on receptor status; Luminal A is ER+, PR+, Her2-, while Luminal B is ER+, PR-/+, Her2+/Ki67 high. Generally Luminal A tumors have a better prognosis, are less aggressive and more differentiated. Luminal B on the other hand, generally have a worse prognosis than Luminal A.[119] Luminal tumors are the most common, with Luminal A being more common than Luminal B.[120] Her2 overexpressing cancers are ER-, PR- and Her2+, which characterizes this cancer subtype.[119] Finally basal-like or triple negative cancers are ER-, PR- and Her2-[120], are the most heterogenous, have the worst prognosis, high expression of proliferation genes, and frequent metastasis.[120]

1.8.2 Standard treatment options of breast cancers

Luminal A and Luminal B breast cancers respond well to hormone therapy. They can be treated with aromatase inhibitors, which result in downregulation of estrogen. Tamoxifen can also be used in these cancers, it will bind ER, preventing ER activity.[120] Previously Her2+ breast cancers had a poor prognosis. Trastuzumab, a monoclonal antibody against Her2 was developed as a targeted therapy to prevent Her2 activation.[120] Following the development of Trastuzumab, Her2+ breast cancer survival has improved. Basal-like breast cancer do not respond to traditional

breast cancer therapies, as there are no hormone receptors to target like in the other subtypes.[120] Basal like cancer are treated with surgery, radiation, and chemotherapy.[119] Due to the lack of response to traditional therapies and propensity to developing resistance, new therapies are needed to treat these cancers.

1.9 Thesis Introduction

1.9.1 Characterizing Tipifarnib

In the first results sub-section of my thesis, I characterized the response of HeLa cells to Tipifarnib. HeLa cells were used due to their competent mitotic checkpoint. In this section, I determined the minimum time required for Tipifarnib treatment, as well as the minimum concentration of Tipifarnib required for loss of Spindly KT localization. In addition, I determined that in accordance with the literature and our labs previous results, that Tipifarnib treatment resulted in a prolonged mitotic duration and increased cell death.

1.9.2 Tipifarnib and Adavosertib combination treatment

The second results sub-section of my thesis investigates the effect of Tipifarnib and Adavosertib combination treatment. We wished to investigate if this combination would be synergistic, resulting in a larger therapeutic window, allowing for lower concentrations to be used while still resulting in cell death. I determined that HeLa and the breast cancer cell lines tested had varying degrees of synergy.

1.9.3 Tipifarnib Resistant cells.

To determine potential causes of resistance to Tipifarnib, Tipifarnib resistant HeLa were generated. These HeLa were then examined for Spindly KT localization, Spindly and FNTB protein

levels. Mitotic duration was also examined, and resistant cells had a prolonged mitotic duration and altered cell fate.

CHAPTER 2: Methods

2.1 Cell Culture

HeLa, HeLa pAAVS1-P-CAG-mCherry-H2B, MDA-MB-231, MDA-MB-468, SK-BR-3, BT-474, cells were grown as a monolayer in high-glucose DMEM (Dulbecco's modified Eagle's medium) supplemented with 2mM L-glutamine and 5% (v/v) FBS (Fetal Bovine Serum). HeLa pAAVS1-P-CAG-mCherry-H2B 1µM Tipi^R were grown in monolayer in high-glucose DMEM (Dulbecco's modified Eagle's medium) supplemented with 1µM Tipifarnib, 2mM L-glutamine and 5% (v/v) FBS (Fetal Bovine Serum). HeLa pAAVS1-P-CAG-mCherry-H2B 2µM Tipi^R were grown in monolayer in in high-glucose DMEM (Dulbecco's modified Eagle's medium) supplemented with 2µM Tipifarnib, 2mM L-glutamine and 5% (v/v) FBS (Fetal Bovine Serum). T-47D and MCF-7 cells were grown as a monolayer in low-glucose DMEM (Dulbecco's modified Eagle's medium) supplemented with 2 L-glutamine, 0.01mg/ml insulin and 10% (v/v) FBS (fetal bovine serum). MCF-10a and HME-1 cells were grown in in MEBM supplemented with SingleQuots (Lonza; CC-3150) (2 mL of bovine pituitary extract, 0.5 mL hydrocortisone, 0.5 mL epidermal growth factor (rHEGF), and 0.5 mL insulin). All cell lines were cultured in a humidified incubator at 37°C with 5% CO_2. Cells were washed with PBS and then trypsinized with 0.05% Trypsin for 5 minutes at 37^{o}C with 5% CO_2. The cells were then split between 1:3-1:5 depending on specific cell line every 2-3 days.

2.1.1 HeLa pAAVS1-P-CAG-mCherry-H2B generation.

HeLa cells were grown to 60% confluency, they were then co-transfected with pAAVS1-P-CAG-mCherry-H2B and pXAT2 as described by Oceguera-Yanez.[1] The transfected cells were then

treated with 1µg/mL puromycin for 2 weeks. Following the confirmation of mCherry-positive cells via microscopy, the cells were then sorte. The positive cells were then seeded with 100 cells per 10cm dish and single cell colonies grown. From these single colonies 6 colonies were mixed to generate the HeLa pAAVS1-P-CAG-mCherry-H2B.

2.1.2 Tipifarnib resistant cell generation.

HeLa pAAVS1-P-CAG-mCherry-H2B cells were seeded into T25 cell culture dishes, once reached 60% confluency, DMSO, 1µM (1µM Tipi^{R}) or 2µM (2µM Tipi^{R}) Tipifarnib was added. Every 3 days cells were split, according to above trypsin protocol if greater than 80% confluency. If the flask was not confluent, the cells were washed with PBS to remove dead cells and debris and then fresh media and Tipifarnib added. Cells were monitored and split every 3-5 days depending on whether they had reached 80% confluency. This was repeated for 30 passages (~3 months), and then Tipifarnib resistance was confirmed by crystal violet assay.

2.2 Small Molecule Inhibitors

Tipifarnib was stored as 25mM stock in DMSO and Adavosertib as 10mM in DMSO at -20^{o}C. Cells were treated with the concentrations indicated. Tipifarnib (Selleckchem, S1453), Adavosertib (Chemie Tek; 955365-80-7), Nocodazole (Sigma, M1404), Monastrol (Selleckchem, S8439).

2.3 Drug Treatments

2.3.1 Tipifarnib treatment for Immunofluorescence experiments

Tipifarnib treatment time optimization: Cells on coverslips were treated with 1.5µM Tipifarnib or equal volume of DMSO solvent control for 12, 18 or 24 hours.

Tipifarnib concentration optimization: Cells on coverslips were treated with 0.097-1.5µM Tipifarnib or equal volume of solvent control DMSO for 12 hours.

2.3.2 Nocodazole kinetochore localization assay

Nocodazole (200ng/mL) was added 30 minutes prior to fixation in the nocodazole kinetochore localization assay.

2.3.3 Mitotic cell assay

Mitotic cell assay for the Tipifarnib resistant cells: Cells seeded on coverslips were treated with 1 or 2µM Tipifarnib or equal volume of solvent control DMSO for 24 hours. Cells were fixed and processed for fluorescence with a pS28-H3 antibody.

2.3.4. Drug treatments for survival assays.

Tipifarnib IC_{50} Crystal Violet assay: Cells were treated with 0.097-25µM Tipifarnib or equal volume of solvent control DMSO.

Adavosertib IC_{50} Crystal Violet assay: Cells were treated with 125-2000nM Adavosertib or equal volume of solvent control DMSO.

Combination treatments for synergy.

Simultaneous: Cells were treated with 0.097-25µM Tipifarnib and 125-2000nM Adavosertib or equal volume of solvent control DMSO for 96 hours.

Tipifarnib first: Cells were treated with 0.097-25µM Tipifarnib or equal volume of solvent control DMSO. 24 hours after Tipifarnib treatment cells were treated with 125-2000nM Adavosertib or equal volume of solvent control.

Adavosertib first: Cells were treated with 125-2000nM Adavosertib or equal volume of solvent control DMSO. 24 hours after Adavosertib treatment cells were treated with 0.097-25µM Tipifarnib or equal volume of solvent control.

2.3.3. HeLa pAAVS1-P-CAG-mCherry H2B cells for high content imaging

HeLa pAAVS-P-CAG-mCherry-H2B cells for high content imaging: Cells were treated 24 hours after seeding. Cells were treated with 0.097-25µM Tipifarnib or equal volume of solvent control DMSO.

Tipifarnib resistant cells for High Content Imaging: Cells were treated 24 hours after seeding. Cells were treated with 0.39-6.2µM Tipifarnib or equal volume of solvent control DMSO.

2.4 Western Blotting

Cells were harvested and processed for western blot as described previously.[2] Protein concentrations of cell extracts were determined with the Pierce BCA assay (Thermo Fischer Scientific, 23225) and samples were standardized by dilution to 20 µg protein per sample. Protein extracts were separated on 10% SDS-polyacrylamide gel for 50 minutes at 200V. PageRuler Plus Prestained protein ladder (Thermo Fisher Scientific; 26619) was used as a molecular weight marker. Proteins were transferred onto nitrocellulose for 10 minutes at 25 V and 2.5mA by Trans-Blot® Turbo Transfer System. Membranes were blocked with Odyssey blocking buffer (LI-COR Biosciences) and probed with rat polyclonal anti-hSpindly antibody (1:1000 dilution, Chan Lab[3]), rabbit anti-Farnesyltransferase B (1:25,000 dilution, Abcam 109625), mouse anti-α-tubulin (1:10,000 dilution, Sigma T5168). Secondary antibodies Alexa Fluor 680 anti-rat (1:1000 dilution, Thermo Fisher Scientific, A21096), Alexa Fluor 680 anti-rabbit (1:1000 dilution, Thermo Fisher Scientific A21109), Alexa Fluor 800 anti-mouse (1:1000 dilution, Thermo Fisher Scientific,

A21057) were used. Total protein was stained using AquaStain Protein Gel stain (Bulldog-Bio). Odyssey IR imager system (LI-COR Biosciences) scanner was used to scan the blots and then analyzed by Image Studio light V5.2 for quantification.

2.5 Fluorescence Microscopy

Cells were seeded on 18-mm^2 coverslips (0.170 +/- 0.005mm, Zeiss, 474030-9000-000) at a density of 50,000 cells/mL in 6 well dish. Coverslips were sterilized by immersion in 95% ethanol and then flamed using a Bunsen burner. Cells on coverslips were treated with Tipifarnib (SelleckChem) at the concentration specified or same volume of solvent control DMSO for the duration specified. When specified, cells were then treated with 200ng/mL nocodazole or equal volume of solvent control DMSO for 30 minutes. Cells were fixed with 3.5% paraformaldehyde in PBS for 7 minutes, permeabilized in KB buffer (50mM Tris/HCl, pH 7.4, 150mM NaCl and 0.1% BSA) with 0.2% Trition X-100 for 5 minutes at room temperature, then rinsed in KB buffer for 5 minutes at room temperature. Rat anti-hSpindly (1:1000 dilution, Chan Lab[3]) and Alexa Fluor 488-conjugated anti-rat (1:1000 dilution, Molecular Probes, A11006) antibodies were used to detect hSpindly. hCENP-F was visualized using rabbit anti-hCENP-F antibody (1:1500, Chan Lab[4]) and AlexaFluor anti-rabbit Texas Red (1:1000, Molecular Probes, T2767) antibodies. Centromeres were visualized using human ACA sera (anti-centromere sera, 1:2000, gift from Dr. Marvin Fritzler, University of Calgary) and Alexa Fluor anti-human 674 (1:1000, Molecular Probes antibodies, A21445). Rat Phospho-S28-H3 antibody (1:2500, Abcam, ab10543), anti-rat 488 DNA was stained with 0.1μg/mL DAPI. Coverslips were mounted with Mowiol mounting media.

A Leica Falcon SP8 microscope was used to collect the images. Cells were visualized with either 100X 1.4NA oil Plan-Apo lens or 25X 0.95 Water HC Fluotar lens. Diode 405nm and White

laser 2 was used. The white light laser was adjusted for 488 nm, 594 nm, and 647nm. Laser power was kept consistent between image acquisition within each experiment. The diode 405nm was detected using a PMT, and the white light laser was detected using 3 hybrid detectors. Images were processed using Adobe Photoshop CS6.

2.6 High Content Imaging

Images were taken with a high-content–automated microscopy imaging system (MetaXpress Micro XLS, software version 6, Molecular Devices) as previously described.[5] Cells were seeded onto 96 well optical bottom plate (Thermo Fisher Scientific, 165395) at density of 1000 per well. Cells were treated with the specified concentrations of Tipifarnib immediately prior to imaging. Single images were captured in each well with a 20X 0.45NA S Plan Fluor ELWD objective with the equipped siCMOS camera using the Texas red bandpass filter set (536/40nm and 624/40 nm). Images were acquired at the center of each well, every 10 minutes for 72 hours. On average 200 cells per well were imaged. The images were then manually analyzed with the MetaXpress software using the mCherry-H2B to monitor changes in DNA organization. Mitotic timing was calculated by the interval between nuclear envelope breakdown (indicated by the first evidence of chromosome condensation) to the onset of anaphase (or chromosome decondensation in the case of mitotic slippage). Only cells that entered mitosis were analyzed for mitotic timing experiments, and the fates of the mitotic cells (and resulting daughter cells) were tracked for the duration of the experiment (72 hours). Cell death was determined by the formation of apoptotic bodies.

2.7 Kinetochore localization quantification code.

Matlab code for the detection and quantification of kinetochore localization was developed by Kaushiki Roy. For the quantification of fluorescence, Spindly and CENP-F kinetochore intensities were measured by determining the total pixel intensity at sister kinetochores. Background subtraction was done as previously described in the literature.[6] Spindly and CENP-F kinetochore intensity were outputted as a ratio to kinetochore intensity. Sister KT from 25 prometaphase cells were analyzed for each protein.

2.8 Crystal Violet assay

Cells were seeded into 96 well plates at either 1000 cells/well (HeLa cells), 2000 cells/well (MDA-MB-231, MDA-MB-468, SK-BR-3, MCF-7, MCF 10a, HME-1 cells), 4000 cells/well (T-47D, BT-474 cells) for 24 hours. Cells were treated as specified with Tipifarnib or Adavosertib or equal volume of solvent control DMSO. After 96-hour treatment, the medium was aspirated then cells were stained with 0.5% Crystal Violet (20% methanol) for 20 minutes as outlined in Feoktistova et al.[7] Crystal violet was then removed, and plates were washed 3X with water and left to air dry for 24 hours. Crystal violet was then resuspended in 200 µL 100% methanol, and absorbance at 570 nm (OD_{570}) was measured using FLUOstar OPTIMA microplate reader (BMG Labtech). Percent surviving attached cells was calculated by subtracting blank wells then normalized with the control set to 100%. The first point on each curve represents the DMSO solvent control. Graphs were plotted using GraphPad Prism V9.

2.9 Reagents and buffers

16% Paraformaldehyde solution (Electron Microscopy Sciences, 15710) was diluted to 3.5% with PBS.

Mowiol Mounting Media

Buffer	Composition
KB and KB-TX	0.01 M Tris-HCl pH 7.5, 0.15 M NaCl, 0.1% BSA (+/- 0.2% Triton X-100)
RIPA buffer	25 mM Tris-HCl pH 7.6, 150 mM NaCl, 1% NP-40, 1% sodium deoxycholate, 0.1% SDS RIPA buffer (Thermo Fisher Scientific, 89900)
Phosphate Buffered Saline (PBS)	137 mM NaCl, 2.7 mM KCl, 4.3 mM Na_2HPO_4, 1.4 mM KH_2PO_4, pH 7
1X SDS-PAGE running buffer (10L)	30.3 g Tris-HCl, pH 8.8, 141.7 g glycine, 10 g SDS
Western Blot transfer buffer	20% Methanol, 60% ddH2O, 20% 5X Transfer buffer Bio Rad, Trans blot turbo kit, 1704270
AquasStain Protein Gel Stain	Bulldog-bio AS001000
2X Laemmli Sample Buffer	65.8 mM Tris-HCl, pH 6.8, 2.1% SDS, 26.3% (w/v) glycerol, 0.01% bromophenol blue Bio Rad, 1610737

Antibody	Host Species	IF dilution	Western Blot dilution	Source
hACA	Human	1:2000	N/A	M. Fritzler, University of Calgary
hCENP-F	Rabbit	1:1500	N/A	Chan et al., 1998
Farnesyltransferase B	Rabbit	N/A	1:25,000	Abcam, ab109625
pS28-H3	rat	1:2500	N/A	Abcam, ab10543
hSpindly	Rat	1:1000	1:1000	Moudgil et al., 2015
Tubulin	Mouse	1:2000	1:10,000	Sigma T5168

CHAPTER 3: Results

3.1 Characterization of cancer cell response to Tipifarnib

It is known that FTI treatment results in loss of Spindly KT localization, and prometaphase arrest.[44,43] However Tipifarnib, the FTI I chose for my experiments had not previously been tested in our lab. Based on experiments with other FTIs, Tipifarnib should have the same effect where the inhibition of farnesylation results in loss of Spindly KT localization. First, I needed to determine the Tipifarnib treatment conditions, and then from there I characterized the response of HeLa cells to Tipifarnib. We selected HeLa to characterize the response to Tipifarnib as the previous FTI work in our lab was done in HeLa cells and Hela cells have a competent mitotic checkpoint.[44]

The first condition that I tested was what is the minimum time required for Tipifarnib treatment to result in the loss of Spindly farnesylation. Previously it has not been determined what the minimum time required for FTI treatment to result in loss of Spindly KT localization, which serves as the indicator for loss of Spindly farnesylation. By investigating the minimum time required for Tipifarnib treatment, we will be able to optimize the conditions for the experiments going forward. If it takes a full 24 hours of FTI treatment, which is the shortest tested thus far in the literature,[44] for loss of Spindly farnesylation, then we will be seeing the effects on the first mitotic division where it is exerting an effect. However, if a shorter treatment duration is sufficient for FTase inhibition, then by looking at these longer time points it is possible we will be examining cells that have already gone through a division, and thus may have abnormalities due to the abnormal mitosis that loss of Spindly KT localization could cause.

To determine if Tipifarnib treatment requires a full 24 hours for loss of farnesylation, or if this occurs after a shorter treatment period, HeLa cells were treated with 1.5 μM Tipifarnib for 12, 18 and 24 hours before fixation (Figure 3.1A) and Spindly kinetochore localization was imaged in prometaphase cells. Prometaphase cells were selected because that is when Spindly KT localization occurs. It is lost in metaphase due to KT shedding upon proper chromosome congression.[37] ACA, an anti-centromere antibody was used to mark the inner KT. This was used in all the following experiments to determine KT localization, via localization of outer KT proteins with ACA. In both Figure 3.1 and Figure 3.2, Spindly KT localization was scored visually as either positive or negative for the cell. This was then calculated as a percentage of cells examined. As shown in Figure 3.1B. Spindly kinetochore localization was lost at all time points examined. When these cells were scored for Spindly KT localization, at all time points tested there was a 100% loss of Spindly KT localization (Figure 3.1C). This indicates that farnesylation is lost by 12hours post Tipifarnib treatment and that 12hrs is a sufficient Tipifarnib treatment duration.

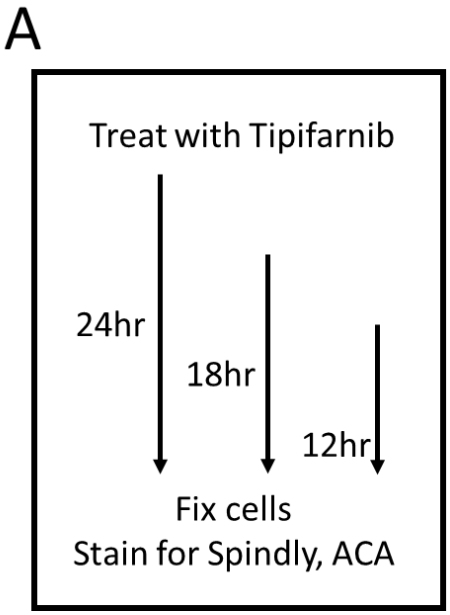

B

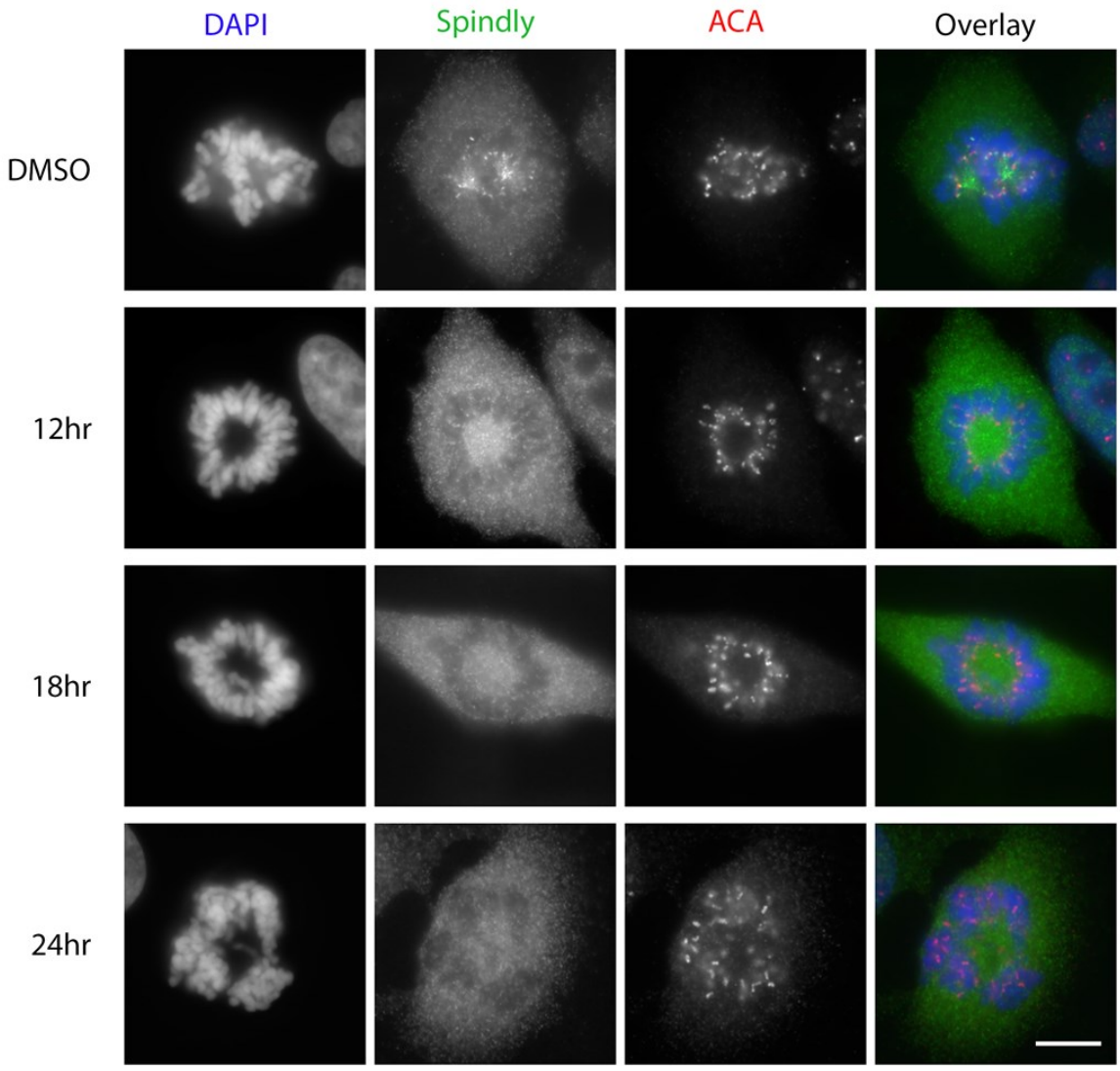

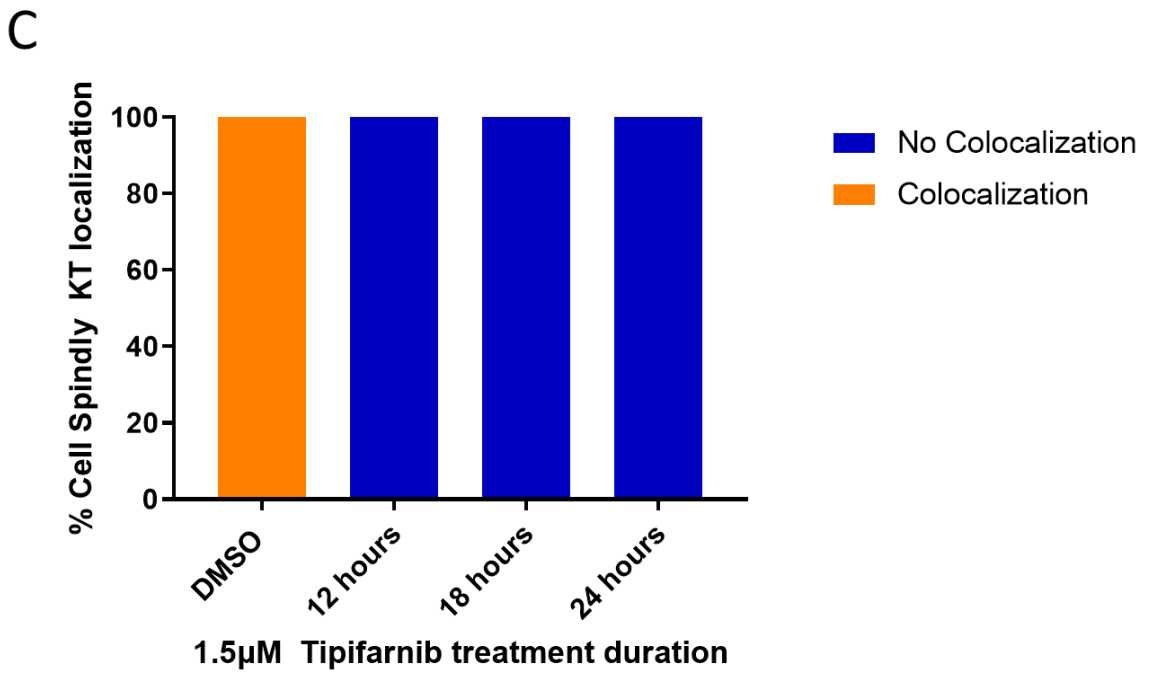

Figure 3.1. Spindly is lost from kinetochores after a 12hr treatment with Tipifarnib. A) Experimental flow chart. HeLa cells were treated with 1.5 µM Tipifarnib for range of time (12, 18, 24 hours) and then fixed and stained for Spindly, ACA (Centromere) and DAPI (DNA). B) Images shown are a single slice from a Z-stack. Laser power was set based on DMSO control and all conditions were imaged using these conditions. C) Spindly KT localization was quantified as either visual positive or negative via localization to ACA. This is then shown as the percent of cells with Spindly KT localization. N = 30 prometaphase cells, 3 biological replicates. Scale bar = 10 µm.

To maximize the sensitivity of this KT localization assay, cells were treated with the microtubule poison, nocodazole 30 minutes prior to fixation (Figure 3.2A). This results in activation of the mitotic checkpoint which then causes maximally expanded kinetochores. Proper mitotic spindle formation relies on the capture of MT at the KT, with large KT accelerating the capture of MT.[121] We treated with nocodazole for 30 minutes, as this is enough time to depolymerize the MT, but not a long enough treatment that it might confound the results we are getting; allowing us to assume that the results observed are due to Tipifarnib treatment alone.

Similar to Tipifarnib alone, Spindly kinetochore localization is lost at all 3 time points (Figure 3.2B), further showing that 12 hours is sufficient for Tipifarnib treatment duration at 1.5 µM. However, in the nocodazole treated cells, 21% of cells still had Spindly KT localization at 12 hours and 14% of cells at 18 hours (Figure 3.2C). This is due to maximal activation of the mitotic checkpoint, which results in kinetochore expansion. Thus, while the more sensitive assay showed some KT localization of Spindly, it was still reduced to only 20% of cell analyzed relative to control.

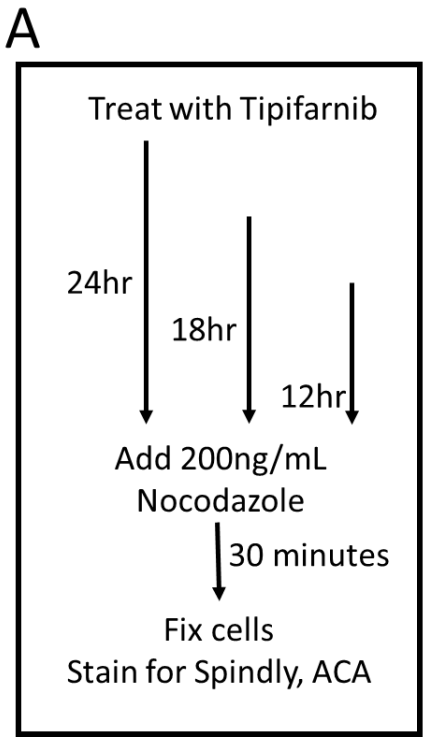

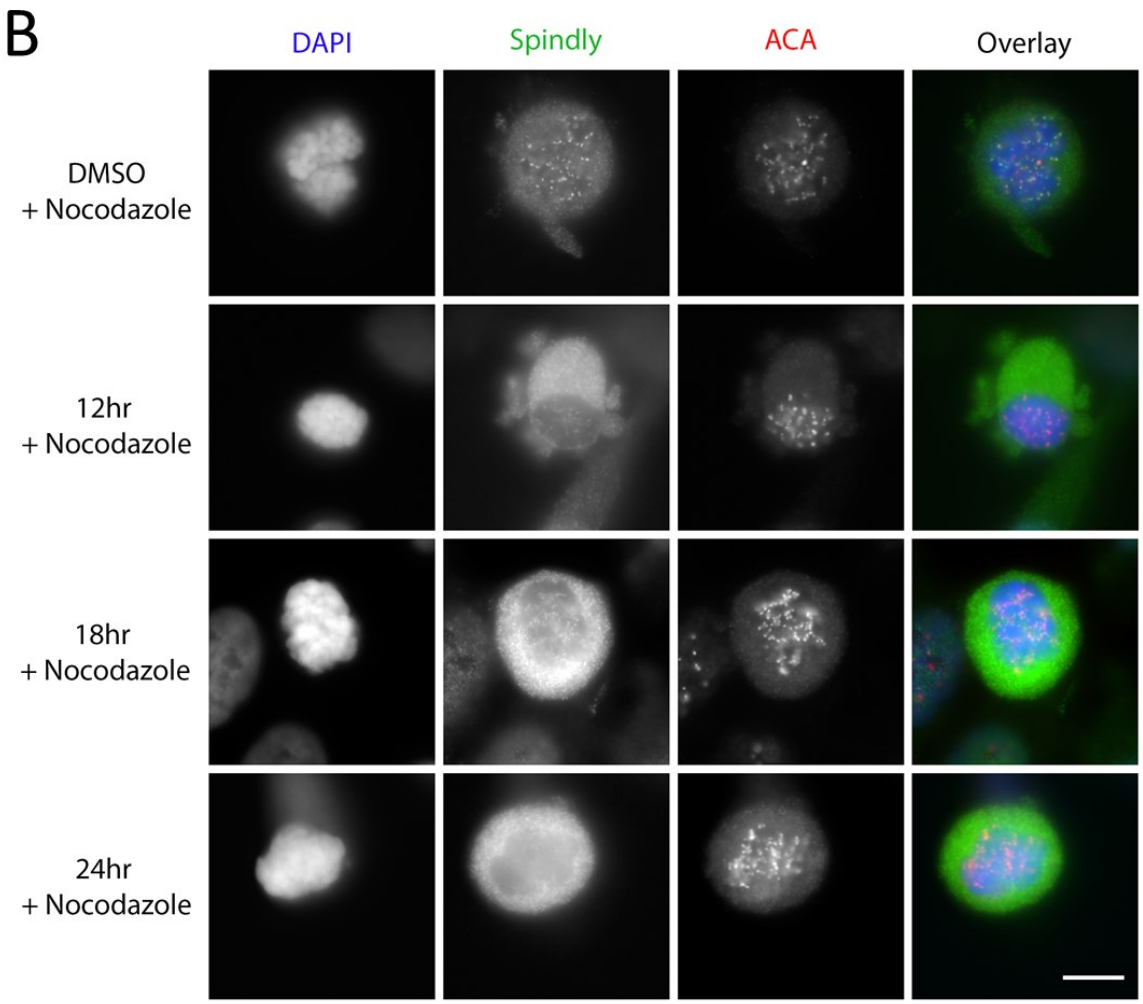
B
DAPI
Spindly
ACA
Overlay
DMSO
+ Nocodazole
12hr
+ Nocodazole
18hr
+ Nocodazole
24hr
+ Nocodazole

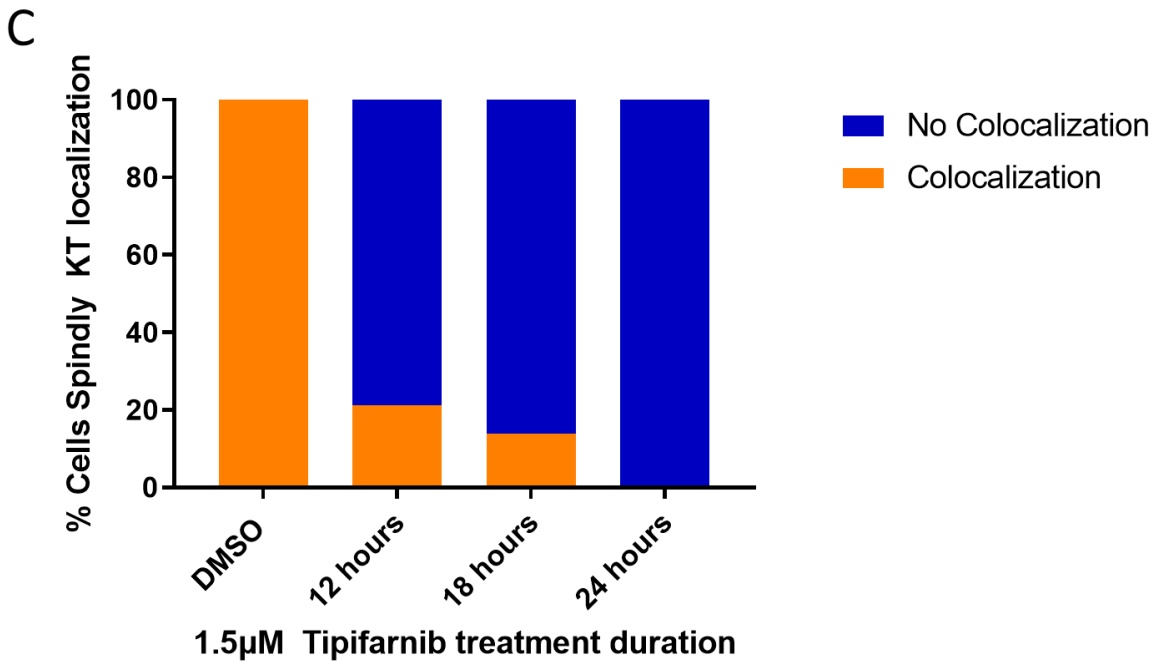

Figure 3.2. Spindly is lost from kinetochores after a 12hr treatment with Tipifarnib and nocodazole. A) Experimental flow chart. HeLa cells were treated with 1.5 µM Tipifarnib for range of time (12, 18, 24 hours) and then treated with 200 ng/mL 30 minutes prior to fixation; fixed and stained for Spindly, ACA (Centromere) and DAPI (DNA). B) Images shown are a single slice from a Z-stack. Laser power was set based of DMSO control and all conditions were imaged using these conditions. C) Spindly KT localization was quantified as either visual positive or negative via localization to ACA. N = 30 prometaphase cells, 3 biological replicates. Scale bar = 10 µm.

As the concentration we tested in the previous time point experiments had not been optimized, we next tested a range of Tipifarnib concentrations for a 12-hour treatment to determine what is the minimum concentration required for loss of Spindly KT localization. HeLa cells were treated with 0.097-1.5 µM Tipifarnib for 12-hours and then stained for Spindly, CENP-F and ACA (Figure 3.3A). We used ACA, which is an anti-centromere antibody, as the constitutive KT marker. While CENP-F was used as a control protein, as it is also a farnesylated protein that is recruited to the outer KT, but its recruitment is not abolished by FTI treatment. By staining for

ACA and CENP-F in addition to Spindly, we are able to determine if Spindly KT localization occurs (Spindly and ACA) and if it is lost (CENP-F and ACA).

As we are treating with a range of Tipifarnib, there is the potential that there will be some partial Spindly recruitment to the KT, if FTase is not fully inhibited. To account for this, Spindly and CENP-F KT localization was determined via quantification of the pixel intensities of Spindly, CENP-F and ACA via a MATLAB code. This allows the potential of partial KT recruitment to be accounted for and analyzed, compared to the previous visual yes/no for Figures 3.1 and 3.2. The pixel intensities for Spindly and CENP-F were determined and calculated as a ratio to ACA (Spindly:ACA and CENP-F:ACA respectively), which were then outputted and graphed as shown in Figures 3.3C and 3.4C.

At all concentrations, Spindly KT recruitment is impaired (Figure 3.3B), with only the solvent control DMSO showing Spindly KT localization. Even at the lowest concentration of 0.097 μM, Spindly KT localization was decreased significantly ($p<0.0001$, student t-test) by more than half, with a median Spindly:ACA ratio of 0.47 (Figure 3.3C). Interestingly across the entire range of Tipifarnib tested, the normalized Spindly:ACA ratio was fairly consistent at ~50% of the control. This indicates that even at the lowest concentration tested (0.097 μM) FTase was comparably inhibited to 1.5 μM. The quantification of Spindly and CENP-F KT localization allows us to see KT localization, that would not be apparent by visual assessment, as shown by the Z-stack slice in Figure 3.3B, where Spindly KT localization appears lost, but when quantified, there is still some Spindly that is recruited. CENP-F recruitment as expected was not abolished by Tipifarnib treatment, and still recruited to the outer KT (Figure 3.3B). While for CENP-F, at 0.097 μM, there

was a significant ($p<0.01$, student t-test) decrease, there was still 92% of KT recruitment compared to control. 0.195, 0.39 and 1.5 µM all resulted in non-significant increases of CENP-F KT localization, while 0.78 µM resulted in a significant ($p<0.01$, student t-test) increase of CENP-F KT localization (Figure 3.3C). From the above, we were able to determine that 0.097 µM of Tipifarnib is sufficient for a significant loss of Spindly KT localization, while CENP-F is not greatly affected by the same concentrations.

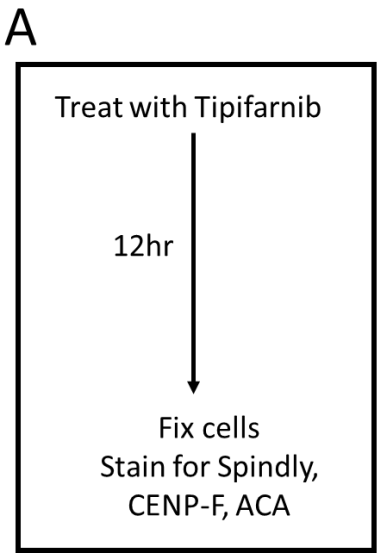

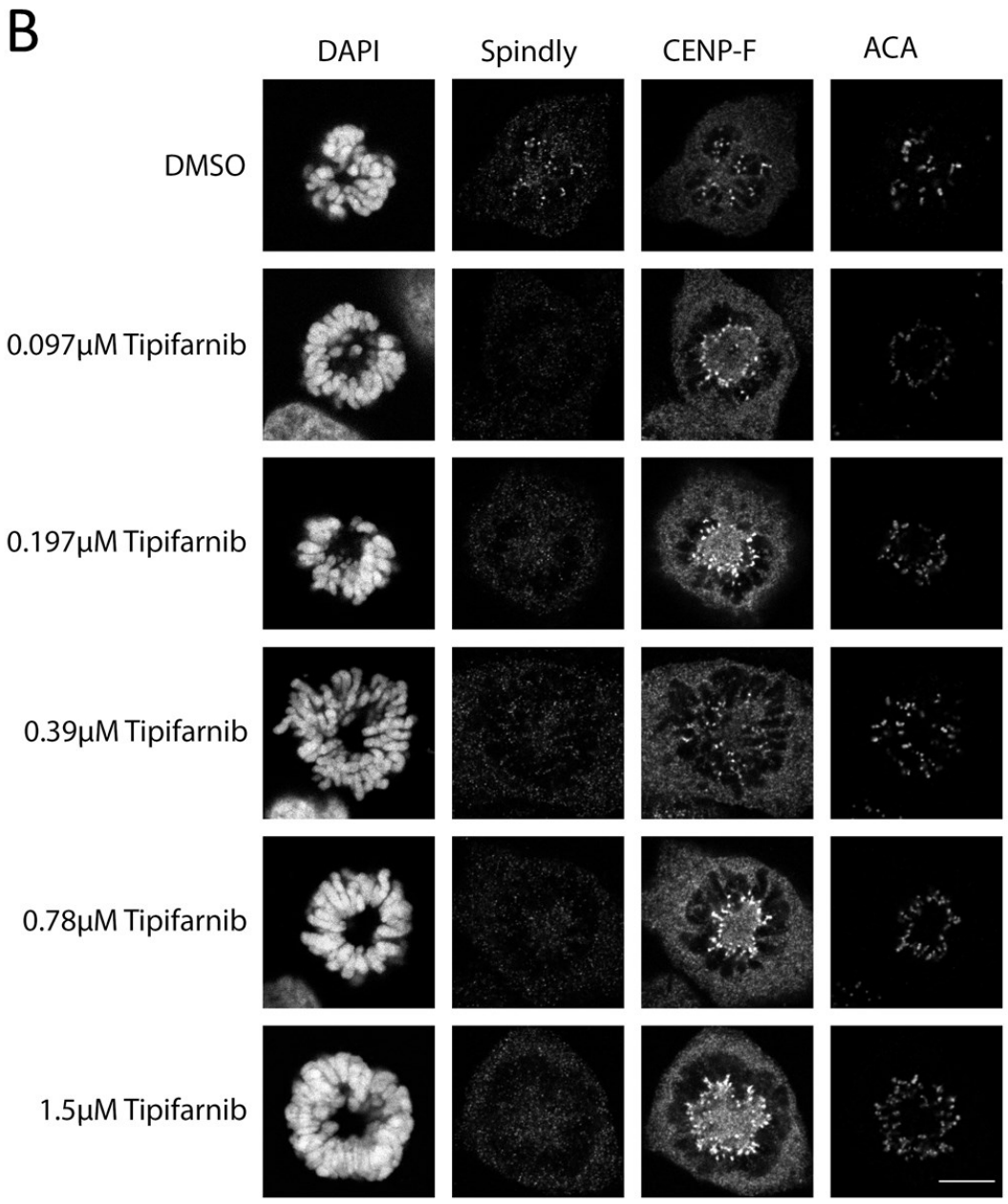
B
DAPI
Spindly
CENP-F
ACA
DMSO
0.097μM Tipifarnib
0.197μM Tipifarnib
0.39μM Tipifarnib
0.78μM Tipifarnib
1.5μM Tipifarnib

C

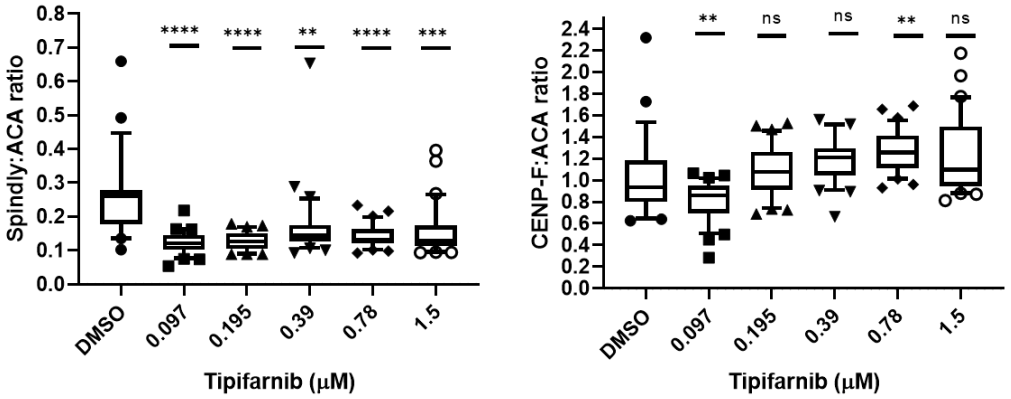

	Spindly		CENP-F	
Tipifarnib (μM)	Median Spindly:ACA ratio	Normalized	Median CENP-F:ACA Ratio	Normalized
DMSO	0.26	1.00	0.94	1.00
0.097	0.12	0.47	0.86	0.92
0.195	0.13	0.48	1.08	1.15
0.39	0.14	0.55	1.21	1.29
0.78	0.13	0.51	1.26	1.34
1.5	0.13	0.49	1.10	1.17

Figure 3.3 0.097μM Tipifarnib is sufficient for loss of Spindly kinetochore localization. A) Experimental flow chart. HeLa cells were treated with 0.097-1.5 μM Tipifarnib for 12 hours. and then fixed and stained for Spindly, CENP-F (outer KT), ACA (KT) and DAPI (DNA). B) Images shown are a single slice from a Z-stack. Laser power was set based on DMSO control and all conditions were imaged using these conditions. Images were enhanced for presentation. C) Spindly and CENP-F KT localization was quantified via MATLAB code, where the pixel intensity from the raw data of Spindly or CENP-F was outputted as a ratio to ACA intensity. Boxes represent interquartile distributions and whiskers represent 10^{th} and 90^{th} percentiles. Points represent the outliers. Statistical comparison between DMSO and Tipifarnib treated cells via student T test, * $p<0.05$, ** $p<0.01$, *** $p<0.001$, **** $p<0.0001$, ns= not significant. Median Spindly:ACA and CENP-F:ACA ratio as shown in the chart, and median ratio normalized to DMSO is shown for each. N = 30 prometaphase cells, 3 biological replicates. Scale bar = 8 μm.

Once again, we wanted to see what Spindly KT localization occurs following Tipifarnib treatment when the mitotic checkpoint is activated by nocodazole. HeLa cells were treated with 0.097-1.5 μM Tipifarnib for 12 hours and with nocodazole 30 minutes prior to fixation in order to maximally activate the mitotic checkpoint (Figure 3.4 A).

Similar to Tipifarnib alone, Spindly KT localization is lost upon Tipifarnib and nocodazole treatment (Figure 3.4B). 0.097 μM Tipifarnib was sufficient to cause a significant ($p<0.0001$, student t-test) decrease in Spindly KT localization. 0.097 μM Tipifarnib and nocodazole resulted in a larger decrease in Spindly KT localization relative to the DMSO control, with an ~70% decrease (Figure 3.4C) compare to the ~50% decrease in Tipifarnib alone (Figure 3.3C). This larger decrease in Spindly KT localization relative to control, is likely due to the mitotic checkpoint being activated, and the KT expanded, which will result in increased Spindly KT localization, and thus a higher ratio in the nocodazole treated control.

Only the 2 lowest concentrations of Tipifarnib tested resulted in a significant change in CENP-F localization. 0.097 μM resulted in a significant ($p<0.0001$, student t-test) decrease to 64% of the solvent control; while 0.195 μM resulted in a significant ($p<0.001$, student t-test) decrease to 88% of solvent control (Figure 3.4C). However, while this decrease is significant, compared to Spindly, there is double the amount of CENP-F to Spindly when treated with 0.097 μM and almost triple when treated with 0.195 μM (Figure 3.3C and Figure 3.4C). The higher concentrations of Tipifarnib tested, resulted in non-significant increases in CENP-F KT localization, indicating that while CENP-F KT localization can be reduced it is to a smaller extent compared to Spindly. Figure 3.3 and 3.4 both show that the lowest concentration of Tipifarnib tested, 0.097 μM is sufficient to result in a significant ($p<0.0001$, student t-test) decrease to 47% (Figure 3.3C) and 32% (Figure 3.4C) of Spindly KT localization relative to the solvent control when treated with Tipifarnib or Tipifarnib and nocodazole respectively. Additionally, 0.097 μM Tipifarnib treatment causes a similar decrease in Spindly KT localization compared to 1.5 μM, with 47% to 49% (Tipifarnib alone Figure 3.3C) and 32% to 23% (Tipifarnib plus nocodazole, Figure 3.4C). This data indicates that

low concentrations Tipifarnib result in comparable inhibition of Spindly KT localization as the higher concentrations.

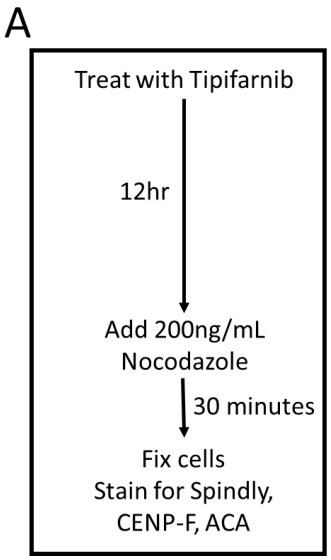

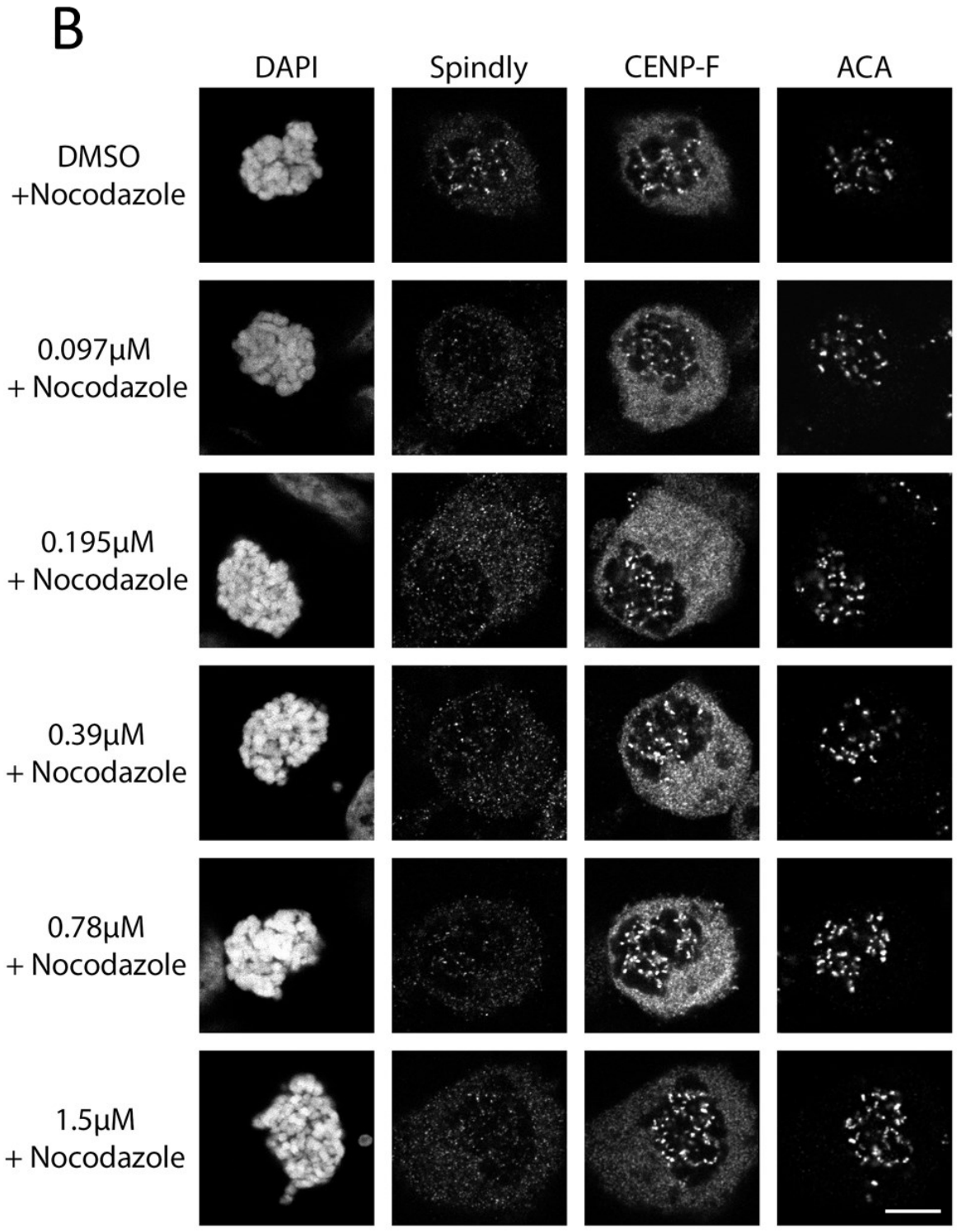
B
DAPI
Spindly
CENP-F
ACA
DMSO
+Nocodazole
0.097μM
+ Nocodazole
0.195μM
+ Nocodazole
0.39μM
+ Nocodazole
0.78μM
+ Nocodazole
1.5μM
+ Nocodazole

C

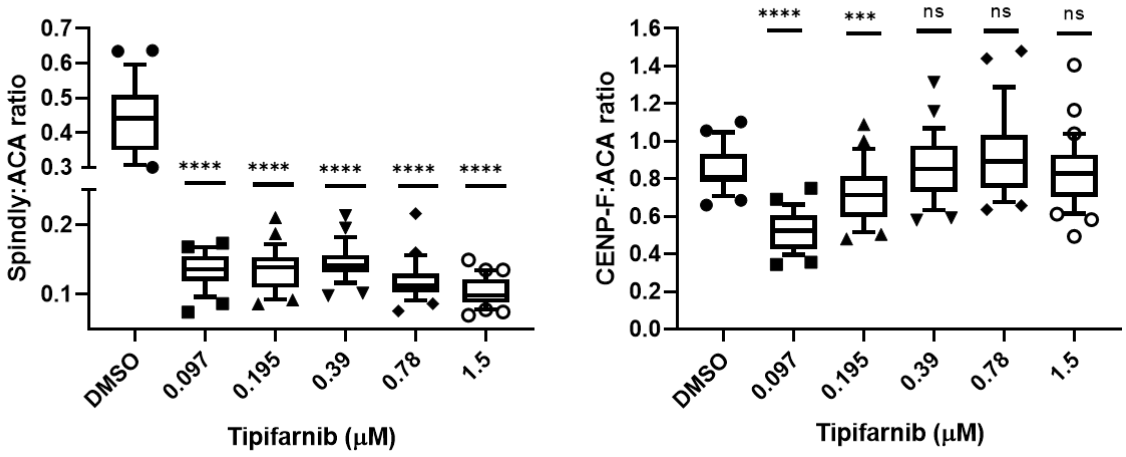

	Spindly		CENP-F	
Tipifarnib + Nocodazole (μM)	Median Spindly:ACA ratio	Normalized	Median CENP-F:ACA Ratio	Normalized
DMSO	0.44	1.00	0.81	1.00
0.097	0.14	0.32	0.52	0.64
0.195	0.14	0.32	0.71	0.88
0.39	0.14	0.32	0.85	1.05
0.78	0.11	0.25	0.89	1.10
1.5	0.10	0.23	0.83	1.02

Figure 3.4 0.097 μM Tipifarnib is sufficient for loss of Spindly kinetochore localization. HeLa cells were treated with 0.097-1.5 μM Tipifarnib for 12 hours and 200 ug/mL of nocodazole was added 30 minutes prior to fixation. Cells were then fixed and stained for Spindly, CENP-F (outer KT), ACA (KT) and DAPI (DNA). A) Experimental flow chart. B) Images shown are a single slice from a Z-stack. Laser power was set based on DMSO control and all conditions were imaged using these conditions. Images enhanced for presentation. C) Spindly and CENP-F KT localization was quantified via MATLAB code, where the raw data pixel intensity of Spindly or CENP-F was outputted as a ratio to ACA intensity. Boxes represent interquartile distributions and whiskers represent 10th and 90th percentiles. Points represent the outliers. Statistical comparison between DMSO and Tipifarnib treated cells via student T test, *** $p<0.001$, **** $p<0.0001$, ns = not significant. Median Spindly:ACA and CENP-F:ACA ratio as shown in the chart, and median ratio normalized to DMSO is shown for each. N = 30 prometaphase cells, 3 biological replicates. Scale bar = 8 μm.

We were able to confirm that in accordance with the literature,[44,43] Tipifarnib treatment resulted in loss of Spindly KT localization. From this we wanted to determine what effect this loss of Spindly KT localization had on the mitotic duration and cell fate. Tipifarnib treatment should

result in a prolonged mitosis duration due to prometaphase arrest, and depending how long this arrest is, could result in cell death. To determine what effects Tipifarnib treatment has on mitotic duration and cell fate we used high content live cell imaging. This allows us to examine a number of treatment conditions in a high throughput manner. HeLa cells stably expressing pAAVS1-P-CAG-mCherry-H2B, which is mCherry-H2B that has been inserted into the safe harbor, PPP1R12C locus where it is stably expressed.[122] These cells were seeded, treated with 0.097-12.5 μM Tipifarnib and then imaged using a high content microscope every 10 minutes for 72 hours (Figure 3.5A). The duration of mitosis was determined from the frame that they enter mitosis, as seen by chromosome condensation and the frame they exit mitosis- denoted by anaphase (Figure 3.5 B, top row). Additionally, cell fate was also tracked, with 3 possible outcomes: survival, death in mitosis or death in interphase. For cell death, both in interphase and mitosis, the frame at which apoptotic bodies formed was used as the frame the cell died, or that mitosis ended for cells that die in mitosis (Figure 3.6B, middle and bottom rows). From this we were then able to calculate the duration of mitosis of each cell and see what effects Tipifarnib treatment has on mitotic duration and cell fate.

The loss of Spindly KT localization when treated with 0.097 μM Tipifarnib (Figure 3.3B) results in a mitotic arrest, with a significant increase in the median mitotic timing from 40 minutes (DMSO), to 80 minutes (0.097 μM), (Figure 3.5C, $p<0.01$, student t-test). With increasing Tipifarnib concentration, there is a significant increase in mitotic duration; with 0.097 μM ($p<0.01$, student t-test), 0.197 μM ($p<0.05$, student t-test), 0.39μM ($p<0.05$, student t-test), and 0.78 μM ($p<0.001$, student t-test) Tipifarnib, all result in increased median mitotic duration to approximately double the DMSO treated control cells (Figure 3.5C). At the higher concentrations

of Tipifarnib tested-1.5, 3.1, 6.2, 12.5 μM, there was a significant ($p<0.0001$, student t-test) increase in median mitotic duration (Figure 3.5C). 1.5 μM and 3.1 μM resulted in increases in median mitotic duration, where they are ~2.5 and 4-fold longer respectively than the control cells. While at the highest concentrations tested, 6.2 μM resulted in a ~8-fold increase, and 12.5 μM resulted in a ~17-fold increase in median mitotic duration (Figure 3.5C).

The increased mitotic duration shown in Figure 3.5C, also resulted in altered cell fate, which is shown in Figure 3.5D. Cell survival (blue), cell death in mitosis (yellow) and death in interphase (purple) is shown and the n in the center of each donut plot is the total number of cells that were tracked over the 72 hours time period, from 16 original parent cells. The increased median mitotic duration, resulted in a lower number of total cells, where 0.097 μM had 78 cells total analyzed, compared to the 131 from the DMSO treated control cells. Tipifarnib treatment ranging from 0.097-3.1 μM, all resulted in a similar number of total cells, ranging from 61-94 (Figure 3.5D). At the higher concentrations tested, 6.2 μM had 34 cells total, a ~4-fold decrease, and 12.5 μM had 16 cells, an ~8-fold decrease in total number of cells (Figure 3.5D). The increased percentage of cells dying in mitosis, appears to correlate with the increased median mitotic duration, where increasing concentrations of Tipifarnib resulted in prolonged mitotic duration and increasing percentage of cells dying in mitosis. The high concentrations tested, 3.1, 6.2 and 12.5 μM resulted in increased percentage of cell death in mitosis, 15.3%, 41.2% and 100% respectively (Figure 3.5D). Other than 0.197 μM Tipifarnib, all other concentrations of Tipifarnib tested, did not result in a large percentage of cells dying in interphase (Figure 3.5D). From this it appears that Tipifarnib treatment results in cell death during mitosis, and if the cell is able to successfully complete mitosis, the cell will continue on in the cell cycle.

A

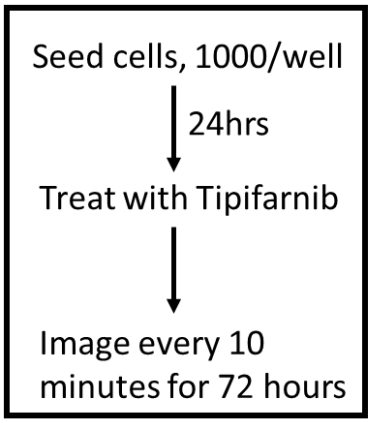
Seed cells, 1000/well
24hrs
Treat with Tipifarnib
Image every 10 minutes for 72 hours

B

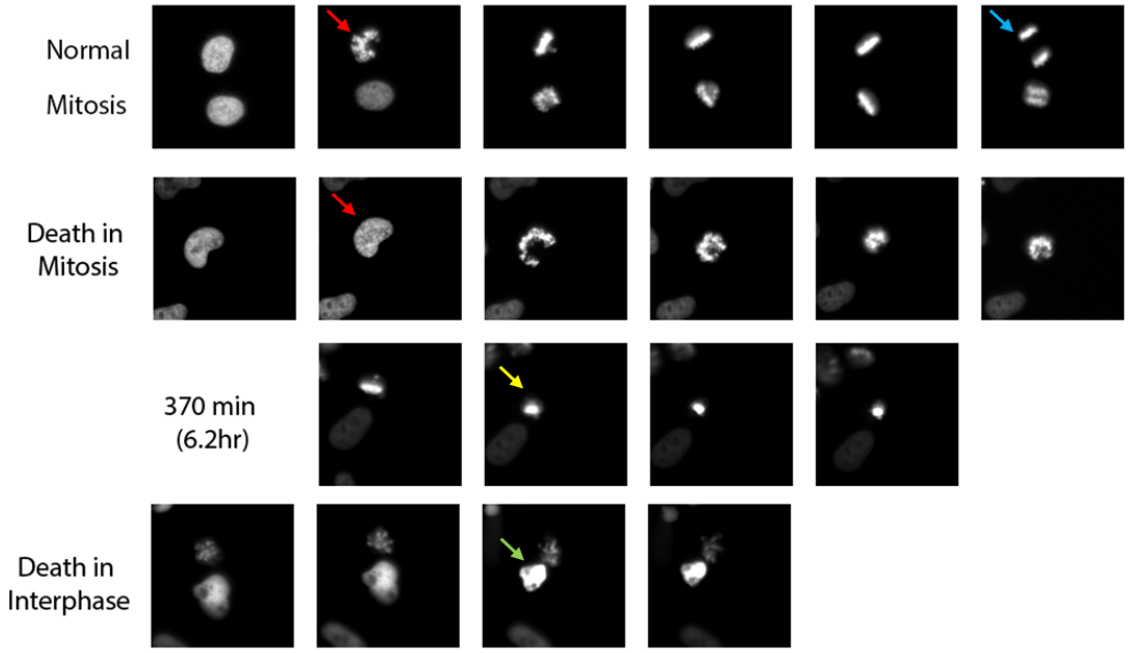
Normal Mitosis
Death in Mitosis
370 min (6.2hr)
Death in Interphase

C

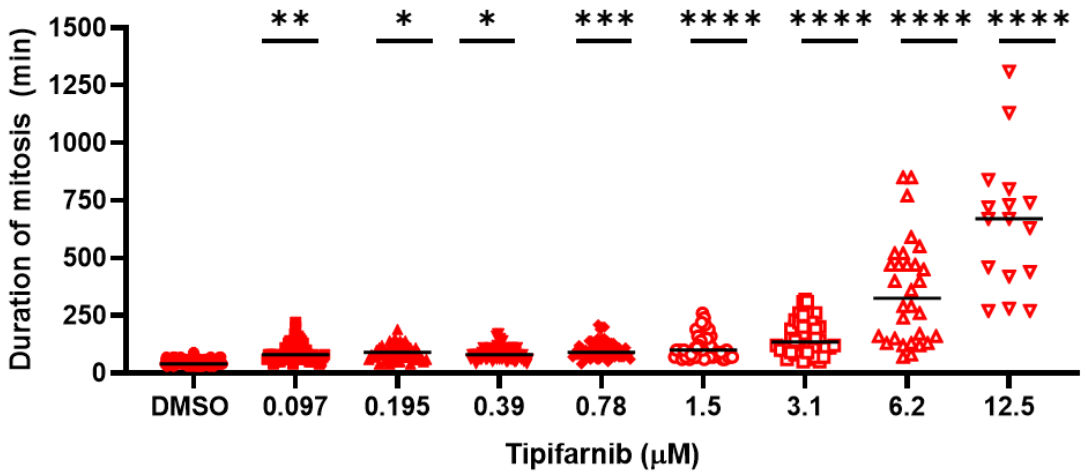

Duration of Mitosis (Min)		
Tipifarnib (μM)	Median	Mean
DMSO	40.0	56.3
0.097	80.0	191.4
0.19	90.0	113.9
0.39	80.0	109.9
0.78	90.0	124.7
1.5	100.0	167.5
3.1	150.0	244.1
6.2	325.0	354.7
12.5	670.0	648.8

D

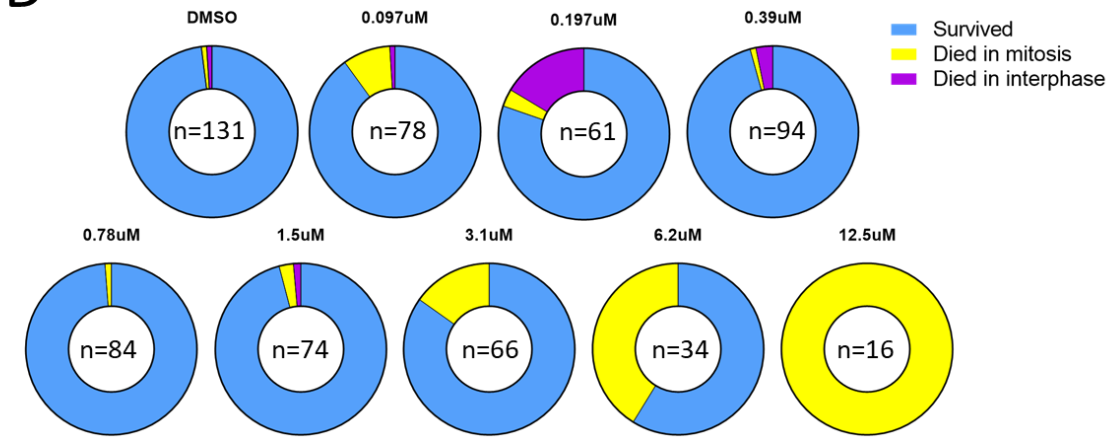

Cell fate (percent)									
	Tipifarnib (µM)								
	DMSO	0.097	0.19	0.39	0.78	1.5	3.1	6.2	12.5
% cells surviving	98.5	89.7	80.3	95.7	98.8	95.9	84.8	58.8	0.0
% cells that died in mitosis	0.8	9.0	3.3	1.1	1.2	2.7	15.2	41.2	100.0
% cells that died in interphase	0.8	1.3	16.4	3.2	0.0	1.4	0.0	0.0	0.0

Figure 3.5 Tipifarnib treatment results in prolonged mitotic arrest. A) Experimental flow chart. HeLa pAAVS1-P-CAG-mCherry-H2B were treated with 0.097-12.5 µM Tipifarnib and then imaged every 10 minutes for 72 hours. Mitotic duration was calculated from chromosome condensation to anaphase. B) Determination of duration of mitosis and classification of phenotypes: 1) normal mitosis – mitosis duration was counted from the first observation of condensed prophase chromosomes (red arrow) to first observation of anaphase (blue arrow); 2) death in mitosis – mitotic duration was counted from prophase to first observation of apoptotic bodies without mitotic exit (yellow arrow); 3) Death in interphase – defined as observation of apoptotic bodies interphase (green arrow). Time-lapse interval was 10 minutes unless otherwise specified. C) 16 initial cells were tracked, with the mitotic duration shown. The median and mean mitotic duration are shown in the table. Statistical significance was determined by One-way ANOVA and Tukey's comparisons test. Asterisk (*) corresponds to significance between DMSO and indicated treatments (* $p<0.05$, ** $p < 0.01$, *** $p<0.001$ and **** $p < 0.0001$), D) Cell fate at 72 hours was noted, and then calculated as a percentage of total cells analyzed. Cells either survived (blue), died in mitosis (yellow) or died in interphase (purple). n inside the donut plots, is the total cells analyzed per condition. Table shows percentage of each cell fate per treatment. N = 16 initial cells, 2 biological replicates.

Our lab has previously shown that the loss of Spindly KT localization due to FTI treatment is not FTI or cell line specific.[44] The experiments discussed to date were to characterize Tipifarnib. Next, I investigated what sensitivity other cell lines have to Tipifarnib. I chose to test a range of breast cancer cell lines that our lab has. The cell lines tested are shown in table 3.1, and together comprise the 4 different molecular sub-types of breast cancer. The cell lines used are MCF-7, T-47D (Luminal A), BT-474 (Luminal B), SK-BR-3 (HER2+), MDA-MB-231, MDA-MB-468 (Triple negative). Additionally, 2 non-tumorigenic cell lines were used, MCF 10a and hTERT-HME-1 (HME-1). These cell lines were used to model the potential effect of Tipifarnib treatment on the non-tumorigenic breast tissue in a patient.

Cell line	Tissue type (ATCC)	Molecular sub-type	Hormone Receptor Status
HeLa	Cervical	N/A	N/A
MDA-MB-231	Mammary gland/breast	Basal, Triple negative	ER-, PR-, HER2-
MDA-MB-468	Mammary gland/breast	Basal, Triple negative	ER-, PR-, HER2-
MCF7	Mammary gland/breast	Luminal A	ER+/PR+, HER2-
T-47D	Mammary gland	Luminal A	ER+, PR+, HER2-
BT-474	Mammary gland/breast	Luminal B	ER+, PR-/+, HER2+ ER+/PR-/+, Ki67 high
SK-BR-3	Mammary gland/breast	HER2+	ER-, PR-, HER2+
MCF 10A*	Mammary gland/breast	N/A	N/A
hTERT-HME-1 (HME-1)	Mammary gland/breast	N/A	N/A

Table 3.1 Molecular subtypes of cell lines used in this study. Cell lines used in this study, with tissue of origin (from ATCC), and molecular classification as well as hormone receptor status.

To determine sensitivity to Tipifarnib, the cell lines were treated with 2 different ranges of Tipifarnib. The more sensitive cell lines: SK-BR-3, MCF-7, MCF 10a were treated with range of 4-25000 nM Tipifarnib, while the other 6 cell lines tested were treated with 97-25000 nM Tipifarnib. The cells were treated for 96 hours before being fixed with crystal violet, and from this the IC_{50} was calculated (Figure 3.6A).

SK-BR-3, MCF-7 and MCF 10a were found to be sensitive cell lines during preliminary tests. These cells were treated with a 1:4 serial dilution ranging from 4-25000 nM. 96 hours post treatment the cells were fixed with crystal violet and the IC_{50} was calculated (Figure 3.6A). MCF 10a was found to be the most sensitive cell line tested with an IC_{50} of 6nM (Figure 3.6B). While

MCF 10a is one of the non-tumorigenic cell lines, it is 7 times more sensitive than the next most sensitive cell line. Why MCF 10a is so sensitive is unknown, however it is possible as FTase as many roles in the cell, that a role for FTase outside mitosis is essential for MCF10a survival, and therefore Tipifarnib treatment results in inhibition of this role. SK-BR-3 and MCF-7 are the other 2 sensitive cell lines, with an IC_{50} of 58nM and 88nM respectively (Figure 3.6B). These 2 cell lines represent 2 different molecular subtypes of breast cancer, with SK-BR-3 being HER2+ and MCF-7 is Luminal A.

The remaining 6 cell lines, HeLa, MDA-MB-231, MDA-MB-468, BT-474, T-47D and HME-1 were treated with a 1:2 serial dilution ranging from 97-25000 nM (Figure 3.6A). 96 hours post treatment cells were fixed with crystal violet and the IC_{50} was calculated. Of these cell lines, HeLa is the most sensitive with an IC_{50} of 416 nM (Figure 3.6C). While this compared to the previous high content data (Figure 3.5), these HeLa cells are more sensitive. It could be that there are a larger proportion of cells dying between 72-96 hours that accounts for the difference in survival. At 72 hrs 390 nM of Tipifarnib resulted in 96% cell survival (Figure 3.5C). Or it could be that when the stable cell line was generated and selected for the resulting population is innately more resistant to Tipifarnib compared to the heterogenous population of HeLa used in this experiment.

The 2 triple negative cell lines, MDA-MB-231 and MDA-MB-468 have similar sensitivity to Tipifarnib, with IC_{50} of 1582 nM and 1730 nM respectively (Figure 3.6C). Triple negative breast cancer are generally harder to treat compared to others due to the lack of hormone receptors, and more epithelial nature[120] and this moderate sensitivity to Tipifarnib could be a potential treatment. Additionally, in MDA-MB-231, FTI treatment has been shown to reduce H-Ras

mediated epidermal growth factor (EGF) induced invasion.[123] This effect could potentially explain why these cells are more sensitive than other cell lines tested.

The second non-tumorigenic cell line I tested is HME-1 a human mammary epithelial cell line that was immortalized with human telomerase (hTERT). The HME-1 cell line has an IC_{50} of 3243 nM and is the second most resistant cell line. It appears whatever effects Tipifarnib is having that is resulting in the cancer cell line deaths does not appear to be resulting in HME-1 cell death. This is promising that Tipifarnib is not resulting in cell death in mammary epithelial cells. This difference is also promising when comparing the 2 triple negative cell lines, which tend to be more epithelial in nature.[120] HME-1 is ~2-fold more resistant to Tipifarnib than either triple negative cell line. Finally, BT-474, a Luminal B cell line, is the most resistant with an IC_{50} of 5664 nM. T-47D, which is a Luminal A cell line like SK-BR-3 but is much more resistant to Tipifarnib and has an IC_{50} of 3022 nM (Figure 3.6C). The 52-fold difference in IC_{50} between T-47D and MCF-7, shows that molecular subtype alone does not predict if a cell line, or subtype, will be sensitive or resistant to Tipifarnib.

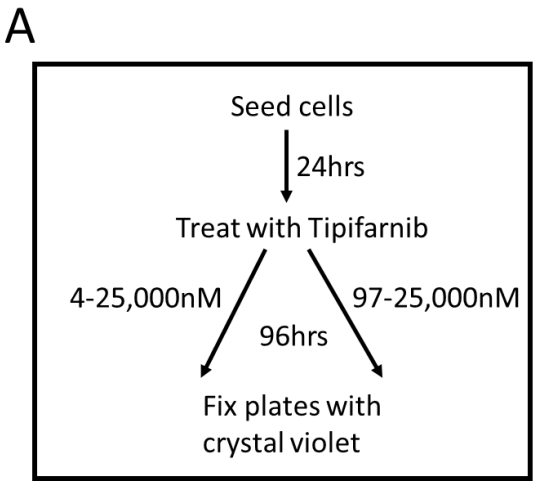

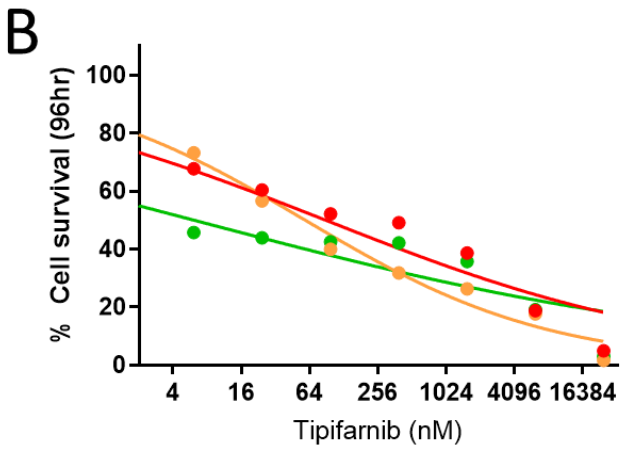

Cell Line	Tipifarnib IC50 (nM)
MCF7	88
SKBR3	58
MCF10a	6

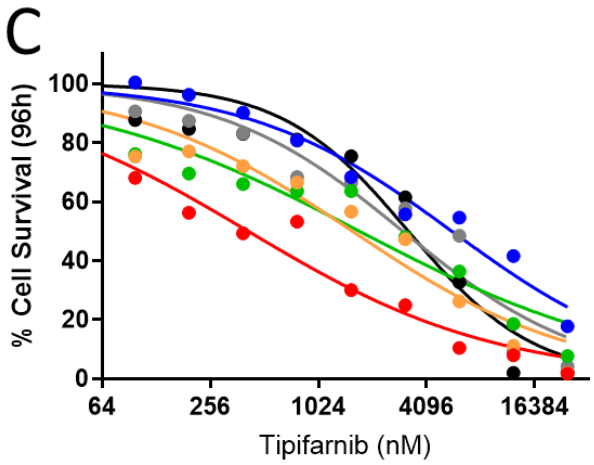

Cell Line	Tipifarnib IC50 (nM)
HeLa	416
MDA-MB-231	1582
MDA-MB-468	1730
BT-474	5664
T47D	3022
HME1	3243

Figure 3.6 Breast cancer cell lines show a varied response to Tipifarnib. A) Experimental flow chart. B) Cells were treated with 4-25000 nM Tipifarnib for 96 hours and then fixed with crystal violet and IC_{50} values determined. IC_{50} values shown in the table. C) Cells were treated with 97-25,000 nM Tipifarnib for 96 hours and then fixed with crystal violet and IC_{50} values determined. IC_{50} shown in table. N = 3, 6 replicates per n, 3 biological replicates

It does not appear that the molecular subtype corresponds to the sensitivity of cell lines to Tipifarnib (Figure 3.6B&C). Some had similar sensitivity, such as the 2 triple negative cell lines

MDA-MB-231 and MDA-MB-468. While the 2 Luminal A cell lines had a 52-fold difference in sensitivity. Molecular subtype alone does not appear to function as an accurate marker of sensitivity and other molecular markers are needed.

As the molecular subtype does not appear to function as a marker of sensitivity, we decided to examine Spindly and Farnesyltransferase β-subunit (FNTB) expression to determine if this correlates to sensitivity or resistance to Tipifarnib. FNTB is the subunit of FTase that binds both the peptide substrate and FPP,[59,60] and is present in equal stoichiometry to the α-subunit, which together comprise FTase. We enriched mitotic populations for the following western blots, as Spindly is a cell cycle regulated protein and its levels peak in mitosis.[37] Additionally, the range of cell lines tested all have different doubling times, from ~24hrs for HeLa cells to 60-80 hours for BT-474 cells. Due to this large range in doubling times an asynchronous population would not provide an accurate comparison of Spindly protein levels in the various cell lines.

Cell lines were treated with nocodazole for 16 hours to arrest cells in mitosis and then mitotic cell were collected via mitotic shake-off and extracts were made (Figure 3.7A). These extracts were then blotted for Spindly and FNTB protein levels in addition to total protein. Spindly and FNTB protein quantification was normalized to total protein and these normalized values are shown in Figure 3.7C.

Looking at Spindly protein levels, it does not appear to correspond to sensitivity or resistance to Tipifarnib seen in Figure 3.6B&C. HeLa cells are in the middle between the resistant and sensitive cell lines in terms of IC_{50} but have the highest levels of Spindly. While BT-474, the most

resistant cell line with an IC_{50} of 5664nM only has 13% of the amount of Spindly compared to HeLa cells.

FNTB on the other hand may relate to Tipifarnib sensitivity or resistance (Figure 3.7B&C). T-47D, one of the resistant cell lines, has approximately 3 times the amount of FNTB relative to HeLa cells and BT-474 cells, the most resistant cell line has 1.87 times relative to HeLa cells. While this shows potential to mark resistance, MCF-10a cells, which is the most sensitive cell line we tested, has 1.89 times the amount of FNTB compared to HeLa while being 70 times more sensitive to Tipifarnib than HeLa.

Neither Spindly nor FNTB protein levels alone appear to be a good marker of Tipifarnib sensitivity or resistance. However, as these 2 proteins work in conjunction, we wanted to see if the ratio of FNTB to Spindly could provide a clearer indicator of Tipifarnib effect. If there is more FNTB, then there could be an increased amount of FTase, requiring higher concentrations of Tipifarnib to fully inhibit.

Only HeLa cells have a higher ratio of Spindly to FNTB protein, in the remaining 8 cell lines there is more FNTB than Spindly, but the degree to which there is more varies by cell lines. In some cell lines this ratio appears to correspond to resistance, HME-1, T-47D, BT-474 all have high ratios of FNTB:Spindly, with 14.94, 9.46, and 12.93 respectively. This could account for the resistance as there is more FTase that needs to be inhibited before Spindly KT recruitment is impaired. However, SK-BR-3, which is one of the most sensitive cell lines has a ratio of 10.64, so it does not appear that this holds true in all cases. Additionally, the 2 triple negative cell lines MDA-MB-231 and MDA-MB-468 have similar IC_{50} values (1582nM and 1730nM respectively); but

have a ~3-fold difference between the FNTB:Spindly ratio, with MDA-MB-231 having 3.98, and MDA-MB-468 being 1.27.

We then compared the ratio of FNTB:Spindly, the normalized Spindly protein level and normalized FNTB level to the cell lines IC_{50} to examine if a trend was present (Figure 3.7D). None of these comparisons appear to act as a clear indicator of sensitivity. Spindly protein vs Tipifarnib IC_{50} shows a trend of increased Spindly protein levels resulting in increased sensitivity to Tipifarnib. Neither Spindly, FNTB or the ratio of FNTB:Spindly appear to act as a consistent marker of sensitivity or resistance. However, if other markers that can predict sensitivity are discovered, this may be able to be used in combination to determine what patients could benefit from Tipifarnib treatment.

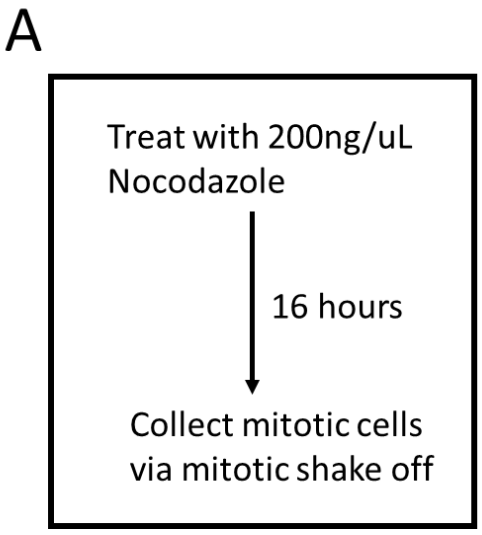

B

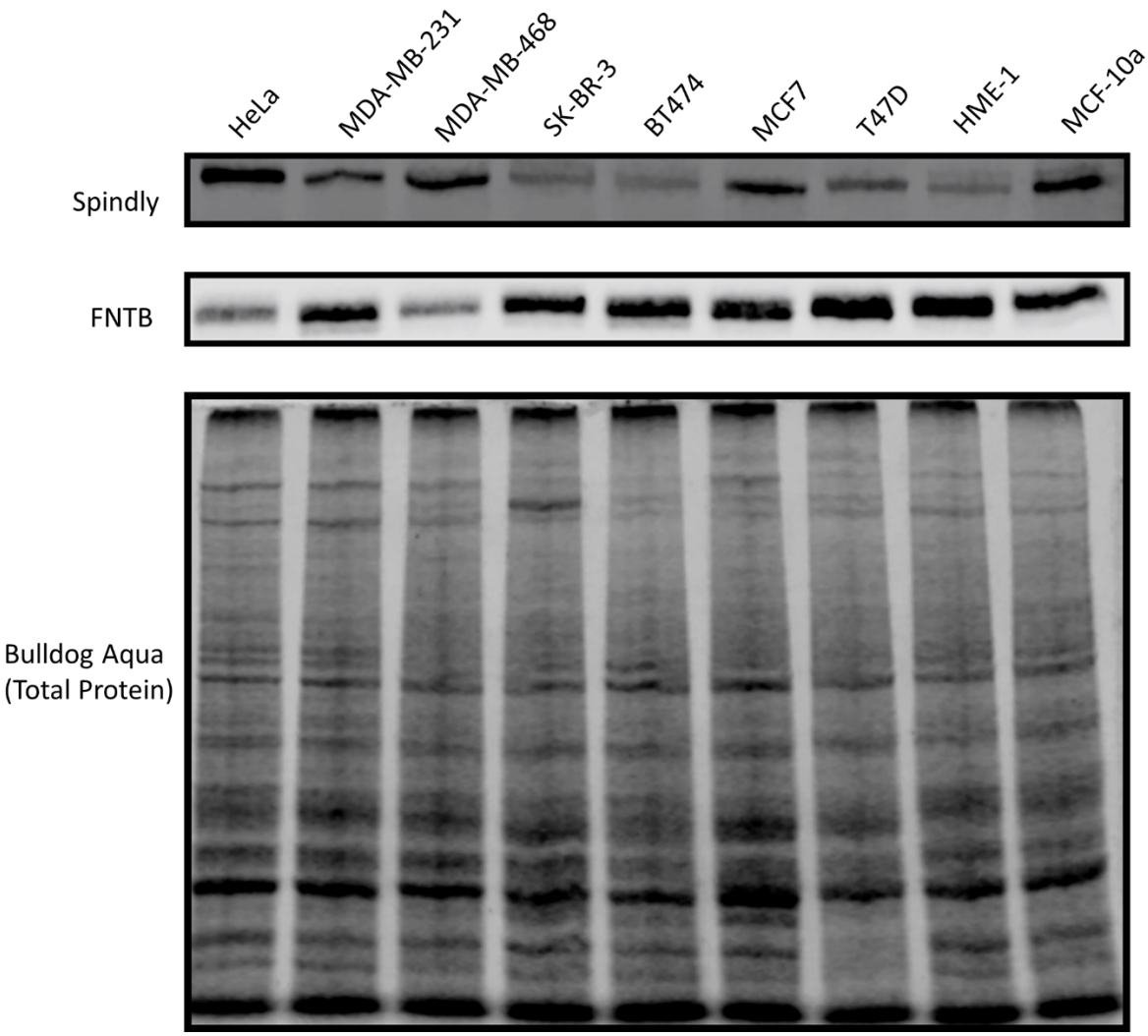

C

			Protein quantification normalized to HeLa	
Cell Line	IC50 (nM)	FNTB:Spindly ratio	Spindly	FNTB
HeLa	415	0.82	1.00	1.00
MM231	1582	3.98	0.29	1.41
MM468	1730	1.27	0.47	0.73
SKBR3	58	10.64	0.12	1.51
BT474	5664	12.93	0.12	1.87
MCF7	88	3.30	0.40	1.59
T47D	3022	9.46	0.27	3.09
HME-1	3243	14.94	0.14	2.62
MCF10a	6	2.92	0.53	1.89

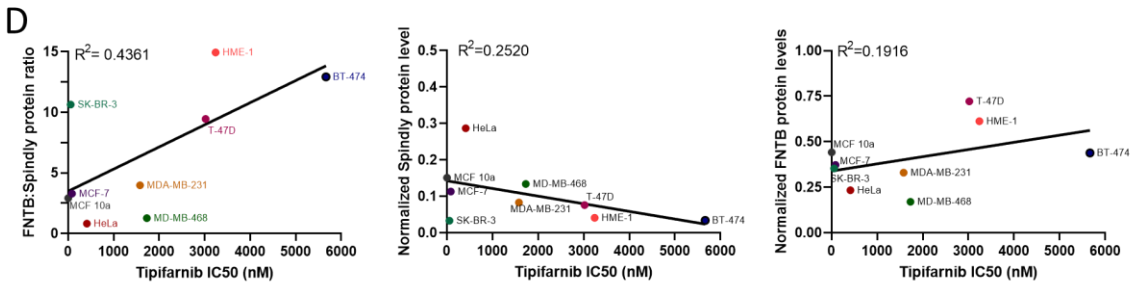

Figure 3.7 Spindly and FNTB levels do not to correspond to Tipifarnib sensitivity or resistance. A) Experimental flow chart. Cells treated with 200 ng/mL nocodazole for 16 hours and then mitotic cells collected via mitotic shake off. Cells were processed for Western Blot and membranes blotted for Spindly and FNTB. Total protein was determined via Bulldog Aqua stain. B) Western blot showing mitotic levels of Spindly and FNTB. Spindly and FNTB quantification is shown relative to total protein, all normalization was done post this calculation. C) Table shows each cell line's IC_{50}, the ratio of FNTB:Spindly and the protein quantification normalized to HeLa for Spindly and FNTB. D) FNTB:Spindly protein ratio, Spindly protein levels and FNTB protein levels plotted with Tipifarnib IC_{50}. Simple regression was done to determine if there was a relationship between protein levels and Tipifarnib IC_{50}. N = 3 biological replicates

3.2 Tipifarnib and Adavosertib combination treatment

Previously our lab had investigated the combination of Adavosertib with various other anti-mitotic agents, each with a different mechanism of action to examine the combined effect. We found that Wee1 inhibition sensitized breast cancer cells to paclitaxel.[105] Another anti-mitotic that was tested was the FTI L-744-832, and it was found to result in longer duration of mitosis, decreased colony formation, and increased cell death in HeLa cells.[124] This portion of my thesis expands upon this preliminary work, by combining Tipifarnib, one of the 2 FTIs that is currently in use for clinical trials, with Adavosertib. I tested the combination of Adavosertib and Tipifarnib in the cell lines shown in table 3.1.

Prior to any combination experiments we needed to determine the IC_{50} for the cell lines to Adavosertib alone. Cells were treated with a range of Adavosertib (125-2000 nM) for 96 hours. Plates were then fixed using crystal violet and IC_{50} was calculated (Figure 3.8A).

The cell lines tested showed a range of sensitivity to Adavosertib. HeLa cells were the most sensitive, with an IC_{50} of 278 nM. The breast cancer cell lines showed a range of sensitivity, with MDA-MB-231 being the most sensitive, with an IC_{50} of 237 nM, to T-47D with an IC_{50} of 824 nM. The 2 non-tumorigenic cell lines, MCF10a and HME-1 had IC_{50} values of 495 nM and 824 nM respectively.

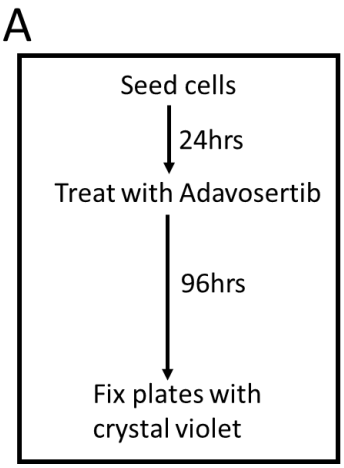

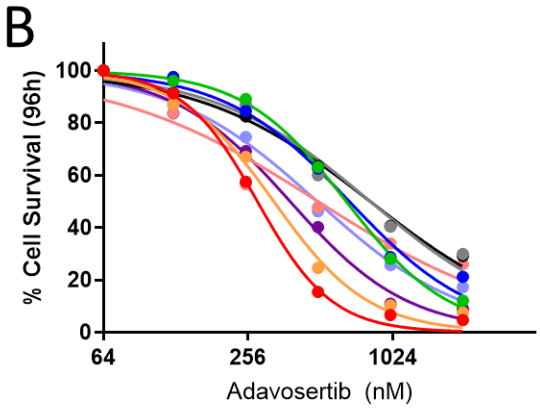

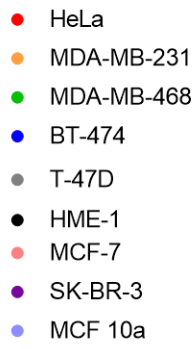

	Adavosertib IC50 (nM)
HeLa	278
MDA-MB-231	327
MDA-MB-468	654
BT-474	675
SKBR3	383
T47D	824
MCF7	500
MCF10a	495
HME1	824

Figure 3.8 Cell lines display range of sensitivity to Adavosertib. A) Experimental flow chart. Cells were treated with 4-25,000 nM Tipifarnib for 96 hours and then fixed with crystal violet and IC_{50} values determined. B) IC_{50} values shown in the table. % cell survival is shown on the y-axis, and concentration of Adavosertib (nM) on the x-axis. C) Cells were treated with 97-25,000 nM Tipifarnib for 96 hours and then fixed with crystal violet and IC_{50} values determined. IC_{50} shown in table. N = 3 biological replicates

Once the IC_{50} was established for each cell line, and the relative sensitivity to Adavosertib and Tipifarnib mono-treatments was known we investigated the results of combination treatment. We wished to see the effect of the combination treatment to determine if the combination is synergistic in any of the cell lines tested. If it is synergistic, this allows for a lower dose of Tipifarnib and Adavosertib to be used compared to either monotreatment.

Cells were treated with a range of Tipifarnib (0.097-25 µM) and Adavosertib (125-2000 nM) for 96 hours, and cell viability was determined using the crystal violet viability assay (Figure 3.9A). From the crystal violet data, percent survival was calculated relative to the solvent control DMSO. This is shown in the cell viability heatmaps in Figure 3.9B, with the concentration of Adavosertib (nM) on the y-axis and concentration of Tipifarnib (nM) on the x-axis. Higher percent survival is shown as darker red, with the darkest being 100% survival. The lighter the colour, the lower the percentage survival, with white being 0% survival. The table below the heat maps shows the most synergistic combination for each cell line, and the IC_{50} the mono-treatment of Tipifarnib and Adavosertib.

Synergy was determined using Bliss CI values, where a value <1, is synergistic, with <0.7 being strongly synergistic. If the value is equal to 1, then the combination is additive and if it is >1.0, then the combination is antagonistic.[118] The Bliss CI score for all concentrations tested are shown

in the heat maps on the right of column of 3.9B. White is antagonistic combinations, grey is additive. If the combination is synergistic, it is teal and if it is strongly synergistic then it is purple.

All cell lines tested showed a range of response, with varying degrees of synergy. MCF 10a had a Bliss CI of 1.01 (Figure 3.9B), meaning the combination of Tipifarnib and Adavosertib is essentially additive. The combination was synergistic in the remaining 8 cell lines tested. MCF-7 had a Bliss CI of 0.96, while it is synergistic, similar to MCF 10a, it is barely so and is closer to being additive. HeLa (Bliss CI=0.72) MDA-MB-231 (Bliss CI=0.90), MDA-MB-468 (Bliss CI=0.81), SK-BR-3 (Bliss CI=0.8), HME-1 (Bliss CI=0.74) were all synergistic combinations (Figure 3.9B). HeLa and HME-1 were both near strong synergy, with Bliss CI of 0.72 and 0.74 respectively. BT-474 (Bliss CI=0.68) and T-47D (Bliss CI=0.46) were both strongly synergistic (Figure 3.9B), with T-47D being the cell line in which the strongest synergy was observed.

The synergistic effect of Tipifarnib and Adavosertib does not appear to correlate with the breast cancer subtype that the cell lines make up. MCF-7 and T-47D are both Luminal A (ER+, PR+, HER2-) cell lines, however MCF-7 is weakly synergistic, with a Bliss CI value of 0.96, while T-47D was the cell line that had the most synergistic combination, with a Bliss CI value of 0.46 (Figure 3.9C). To achieve 50% cell death with Tipifarnib or Adavosertib monotreatment in T-47D, it required 6250 nM Tipifarnib or 1000 nM Adavosertib. While the combination treatment required just 97 nM and 500 nM of Tipifarnib and Adavosertib respectively, to result in 50% cell death and the most synergistic combination was 97 nM Tipifarnib and 125 nM Adavosertib. This is much lower than either mono-treatment alone. T-47D was one of the most resistant cell lines

to Tipifarnib, and this combination treatment resulted in a 31-fold decrease in the concentration of Tipifarnib required.

BT-474 was the cell line most resistant to Tipifarnib with an IC_{50} of 5664 nM; when treated with the combination treatment, it was strongly synergistic (Bliss CI=0.68, Figure 3.9B). Additionally, the concentration at which it was most synergistic was 195 nM Tipifarnib and 250 nM Adavosertib, which is an almost 30-fold decrease in the concentration of Tipifarnib required relative to the IC_{50}. The effectiveness of the Tipifarnib Adavosertib combination treatment in both BT-474 and T-47D, resulting in much lower concentrations of Tipifarnib, and Adavosertib to a lesser extent, emphasizes the benefits of exploiting synergy, cells that might survive either drug alone, are killed at much lower doses when these drugs are used in combination. Based of this data, the combination of Tipifarnib and Adavosertib is synergistic to varying degrees depending on the cell line tested and this does not appear to be molecular subtype specific. However, if it can be elucidated which cell lines will be more responsive to this therapy, it could indicate eventually which patients in the clinic could benefit from the combination.

A

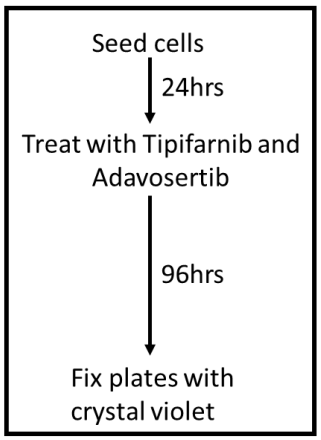
Seed cells
24hrs
Treat with Tipifarnib and Adavosertib
96hrs
Fix plates with crystal violet

B

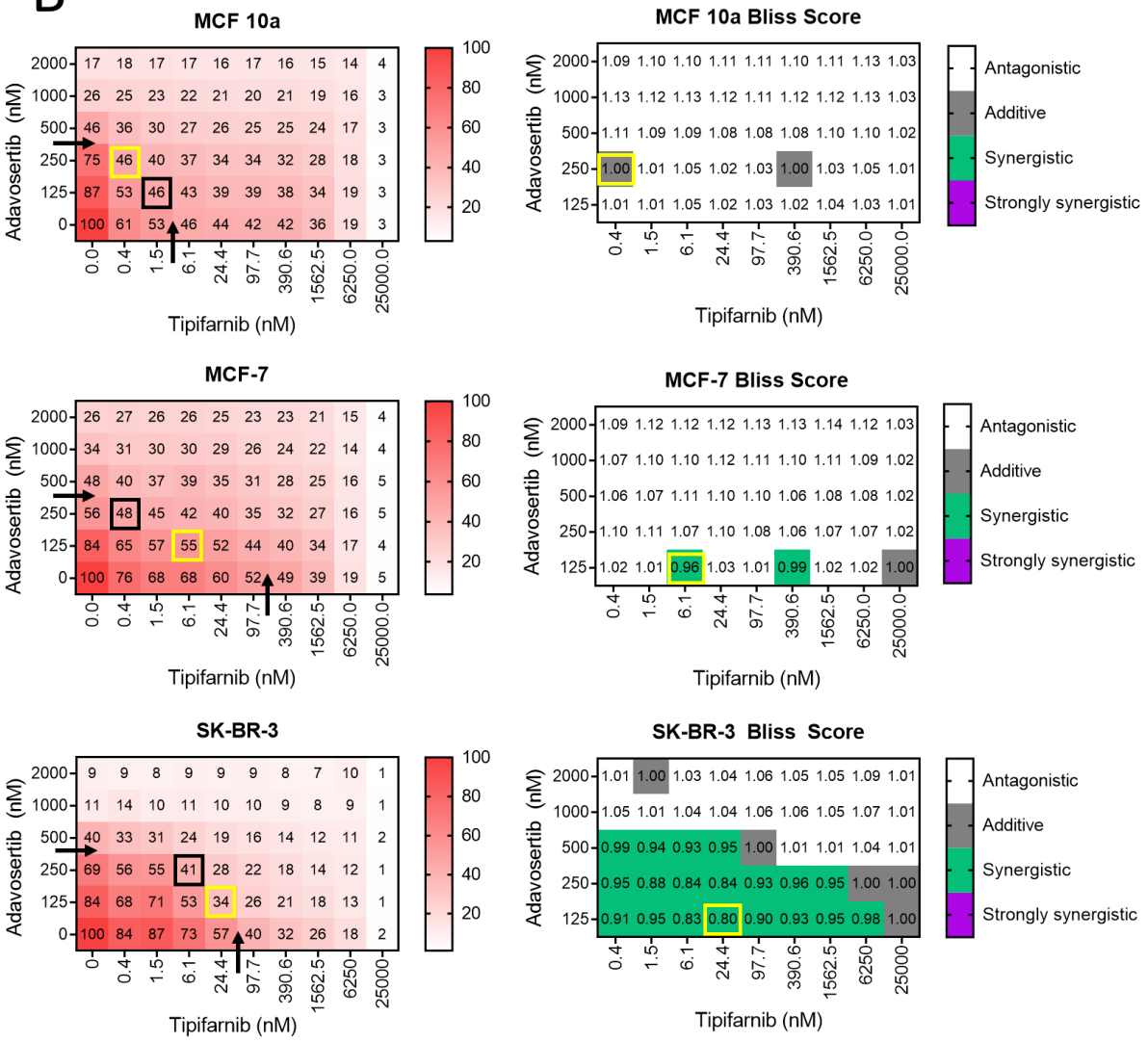
MCF 10a
MCF 10a Bliss Score
MCF-7
MCF-7 Bliss Score
SK-BR-3
SK-BR-3 Bliss Score
Adavosertib (nM)
Tipifarnib (nM)
Antagonistic
Additive
Synergistic
Strongly synergistic

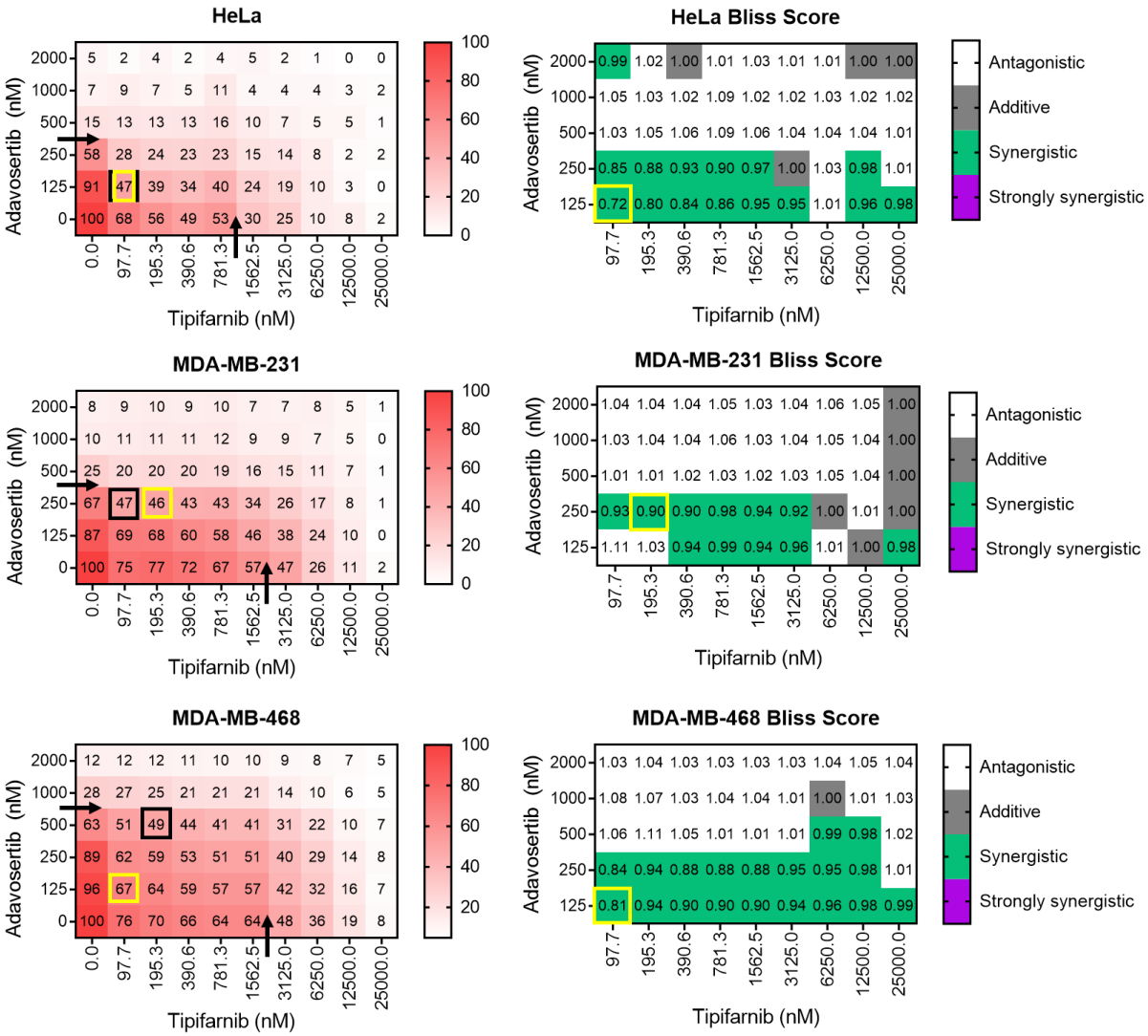
HeLa
Adavosertib (nM)
2000 5 2 4 2 4 5 2 1 0 0
1000 7 9 7 5 11 4 4 4 3 2
500 15 13 13 13 16 10 7 5 5 1
250 58 28 24 23 23 15 14 8 2 2
125 91 47 39 34 40 24 19 10 3 0
0 100 68 56 49 53 30 25 10 8 2
0.0 97.7 195.3 390.6 781.3 1562.5 3125.0 6250.0 12500.0 25000.0
Tipifarnib (nM)
100 80 60 40 20 0
HeLa Bliss Score
Adavosertib (nM)
2000 0.99 1.02 1.00 1.01 1.03 1.01 1.01 1.00 1.00
1000 1.05 1.03 1.02 1.09 1.02 1.02 1.03 1.02 1.02
500 1.03 1.05 1.06 1.09 1.06 1.04 1.04 1.04 1.01
250 0.85 0.88 0.93 0.90 0.97 1.00 1.03 0.98 1.01
125 0.72 0.80 0.84 0.86 0.95 0.95 1.01 0.96 0.98
97.7 195.3 390.6 781.3 1562.5 3125.0 6250.0 12500.0 25000.0
Tipifarnib (nM)
Antagonistic
Additive
Synergistic
Strongly synergistic
MDA-MB-231
Adavosertib (nM)
2000 8 9 10 9 10 7 7 8 5 1
1000 10 11 11 11 12 9 9 7 5 0
500 25 20 20 20 19 16 15 11 7 1
250 67 47 46 43 43 34 26 17 8 1
125 87 69 68 60 58 46 38 24 10 0
0 100 75 77 72 67 57 47 26 11 2
0.0 97.7 195.3 390.6 781.3 1562.5 3125.0 6250.0 12500.0 25000.0
Tipifarnib (nM)
100 80 60 40 20 0
MDA-MB-231 Bliss Score
Adavosertib (nM)
2000 1.04 1.04 1.04 1.05 1.03 1.04 1.06 1.05 1.00
1000 1.03 1.04 1.04 1.06 1.03 1.04 1.05 1.04 1.00
500 1.01 1.01 1.02 1.03 1.02 1.03 1.05 1.04 1.00
250 0.93 0.90 0.90 0.98 0.94 0.92 1.00 1.01 1.00
125 1.11 1.03 0.94 0.99 0.94 0.96 1.01 1.00 0.98
97.7 195.3 390.6 781.3 1562.5 3125.0 6250.0 12500.0 25000.0
Tipifarnib (nM)
Antagonistic
Additive
Synergistic
Strongly synergistic
MDA-MB-468
Adavosertib (nM)
2000 12 12 12 11 10 10 9 8 7 5
1000 28 27 25 21 21 21 14 10 6 5
500 63 51 49 44 41 41 31 22 10 7
250 89 62 59 53 51 51 40 29 14 8
125 96 67 64 59 57 57 42 32 16 7
0 100 76 70 66 64 64 48 36 19 8
0.0 97.7 195.3 390.6 781.3 1562.5 3125.0 6250.0 12500.0 25000.0
Tipifarnib (nM)
100 80 60 40 20
MDA-MB-468 Bliss Score
Adavosertib (nM)
2000 1.03 1.04 1.03 1.03 1.03 1.03 1.04 1.05 1.04
1000 1.08 1.07 1.03 1.04 1.04 1.01 1.00 1.01 1.03
500 1.06 1.11 1.05 1.01 1.01 1.01 0.99 0.98 1.02
250 0.84 0.94 0.88 0.88 0.88 0.95 0.95 0.98 1.01
125 0.81 0.94 0.90 0.90 0.90 0.94 0.96 0.98 0.99
97.7 195.3 390.6 781.3 1562.5 3125.0 6250.0 12500.0 25000.0
Tipifarnib (nM)
Antagonistic
Additive
Synergistic
Strongly synergistic

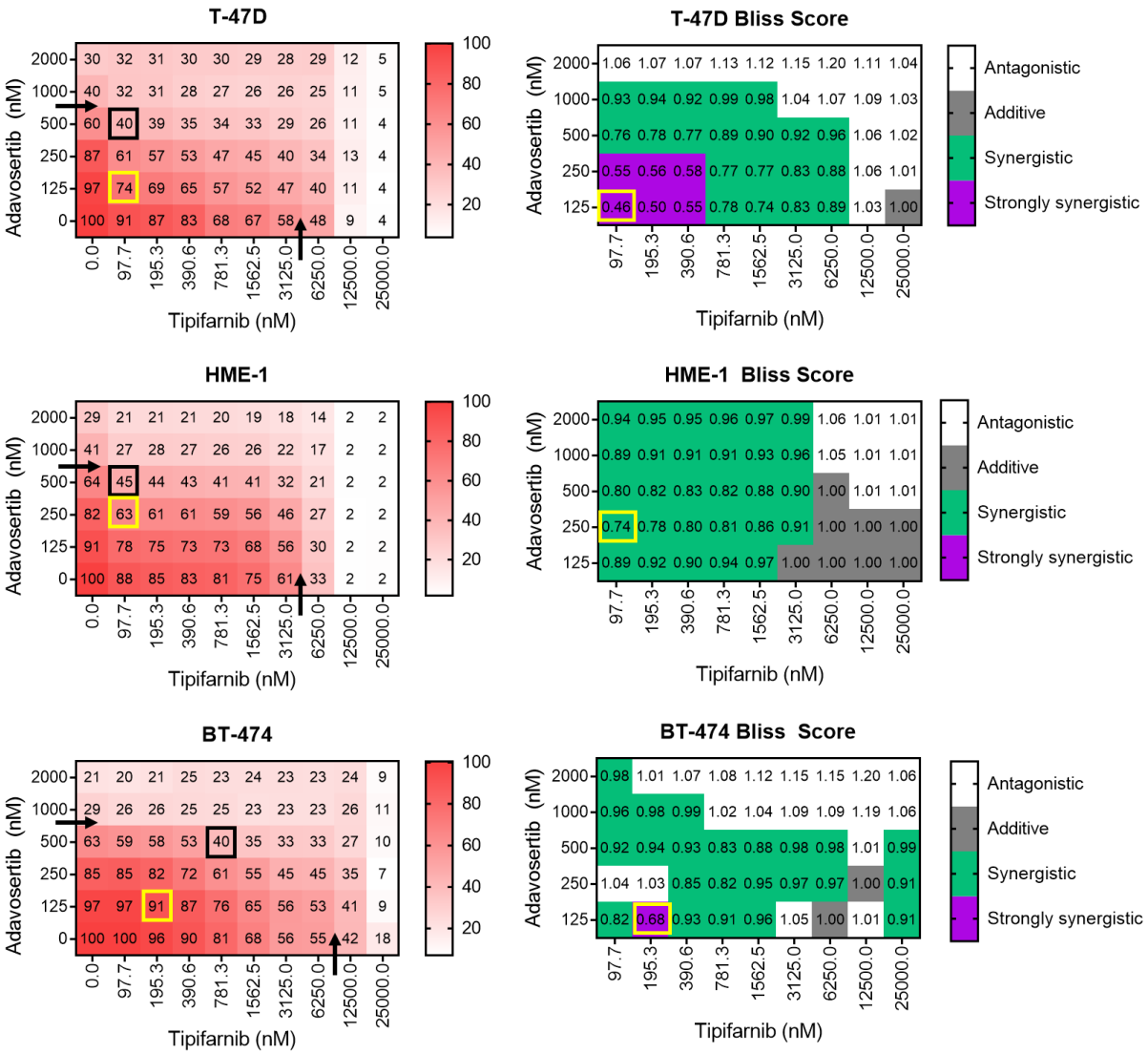

C

Cell Line	Bliss CI	Tipifarnib (nM)	Adavosertib (nM)	Tipifarnib IC50 (nM)	Adavosertib IC50 (nM)
HeLa	0.72	97.7	125	416	278
MDA-MB-231	0.9	195.3	250	1582	327
MDA-MB-468	0.81	97.7	125	1730	654
BT-474	0.68	195.3	125	5664	675
SKBR3	0.8	24.4	125	58	383
T47D	0.46	97.7	125	3022	824
MCF7	0.96	6.1	125	88	500
MCF10a	1.01	0.4	125	6	495
HME1	0.74	97.7	250	3243	824

Figure 3.9 Tipifarnib and Adavosertib combination treatment is synergistic to varying degrees in different cell lines A) Experimental flow chart. Cells were seeded and treated with range of Tipifarnib and Adavosertib for 96 hours. Plates were fixed with crystal violet and percent

survival calculated. B) Left column, Cell viability heat maps are shown with concentration of Adavosertib (nM) on the y-axis and concentration of Tipifarnib (nM) on the x-axis. Colour bars indicate percentage survival normalized to untreated cells. Arrow is the concentration at which 50% cell survival occurred for each drug alone. The black box is 50% cell survival of combination treatment and the yellow box is the combination that resulted in the most synergistic combo. Right column, Bliss score map of all concentrations. Antagonistic= white, additive= grey, synergistic= teal, strongly synergistic= purple. Most synergistic combination shown with yellow box. Values shown were the mean of n=3. C) Bliss combination indices (CIs) at indicated drug concentrations were calculated. A Bliss CI of less than 1 indicates synergy, a CI of less than 0.7 strong synergy, and a CI of greater than 1 antagonism. The most synergistic combination Tipifarnib and Adavosertib and the mono-treatment IC_{50} are shown. Synergy was calculated from mean of n = 3.

Tipifarnib and Adavosertib result in mitotic arrest through differing mechanisms. Adavosertib results in premature entry into mitosis and prolonged mitotic duration due to the inhibition of Wee1,[110] while FTI treatment both in the literature (L744832, FTI-277) and my own results (Figure 3.1) causes a prolonged mitotic arrest due to loss of Spindly mediated dynein/dynactin KT localization.[44,43] Tipifarnib treatment inhibits Spindly farnesylation, therefore if Spindly has already been farnesylated prior to Tipifarnib treatment, the mitosis will proceed as normal without a prometaphase arrest. As Adavosertib treatment results in premature entry to mitosis and has been shown to cause this mitotic entry only a few hours following treatment, Spindly could be farnesylated and thus the effects of Tipifarnib will not be seen. We wished to investigate whether the order in which Tipifarnib and Adavosertib treatment occurs alters the synergy observed.

The order of addition experiments was tested in a subset of cell lines. HeLa, MDA-MB-231, MDA-MB-468 and BT-474 were selected for the following reasons: HeLa which were used for the previous Tipifarnib characterization, MDA-MB-231 and MDA-MB-468 which both have

moderate sensitivity to Tipifarnib treatment alone. Finally, BT-474 was selected as it was the most resistant to Tipifarnib, with an IC_{50} of 5664 nM and was a strongly synergistic combination.

Cells were seeded and then after 24 hours treated with one of three conditions. Simultaneous addition was the same as seen in Figure 3.9, where both Tipifarnib and Adavosertib were added together. Tipifarnib first, the cells were first treated with Tipifarnib, and then 24 hours following this treatment Adavosertib was added. Adavosertib first, cells were treated with Adavosertib, and then 24 hours later they were treated with Tipifarnib (Figure 3.10A). The 24-hour delay between the 2 staggered additions was selected as when these experiments were initiated the shortest time that FTI treatment was known to result in loss of Spindly KT localization was 24 hours. All plates were treated for a total of 96 hours from the time when the first drug was added (or both in the case of the simultaneous addition), and then the crystal violet viability assay was performed. Percent survival was calculated relative to the solvent control, DMSO, and this is shown in the cell viability heat maps in Figure 3.10B. The cell viability heat maps are the same as seen in Figure 3.9B, where the concentration of Adavosertib (nM) is on the y-axis and concentration of Tipifarnib (nM) on the x-axis. The higher percent cell survival is shown as darker red, with the darkest being 100% survival. While the lighter the colour, the lower the percentage cell survival, with white being 0% survival. Synergy was determined using Bliss CI values, where a value <1, is synergistic, with <0.7 being strongly synergistic. If the value is equal to 1, then the combination is additive and if it is >1.0, then the combination is antagonistic.[118]

For HeLa cells, when the two drugs are added simultaneously or Tipifarnib first, the same concentrations of Tipifarnib and Adavosertib alone result in 50% cell survival (black arrows, Figure

3.10B). Additionally, the same combination is the most synergistic, 97 nM Tipifarnib and 125 nM Adavosertib, but the Bliss CI scores are different, with simultaneous addition being slightly more synergistic with a Bliss score of 0.72 vs. 0.78 for Tipifarnib first. When Adavosertib is added first, a much higher concentration of Tipifarnib alone is required for 50% cell survival, 3125 nM compared to the 390 nM for Tipifarnib first, an 8-fold increase. It also requires a lower concentration of Adavosertib, 250 nM instead of 500 nM. The combination of 97 nM Tipifarnib and 125 nM Adavosertib is less synergistic with a Bliss CI of 0.92 (Figure 3.10C).

Similar to HeLa cells, when the 2 drugs are added simultaneously or Tipifarnib first in MDA-MB-231 cells, the same concentrations result in 50% survival as monotreatment's, 500 nM Adavosertib and 3125 nM Tipifarnib (Figure 3.10B). Adavosertib first, required a lower concentration of Adavosertib, 250 nM but again a higher concentration of Tipifarnib, 6250 nM (Figure 3.10B). When looking at the most synergistic combination in the simultaneous addition- 97nM Tipifarnib and 250 nM Adavosertib in Tipifarnib first was slightly more synergistic with a Bliss CI of 0.89 compared to the simultaneous addition Bliss CI of 0.90. As these values are so close it appears that in MDA-MB-231 cells, either simultaneous addition or Tipifarnib first seem to have the same result, with an equally synergistic combination. When Adavosertib was added first, the combination that was equally synergistic in both simultaneous and Tipifarnib first is now an antagonistic combination, with a Bliss CI of 1.07.

The above trend seen in HeLa and MDA-MB-231 cells is also seen in MDA-MB-468 cells. The concentration of either treatment alone that results in 50% cell survival are identical in the simultaneous addition and Tipifarnib first, 1000 nM Adavosertib, 3125 nM Tipifarnib. And that

when treating with Adavosertib first, a lower concentration of Adavosertib, 500 nM and a higher concentration of Tipifarnib, 12500 nM is required (Figure 3.10B). When looking at the most synergistic combination when treated with Tipifarnib and Adavosertib simultaneously was the most synergistic at 195 nM Tipifarnib and 500 nM Adavosertib with a Bliss CI of 0.81, and both Tipifarnib first and Adavosertib first are less synergistic, with Bliss CI of 0.88 and 0.94 respectively.

BT-474 again follows the same trend, where both simultaneous and Tipifarnib first have identical concentrations for either compound alone to result in 50% cell survival, with 1000 nM Adavosertib, and 12500 nM Tipifarnib. When treated with Adavosertib first, again the same is seen where a lower concentration of Adavosertib is required for 50% cell survival, 500 nM, and 25000 nM Tipifarnib is required (Figure 3.10B). The combination that is the most synergistic in the simultaneous treatment was 195 nM Tipifarnib and 125 nM Adavosertib, with a Bliss CI of 0.68. When treated with Tipifarnib first, this combination is now antagonistic, and when treated with Adavosertib first, there is very little cell killing at this combination of Tipifarnib and Adavosertib (195 nM Tipifarnib and 125 nM Adavosertib) (Figure 3.10B&C).

When comparing simultaneous addition to Tipifarnib first, in the 4 cell lines tested, the same concentration is required to result in 50% cell survival from either compound alone, and in HeLa, MDA-MB-231, MDA-MB-468 but not BT-474 cells they result in similar synergistic values. The antagonistic relationship in BT-474 cells may be due to the long doubling time. It is possible that the BT-474 cells did not have a large percentage entering mitosis prior to Adavosertib treatment, and that the premature mitotic entry due to Adavosertib treatment is needed for this combination to be synergistic. While when the cell lines were treated with Adavosertib first, it

resulted in a lower concentration of Adavosertib for 50% cell survival but a higher concentration of Tipifarnib being required. Additionally, in all cell lines treated with Adavosertib first, there is a lower percent cell survival compared to Tipifarnib first. It is possible that the increased cell killing observed was due to Adavosertib and not the combination treatment. Altering the order of the addition did not make the combination more synergistic, in all cases it made it less synergistic, or antagonistic in some cases. Based on this we did not proceed further with these experiments as staggering the addition did not greatly increase synergy.

A

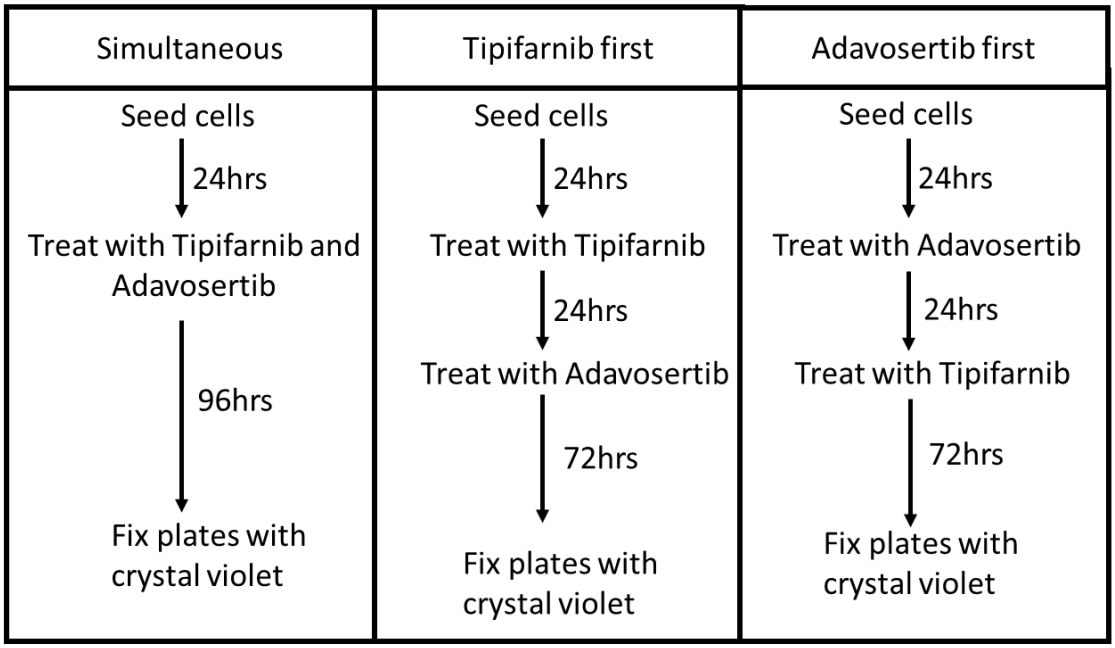

B

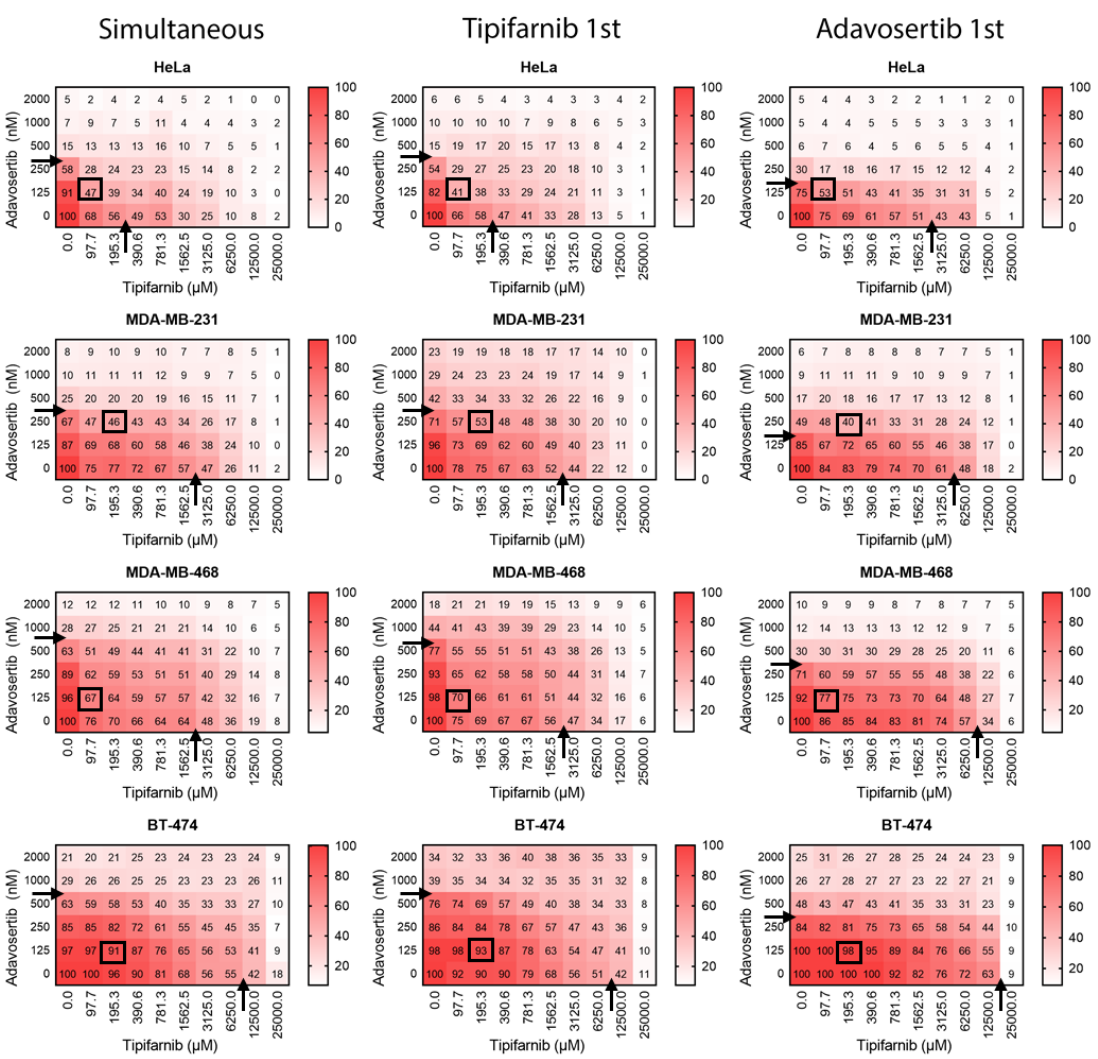

C

	Concentration		Simultaneous		Tipifarnib First		Adavosertib first	
	Tipifarnib(nM)	Adavosertib (nM)	Bliss CI	% Survival	Bliss CI	% Survival	Bliss CI	% Survival
HeLa	97.7	125	0.72	47	0.78	41	0.92	53
MDA-MB-231	195.3	250	0.90	46	0.89	53	1.07	40
MDA-MB-468	97.7	125	0.81	67	0.88	70	0.94	77
BT-474	195	125	0.68	91	1.53	93	0**	98

Figure 3.10 Order of Addition. A) Experimental flow chart. Cells were seeded and treated with either Simultaneous, Tipifarnib first or Adavosertib first for 96 hours. Plates were fixed with crystal violet and percent survival calculated. B) Cell viability heat maps are shown with concentration of Adavosertib (nM) on the y-axis and concentration of Tipifarnib (nM) on the x-axis. Color bars indicate percentage survival normalized to untreated cells. Arrow is the concentration at which 50% cell survival occurred. The black box is 50% cell survival of

combination treatment Mean of n=3 is shown. C) Bliss combination indices (CIs) at indicated drug concentrations were calculated. A Bliss CI of less than 1 indicates synergy, a CI of less than 0.7 strong synergy, and a CI of greater than 1 antagonism. The most synergistic combination Tipifarnib and Adavosertib and the mono-treatment IC_{50} are shown. Synergy was calculated from mean of n = 3.

3.3 Tipifarnib resistant cells

As the levels of Spindly and FNTB did not correspond to Tipifarnib sensitivity or resistance we wanted to investigate how cells might acquire resistance to Tipifarnib. HeLa pAAVS1-P-CAG-mCherry-H2B cells were treated with 1µM and 2µM Tipifarnib for 3 months. 1µM and 2µM Tipifarnib was selected based on the IC_{50} of the parental cell line, which is 1459 nM. Initially the majority of cells died, however after a few weeks the surviving population took over, generating the resistant cells. These surviving Tipifarnib resistant cells were used for the following experiments. The parental cell line is labelled as parental, and the 1µM and 2µM resistant cells as 1µM Tipi^R and 2µM Tipi^R respectively.

Prior to any experiments being completed, we verified that the resistant cells had a higher IC_{50} relative to the parental cell line. Cells were treated with a 0.097-25 µM Tipifarnib for 72 hours and then fixed with crystal violet. Percent survival relative to the control (DMSO) was calculated and from this IC_{50} was determined (Figure 3.11A).

As shown in figure 3.11B the resistant cells have increased IC_{50} values, with 1µM Tipi^R having an IC_{50} of 2136 nM and 2µM Tipi^R having an IC_{50} of 4752 nM. This is a 1.46- and 3.3-fold increase respectively relative to the parental cell line. The parental cell line has a different IC_{50} compared to the HeLa used in the previous experiments. This is due to the selection that was required for the generation of the HeLa pAAVS1-P-CAG-mCherry-H2B. The cells were transfected and then

underwent puromycin selection to kill any cells that were not positive. Following this selection, single colonies were grown and selected, and 6 colonies were mixed to form the parental population of cells. This higher IC_{50} in these cells is most likely due to the cells that formed this parental population having a higher resistance to Tipifarnib compared to the heterogenous population of HeLa cells used in the previous experiments.

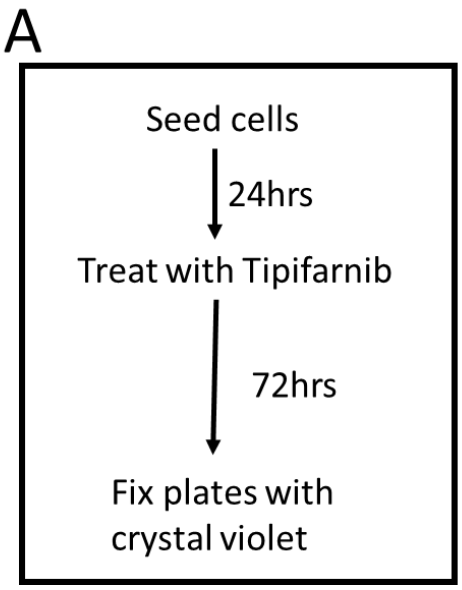

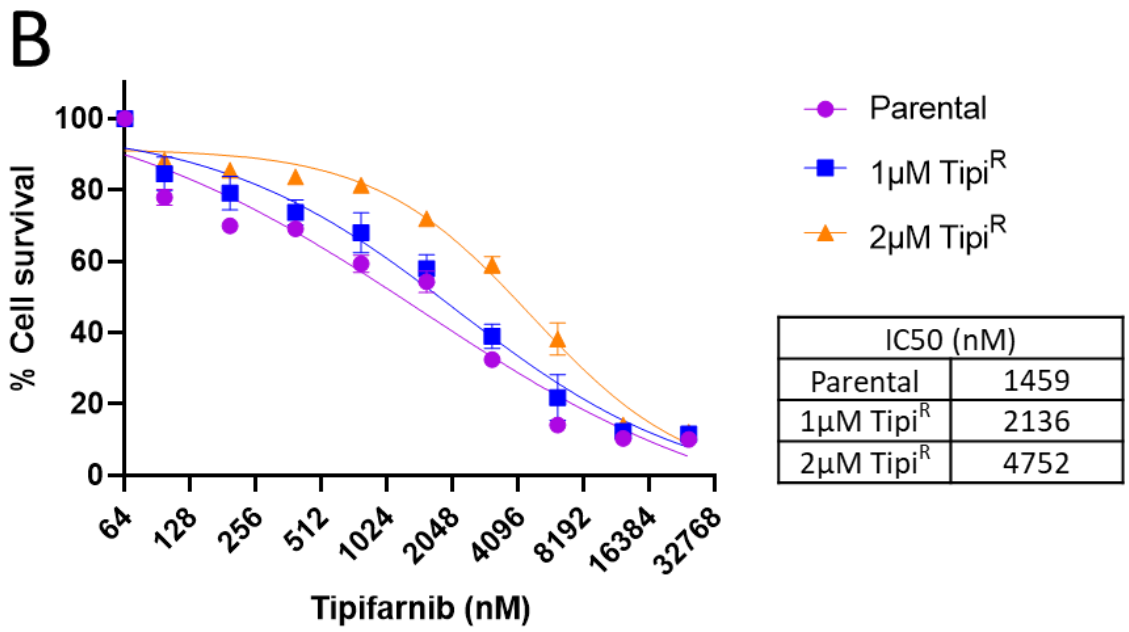

IC50 (nM)	
Parental	1459
1μM Tipi^R	2136
2μM Tipi^R	4752

Figure 3.11 Tipifarnib resistant cells have increased resistance to Tipifarnib. A) Experimental flow chart. Cells were seeded, treated with range of Tipifarnib (97-25,000 nM) for 72 hours. Plates were fixed with crystal violet and percent survival calculated. B) Percent cell survival y-axis, concentration of Tipifarnib (nM) on the X-Axis. IC_{50} in nM shown in table. N = 6 per replicate, 3 biological replicates

Once the resistance had been confirmed, we investigated the protein levels of Spindly and FNTB to determine if this is resistance was due to upregulation of either of these proteins. In Figure 3.7 Spindly and FNTB levels were examined only in mitotic cells, as Spindly is a mitotic protein. For the following experiment we compared interphase and mitotic extracts, as Spindly protein levels oscillate during the cell cycle and peak in mitosis.[37] Since these cells are acquiring resistance through unknown mechanisms we wanted to determine if the increase in Spindly protein levels from interphase to mitosis occurs in the resistant cells. In order to enrich for mitotic cells, cells were treated with nocodazole for 16 hours, which resulted in mitotic arrest due to microtubule depolymerization and mitotic checkpoint activation. The mitotic cells were collected

from these dishes via mitotic shake off, to ensure that any cells that remained in interphase were not collected as they were attached to the plate. The interphase extracts were collected from an asynchronous dish where the mitotic cells were removed prior to collection by mitotic shake off (Figure 3.12A). These extracts were then blotted for Spindly and FNTB.

As shown in Figure 3.12, in the parental cell line, the mitotic cells have 2.7 times the interphase levels of Spindly, consistent with what is known in the literature.[37] Both the 1μM Tipi^R and 2μM Tipi^R have increased mitotic Spindly levels, with a 1.4 and 1.7 fold increase respectively relative to parental mitotic Spindly. However, while there is this increase in mitotic Spindly, there is a larger fold increase of Spindly protein levels in interphase. 1μM Tipi^R and 2μM Tipi^R have a 3.2- and 4.1-fold increase respectively of interphase Spindly protein expression compared to parental. This results in almost identical levels of Spindly in interphase and mitosis in the resistant cells. 1μM Tipi^R only has a 1.2-fold increase, and 2μM Tipi^R has only a 1.1-fold increase relative to interphase protein levels (Figure 3.12B). This indicates that Spindly levels are no longer oscillating with the cell cycle and peaking in mitosis, but rather in these resistant cells appears to be at a higher consistent basal level with only a small increase in mitosis compared to the parental cells. In the parental cell line, there is not a large difference in the expression of FNTB in interphase or mitotic cells, with 1.0 and 1.4 respectively (Figure 3.12B), as FNTB is expressed throughout the cell cycle and farnesylates its substrates. Mitotic FNTB does appear to have a post translational modification, which results in the shift that is seen in all of the mitotic lanes (Figure 3.12B). The resistant cell lines have increased protein levels of FNTB, the 1μM Tipi^R and 2μM Tipi^R have a 2.3- and 2.6-fold increase in interphase FNTB respectively relative to the parental cell line. The same is seen with increased levels of mitotic FNTB in the 2 resistant cell lines.

In addition to looking at the change in Spindly and FNTB levels in interphase and mitosis, I also wanted to determine if the Spindly to FNTB ratio, is altered in the resistant cells, since Spindly and FNTB work in conjunction. In the interphase cells, the 1µM Tipi^R Spindly:FNTB ratio is 1.4 and 2µM Tipi^R is 1.6, compared to 1.0 in the parental cells. In the mitotic cells, the 1µM Tipi^R and 2µM Tipi^R have decreased Spindly:FNTB ratios, of 1.2 and 1.7 respectively compared to 1.9 in the parental cells. This means that there is less Spindly relative to the amount of FNTB. This could account for the resistance, as more FNTB protein being present, results in more farnesyltransferase that needs to be inhibited to prevent Spindly farnesylation.

The resistant cell lines show increased Spindly and FNTB protein expression relative to the parental, which could be what accounts for the increased resistance to Tipifarnib. Unlike what was seen in Figure 3.7, where Spindly and FNTB expression did not correspond to resistance; it appears that in the cells that resistance was generated, increased Tipifarnib resistance resulted in increased Spindly and FNTB protein levels.

A

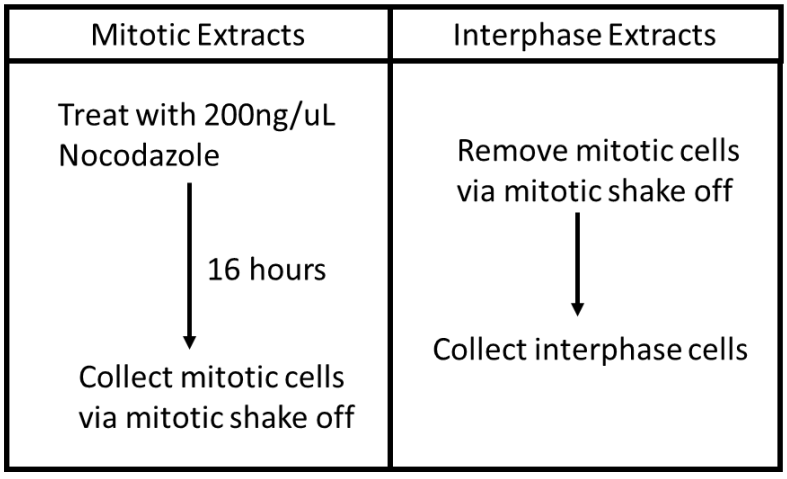

B

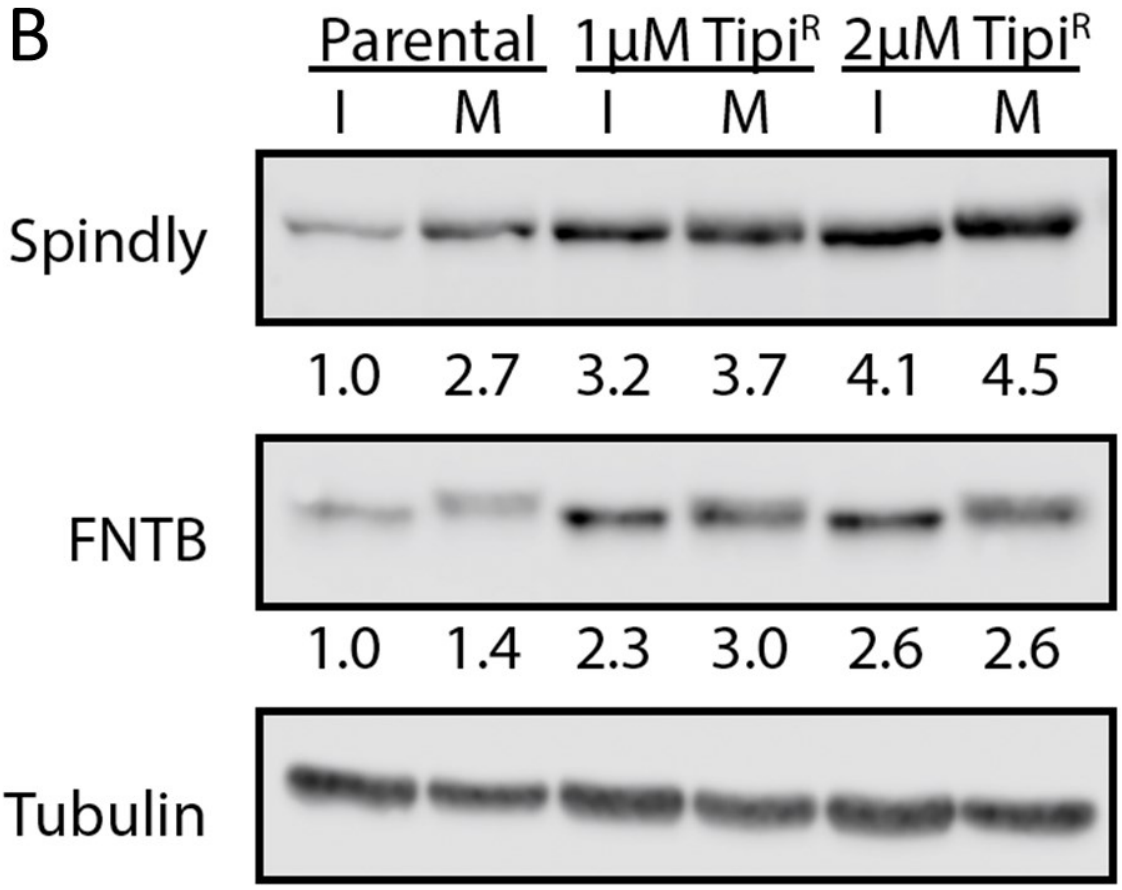

C

	Interphase			Mitosis		
	Parental	1uM-R	2uM-R	Parental	1uM-R	2uM-R
Spindly	1	3.2	4.1	1.0	1.4	1.7
FNTB	1	2.3	2.6	1.0	2.1	1.9

	Interphase			Mitosis		
	Parental	1uM-R	2uM-R	Parental	1uM-R	2uM-R
Spy:FNTB ratio	1.0	1.4	1.6	1.9	1.2	1.7
FNTB:Spy ratio	1.0	0.7	0.6	0.5	0.8	0.6

Figure 3.12. Spindly and FNTB protein levels increased in the resistant cell lines. A) Experimental flow chart. Mitotic extracts treated with 200 ng/μL nocodazole for 16 hours, mitotic cells collected by mitotic shake-off and prepared for western blot. Interphase extracts had mitotic cells removed via mitotic shake-off and remaining attached interphase cells collected and processed for western blot. B) Tipifarnib resistant cell lysate analyzed by immunoblot for total levels of Spindly, FNTB and Tubulin in Interphase (I) and Mitotic (M)

extracts. Average quantification normalized to Tubulin is shown below each blot for Spindly and FNTB. C) Ratio of Spindly and FNTB in resistant cell lines, Interphase and mitotic levels normalized to their respective parental level. Top table, levels of Spindly and FNTB normalized to the parental interphase and mitosis respectively. Bottom table, Spindly:FNTB and FNTB:Spindly ratios normalized to parental interphase. N = 2

As there is increased Spindly and FNTB protein levels in the resistant cells, we theorized that this could result in increased Spindly kinetochore localization, as the mechanism through which the cells are resistant to Tipifarnib. To test this, immunofluorescence experiments were carried out examining Spindly kinetochore localization in the parental, 1μM Tipi^{R} and 2uM Tipi^{R} cell lines. Cells were stained for Spindly or CENP-F and ACA to mark the kinetochore and Spindly KT localization was examined (Figure 3.13A). The Tipifarnib resistant cell lines do not display increased Spindly kinetochore localization even though the protein levels are increased (Figure 3.13B). While these resistant cells have higher levels of Spindly and FNTB, this is not resulting in Spindly KT localization as we first thought based on the results from Figure 3.12. It does not appear the mechanism of resistance results in increased Spindly KT localization in the presence of Tipifarnib.

A

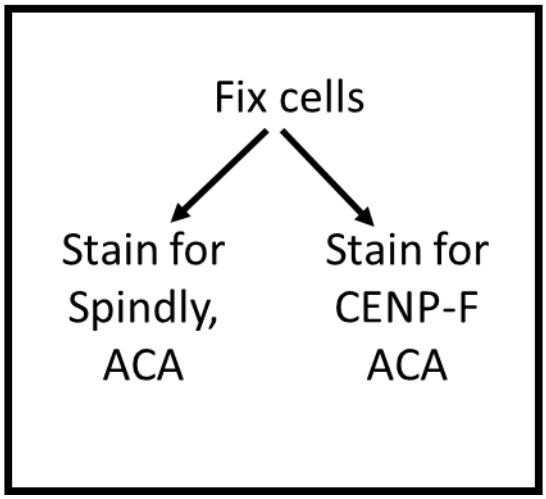

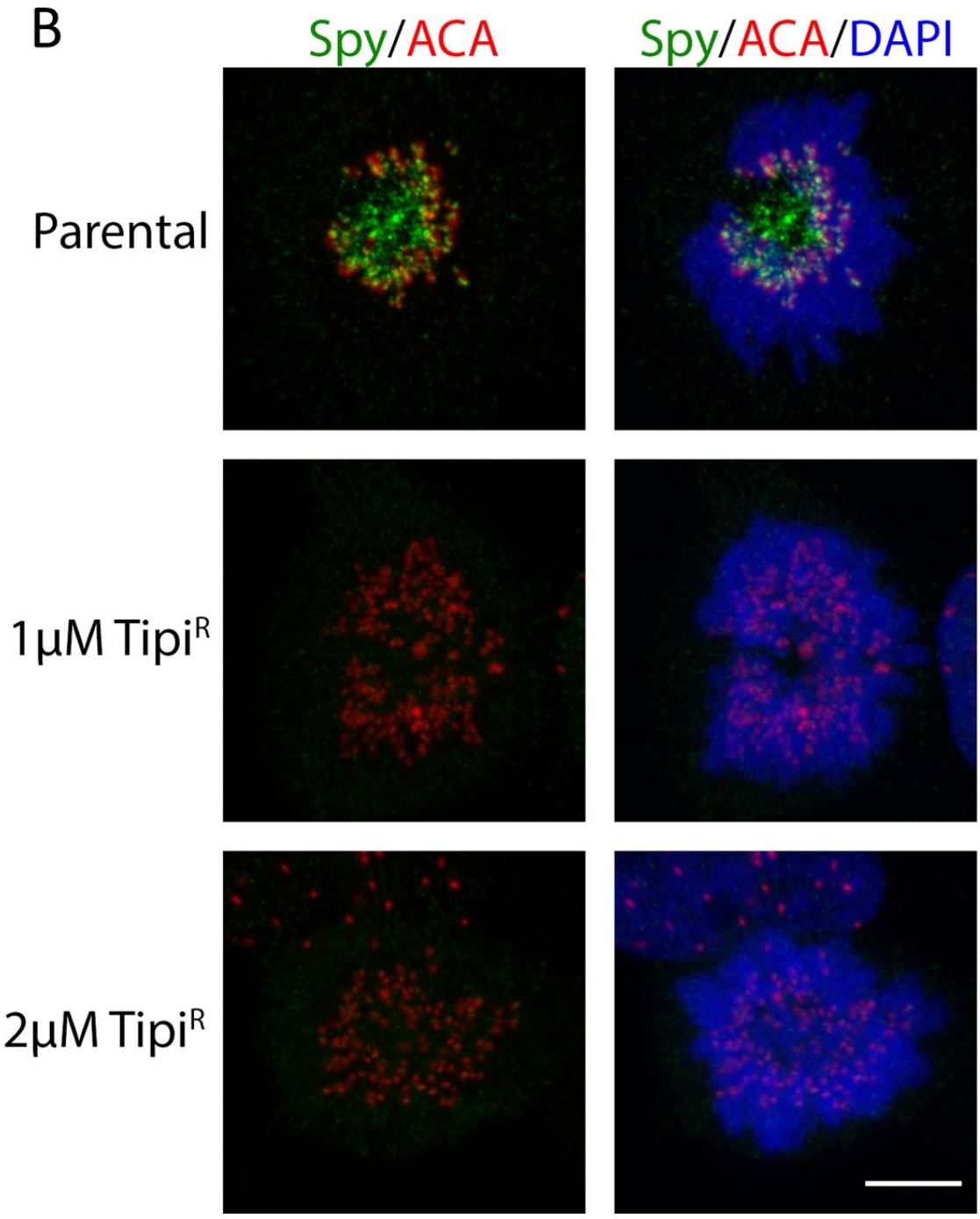
B
Spy/ACA
Spy/ACA/DAPI
Parental
1μM Tipi^R
2μM Tipi^R

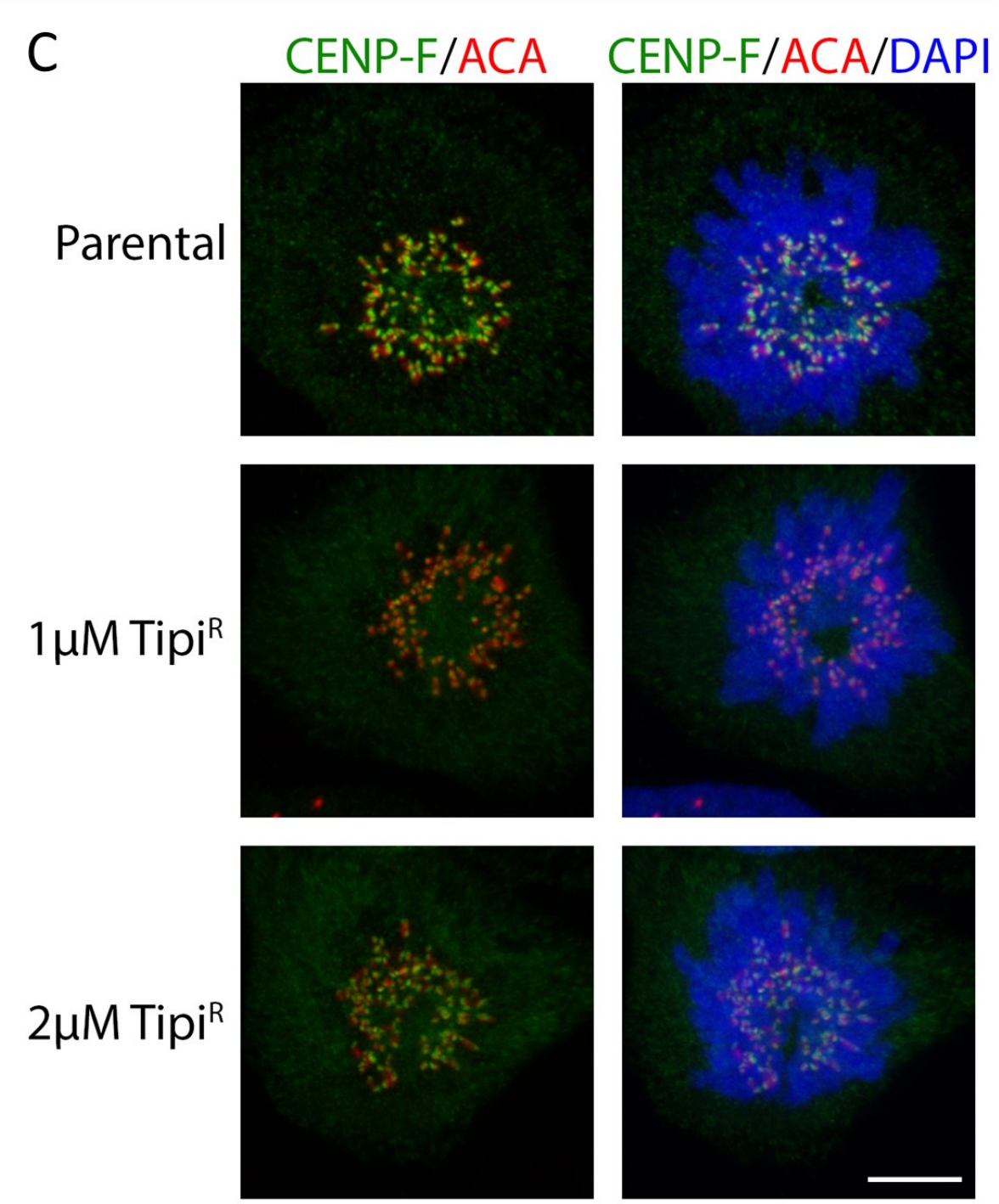

Figure 3.13 Tipifarnib resistant cells have decreased Spindly KT localization while CENP-F KT localization is unchanged. A) Experimental flow chart is shown. Cells were stained for either Spindly and ACA (B) or CENP-F and ACA(C). Maximum projections are shown. Spindly (B) or CENP-F (C) are green, ACA (Kinetochore) is red and DAPI marking the DNA is blue. Scale bar = 5 μm. n = 2 biological replicates, 25 prometaphase cells per replicate.

To further investigate Spindly KT localization in the resistant cells we treated the cells with nocodazole or monastrol. We tested these two inhibitors as they inhibit mitosis through different mechanisms. Nocodazole is a MT poison that inhibits the formation of the mitotic spindle, which results in maximal mitotic checkpoint activation. While monastrol inhibits Eg5, a kinesin that is required for spindle pole separation and monastrol treatment results in cells with monopolar spindles thus activating the mitotic checkpoint. By testing these two inhibitors we can determine if there is a difference in Spindly KT localization depending on how the checkpoint is activated. Following nocodazole or monastrol treatment, the cells were fixed and stained for either Spindly and ACA or CENP-F and ACA and then imaged (Figure 3.14A).

Consistent with what was seen in Figure 3.13B., upon checkpoint activation, Spindly KT localization was still decreased in the resistant cell lines compared to parental (Figure 3.14B). And again, consistent with Figure 3.13C, CENP-F KT localization is unaffected in these resistant cells (Figure 3.14C). This confirms what we observed in Figure 3.13, that even with the activated mitotic checkpoint, Spindly KT localization is still inhibited by Tipifarnib in these resistant cells. So, the mechanism through which these cells have developed resistance is not through persistent Spindly kinetochore localization.

A

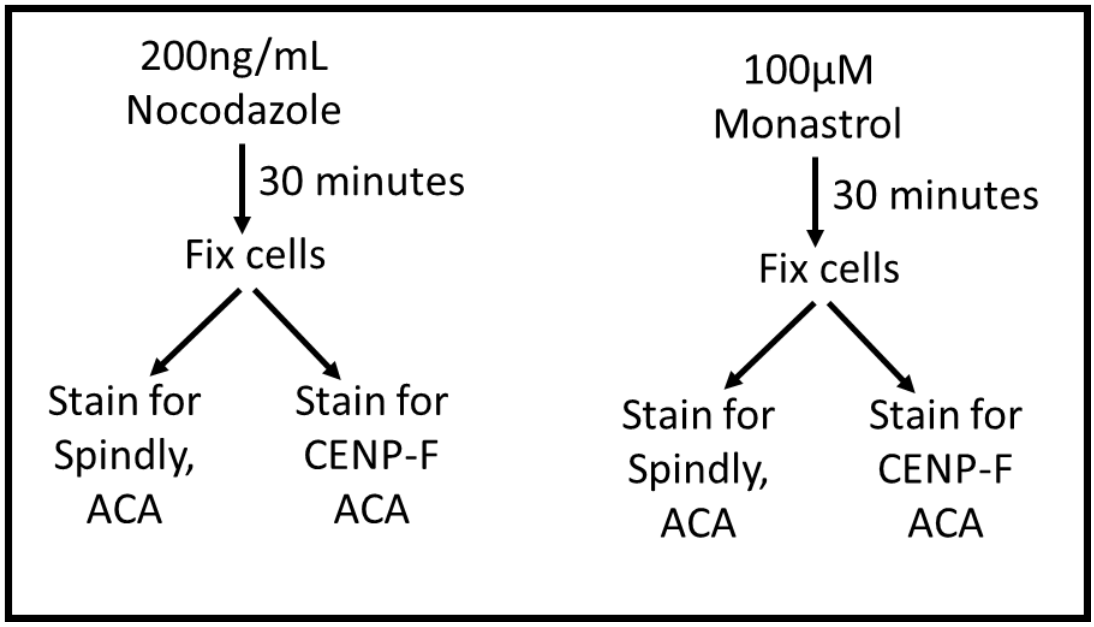
200ng/mL
Nocodazole
30 minutes
Fix cells
Stain for
Spindly,
ACA
Stain for
CENP-F
ACA
100µM
Monastrol
30 minutes
Fix cells
Stain for
Spindly,
ACA
Stain for
CENP-F
ACA

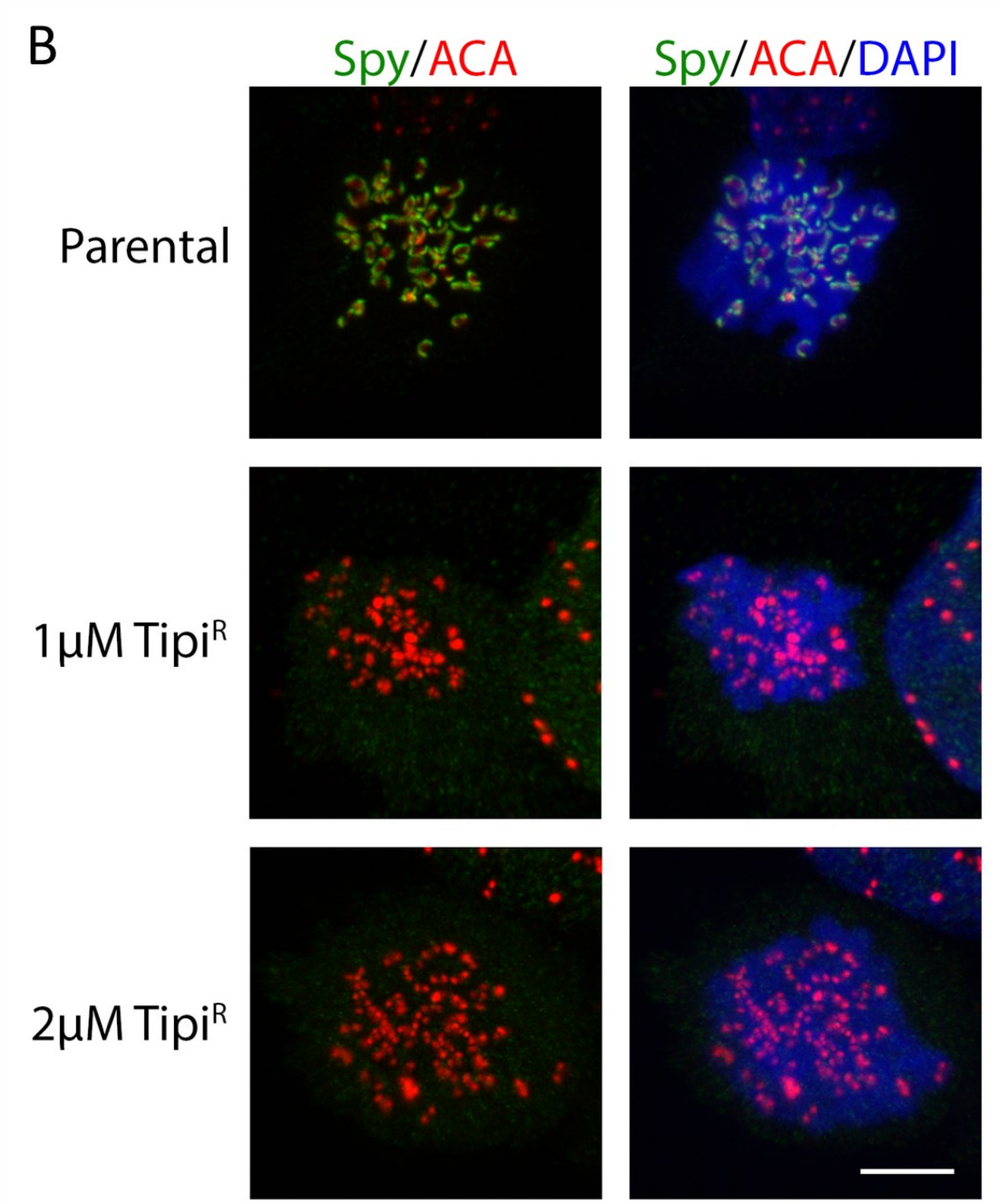
B
Spy/ACA
Spy/ACA/DAPI
Parental
1μM Tipi^R
2μM Tipi^R

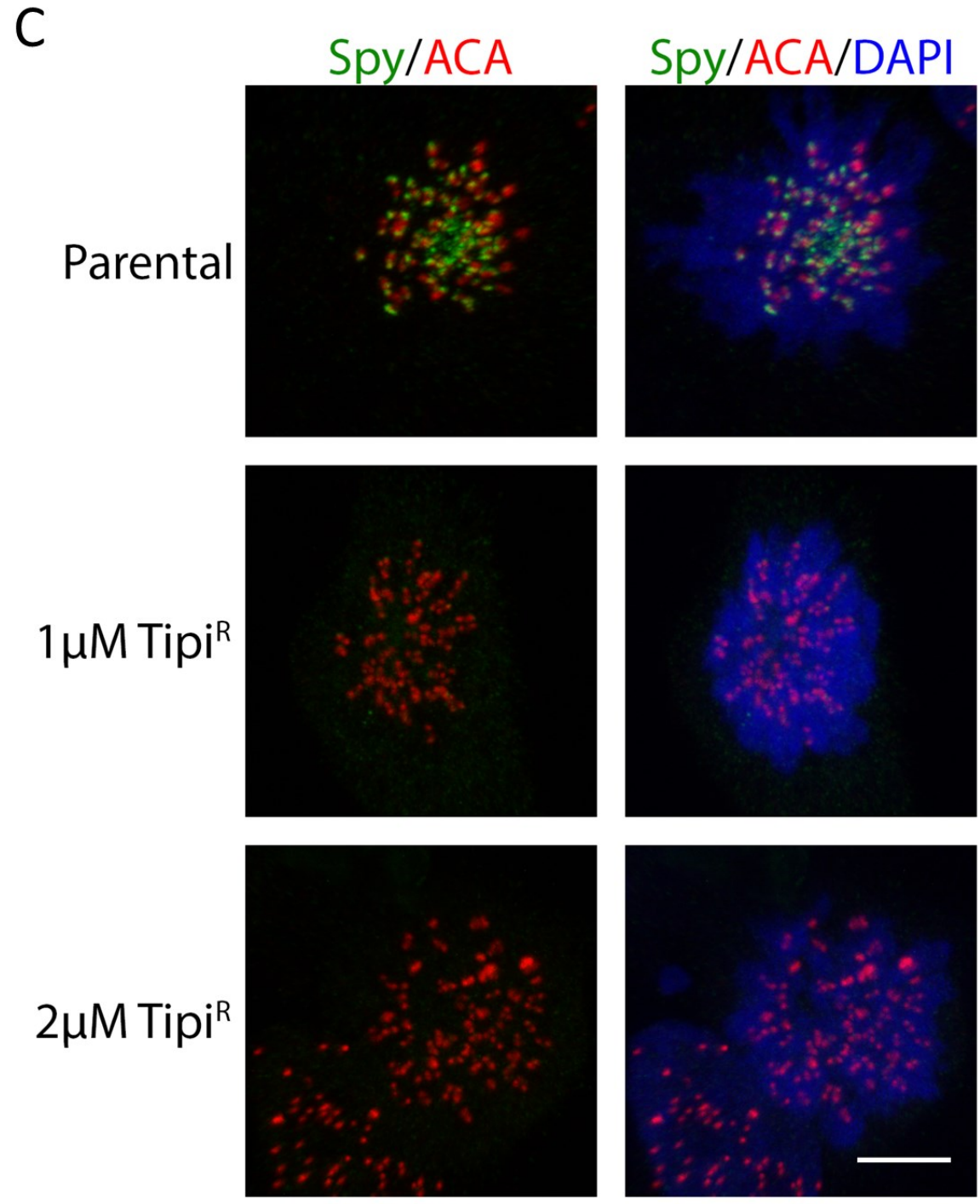
C
Spy/ACA
Spy/ACA/DAPI
Parental
1μM Tipi^R
2μM Tipi^R

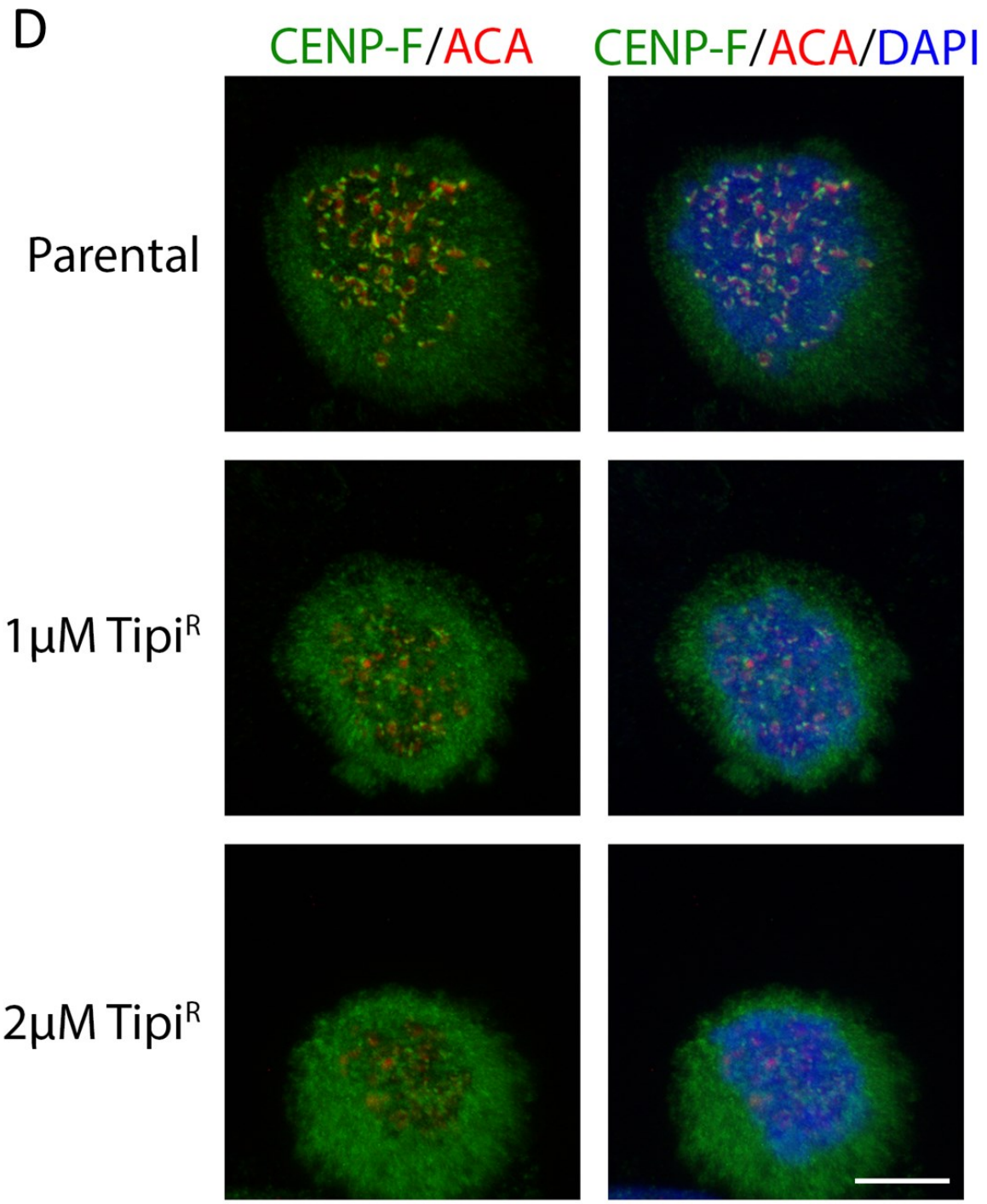
D
CENP-F/ACA
CENP-F/ACA/DAPI
Parental
1μM Tipi^R
2μM Tipi^R

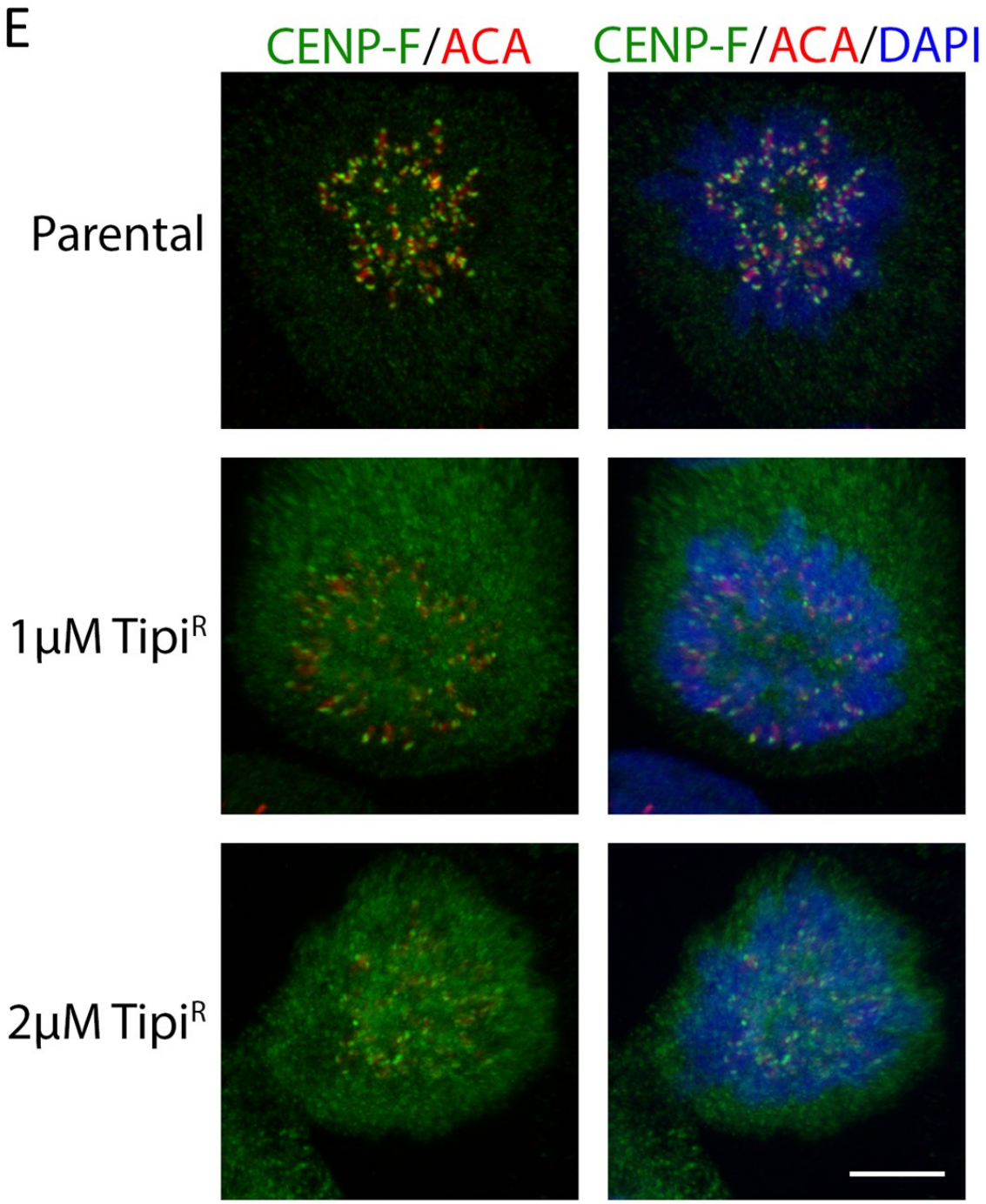

Figure 3.14 Tipifarnib resistant cells have decreased Spindly KT localization while CENP-F KT localization is unchanged with nocodazole or monastrol treatment. A) Experimental flow chart is shown. Cells were treated with 200 ng/mL nocodazole (B, D) or monastrol (C, E) for 30 minutes and then stained for either Spindly and ACA (B, D) or CENP-F and ACA (C, E). Maximum projections are shown. Spindly (B) or CENP-F (C) are green, ACA (kinetochore) is red and DAPI

marking the DNA is blue. Scale bar = 5 µm. n = 2 biological replicates, 25 prometaphase cells per replicate.

As we determined that the resistant cells do not have Spindly KT localization, we wished to investigate what percentage of cells are in mitosis in an asynchronous population. The prometaphase arrest due to lack of Spindly KT localization should result in an increased percentage of mitotic cells in the resistant cells. Additionally, to compare the resistance that was generated over the 3-month selection and what effect the same concentration of Tipifarnib have on parental cells, the parental cells were treated with 1µM and 2µM for 24 hours prior to fixation. These cells were then stained for pS28 H3, which is a marker of mitotic cells (Figure 3.15A). From these images, the percentage of cells in mitosis was calculated.

Representative images are shown in Figure 3.15B, where mitotic cells are marked by pS28 H3 staining. The total number of pS28 H3 positive cells was counted and percent mitotic cells was determined. Parental cells when treated with Tipifarnib resulted in a non-significant increase in the percent of mitotic cells to 4.1% and 6.1% for 1 µM and 2 µM respectively. The parental treated with 1 µM Tipifarnib results in a lower percent mitotic cells compared to the 1µM Tipi^{R} cells, with 4.1% vs. 5.3% respectively. While the parental cells treated with 2 µM had 6.1% mitotic cells and 2µM Tipi^{R} was 5.8%. (Figure 3.15C). The percentage of mitotic cells was comparable between the resistant cell lines and the parental cells treated with the same concentration of Tipifarnib.

As FTI treatment is known to result in prometaphase arrest,[44,43] I wanted to determine if the increased percentage of mitotic cells upon Tipifarnib treatment of parental cells and the

resistant cell lines is due to a prometaphase arrest. To determine if this is true, the mitotic cells were classified as either prophase, prometaphase, metaphase, or anaphase/telophase based of the chromosome morphology. The parental cells treated with Tipifarnib, resulted in an increase in the percentage of cells in prometaphase from 31.5% (parental + DMSO) to 47.4% (parental + 1 μM) and 63% (parental + 2 μM) (Figure 3.15D). After the chromosomes have properly congressed and the cell has proceeded to metaphase, the cell cycle appears to continue per usual.

The 1μM Tipi^R and 2μM Tipi^R cell lines have the expected higher percentage of prometaphase cells, with 47.6% and 56.9% respectively (Figure 3.15D), which is 1.5- and 1.8-fold increase compared to the parental cell line. When comparing the parental + 1 μM Tipifarnib to 1μM Tipi^R they had almost identical percentages of prometaphase cells, with 47.4% and 47.6% (Figure 3.15D). Parental + 2 μM Tipifarnib had a higher percentage of prometaphase cells compared to the 2μM Tipi^R, with 63% vs 56.9% (Figure 3.15D). It appears at this 24-hour treatment, the prometaphase arrest seen in the parental cells when treated with 2 μM Tipifarnib results in a longer prometaphase arrest compared to the cells that have developed resistance. While the resistant cells do display a prometaphase arrest, there is the potential that it is a shorter prometaphase arrest compared to the parental cell line. This could account for the cell survival and resistance to Tipifarnib.

A

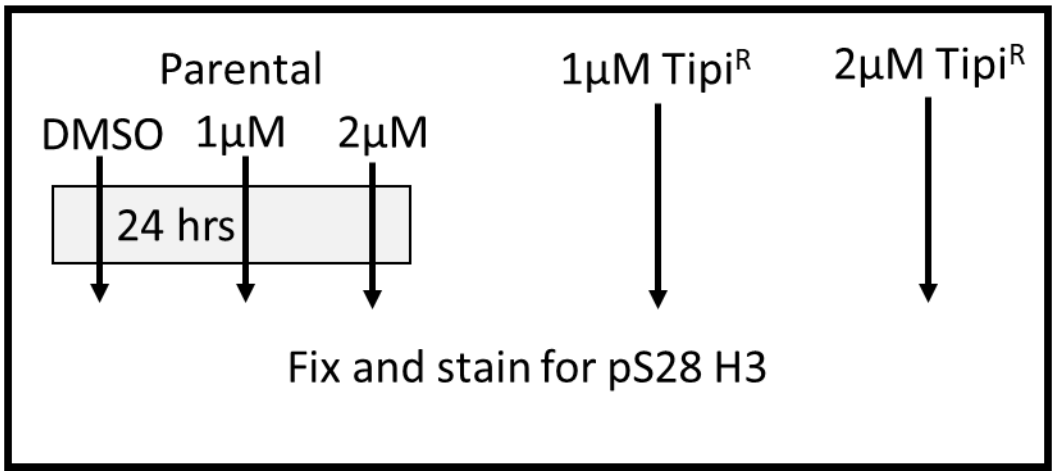
Parental
DMSO
1μM
2μM
24 hrs
1μM Tipi^R
2μM Tipi^R
Fix and stain for pS28 H3

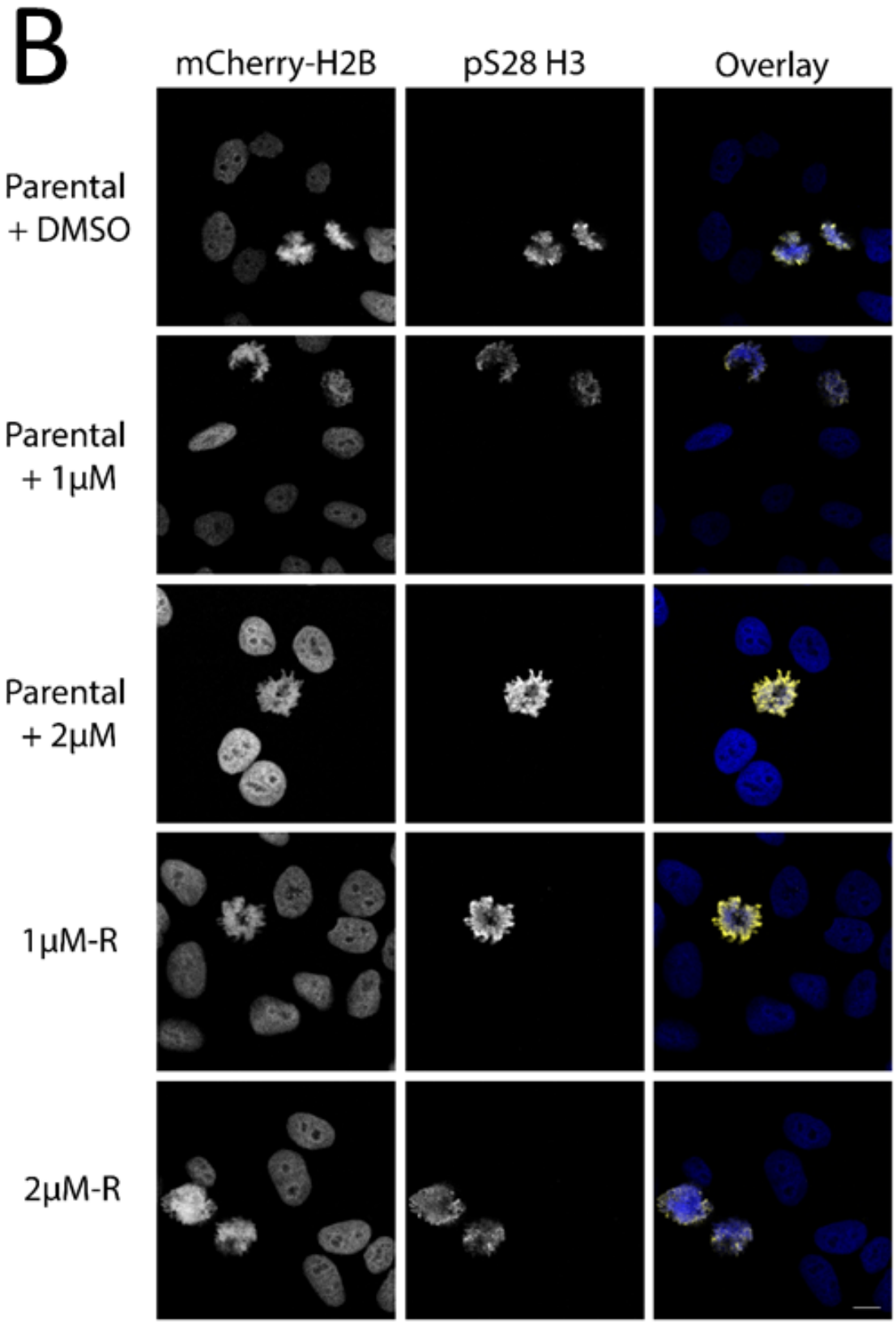
B
mCherry-H2B
pS28 H3
Overlay
Parental
+ DMSO
Parental
+ 1μM
Parental
+ 2μM
1μM-R
2μM-R

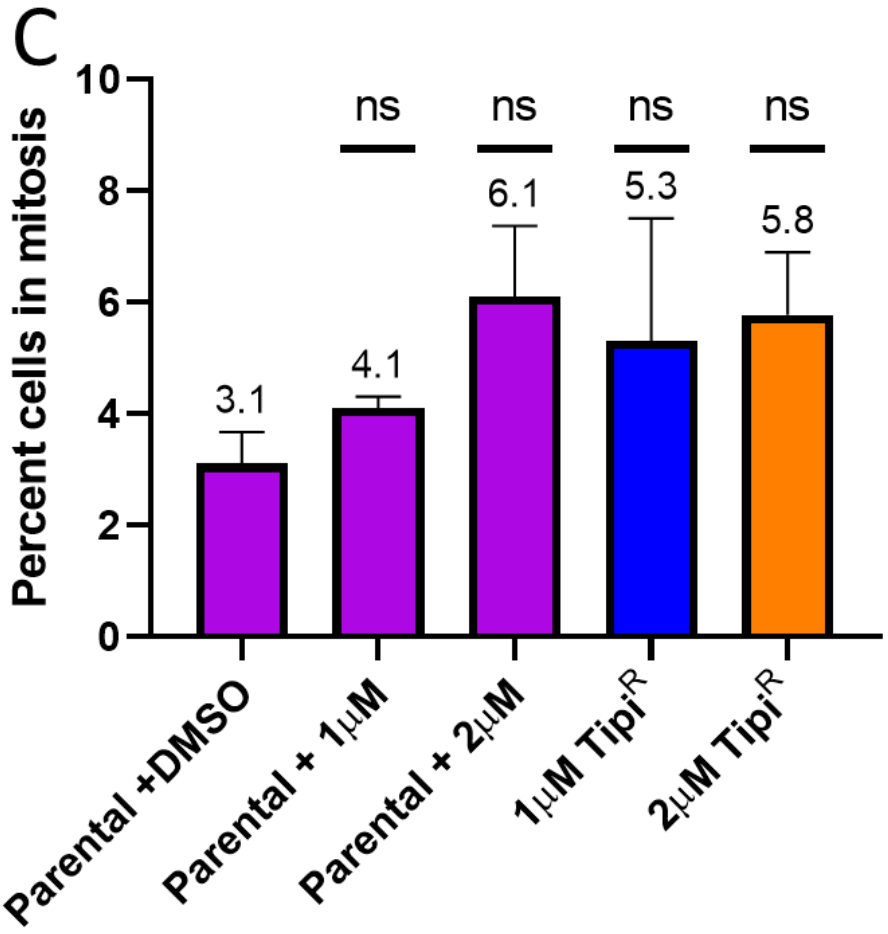
C
Percent cells in mitosis
10
8
6
4
2
0
ns
ns
ns
ns
3.1
4.1
6.1
5.3
5.8
Parental +DMSO
Parental + 1μM
Parental + 2μM
1μM Tipi^R
2μM Tipi^R

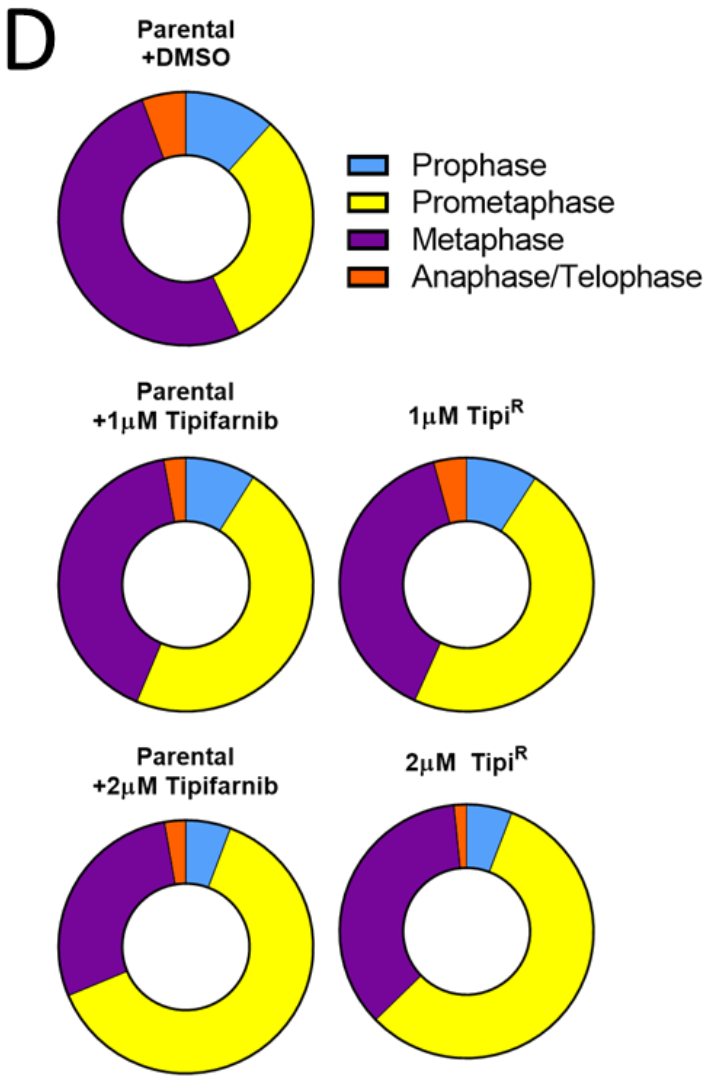

	Prophase	Prometaphase	Metaphase	Anaphase/Telophase
Parental + DMSO	11.6	31.5	51.3	5.6
Parental + 1uM	8.9	47.4	40.9	2.8
Parental + 2uM	5.7	63.0	28.6	2.7
1uM-R	9.1	47.6	39.1	4.2
2uM-R	5.8	56.9	35.7	1.6

Figure 3.15 Tipifarnib resistant cells show an increase in percentage of mitotic cells. A) Experimental flow chart. Parental cells were treated with 1 μM or 2 μM Tipifarnib or equal volume solvent control (DMSO) for 24 hours, then treated parental cells, and untreated 1μM Tipi^R and 2μM Tipi^R cells were fixed and stained for pS28 H3. B) Representative images of pS28 H3 positive cells. C) Percentage of mitotic cells mean on top of SEM bar, ns = not significant. D) Mean percentage of cells in each phase of mitosis. n in center of donut plot is the total number of mitotic cells examined. Blue= prophase, yellow= prometaphase, purple= metaphase,

orange= anaphase/telophase. Table below shows the percentage. Scale bar = 10 μm; n = 3, >500 cells per replicate

As expected, Figure 3.15 showed an increase in the percentage of mitotic cells in the resistant cell lines compared to the parental cells, with a prometaphase arrest. To further investigate this we did high content imaging to determine how mitotic duration and cell fate are altered in these resistant cells. The parental, 1μM Tipi^R and 2μM Tipi^R were seeded, and then treated with 0.39-6.25 μM, then imaged every 10 minutes for 72 hours (Figure 3.16A). From this imaging data, mitotic duration and cell fate were determined. Mitotic duration was measured from the first observation of condensed prophase chromosomes to first observation of anaphase. The cell fate phenotypes were classified as: 1) normal mitosis – mitosis duration was counted from the first observation of condensed prophase chromosomes to first observation of anaphase; 2) death in mitosis – mitotic duration was counted from prophase to first observation of apoptotic bodies without mitotic exit; 3) Death in interphase – defined as observation of apoptotic bodies during interphase. From this we were then able to calculate the duration of mitosis of each cell and see what effects Tipifarnib treatment has on mitotic duration and cell fate.

Tipifarnib treatment resulted in increased mitotic duration in all cell lines tested, the parental and both resistant cell lines. However, the extent to which it increased the mitotic duration is different depending on the cell line. The parental cells had a significant increase ($p<0.0001$, 2-way ANOVA) in all concentrations of Tipifarnib tested (0.39, 0.78, 1.5, 3.1, 6.2 μM) (Figure 3.16 B&C). There was an increase in mitotic duration from 40 minutes when treated with

the control, to 110 minutes when treated with 0.39 μM. The median mitotic duration for 0.39, 0.78, 1.5 and 3.1 μM Tipifarnib are all in the range of 110-130 minutes. Only the highest concentration tested, 6.2 μM resulted in a median mitotic duration of 210 minutes (Figure 3.16 B&C).

Both resistant cell lines had varying levels of significant increase in mitotic duration. Neither 1μM Tipi^R nor 2μM Tipi^R showed a significant increase in mitotic duration when treated with 0.39 μM Tipifarnib. The remaining concentrations tested in the 1μM Tipi^R resulted in significant increase, with 0.78 μM increasing median mitotic duration to 130 minutes ($p<0.001$, 2-way ANOVA), 1.5 μM having median mitotic duration of 100 minutes ($p<0.01$, 2-way ANOVA). Both 3.1 and 6.2 μM in the 1μM Tipi^R cells resulted in significant increases of to 170 and 400 minutes respectively ($p<0.0001$, 2-way ANOVA). The 2μM Tipi^R, 0.78 μM Tipifarnib only resulted in a small increase in median mitotic duration from 70 to 100 minutes ($p<0.05$, 2-way ANVOA). Both 1.5 and 3.1 μM Tipifarnib resulted in increased median mitotic duration to 110 and 120 minutes, respectively ($p<0.05$, 2-way ANOVA). Only the highest concentration tested 6.2 μM resulted in increased median mitotic duration to >120 minutes, increasing it to 280 minutes ($p<0.0001$, 2-way ANOVA) (Figure 3.16 B&C).

Comparing the parental to resistant cell lines, at lower concentrations of Tipifarnib, the resistant cell lines are affected to a lesser extent than the parental. Only at the highest concentration tested, 6.2 μM, was the change in mitotic duration equally significant ($p<0.0001$, 2-way ANOVA) in all 3 cell lines. As one would expect, the resistant cell lines have less significant

increases in the mitotic duration, with 1µM Tipi^{R} having more significant increases than 2µM Tipi^{R} at lower concentrations.

Figure 3.16D, shows an enlarged Figure 3.16B, and in 3.16E, the significance compared to parental DMSO is shown. Both 1µM Tipi^{R} and 2µM Tipi^{R} have no significant increase in mitotic duration when treated with DMSO compared to parental. Every concentration other than 1µM Tipi^{R} treated with 0.39 µM Tipifarnib resulted in a significant ($p<0.0001$, one-way ANOVA) increase in mitotic duration.

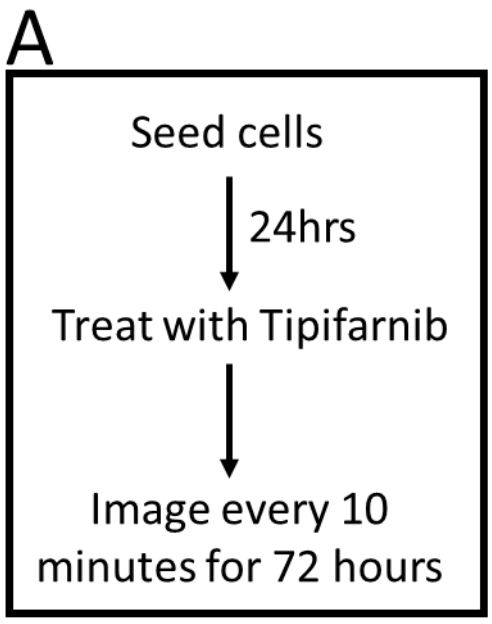

B

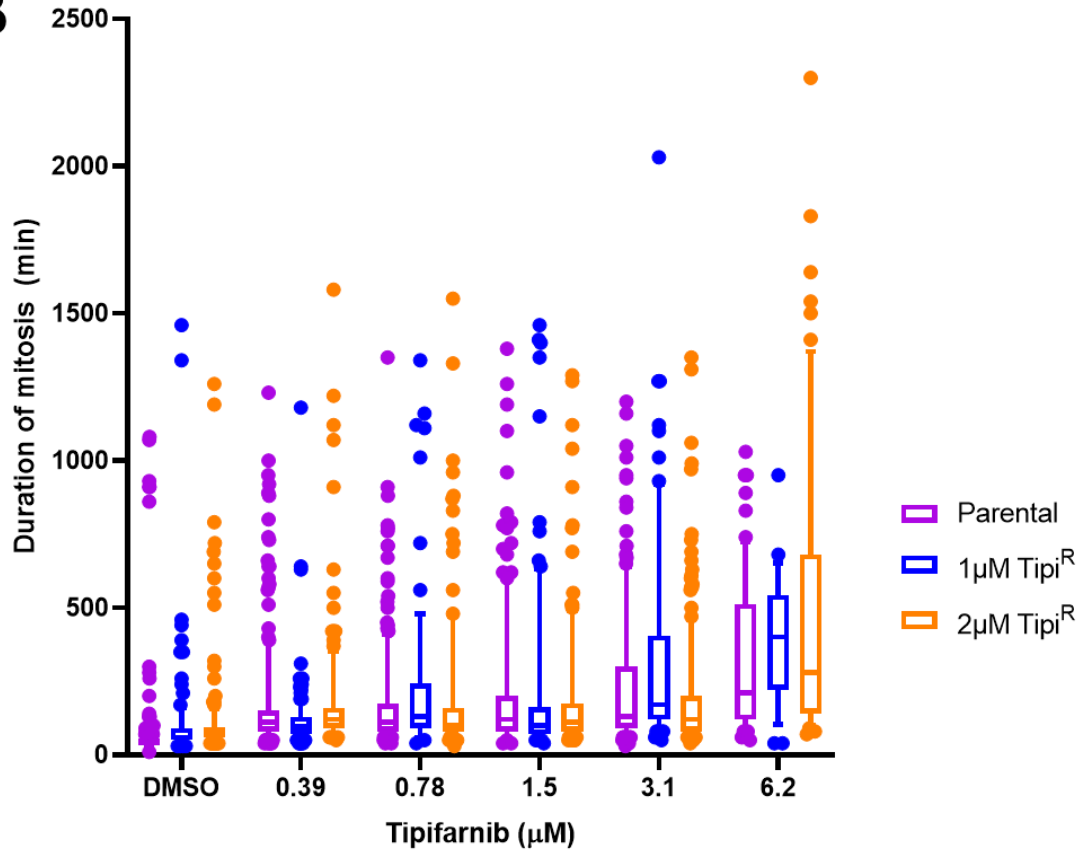

C

	Parental			1μM Tipi^R			2μM Tipi^R		
Treatment (μM)	Median (min)	Mean (min)	Significance	Median (min)	Mean (min)	Significance	Median (min)	Mean (min)	Significance
DMSO	40.0	61.3		60.0	102.1		70.0	102.1	
0.39	110.0	170.7	****	95.0	116.3	ns	120.0	116.3	ns
0.78	110.0	173.6	****	130.0	235.0	***	100.0	235.0	*
1.5	120.0	216.5	****	100.0	210.3	**	110.0	210.3	**
3.1	130.0	248.2	****	170.0	350.1	****	120.0	350.1	**
6.2	210.0	338.7	****	400.0	390.8	****	280.0	390.8	****

D

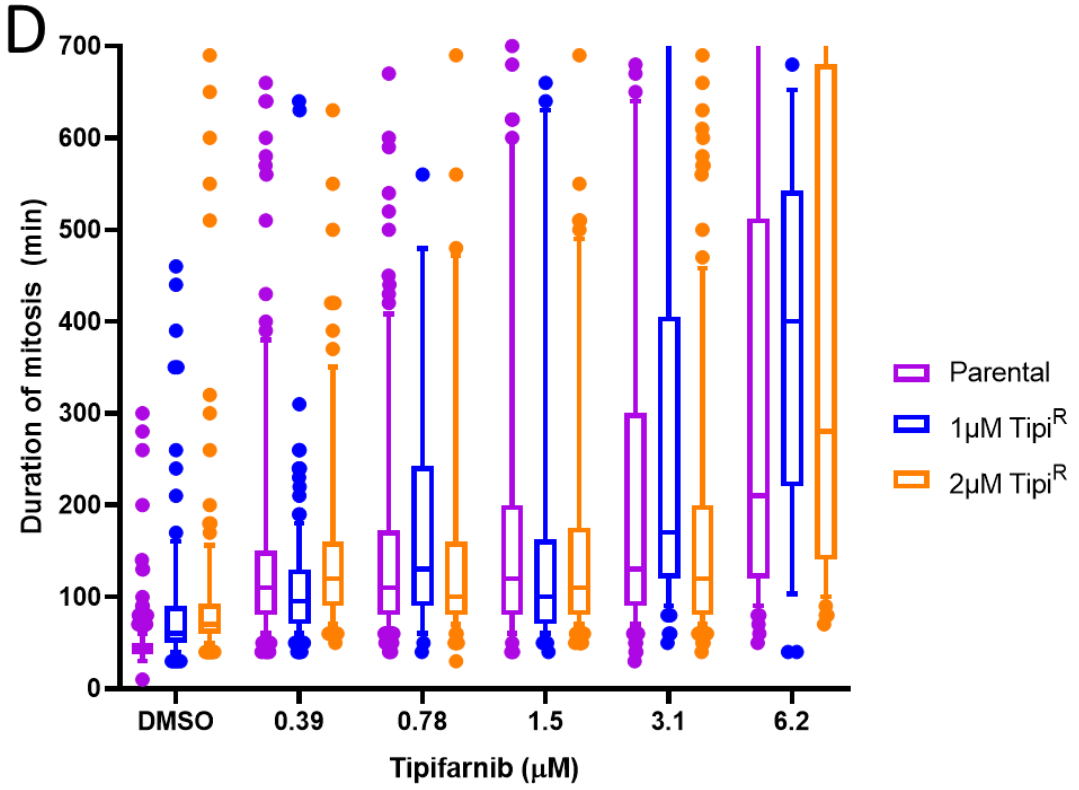

E

	Parental			1μM Tipi^R			2μM Tipi^R		
Treatment (μM)	Median (min)	Mean (min)	Significance	Median (min)	Mean (min)	Significance	Median (min)	Mean (min)	Significance
DMSO	40.0	61.3		60.0	102.1	ns	70.0	102.1	ns
0.39	110.0	170.7	****	95.0	116.3	ns	120.0	116.3	****
0.78	110.0	173.6	****	130.0	235.0	****	100.0	235.0	****
1.5	120.0	216.5	****	100.0	210.3	****	110.0	210.3	****
3.1	130.0	248.2	****	170.0	350.1	****	120.0	350.1	****
6.2	210.0	338.7	****	400.0	390.8	****	280.0	390.8	****

Figure 3.16 Tipifarnib resistant cells have altered mitotic timing. A) Experimental flow chart. HeLa pAAVS1-P-CAG-mCherry-H2B were treated with 0.097-12.5 μM Tipifarnib and then imaged every 10 minutes for 72 hours. Mitotic duration was calculated from chromosome condensation to anaphase. B) 16 initial cells were tracked, with the mitotic duration shown. 2 separate replicates are shown. C) Statistical significance was determined by Two-way ANOVA and Dunnets comparisons test. Asterisk (*) corresponds to significance between parental DMSO and indicated treatments (* $p<0.05$, ** $p < 0.01$, *** $p<0.001$ and **** $p < 0.0001$), D) Graph from B enlarged, with upper portion removed. E) Statistical significance was determined by One-way ANOVA and Tukey's comparisons test. Asterisk (*) corresponds to significance between each individual cell line DMSO and indicated treatments (* $p<0.05$, ** $p < 0.01$, *** $p<0.001$ and **** $p < 0.0001$). N = 16 initial cells, 2 biological replicates.

From the above experiment, we also determined the cell fate of all cells tracked. The 3 possible outcomes were survival, or that the cell was alive at the end of the 72 hours, death in mitosis or death in interphase. This cell fate is shown as a percentage in the donut plots, with the total cells analyzed shown in the center (Figure 3.17). The parental cell line with increasing concentration of Tipifarnib had increasing percentage of cell death in mitosis, with a small increase in the cells dying in interphase. When the parental cells were treated with 6.2 μM Tipifarnib, approximately 50% of the cells died, with 44.1% being in mitosis and only 5% in interphase (Figure 3.17). This shows that the cell death that we are seeing with Tipifarnib treatment is due to the mitotic arrest, and it is not the cells exiting mitosis and dying in interphase due to errors during mitosis.

The 1μM Tipi^{R} cell line had increasing cell death in interphase with the increasing concentrations of Tipifarnib. It appears these cells are able to deal with the altered mitosis, successfully exit however any errors or improper segregation may have led to death in interphase. It is not until 3.1 μM that there is a similar percentage of cells dying in mitosis (20%) to the parental cell line (Figure 3.17). At 6.2 μM, the majority of the cells are dying in mitosis (85.2%), so whatever compensatory mechanism the cells are using to be resistant, seems to be insufficient at this higher concentration as there is a lower percentage of surviving cells relative to both the parental and 2μM Tipi^{R} cell lines. However, as the 1μM Tipi^{R} cells are dying, there is a lower number of total cells analyzed, so there is potential that the cells analyzed were ones that died, while if others were selected then there could potentially be a higher percentage of surviving cells.

The 2μM Tipi^R cell line does not have a large percentage of cell death until the highest concentration of 6.2 μM. At 6.2 μM, more cells are dying in mitosis (28%) than interphase (17%) (Figure 3.17), so even when a higher percentage of cells are dying, it is occurring in mitosis and not the interphase after. This could be similar to the 1μM Tipi^R in that by whatever mechanism the cells have developed resistance, it is not able to rescue the cells from treatment at this concentration.

Both of the resistant cell lines take longer to divide than the parental line. This is shown by looking at the DMSO treated cells, where parental had 422 cells analyzed, compared to 147 for 1μM Tipi^R and 184 for 2μM Tipi^R (Figure 3.17). However, when treated with 0.39 μM Tipifarnib, the total number of parental cells analyzed goes down by more than half to 204, while the resistant cells increase for 1μM Tipi^R to 177 and decrease to 147 for 2μM Tipi^R. The decrease in the total number of cells analyzed can be explained by the parental cells dying at a greater rate, with ~10% of cells dying when treated with Tipifarnib compared to 2.6% in the control. Both resistant cell lines have a similar percentage of cells dying in the DMSO treated control and 0.39 μM (Figure 3.17). In addition to this increased cell death, the prolonged mitotic duration can make it so that the cells are dividing fewer times compared to the control parental. The resistant cell lines are also less affected for the total number of cells, as 1μM Tipi^R does not have the total number of cells analyzed halved until treated with 3.1 μM and 2μM Tipi^R had more than 100 cells analyzed until 6.2 μM. While these percentage do provide some insight into the effect of Tipifarnib treatment on cell fate, they do not show the total picture.


Parental DMSO
n=422
1μM Tipi^R DMSO
n=147
2μM Tipi^R DMSO
n=184
Parental 0.39μM
n=204
1μM Tipi^R 0.39μM
n=177
2μM Tipi^R 0.39μM
n=147
Parental 0.78μM
n=176
1μM Tipi^R 0.78μM
n=85
2μM Tipi^R 0.78μM
n=142
Parental 1.5μM
n=145
1μM Tipi^R 1.5μM
n=94
2μM Tipi^R 1.5μM
n=129
Parental 3.1μM
n=134
1μM Tipi^R 3.1μM
n=60
2μM Tipi^R 3.1μM
n=182
Parental 6.2μM
n=59
1μM Tipi^R 6.2μM
n=27
2μM Tipi^R 6.2μM
n=64
Survived
Died in mitosis
Died in interphase

Parental cell fate (percent)						
	DMSO	0.39µM	0.78µM	1.5µM	3.1µM	6.2µM
% cells surviving	97.4	90.2	88.6	83.4	73.1	50.8
% cells that died in mitosis	0.7	8.8	9.1	13.1	25.4	44.1
% cells that died in interphase	1.9	1.0	2.3	3.4	1.5	5.1

1uM-R cell fate (percent)						
	DMSO	0.39µM	0.78µM	1.5µM	3.1µM	6.2µM
% cells surviving	89.8	88.7	75.3	84.0	60.0	7.4
% cells that died in mitosis	4.8	4.0	7.1	8.5	20.0	85.2
% cells that died in interphase	5.4	7.3	17.6	7.4	20.0	7.4

2uM-R cell fate (percent)						
	DMSO	0.39µM	0.78µM	1.5µM	3.1µM	6.2µM
% cells surviving	95.7	94.6	88.0	90.7	90.1	54.7
% cells that died in mitosis	1.1	2.0	7.0	4.7	4.9	28.1
% cells that died in interphase	3.3	3.4	4.9	4.7	4.9	17.2

Figure 3.17 Tipifarnib resistant cells have similar cell fates after Tipifarnib treatment. TipiR cells were treated with a range of Tipifarnib (6.2-0.39 uM) and imaged for 72 hours. Cell fate at 72 hours was noted, and then calculated as a percentage of total cells analyzed. Cells either survived (blue), died in mitosis (yellow) or died in interphase (purple). n inside the donut plots, is the total cells analyzed per condition. Table shows percentage of each cell fate per treatment. N = 16 initial cells, 2 biological replicates.

As the donut plots in Figure 3.17 do not show what is occurring at the different time points the dendrograms in Figure 3.18 based on the Figure 3.16 high content experiment allow this to be examined. The dendrogram shows how long the mitotic duration is and how long the duration between mitosis is. Yellow line indicates that the cell is in interphase. Blue line indicates that the cell is in mitosis. If the yellow or blue line end in a black line, it indicates that the cell died in interphase or mitosis respectively. While proper mitotic division is shown by a fork, where the daughter cells are shown, which were then tracked going forward from that point. The x-axis shows the time in hours, and the Y-axis is the starting cell at frame 1. Figure 3.18A shows a legend of the different potential outcomes shown in the dendrograms. In this experiment we saw 6

different potential outcomes: 1. Successful mitosis, resulting in 2 daughter cells; 2. tripolar division, where the mitotic division resulted in 3 daughter cell; 3. mitotic slippage, where the chromosomes never segregated and decondense into a single cell; 4. mitotic division resulting in a binucleated cell; 5. cell death in mitosis; or 6. cell death in interphase. Figure 3.18B shows an example of each of the above outcomes, with stills from the video that was analyzed.

Comparing the parental (Figure 3.18C-H) to the 1μM Tipi^R (Figure 3.18I-N) and 2μM Tipi^R (Figure 3.18O-T) cell lines the parental cells divide more often than both resistant cell lines, indicating that the doubling time in the resistant cells is increased. This increased doubling time is also shown by the treatment of parental cells with Tipifarnib resulting in a decrease in the total number of divisions. Parental treated with DMSO (Figure 3.18C) generally divided 4 to5 times in the 72 hours depending how early in the video the first division occurred; compared to parental treated with 0.78 μM Tipifarnib (Figure 3.18E), where the cells divided on average of 3 times total. The prolonged mitotic duration that is seen, results in a decrease in the total number of cell divisions that occur.

When the parental cells were treated with Tipifarnib, generally there was one or 2 successful divisions within the first 36 hours. After 36 hours, there was either an increase in the dying or mitosis took much longer (Figure 3.18E&F). At the higher concentrations of Tipifarnib, this increase in cell death or prolonged mitosis was seen earlier. With 3.1 μM Tipifarnib resulted in prolonged mitosis after ~24 hours (Figure 3.18G). In contrast, when the parental cells were treated with 6.2 μM Tipifarnib this prolonged mitosis was occurring within 8 hours (Figure 3.18H). In addition, the total number of divisions decreased with increasing concentration of Tipifarnib,

as was shown in the donut plots in Figure 3.17, where less divisions result in less total cells analyzed.

The resistant cell lines both showed an increased number of abnormal mitosis when untreated with Tipifarnib. Both 1µM Tipi^{R} and 2µM Tipi^{R} had divisions resulting in binucleated cells, and tripolar divisions (Figure 3.18 I&O). However, when parental and Tipifarnib resistant cells were treated with Tipifarnib, for example 1.5 µM, the parental cells are now having the abnormal divisions while the resistant cells are having normal bipolar division (Figure 3.18 F, L&R).

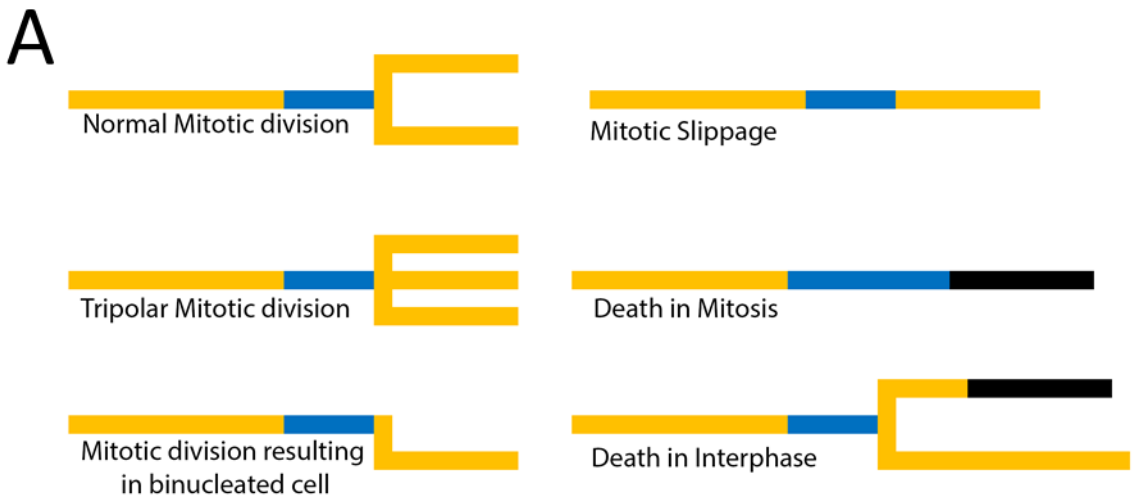

B

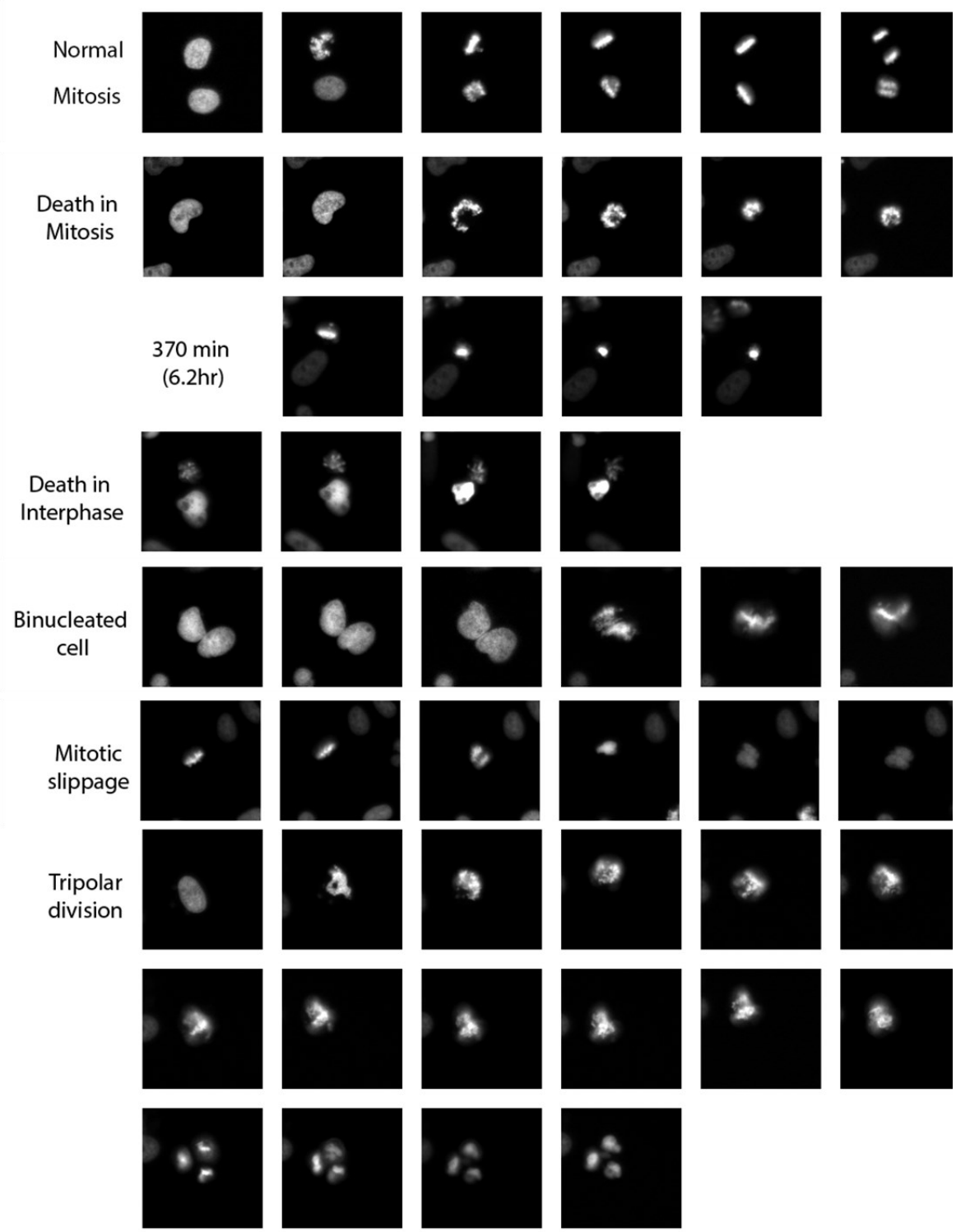
Normal
Mitosis
Death in
Mitosis
370 min
(6.2hr)
Death in
Interphase
Binucleated
cell
Mitotic
slippage
Tripolar
division

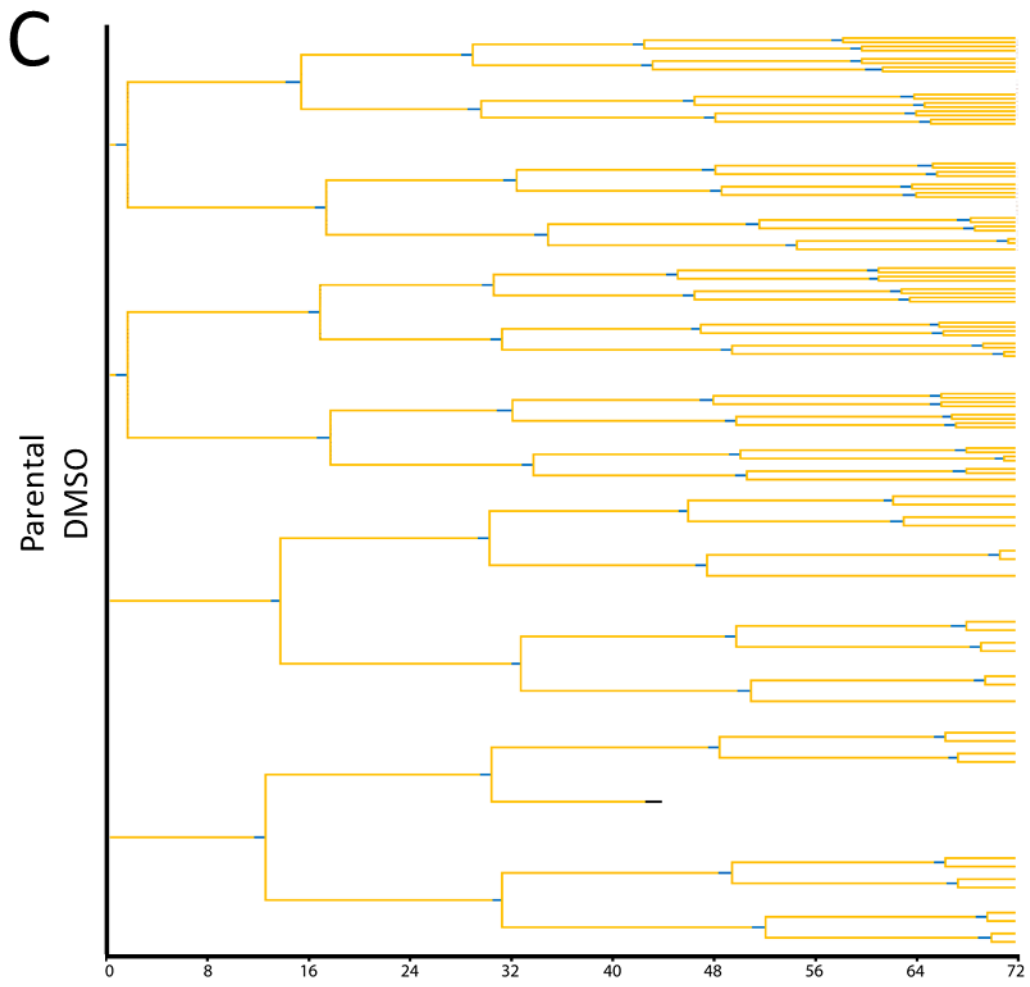
C
Parental
DMSO
0
8
16
24
32
40
48
56
64
72

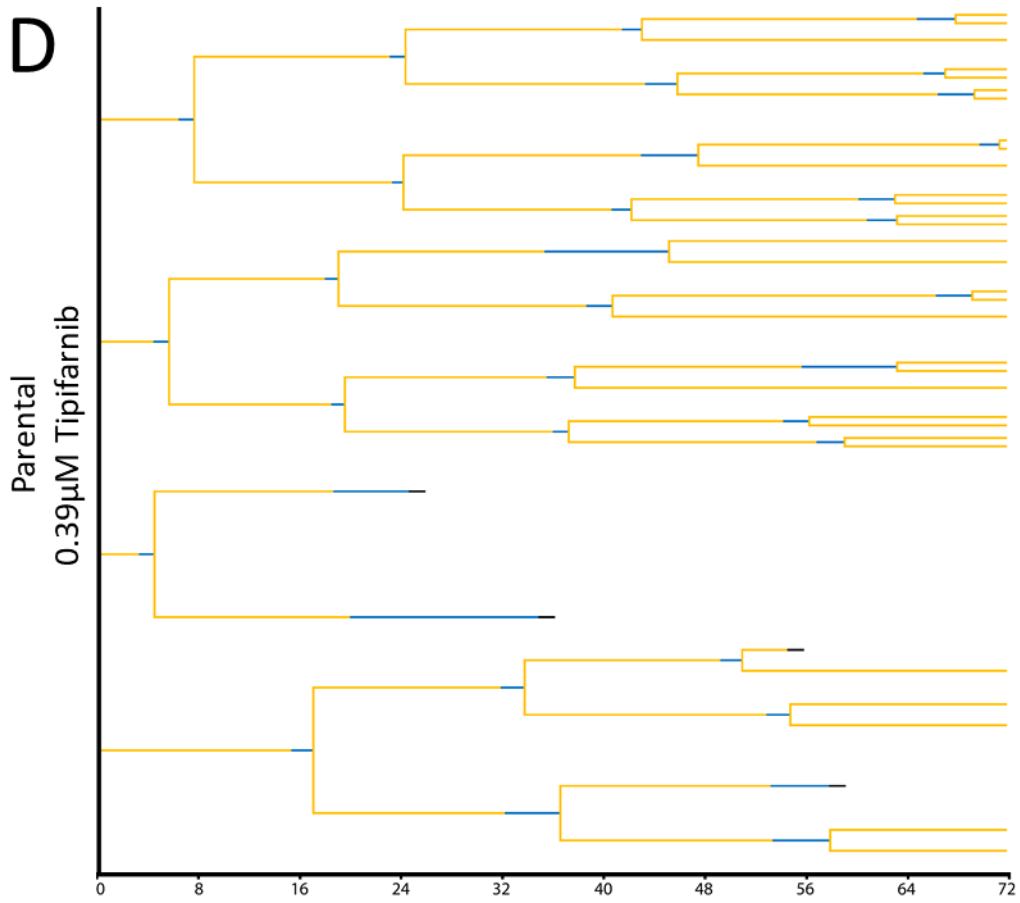
D
Parental
0.39μM Tipifarnib
0
8
16
24
32
40
48
56
64
72

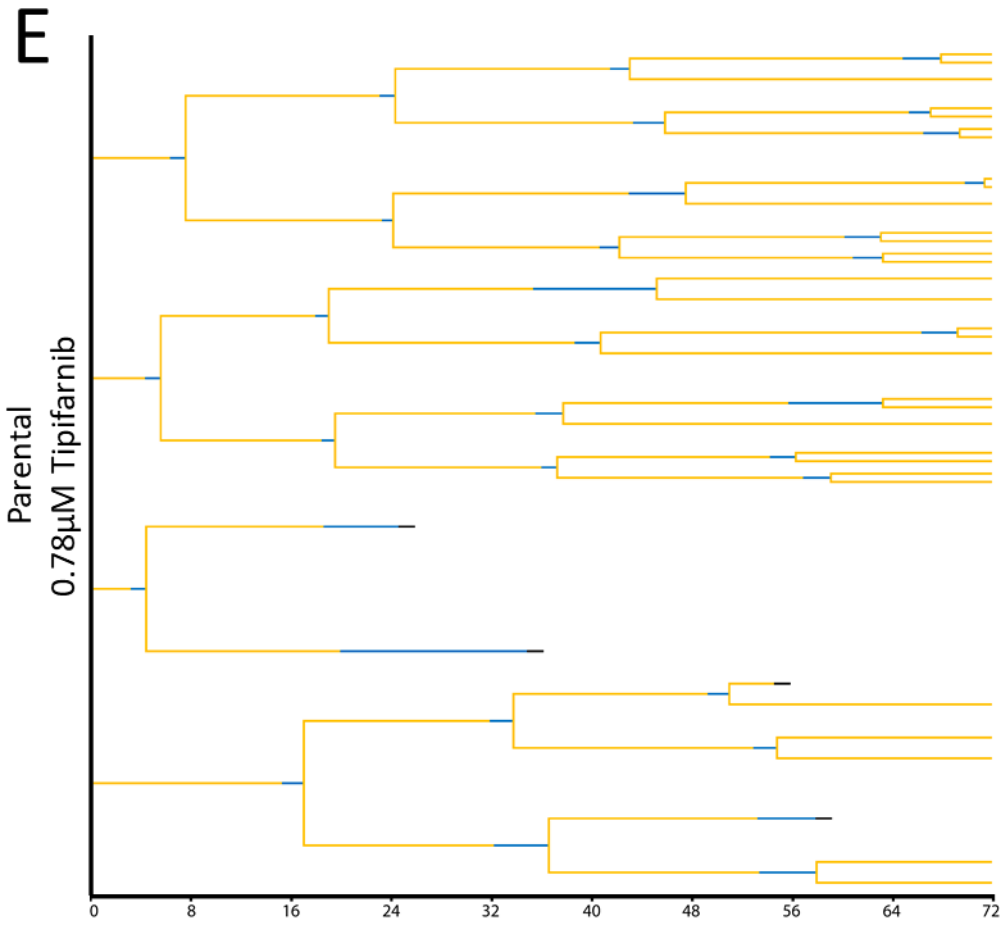
E
Parental
0.78μM Tipifarnib
0
8
16
24
32
40
48
56
64
72

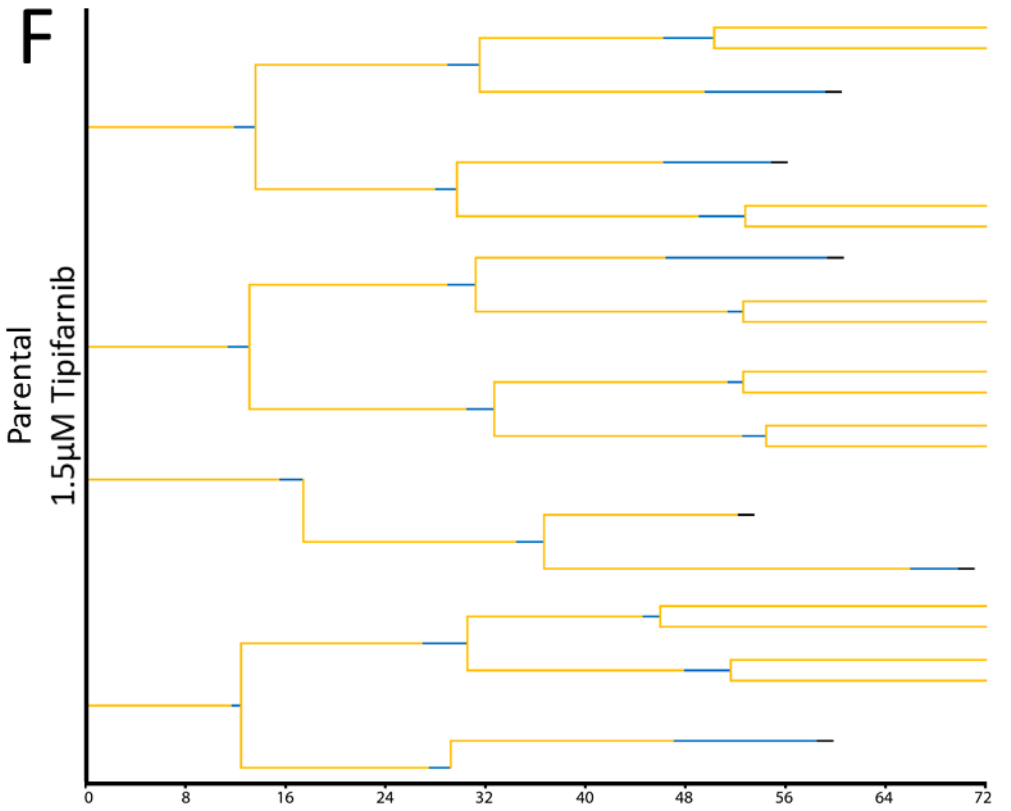
F
Parental
1.5μM Tipifarnib
0
8
16
24
32
40
48
56
64
72

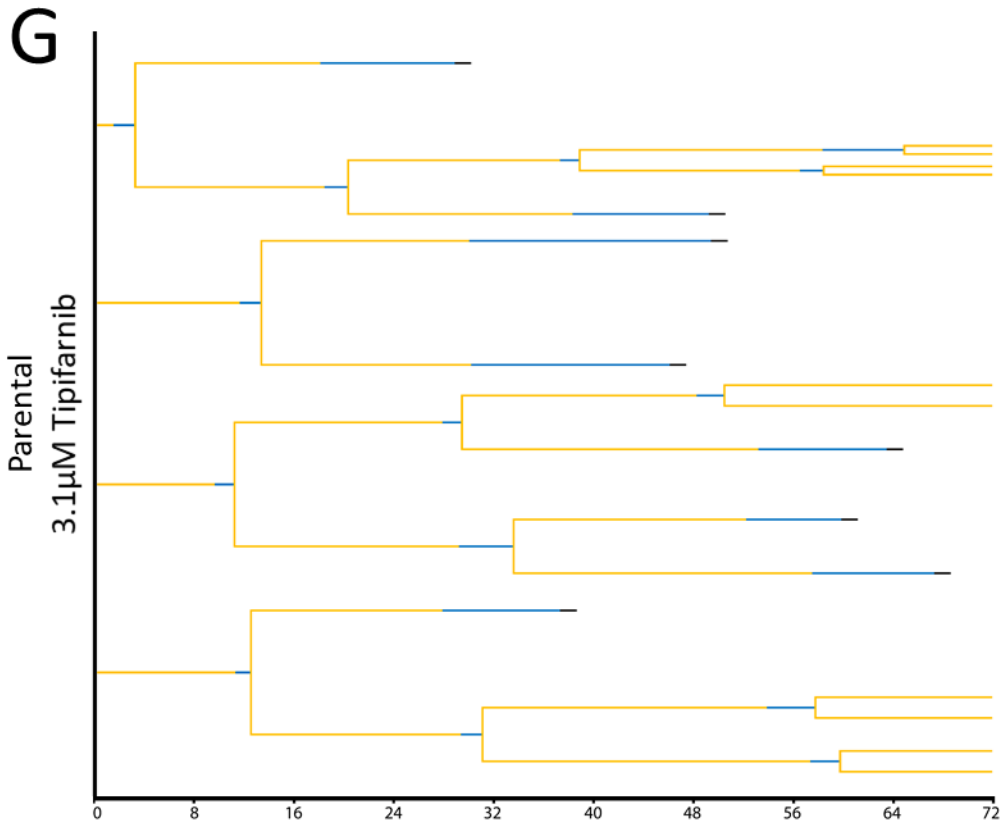
G
Parental
3.1μM Tipifarnib
0
8
16
24
32
40
48
56
64
72

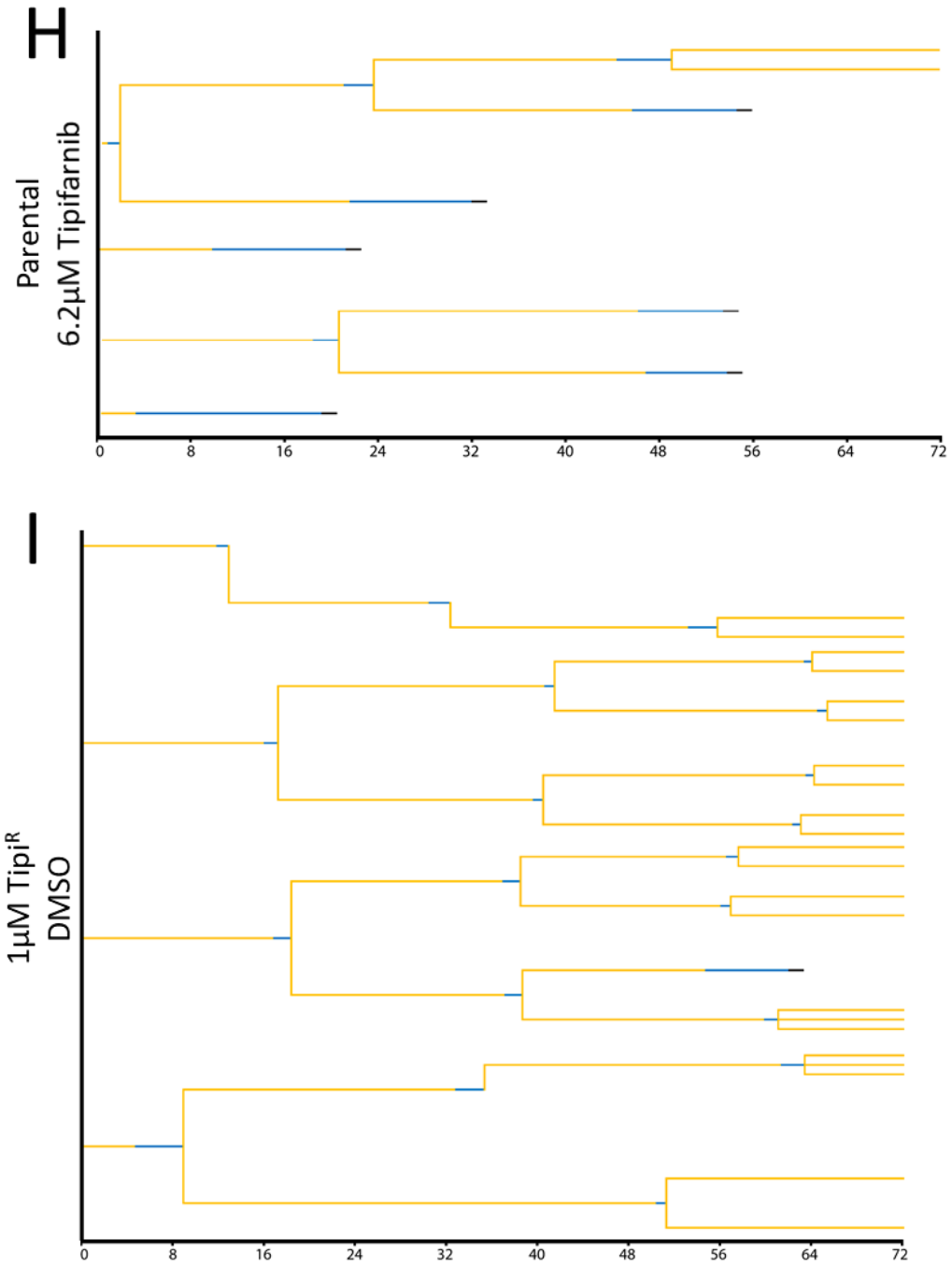
H
Parental
6.2μM Tipifarnib
0
8
16
24
32
40
48
56
64
72
I
1μM Tipi^R
DMSO
0
8
16
24
32
40
48
56
64
72

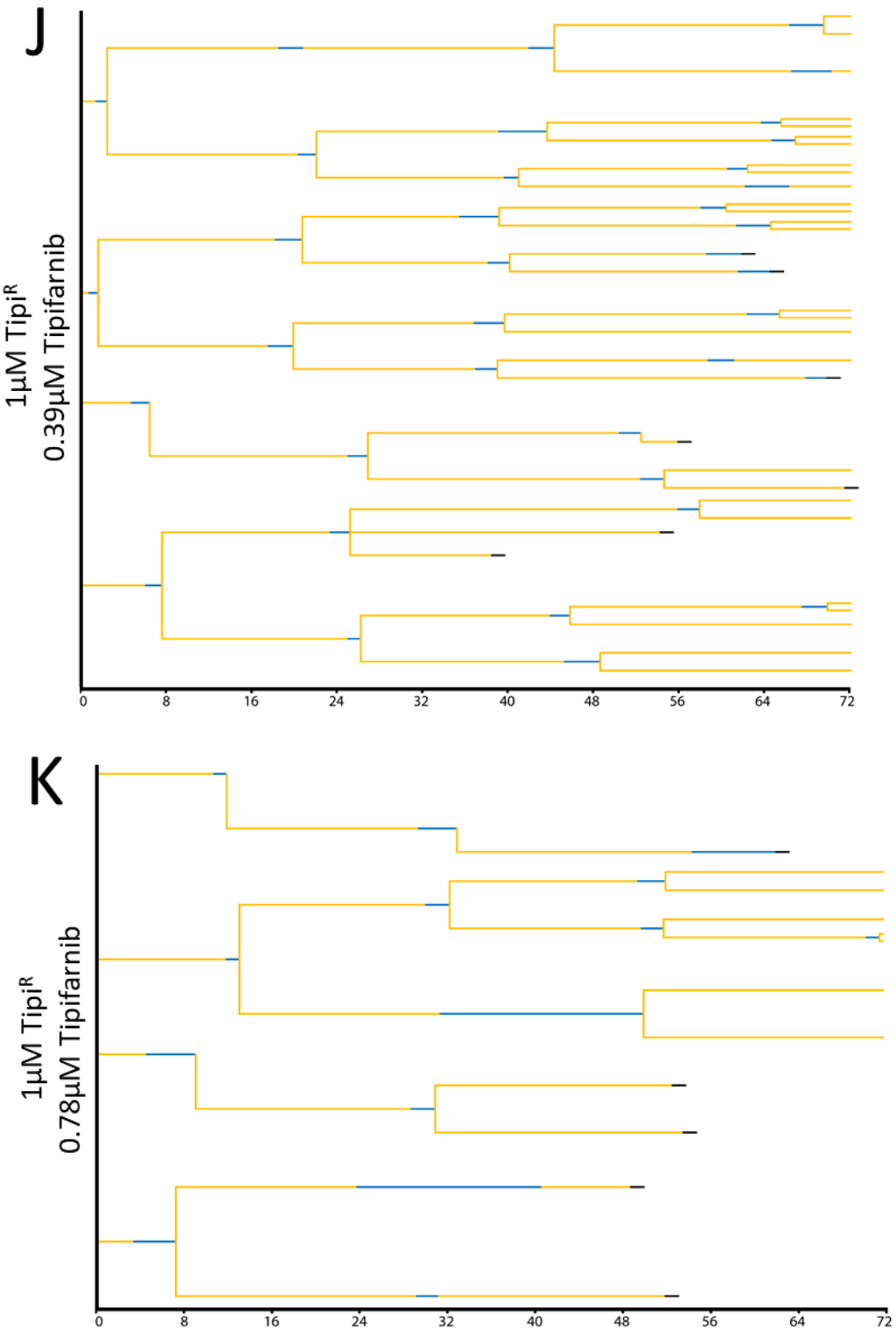
J
1μM Tipi^R
0.39μM Tipifarnib
0
8
16
24
32
40
48
56
64
72
K
1μM Tipi^R
0.78μM Tipifarnib
0
8
16
24
32
40
48
56
64
72

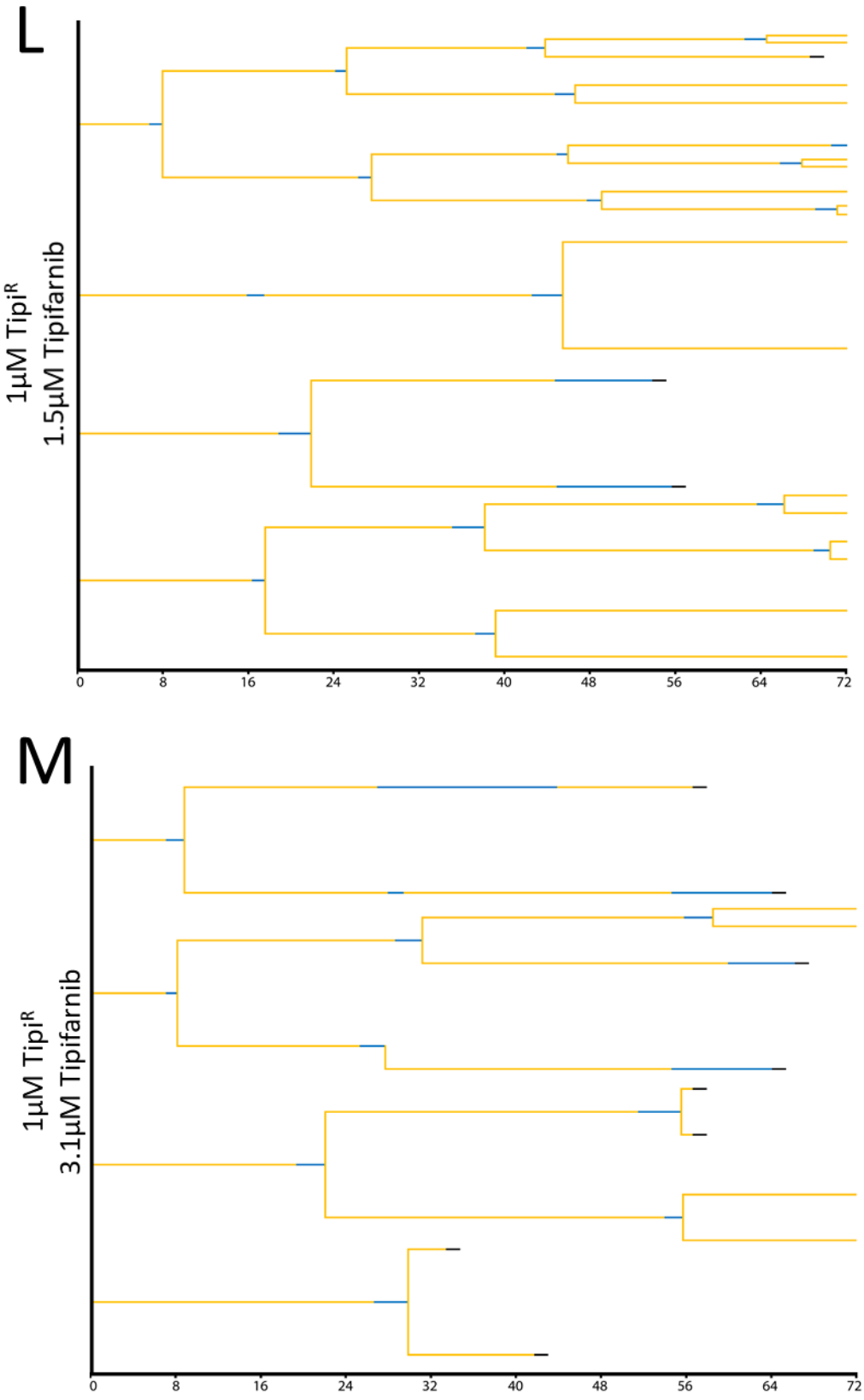
L
1μM Tipi^R
1.5μM Tipifarnib
0
8
16
24
32
40
48
56
64
72
M
1μM Tipi^R
3.1μM Tipifarnib
0
8
16
24
32
40
48
56
64
72

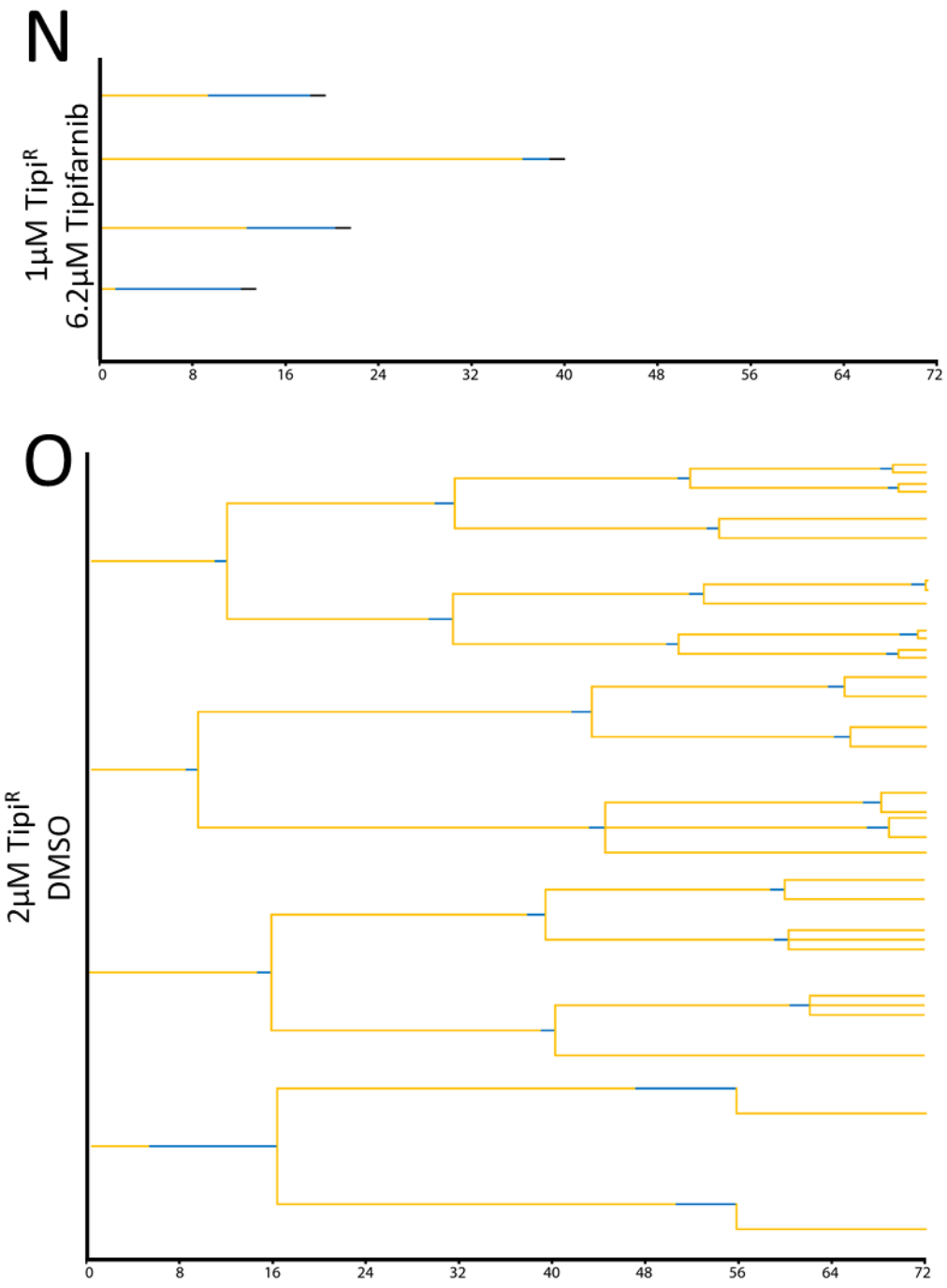
N
1μM Tipi^R
6.2μM Tipifarnib
0
8
16
24
32
40
48
56
64
72
O
2μM Tipi^R
DMSO
0
8
16
24
32
40
48
56
64
72

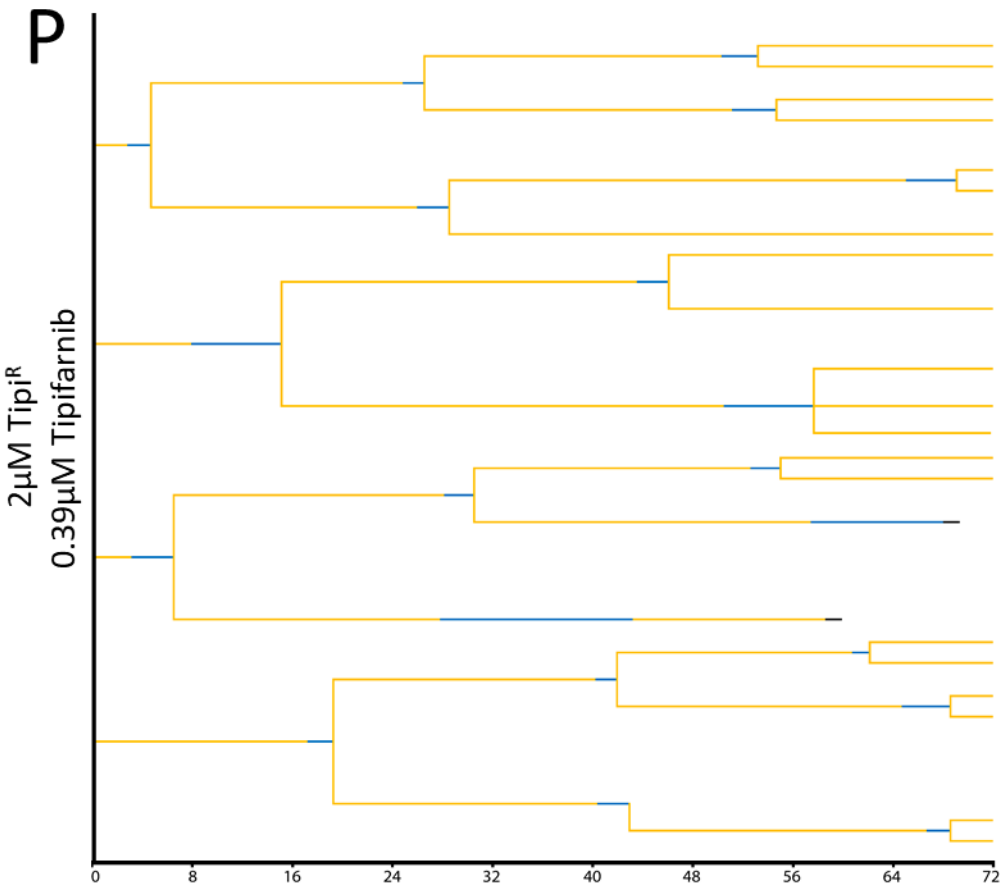
P
2μM Tipi^R
0.39μM Tipifarnib
0
8
16
24
32
40
48
56
64
72

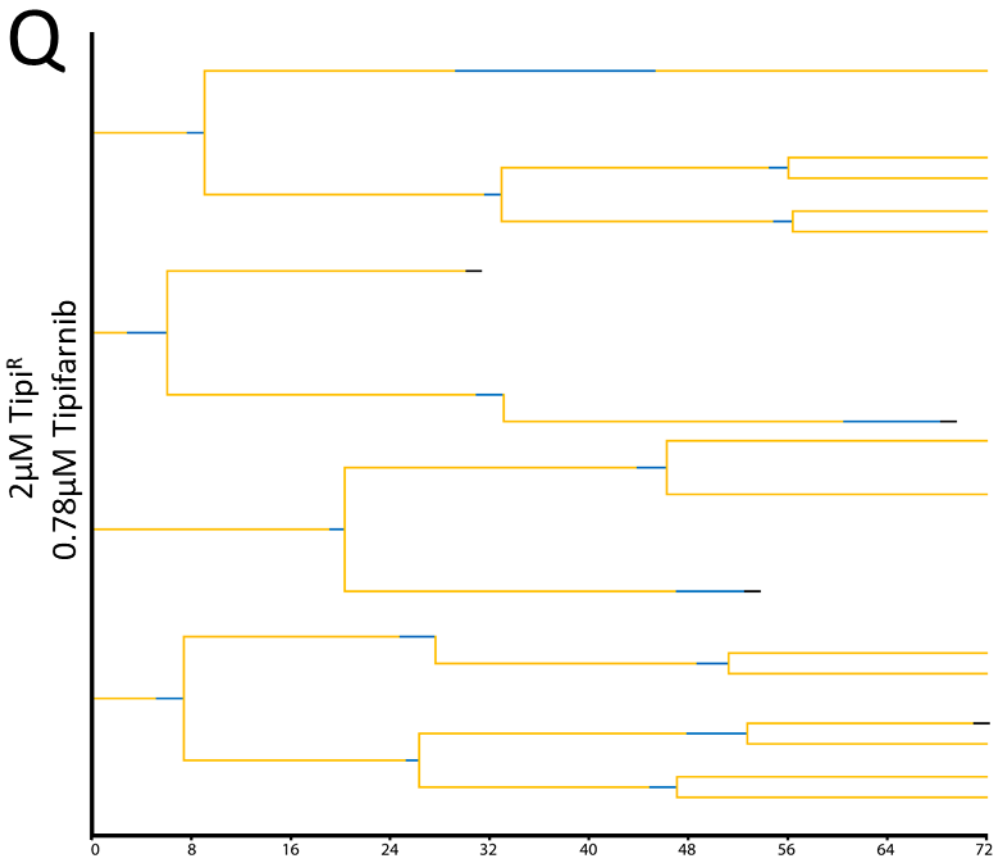
Q
2μM Tipi^R
0.78μM Tipifarnib
0
8
16
24
32
40
48
56
64
72

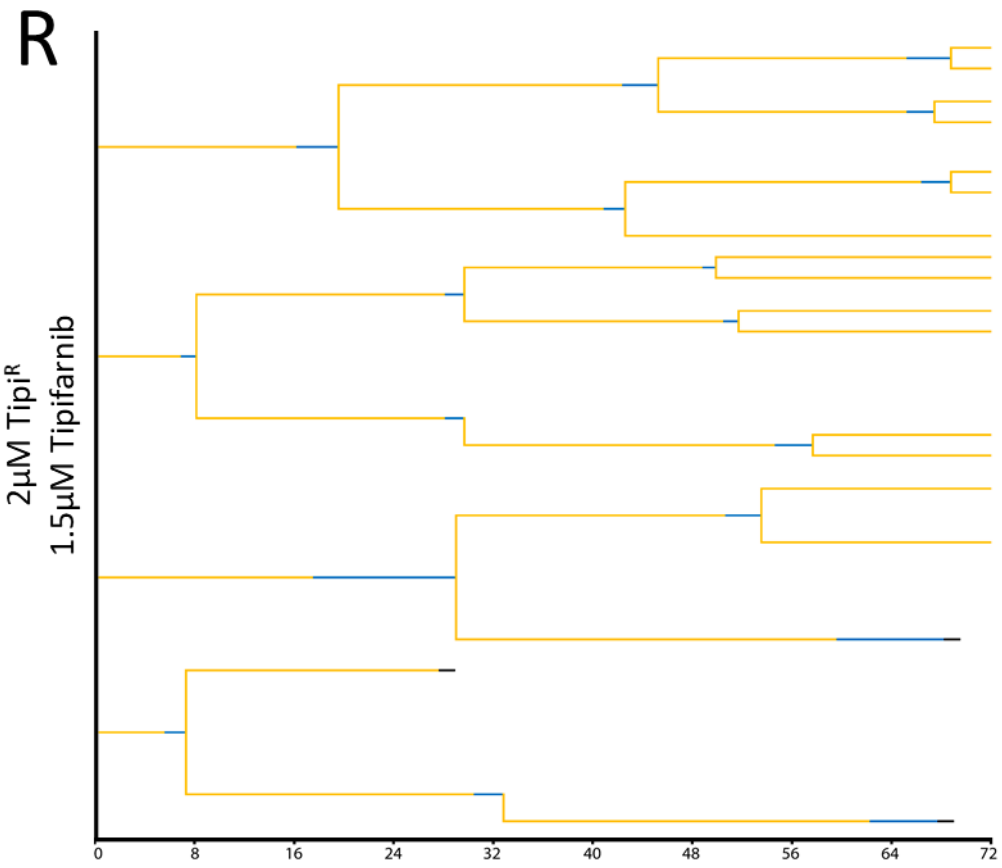
R
2μM Tipi^R
1.5μM Tipifarnib
0
8
16
24
32
40
48
56
64
72

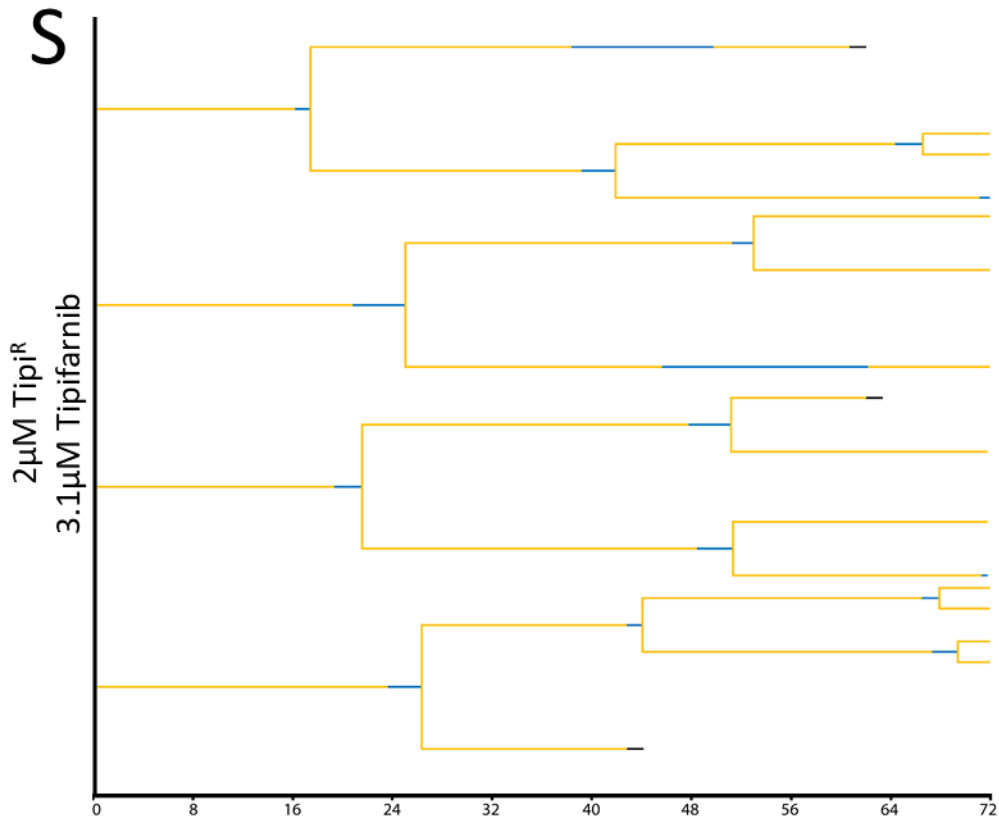
S
2μM Tipi^R
3.1μM Tipifarnib
0
8
16
24
32
40
48
56
64
72

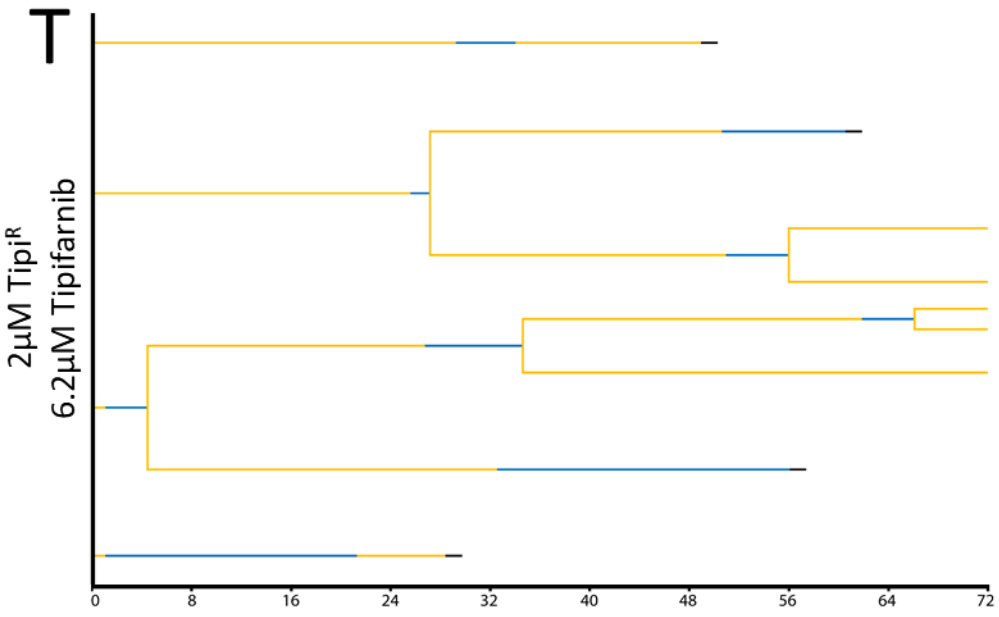
T
2μM Tipi^R
6.2μM Tipifarnib
0
8
16
24
32
40
48
56
64
72

3.18 Tipifarnib resistant cells show increased mitotic duration. Parental, 1µM Tipi^R 2µM Tipi^R cells were treated with a range of Tipifarnib (0.39-6.2 µM) for 72 hours and imaged every 10 minutes. Cell fate dendrograms are shown in C-T. Line graph for individual cells tracked by time-lapse microscopy is shown. A fork indicates cell division. The X-axis shows time in hours. Yellow = interphase, blue = mitosis, black = cell death. A) Dendrogram legend, showing the possible outcomes that are shown in the dendrograms. B) Examples of each cell fate stills from one of the videos analyzed. C-H, parental cells treated with DMSO (C), 0.39 µM (D), 0.78 µM (E), 1.5 µM (F), 3.1 µM (G), 6.2 µM (H). I-N, 1µM Tipi^R treated with DMSO (I), 0.39 µM (J), 0.78 µM (K), 1.5 µM (L), 3.1 µM (M), 6.2 µM (N). O-T, 2µm Tipi^R treated with DMSO (O), 0.39 µM (P), 0.78 µM (Q), 1.5 µM (R), 3.1 µM (S), 6.2 µM (T).

CHAPTER 4: Discussion and Conclusions

4.1 Characterization of Tipifarnib

Spindly KT recruitment requires farnesylation in order to interact with the RZZ complex. KT localized Spindly then recruits dynein/dynactin to the KT allowing for proper chromosome congression.[44,43] Previously our laboratory and others have shown that FTI treatment phenocopies Spindly KD, resulting in inhibition of Spindly KT localization and prometaphase arrest.[44,43] I have determined the minimum time and Tipifarnib concentration required for loss of Spindly KT localization to be 12 hours and 97nM. When testing different concentrations of Tipifarnib (97-1500 nM) at 12 hours, there are still partial (~50% relative to control) Spindly KT localization and similar residual levels of Spindly at KT with either 97 nM or 1500 nM Tipifarnib treatment (Figure 3.3 and Figure 3.4). While there is still partial recruitment at 12 hours with 1500 nM, I believe that FTase is fully inhibited because at 96 hours the IC_{50} is 416nM (Figure 3.6). 1500 nM is 3 times the 96 hours IC_{50} and cell death was not observed due to the short duration of the experiment. CENP-F is another outer KT protein that has been shown to require farnesylation to be recruited to the KT. However, there are conflicting reports in the literature about the effect of FTI treatment on CENP-F recruitment. One report showed that FTI treatment impairs CENP-F KT localization,[125] however our laboratory has previously shown that FTI treatment does not impair CENP-F KT localization,[44] and in my own experiments Tipifarnib treatment does not abolish CENP-F KT localization (Figure 3.3, 3.4). Therefore, I believe that Spindly is the primary target of Tipifarnib in mitosis.

Currently what is causing this partial Spindly KT recruitment is unknown, however, it is known that non-farnesylated Spindly is not recruited to the KT[44], and there is mitotic arrest and cell killing at these concentrations. I propose two potential mechanisms. First I propose that as farnesylation is a non-reversible post-translational modification, and it is known that Spindly is not fully degraded following exit from mitosis,[37] this pool of farnesylated Spindly will be able to bind to the RZZ complex in the next mitosis. The exact amount of the residual pool of Spindly following mitosis has not be quantified and how this relates to the minimum functional pool of Spindly required for dynein/dynactin KT recruitment and proper chromosome congression is not known.

The second possibility that leads to the difference observed between Spindly KT localization and the observed mitotic arrest and cell killing at longer time points, is if Spindly is farnesylated in interphase. It is unknown if Spindly requires farnesylation for its role in cell migration, only Spindly knockdown has been examined.[39,49] The only Tipifarnib treatment time point that had Spindly KT localization quantified was 12 hours. The previous experiment that included 18 and 24 hours were preliminary experiments where localization was determined as either yes or no visually for the whole cell. As only the 12 hour time point was quantified, if Spindly is farnesylated in interphase, then this could explain the pool of farnesylated Spindly present at the mitotic KT. Spindly protein levels peak in mitosis, however there is Spindly protein present at the G1/S transition in HeLa cells,[37] with the 12-hour treatment, potentially the interphase pool of Spindly is farnesylated. However, following Tipifarnib treatment, the Spindly protein that is then produced in G2 is not farnesylated and this is what results in the partial Spindly KT localization. If this is true, then the minimum treatment time will need to be adjusted to ensure that both the

remnant Spindly from the previous mitotic division and any interphase Spindly is also unfarnesylated, and therefore unable to be recruited to the KT. This would also account for the mitotic arrest and cell killing seen at 96 hours, as this pool of farnesylated Spindly would by gradually depleted due to turnover, resulting in the later division having no Spindly KT localization.

The existence of a residual farnesylated Spindly pool is also supported by the nocodazole KT localization assay. The treatment with nocodazole results in maximally expanded KTs, where there will be more RZZ complexes at KTs,[42] which can then bind more farnesylated Spindly. HeLa cells treated with 97-1500 nM Tipifarnib and nocodazole 30 minutes prior to fixation, resulted in Spindly KT localization that was decreased to ~32-23% relative to control depending on which concentration was examined (Figure 3.4). This reduction is presumably due to the increase in kinetochore size in the nocodazole treated cells and a finite pool of farnesylated Spindly following Tipifarnib that is able to localize to the KT via interaction with the RZZ complex. The reduction in Spindly KT localization when treated with 97 nM Tipifarnib alone is 47% relative to control while 97 nM Tipifarnib + nocodazole is 32%. These experiments were done simultaneously, with the only difference being if nocodazole was added 30 minutes prior to fixation. This 15% difference in Spindly KT localization supports our belief that the Spindly KT recruitment seen is due to a residual pool of farnesylated Spindly.

Both FTI treatment and Spindly knockdown result in a prometaphase arrest. This prometaphase arrest results in prolonged mitotic duration.[44] As expected, I found that Tipifarnib treatment also resulted in increased mitotic duration (Figure 3.5). When treated with 97 nM,

there was a doubling of the median mitotic duration relative to the solvent control, 80 minutes, compared to 40 minutes (Figure 3.5). When treated with 1500 nM, there was a median mitotic duration of 100 minutes (Figure 3.5). While there appears to be comparable levels of Spindly KT localization (Figure 3.3C), at the higher concentrations of Tipifarnib there is a longer mitotic duration. We do not know what is causing this difference in mitotic duration while the Spindly KT localization is comparable between the different Tipifarnib concentrations tested. We wish to determine if the difference observed in Spindly KT recruitment and mitotic arrest is mechanistically due to the recruitment of dynein/dynactin to KTs. If the partial recruitment of Spindly to the KT is sufficient to recruit enough dynein/dynactin to ensure chromosome congression and mitotic checkpoint silencing, the observed difference in Spindly KT localization seen with the nocodazole KT localization assay may explain the prolonged mitotic delay. I propose to examine dynein/dynactin kinetochore recruitment. Is there a comparable level of dynein/dynactin recruited in the cells treated with 97 nM and 1500 nM, or does the slightly lower Spindly:ACA ratio result in lower dynein/dynactin recruitment which then results in the prolonged mitotic duration? If dynein/dynactin recruitment also decreases further in a Tipifarnib dose dependent manner, that would account for the increased percentage of prometaphase cells seen with increasing concentrations of Tipifarnib and the increased median mitotic duration. However, if this is not true, then it is possible that Spindly has other unknown mitotic functions that will require further investigation. Alternatively, FTIs might be inhibiting other mitotic targets or functions.

To further understand Spindly farnesylation and the effects of Tipifarnib, understanding where in the cell cycle Spindly is farnesylated is invaluable. I propose to determine when in the

cell cycle Spindly is farnesylated by using metabolic labeling with an alkynyl-farnesol and CLICK chemistry.[126] By collecting samples at various time points throughout the cell cycle, this will allow us to determine when Spindly is farnesylated. It will also answer the previous question of a pool of farnesylated Spindly in interphase prior to the increased protein levels that peak in mitosis. This information will also then further inform the minimum treatment time required for Tipifarnib and to determine if Spindly is degraded following the exit from mitosis as CENP-F is, or if there is a residual pool that is present in the next cell cycle.

Spindly is farnesylated by FTase, which is comprised of the alpha and beta subunits, that work in conjunction to farnesylate target proteins.[56] Tipifarnib inhibits FTase through binding in the substrate binding site,[95] therefore, if there is more FTase, then more Tipifarnib will be required to fully inhibit farnesylation. Sensitivity does not appear to correspond to levels of Spindly and FNTB in all cell lines tested. When examining the ratio of FNTB:Spindly, Spindly protein levels or FNTB protein levels to Tipifarnib IC_{50}, none of these combinations act as a clear indicator for sensitivity or resistance. There is no clear relationship that can be observed, in some cases, such as SK-BR-3, it appears that higher Spindly levels generally correspond to higher sensitivity, while the lower Spindly protein levels correspond to the more resistant cell lines, e.g. BT-474 (Figure 3.7). More investigation will be required to determine what molecular markers serve as predictors for cell line response to Tipifarnib treatment.

Normally, the non-tumorigenic control is used to show if the treatment has a viable therapeutic window. In our experiments MCF 10a, one of the 2 non-tumorigenic controls is extremely sensitive via an unknown mechanism. The other non-tumorigenic control tested, HME-

1, is very resistant to Tipifarnib. I believe the extreme sensitivity of MCF 10a to Tipifarnib is cell line specific and not representative of what would happen in a patient, as Tipifarnib has been shown to have viable therapeutic window in clinical trials. To confirm this, I can test Tipifarnib in primary patient cell lines, to determine if it is excessively toxic to the non-tumorigenic mammary epithelial cells or if the extreme Tipifarnib sensitivity is MCF10a specific.

4.2 Tipifarnib & Adavosertib combination treatment

Synergistic combinations allow for lower doses of either treatment then when used alone.[117] This can help minimize side effects, as at the lower concentrations, the goal is to spare the normal non-cancerous cells. The combination of Tipifarnib and Adavosertib exhibited synergy that was not specific to particular breast cancer subtype, instead there was varying degrees of synergy, ranging from strongly synergistic to weakly synergistic.

To further understand the synergistic mechanism that is occurring, I propose to do live cell imaging of these cells to determine what effects the combination treatment is having at the different concentrations. Of the cell lines tested, HeLa and MDA-MB-231 have shorter division times, ~24 hours, so by using these cells to examine mitotic timing I will be able to examine 3-4 divisions per cell. While if I tested BT-474, which has a doubling time of ~60-80 hours then only one division may be observed. I expect to see prolonged mitotic arrest with increasing concentration of either Tipifarnib or Adavosertib. Additionally, with increasing Adavosertib there should be a shorter interphase duration between mitotic divisions, due to Adavosertib mediated premature mitotic entry. This will allow us to further understand the synergistic mechanism of combining Tipifarnib and Adavosertib on mitosis.

In order to determine if staggering the addition of Tipifarnib and Adavosertib would increase synergy we tested this with a 24-hour delay between the two drugs. We found that altering the order in which the compounds were added, did not make the combination more synergistic, in fact it made it less synergistic in all cases. When Adavosertib was added first in all cases, a lower dose of Adavosertib resulted in 50% cell killing compared to either simultaneous or Tipifarnib first addition (Figure 3.10). This indicates that Adavosertib is the dominant drug when added first in the combination treatment. But when they are added simultaneously or with Tipifarnib first it does not appear to be the dominant drug.

4.3 Tipifarnib Resistant cells

The mechanism through which cancer cells develop resistance is not always known. However, it is known that the treatment used can apply selective pressures and select for the resistant population.[127] This can then lead to relapses in patients. We were able to develop resistant cells *in vitro*, through persistent culture with Tipifarnib, similar to what might be seen in the clinic. A previous example of resistance that our lab had tested, was Myt1 overexpression resulting in Adavosertib resistance.[128] While Adavosertib only inhibits Wee1, Myt1 inhibition of Cdk1 is sufficient to overcome the aberrant Cdk1 activity that occurs following Adavosertib treatment.[128] First we investigated if Spindly or FNTB protein levels are increased in the Tipifarnib resistant cells. While there is an increase in the protein levels (Figure 3.12), this does not result in Spindly KT localization in the presence of Tipifarnib (Figure 3.13, 3.14). The increase in FNTB protein levels could result in increased active FTase, which then would require more Tipifarnib in order for its activity to be fully inhibited and could potentially lead to resistance. However, the increased FNTB

levels do not result in increased Spindly KT localization (Figure 3.13, 3.14) therefore if the mechanism of action is FNTB mediated it is not through Spindly farnesylation. The mechanism of resistance in the Tipifarnib resistant cells is not through rescuing Spindly KT localization in the presence of Tipifarnib.

The implications is that Tipifarnib might potentially have other targets. There may be other mitotic proteins that are able to compensate for Spindly function, which is resulting in the survival in the presence of Tipifarnib. Alternatively, the resistance may be due to dynein/dynactin recruitment independent of Spindly. The increased mitotic duration of the resistant cell lines indicates a partial functional rescue. Impairing dynein/dynactin KT recruitment results in prometaphase arrest,[129,130,131,132] however resistant cells readily undergo anaphase despite having a delay (Figure 3.15). If dynein/dynactin is still recruited to KTs but at a reduced level, it might be through a less efficient mechanism. In order to investigate this, dynein/dynactin KT localization will be examined in the parental and resistant cells. If there is dynein/dynactin localization in the resistant cells comparable to the parental cells, this suggests dynein/dynactin may be recruited through a different adaptor protein, which could be the mechanism of action through which the Tipifarnib resistant cells survive.

The Tipifarnib resistant cell lines have increased Spindly protein levels relative to parental (Figure 3.12), however this does not result in increased Spindly KT localization. When treated with Tipifarnib, as with other FTIs, this results in prometaphase arrest.[44] Parental and Tipifarnib resistant cells, when treated with the same concentrations of Tipifarnib result in comparable percentages of prometaphase cells (Figure 3.15). Whatever mechanism through which Tipifarnib

resistance was developed does not appear to shorten the prometaphase arrest seen when treating parental cells with either 1 μM or 2 μM Tipifarnib. The prometaphase delay results in prolonged median mitotic duration (Figure 3.16) and increased cell death with increasing Tipifarnib concentrations consistent with previous work with other FTIs.[44,43]

One of the common mechanisms through which cells develop resistance is through the expression of multidrug resistance pumps. However, I do not believe this to be the case for the Tipifarnib resistant cells, because if multidrug resistant pumps were responsible for Tipifarnib resistance, then Tipifarnib would be actively pumped out from the cell and Spindly would be farnesylated. Due to the lack of Spindly KT localization I do not believe that multidrug resistant pumps are the cause of Tipifarnib resistance. Another potential mechanism of resistance is that there are compensatory mechanisms for chromosome congression. Chromosome congression is achieved through multiple redundant force generating mechanisms, and it is the balance of forces that result in alignment of chromosomes at the metaphase plate. Spindly-Dynein/dynactin is one of these force generating mechanisms. Other mitotic forces might be altered to compensate for the lack of dynein/dynactin to achieve chromosome congression (Figure 4.1). The mechanism of compensation does not appear to be perfect, as we still observe a prometaphase delay however the cells eventually do divide and survive. It is already known that Spindly-dynein/dynactin counters the polar ejection forces of the chromokinesin hKid,[37] and therefore other balancing mitotic forces may be altered to allow chromosome congression and thus causing the resistance. The high content analysis of the Tipifarnib resistant cells supports this notion. When resistant cells were treated with DMSO only, there was an increased number of abnormal mitotic division, where binucleated cells or tripolar divisions frequently occurred.

This suggests that the resistant cell lines are addicted to Tipifarnib and the balance of mitotic forces required for chromosome congression is disturbed when Tipifarnib is removed resulting in abnormal division. Potentially these mitotic forces can be manipulated via siRNA knockdown to examine the effect on Tipifarnib resistant chromosome congression. If the siRNA KD results in death of the resistant cells, this will suggest that it is a potential synthetic lethality partner. Further investigation is required to determine if the mechanism of resistance is due to an alternative mechanism for chromosome congression.

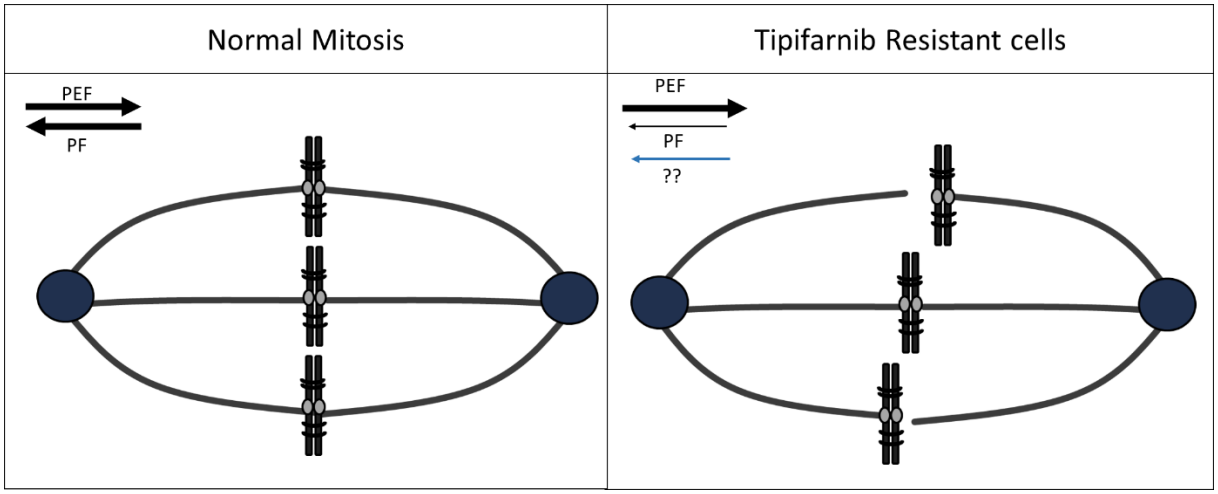

Figure 4.1 Tipifarnib resistance mechanism. The potential mechanism of resistance. In normal mitosis, the polar ejection forces (PEF) and dynein/dynactin mediated poleward forced (PF) are balanced and proper chromosome congression occurs. In the resistant cells the PF are decreased most likely due to lack of Spindly mediated dynein/dynactin recruitment but there is another unknown force that compensates resulting in proper chromosome congression.

4.4 Conclusions

Tipifarnib inhibits Spindly KT localization as expected and this inhibition occurs at a much shorter time period than expected. Previously FTI treatment had not been tested for shorter than 24 hours and we found that 12 hours is sufficient for impaired Spindly KT localization and prolonged mitotic duration. Neither Spindly nor FNTB protein levels are able to function as a

marker for Tipifarnib sensitivity. Further investigation is required to determine if there are any markers to determine who would benefit from treatment with Tipifarnib.

Tipifarnib is synergistic when combined with Adavosertib to varying degrees of synergy. This does not appear to be breast cancer subtype specific. Further investigation into what acts as prognostic markers may elucidate who will benefit from this treatment. Now that I have shown that Tipifarnib and Adavosertib are synergistic combination *in vitro*, I wish to determine if this also occurs *in vivo*. I propose to use a xenograft mouse model to determine if the synergy seen *in vitro* also occurs *in vivo*. In parallel to this, we will be investigating the mechanism of resistance to better understand this mechanism *in vitro*. The combination of these two approaches, will allow us to examine if there are other potential therapeutic targets which then can be examined in the TGCA database to determine if a potential population of patients may benefit. At this point we will be able to test appropriate patient samples and examine whether what we have observed *in vitro* in cell lines occurs in the patients.

The characterization of the Tipifarnib resistant cell lines is still incomplete and ongoing, with only minimal investigation having been completed in this thesis. I found that they have increased Spindly protein expression, however this does not lead to the rescue of Spindly KT localization. The lack of Spindly KT localization seen in the resistant cells results in a prolonged mitotic duration, however the increase in mitotic duration when treated with Tipifarnib is a less significant increase compared to the parental cell line. Further investigation into these resistant cells will allow us to better understand the resistance mechanisms.

My research will allow us to better understand Tipifarnib and farnesylation as a cancer therapeutic target and as an anti-mitotic agent. By further investigating this mechanism we will be able to better understand how chromosome congression works, and if there is a potential therapeutic target or synthetic lethal partner that can be targeted in combination with Tipifarnib.

References:

1. Mcintosh, J. R. (2016). *Mitosis*. *Cold Spring Harb. Perspect. Biol.* 1–16

2. Vermeulen, K., Van Bockstaele, D. R. & Berneman, Z. N. (2003). *The cell cycle: A review of regulation, deregulation and therapeutic targets in cancer*. *Cell Prolif.* **36,** 131–149

3. Pavletich, N. P. (1999). *Mechanisms of cyclin-dependent kinase regulation: Structures of Cdks, their cyclin activators, and Cip and INK4 inhibitors*. *J. Mol. Biol.* **287,** 821–828

4. Lim, S. & Kaldis, P. (2013). *Cdks, cyclins and CKIs: roles beyond cell cycle regulation*. *Development* **140,** 3079–3093

5. Jorgensen, P. & Tyers, M. (2004). *How cells coordinate growth and division*. *Curr. Biol.* **14,** 1014–1027

6. Kastan, M. B. & Bartek, J. (2004). *Cell-cycle checkpoints and cancer*. *Nature* **432,** 316–323

7. Timofeev, O., Cizmecioglu, O., Settele, F., Kempf, T. & Hoffmann, I. (2010). *Cdc25 phosphatases are required for timely assembly of CDK1-cyclin B at the G2/M transition*. *J. Biol. Chem.* **285,** 16978–16990

8. Rieder, C. L. & Khodjakov, A. (2003). *Mitosis through the microscope: Advances in seeing inside live dividing cells*. *Science (80-.).* **300,** 91–96

9. Walczak, C. E., Cai, S. & Khodjakov, A. (2010). *Mechanisms of chromosome behaviour during mitosis*. *Nat. Rev. Mol. Cell Biol.* **11,** 91–102

10. Cheeseman, I. M. (2014). *The Kinetochore*. *Cold Spring Harb. Perspect. Biol.* **6,** 1–18

11. Pesenti, M. E., Weir, J. R. & Musacchio, A. (2016). *Progress in the structural and functional characterization of kinetochores*. *Curr. Opin. Struct. Biol.* **37,** 152–163

12. Musacchio, A. (2015). *The Molecular Biology of Spindle Assembly Checkpoint Signaling Dynamics*. *Curr. Biol.* **25,** R1002–R1018

13. Cianfrocco, M. A., Desantis, M. E., Leschziner, A. E. & Reck-Peterson, S. L. (2015). *Mechanism and Regulation of Cytoplasmic Dynein*. *Annu. Rev. Cell Dev. Biol.* **31,** 83–108

14. McKenney, R. J., Huynh, W., Tanenbaum, M. E., Bhabha, G. & Vale, R. D. (2014). *Activation of cytoplasmic dynein motility by dynactin-cargo adapter complexes*. *Science (80-.).* **345,** 337–341

15. Schlager, M. A., Hoang, H. T., Urnavicius, L., Bullock, S. L. & Carter, A. P. (2014). *In vitro reconstitution of a highly processive recombinant human dynein complex* . *EMBO J.* **33,** 1855–1868

16. Kardon, J. R. & Vale, R. D. (2009). *Regulators of the cytoplasmic dynein motor*. *Nat. Rev. Mol. Cell Biol.* **10,** 854–865

17. Berto, A. & Doye, V. (2018). *Regulation of Cenp-F localization to nuclear pores and kinetochores*. *Cell Cycle* **17,** 2122–2133

18. Feng, J., Huang, H. & Yen, T. J. (2006). *CENP-F is a novel microtubule-binding protein that is essential for kinetochore attachments and affects the duration of the mitotic*

checkpoint delay. *Chromosoma* **115,** 320–329

19. Vergnolle, M. A. S. & Taylor, S. S. (2007). *Cenp-F Links Kinetochores to Ndel1/Nde1/Lis1/Dynein Microtubule Motor Complexes*. *Curr. Biol.* **17,** 1173–1179

20. Hussein, D. & Taylor, S. S. (2002). *Farnesylation of Cenp-F is required for G2/M progression and degradation after mitosis*. *J. Cell Sci.* **115,** 3403–3414

21. Ciossani, G. *et al.* (2018). *The kinetochore proteins CENP-E and CENP-F directly and specifically interact with distinct BUB mitotic checkpoint Ser / Thr kinases*. **293,** 10084–10101

22. Li, R. & Murray, A. W. (1991). *Feedback Control of Mitosis in budding Yeast*. *Cell* **66,** 519–531

23. Hoyt, M. A., Totis, L. & Roberts, B. T. (1991). *S. cerevisiae genes required for cell cycle arrest in response to loss of microtubule function*. *Cell* **66,** 507–517

24. Weiss, E. & Winey, M. (1996). *The Saccharomyces cerevisiae spindle pole body duplication gene MPS1 is part of a mitotic checkpoint*. *J. Cell Biol.* **132,** 111–123

25. Elledge, S. J. (1996). *Cell cycle checkpoints: Preventing an identity crisis*. *Science (80-.).* **274,** 1664–1672

26. Primorac, I. & Musacchio, A. (2013). *Panta rhei: The APC/C at steady state*. *J. Cell Biol.* **201,** 177–189

27. Murray, A. W., Solomon, M. J. & Kirschner, M. W. (1989). *The role of cyclin synthesis and degradation in the control of maturation promoting factor activity*. *Nature* **339,** 280–286

28. De Antoni, A., Pearson, C., Cimini, D., Canman, J. C., Sala, V., Faretta, M., Salmon, E.D., Musacchio, A. (2014). *The Mad1/Mad2 Complex as a Template for Mad2 Activation in the Spindle Assembly Checkpoint. Curr. Biol.* **91,** 20–22

29. Michel, L. *et al.* (2004). *Complete loss of the tumor suppressor MAD2 causes premature cyclin B degradation and mitotic failure in human somatic cells*. *Proc. Natl. Acad. Sci. U. S. A.* **101,** 4459–4464

30. Williams, B. C., Li, Z., Liu, S. & Williams, E., Leung, G., Yen, T. J., G. M. L. (2003). *Zwilch, a new component of hte Zw10/ROD complex required for Kinetochore functions*. *Mol. Biol. Cell* **14,** 1379–1391

31. Zhang, G., Lischetti, T., Hayward, D. G. & Nilsson, J. (2015). *Distinct domains in Bub1 localize RZZ and BubR1 to kinetochores to regulate the checkpoint*. *Nat. Commun.* **6,**

32. Kops, Geert J.P.L., Kim, Yumi., Weaver, Beth A.A., Mao, Yinghui, Mao., McLeod, Ian., Yates III, John R., Tagaya, Mitsuo., Cleveland, Don W. (2005). *Zw10 links mitotic checkpoint signaling to the structural kinetochore*. *J. Cell Biol.* **16,** 49–60

33. Buffin, E., Lefebvre, C., Huang, J., Gagou, M. E. & Karess, R. E. (2005). *Recruitment of Mad2 to the kinetochore requires the Rod/Zw10 complex*. *Curr. Biol.* **15,** 856–861

34. Griffis, E. R., Stuurman, N. & Vale, R. D. (2007). *Spindly, a novel protein essential for*

silencing the spindle assembly checkpoint, recruits dynein to the kinetochore. *J. Cell Biol.* **177,** 1005–1015

35. Yamamoto, T. G., Watanabe, S., Essex, A. & Kitagawa, R. (2008). *Spdl-1 functions as a kinetochore receptor for MDF-1 in Caenorhabditis elegans*. *J. Cell Biol.* **183,** 187–194

36. Chan, Y. W. *et al.* (2009). *Mitotic control of kinetochore-associated dynein and spindle orientation by human Spindly*. *J. Cell Biol.* **185,** 859–874

37. Barisic, M., Sohm, B., Mikolcevic, P., Wandke, C., Rauch, V., Ringer, T., Hess, M., Bonn, G., Geley, S. (2010). *Spindly/CCDC99 Is Required for Efficient Chromosome Congression and Mitotic Checkpoint Regulation*. *Mol. Biol. Cell* **21,** 1968–1981

38. Gassmann, R. *et al.* (2010). *Removal of Spindly from microtubule-attached kinetochores controls spindle checkpoint silencing in human cells*. *Genes Dev.* **24,** 957–971

39. Conte, C., Baird, M. A., Davidson, M. W. & Griffis, E. R. (2018). *Spindly is required for rapid migration of human cells*. *Biol. Open* **7,**

40. Clemente, G. D. *et al.* (2018). *Requirement of the Dynein-adaptor spindly for mitotic and post-mitotic functions in Drosophila*. *J. Dev. Biol.* **6,** 1–23

41. Hoogenraad, C. C. & Akhmanova, A. (2016). *Bicaudal D Family of Motor Adaptors: Linking Dynein Motility to Cargo Binding*. *Trends Cell Biol.* **26,** 327–340

42. Sacristan, C. *et al.* (2018). *Dynamic kinetochore size regulation promotes microtubule capture and chromosome biorientation in mitosis*. *Nat. Cell Biol.* **20,** 800–810

43. Holland, A. J. *et al.* (2015). *Preventing farnesylation of the dynein adaptor Spindly contributes to the mitotic defects caused by farnesyltransferase inhibitors*. *Mol. Biol. Cell* **26,** 1845–1856

44. Moudgil, D. K. *et al.* (2015). *A novel role of farnesylation in targeting a mitotic checkpoint protein, human spindly, to kinetochores*. *J. Cell Biol.* **208,** 881–896

45. Mosalaganti, S. *et al.* (2017). *Structure of the RZZ complex and molecular basis of its interaction with Spindly*. *J. Cell Biol.* **216,** 961–981

46. Gama, J. B. *et al.* (2017). *Molecular mechanism of kinetochore dynein recruitment by the Rod/Zw10/Zwilch complex and Spindly*. *J. Cell Biol.* **216,** 654–672

47. Krenn, V. & Musacchio, A. (2015). *The Aurora B kinase in chromosome bi-orientation and spindle checkpoint signaling*. *Front. Oncol.* **5,**

48. Gurden, M. D., Anderhub, S. J., Faisal, A. & Linardopoulos, S. (2018). *Aurora B prevents premature removal of spindle assembly checkpoint proteins from the kinetochore: A key role for Aurora B in mitosis*. *Oncotarget* **9,** 19525–19542

49. Conte, C., Griffis, E. R., Hickson, I. & Perez-Oliva, A. B. (2018). *USP45 and Spindly are part of the same complex implicated in cell migration*. *Sci. Rep.* **8,** 1–13

50. Silva, P. M. A. *et al.* (2017). *Suppression of spindly delays mitotic exit and exacerbates cell death response of cancer cells treated with low doses of paclitaxel*. *Cancer Lett.* **394,** 33–42

51. Zhang, F. L. & Casey, P. J. (1996). *Protein Prenylation: Molecular Mechanisms and Functional Consequences*. *Annu. Rev. Biochem.* **65,** 241–269

52. Kamiya, Y. *et al.* (1979). *Structure of rhodotorucine A, a peptidyl factor, inducing mating tube formation in Rhodosporidium toruloides*. *Agric. Biol. Chem.* **43,** 363–369

53. Schmidt, R. A., Schneider, C. J. & Glomset, J. A. (1984). *Evidence of post-translational incorporation of a product of mevalonic acid into Swiss 3T3 cell proteins*. *J. Biol. Chem.* **259,** 10175–10180

54. Goldstein, J. L. & Brown, M. S. (1995). *Regulation of the mevalonate pathway in plants*. *Nature* **343,** 425–430

55. Powers, S. *et al.* (1986). *RAM, a gene of yeast required for a functional modification of RAS proteins and for production of mating pheromone a-factor*. *Cell* **47,** 413–422

56. Reiss, Y., Goldstein, J. L., Seabra, M. C., Casey, P. J. & Brown, M. S. (1990). *Inhibition of purified p21ras farnesyl:protein transferase by Cys-AAX tetrapeptides*. *Cell* **62,** 81–88

57. Schaber, M. D. *et al.* (1990). *Polyisoprenylation of Ras in Vitro by a Farnesyl-Protein Transferase"*. *J. Biol. Chem.* **265,** 14701–14704

58. Chen, W. J., Andres, D. A., Goldstein, J. L. & Brown, M. S. (1991). *Cloning and expression of a cDNA encoding the α subunit of rat p21(ras) protein farnesyltransferase*. *Proc. Natl. Acad. Sci. U. S. A.* **88,** 11368–11372

59. Chen, W. J., Andres, D. A., Goldstein, J. L., Russell, D. W. & Brown, M. S. (1991). *cDNA*

cloning and expression of the peptide-binding β subunit of rat p21rasfarnesyltransferase, the counterpart of yeast DPR1/RAM1. *Cell* **66,** 327–334

60. Tschantz, W. R., Furfine, E. S. & Casey, P. J. (1997). *Substrate binding is required for release of product from mammalian protein farnesyltransferase*. *J. Biol. Chem.* **272,** 9989–9993

61. Reiss, Y., Brown, M. S. & Goldstein, J. L. (1992). *Divalent cation and prenyl pyrophosphate specificities of the protein farnesyltransferase from rat brain, a zinc metalloenzyme*. *J. Biol. Chem.* **267,** 6403–6408

62. Reiss, Y. *et al.* (1991). *Nonidentical subunits of p21(H-ras) farnesyltransferase. Peptide binding and farnesyl pyrophosphate carrier functions*. *J. Biol. Chem.* **266,** 10672–10677

63. Mijimolle, N. *et al.* (2005). *Protein farnesyltransferase in embryogenesis, adult homeostasis, and tumor development*. *Cancer Cell* **7,** 313–324

64. Farnsworth, C. C., Gelb, M. H. & Glomset, J. A. (1990). *Identification of geranylgeranyl-modified proteins in HeLa cells*. *Science (80-.).* **247,** 320–322

65. Cox, A. D., Hisaka, M. M., Buss, J. E. & Der, C. J. (1992). *Specific isoprenoid modification is required for function of normal, but not oncogenic, Ras protein. Mol. Cell. Biol.* **12,** 2606–2615

66. Yokoyama, K., Goodwin, G. W., Ghomashchi, F., Glomset, J. A. & Gelb, M. H. (1991). *A protein geranylgeranyltransferase from bovine brain: Implications for protein prenylation*

specificity. *Proc. Natl. Acad. Sci. U. S. A.* **88,** 5302–5306

67. Moores, S. L. *et al.* (1991). *Sequence dependence of protein isoprenylation*. *J. Biol. Chem.* **266,** 14603–14610

68. Casey, P. J., Thissen, J. A. & Moomaw, J. F. (1991). *Enzymatic modification of proteins with a geranylgeranyl isoprenoid*. *Proc. Natl. Acad. Sci. U. S. A.* **88,** 8631–8635

69. Jackson, J. H. *et al.* (1990). *Farnesol modification of Kirsten-ras exon 4B protein is essential for transformation*. *Proc. Natl. Acad. Sci. U. S. A.* **87,** 3042–3046

70. Van Cutsem, E. *et al.* (2004). *Phase III trial of gemcitabine plus tipifarnib compared with gemcitabine plus placebo in advanced pancreatic cancer*. *J. Clin. Oncol.* **22,** 1430–1438

71. Palsuledesai, C. C. & Distefano, M. D. (2015). *Protein Prenylation: Enzymes, Therapeutics, and Biotechnology Applications*.

72. Norbert Berndt, Andrew D. Hamilton, S. M. S. (2012). *Targeting protein prenylation for cancer therapy*. *Nat* **23,** 1–7

73. Zhang, B., Fenton, R. G. & Prendergast, G. C. (2002). *Farnesyltransferase inhibitors reverse Ras-mediated inhibition of Fas gene expression*. *Cancer Res.* **62,** 450–458

74. Takada, Y., Khuri, F. R. & Aggarwal, B. B. (2004). *Protein farnesyltransferase inhibitor (SCH 66336) abolishes NF-κB activation induced by various carcinogens and inflammatory stimuli leading to suppression of NF-κB-regulated gene expression and up-regulation of apoptosis*. *J. Biol. Chem.* **279,** 26287–26299

75. Crespo, N. C., Ohkanda, J., Yen, T. J., Hamilton, A. D. & Sebti, S. M. (2001). *The Farnesyltransferase Inhibitor, FTI-2153, Blocks Bipolar Spindle Formation and Chromosome Alignment and Causes Prometaphase Accumulation during Mitosis of Human Lung Cancer Cells*. *J. Biol. Chem.* **276,** 16161–16167

76. Crespo, N. C. *et al.* (2002). *The farnesyltransferase inhibitor, FTI-2153, inhibits bipolar spindle formation during mitosis independently of transformation and Ras and p53 mutation status*. *Cell Death Differ.* **9,** 702–709

77. Lerner, E. C. *et al.* (1995). *Ras CAAX peptidomimetic FTI-277 selectively blocks oncogenic Ras signaling by inducing cytoplasmic accumulation of inactive Ras-Raf complexes*. *J. Biol. Chem.* **270,** 26802–26806

78. Sun, J., Sebti, S. M., Qian, Y. & Hamilton, A. D. (1995). *Ras CAAX Peptidomimetic FTI 276 Selectively Blocks Tumor Growth in Nude Mice of a Human Lung Carcinoma with K-Ras Mutation and p53 Deletion*. *Cancer Res.* **55,** 4243–4247

79. Mangues, R. *et al.* (1998). *Antitumor effect of a farnesyl protein transferase inhibitor in mammary and lymphoid tumors overexpressing N-ras in transgenic mice*. *Cancer Res.* **58,** 1253–1259

80. Omer, C. A. *et al.* (2000). *Mouse mammary tumor virus-Ki-rasB transgenic mice develop mammary carcinomas that can be growth-inhibited by a farnesyl:protein transferase inhibitor*. *Cancer Res.* **60,** 2680–2688

81. Delmas, C. *et al.* (2003). *The Farnesyltransferase Inhibitor R115777 Reduces Hypoxia and*

Matrix Metalloproteinase 2 Expression in Human Glioma Xenograft. *Clin. Cancer Res.* **9,** 6062–6068

82. Moasser, M. M. *et al.* (1998). *Farnesyl transferase inhibitors cause enhanced mitotic sensitivity to taxol and epothilones*. *Proc. Natl. Acad. Sci. U. S. A.* **95,** 1369–1374

83. Eriksson, M. *et al.* (2003). *Recurrent de novo point mutations in lamin A cause Hutchinson-Gilford progeria syndrome*. *Nature* **423,** 293–298

84. Young, S. G., Fong, L. G. & Michaelis, S. (2005). *Prelamin A, Zmpste24, misshapen cell nuclei, and progeria - New evidence suggesting that protein farnesylation could be important for disease pathogenesis*. *J. Lipid Res.* **46,** 2531–2558

85. Mallampalli, M. P., Huyer, G., Bendale, P., Gelb, M. H. & Michaelis, S. (2005). *Inhibiting farnesylation reverses the nuclear morphology defect in a HeLa cell model for Hutchinson-Gilford progeria syndrome*. *Proc. Natl. Acad. Sci. U. S. A.* **102,** 14416–14421

86. Yang, S. H. *et al.* (2010). *Assessing the effi cacy of protein farnesyltransferase inhibitors in mouse models of progeria*. *J. Lipid Res.* **51,** 400–405

87. Gordon, L. B. *et al.* (2012). *Clinical trial of a farnesyltransferase inhibitor in children with Hutchinson-Gilford progeria syndrome*. *Proc. Natl. Acad. Sci. U. S. A.* **109,** 16666–16671

88. Gordon, L. B. *et al.* (2016). *Clinical Trial of the Protein Farnesylation Inhibitors Lonafarnib, Pravastatin, and Zoledronic Acid in Children with Hutchinson-Gilford Progeria Syndrome*. *Circulation* **134,** 114–125

89. Gordon, L. B. *et al.* (2018). *Association of lonafarnib treatment vs no treatment with mortality rate in patients with Hutchinson-Gilford progeria syndrome*. *JAMA - J. Am. Med. Assoc.* **319,** 1687–1695

90. Eastman, R. T., Buckner, F. S., Yokoyama, K., Gelb, M. H. & Van Voorhis, W. C. (2006). *Fighting parasitic disease by blocking protein farnesylation*. *J. Lipid Res.* **47,** 233–240

91. Carrico, D. *et al.* (2004). *In vitro and in vivo antimalarial activity of peptidomimetic protein farnesyltransferase inhibitors with improved membrane permeability*. *Bioorganic Med. Chem.* **12,** 6517–6526

92. Kraus, J. M. *et al.* (2010). *Second generation analogues of the cancer drug clinical candidate tipifarnib for anti-chagas disease drug discovery*. *J. Med. Chem.* **53,** 3887–3898

93. Fletcher, S. *et al.* (2008). *Potent, plasmodium-selective farnesyltransferase inhibitors that arrest the growth of malaria parasites: Structure-activity relationships of ethylenediamine-analogue scaffolds and homology model validation*. *J. Med. Chem.* **51,** 5176–5197

94. Nallan, L. *et al.* (2005). *Protein farnesyltransferase inhibitors exhibit potent antimalarial activity*. *J. Med. Chem.* **48,** 3704–3713

95. End, D. W. *et al.* (2001). *Characterization of the antitumor effects of the selective farnesyl protein transferase inhibitor R115777 in vivo and in vitro*. *Cancer Res.* **61,** 131–137

96. Li, T. *et al.* (2009). *Phase II trial of the farnesyltransferase inhibitor tipifarnib plus*

fulvestrant in hormone receptor-positive metastatic breast cancer: New York Cancer Consortium Trial P6205. *Ann. Oncol.* **20,** 642–647

97. Shen, M. *et al.* (2015). *Farnesyltransferase and geranylgeranyltransferase I: Structures, mechanism, inhibitors and molecular modeling*. *Drug Discov. Today* **20,** 267–276

98. Russell, P. & Nurse, P. (1987). *Negative regulation of mitosis by wee1+, a gene encoding a protein kinase homolog*. *Cell* **49,** 559–567

99. Perry, J. A. & Kornbluth, S. (2007). *Cdc25 and Wee1: Analogous opposites? Cell Div.* **2,** 1–12

100. Blackford, A. N. & Jackson, S. P. (2017). *ATM, ATR, and DNA-PK: The Trinity at the Heart of the DNA Damage Response*. *Mol. Cell* **66,** 801–817

101. Geenen, J. J. J. & Schellens, J. H. M. (2017). *Molecular pathways: Targeting the protein kinase Wee1 in cancer*. *Clin. Cancer Res.* **23,** 4540–4544

102. Matheson, C. J., Backos, D. S. & Reigan, P. (2016). *Targeting WEE1 Kinase in Cancer*. *Trends Pharmacol. Sci.* **37,** 872–881

103. Du, X. *et al.* (2020). *Structure-activity relationships of Wee1 inhibitors: A review*. *Eur. J. Med. Chem.* **203,** 112524

104. Sullivan, M. & Morgan, D. O. (2007). *Finishing mitosis, one step at a time*. *Nat. Rev. Mol. Cell Biol.* **8,** 894–903

105. Lewis, C. W. *et al.* (2017). *Prolonged mitotic arrest induced by Wee1 inhibition sensitizes breast cancer cells to paclitaxel*. *Oncotarget* **3,** 1–6

106. Do, K., Doroshow, J. H. & Kummar, S. (2013). *Wee1 kinase as a target for cancer therapy*. *Cell Cycle* **12,** 3348–3353

107. Toledo, C. M. *et al.* (2015). *Genome-wide CRISPR-Cas9 Screens Reveal Loss of Redundancy between PKMYT1 and WEE1 in Glioblastoma Stem-like Cells*. *Cell Rep.* **13,** 2425–2439

108. Potapova, T. A., Sivakumar, S., Flynn, J. N., Li, R. & Gorbsky, G. J. (2011). *Mitotic progression becomes irreversible in prometaphase and collapses when Wee1 and Cdc25 are inhibited*. *Mol. Biol. Cell* **22,** 1191–1206

109. Aarts, M. *et al.* (2012). *Forced mitotic entry of S-phase cells as a therapeutic strategy induced by inhibition of WEE1*. *Cancer Discov.* **2,** 524–539

110. Hirai, H. *et al.* (2009). *Small-molecule inhibition of Wee1 kinase by MK-1775 selectively sensitizes p53-deficient tumor cells to DNA-damaging agents*. *Mol. Cancer Ther.* **8,** 2992–3000

111. Hirai, H. *et al.* (2009). *Small-molecule inhibition of Wee1 kinase by MK-1775 selectively sensitizes p53-deficient tumor cells to DNA-damaging agents*. *Mol. Cancer Ther.* **8,** 2992–3000

112. Pfister, S. X. *et al.* (2015). *Inhibiting WEE1 Selectively Kills Histone H3K36me3-Deficient Cancers by dNTP Starvation*. *Cancer Cell* **28,** 557–568

113. Bukhari, A. B. *et al.* (2019). *Inhibiting Wee1 and ATR kinases produces tumor-selective synthetic lethality and suppresses metastasis*. *J. Clin. Invest.* **129,** 1329–1344

114. O'Neil, N. J., Bailey, M. L. & Hieter, P. (2017). *Synthetic lethality and cancer*. *Nat. Rev. Genet.* **18,** 613–623

115. Bryant, H. E. *et al.* (2005). *Specific killing of BRCA2-deficient tumours with inhibitors of poly(ADP-ribose) polymerase*. *Nature* **434,** 913–917

116. Farmer, H. *et al.* (2005). *Targeting the DNA repair defect in BRCA mutant cells as a therapeutic strategy*. *Nature* **434,** 917–921

117. Foucquier, J. & Guedj, M. (2015). *Analysis of drug combinations: current methodological landscape*. *Pharmacol. Res. Perspect.* **3,**

118. BLISS, C. I. (1956). *The calculation of microbial assays. Bacteriol. Rev.* **20,** 243–258

119. Senkus, E. *et al.* (2015). *Primary breast cancer: ESMO Clinical Practice Guidelines for diagnosis, treatment and follow-up*. *Ann. Oncol.* **26,** v8–v30

120. Dai, X. *et al.* (2015). *Breast cancer intrinsic subtype classification, clinical use and future trends*. *Am. J. Cancer Res.* **5,** 2929–2943

121. Magidson, V. *et al.* (2015). *Adaptive changes in the kinetochore architecture facilitate proper spindle assembly*. *Nat. Cell Biol.* **17,** 1134–1144

122. Oceguera-Yanez, F. *et al.* (2016). *Engineering the AAVS1 locus for consistent and scalable*

transgene expression in human iPSCs and their differentiated derivatives. *Methods* **101,** 43–55

123. Lee, K. H., Koh, M. & Moon, A. (2016). *Farnesyl transferase inhibitor FTI-277 inhibits breast cell invasion and migration by blocking H-Ras activation*. *Oncol. Lett.* **12,** 2222–2226

124. Lewis, C. W. (2020). The role of Wee1 and Myt1 in breast cancer.

125. Schafer-Hales, K. *et al.* (2007). *Farnesyl transferase inhibitors impair chromosomal maintenance in cell lines and human tumors by compromising CENP-E and CENP-F function*. *Mol. Cancer Ther.* **6,** 1317–1328

126. Charron, G., Tsou, L. K., Maguire, W., Yount, J. S. & Hang, H. C. (2011). *Alkynyl-farnesol reporters for detection of protein S-prenylation in cells*. *Mol. Biosyst.* **7,** 67–73

127. Mansoori, B., Mohammadi, A., Davudian, S., Shirjang, S. & Baradaran, B. (2017). *The different mechanisms of cancer drug resistance: A brief review*. *Adv. Pharm. Bull.* **7,** 339–348

128. Lewis, C. W. *et al.* (2019). *Upregulation of MyT1 promotes acquired resistance of cancer cells to WEE1 inhibition*. *Cancer Res.* **79,** 5971–5985

129. Howell, B. J. *et al.* (2001). *Cytoplasmic dynein/dynactin drives kinetochore protein transport to the spindle poles and has a role in mitotic spindle checkpoint inactivation*. *J. Cell Biol.* **155,** 1159–1172

130. Echeverri, C. J., Paschal, B. M., Vaughan, K. T. & Vallee, R. B. (1996). *Molecular characterization of the 50-kD subunit of dynactin reveals function for the complex in chromosome alignment and spindle organization during mitosis*. *J. Cell Biol.* **132,** 617–633

131. Gaetz, J. & Kapoor, T. M. (2004). *Dynein/dynactin regulate metaphase spindle length by targeting depolymerizing activities to spindle poles*. *J. Cell Biol.* **166,** 465–471

132. Goshima, G. & Vale, R. D. (2003). *The roles of microtubule-based motor proteins in mitosis: Comprehensive RNAi analysis in the Drosophila S2 cell line*. *J. Cell Biol.* **162,** 1003–1016